Upstream Binding Factor, an evolutionarily conserved protein that organises ribosomal gene chromatin

Christine Ann Marie Colleran

Centre for Chromosome Biology,
School of Natural Sciences,
National University of Ireland Galway

A thesis submitted to the National University of Ireland Galway for the degree of Doctor of Philosophy

September 2012

Supervisor: Professor Brian McStay

Abbreviations

ActD	Actinomycin D
ARF	alternate reading frame
BLAST	Basic Local Alignment Search Tool
bp	base pair
BSA	bovine serum albumin
Cdk	cyclin dependent kinases
cDNA	complementary DNA
CF	core factor
ChIP	chromatin immunoprecipiation
CSB	cockayne syndrome protein B
Da	dalton
DAPI	4'-6-diamidino-2-phenylindole
DMEM	dulbecco's modified eagle's medium
DMSO	dimethyl sulfoxide
DNA	deoxyribonucleic acid
dNTPs	deoxynucleotide triphosphate
ds	double stranded
ECL	enhanced chemiluminescence
EGF	epidermal growth factor
EGFR	EGF receptor
EST	expressed sequence tags
FACS	fluorescence activated cell sorting
FBS	foetal bovine serum
FISH	fluorescence in situ hybridisation
FOA	fluroorotic acid
GFP	green fluorescent protein
GST	glutathione *S*-transferase
HAT	histone acteyltransferase
HMG	high mobility group
hr	hour
HRP	horseradish peroxidase
IgG	Immunoglobulin G
IGS	intergenic spacer
JNK2	c-jun N-terminal protein kinasae 2
kb	kilo-base
LB	Luria broth
MAPK	mitogen-activated protein kinase
MEM	minimum essential medium
min	minute
ml	millilitre
nm	nanometre
NOR	nucleolar organiser region
O/N	over night
OD	optical density
orf	open reading frame
PARP	poly (ADP-ribose) polymerase
PBS	phosphate buffered saline
PCR	polymerase chain reaction
PFA	paraformaldehyde

PI	propidium iodide
PI3K	phosphatidylinositol 3-kinase
PIC	Pre-Initiation Complex
PP2A	phosphatase 2A
PTRF	Polymerase I and Transcript Release Factor
RISC	RNA-induced silencing complex
RNA	ribonucleic acid
RNAi	RNA interference
RNase	ribonuclease
RP	ribosomal protein
RPE	retinal pigment epithelial
rpm	revolutions per minute
RT	room temperature
SANT	switching-defective protein 3 (Swi3), adaptor 2 (Ada2), nuclear receptor co-repressor (N-CoR), transcription factor (TF)IIIB
SDS	sodium dodecyl sulfate
sec	second
shRNA	short hairpin RNA
SILAC	stable isotope labelling with amino acids in cell culture
SL1	selectivity factor 1
SLD	SANT-like domain
SNAP	SILAC nucleosome affinity purification
snoRNA	small nucleolar RNA
snoRNP	small nucleolar ribonucleoprotein
snRNA	small nuclear RNA
SSC	saline-sodium citrate
SSU	small sub-unit
TBP	TATA-binding protein
TEM	transmission electron microscopy
TERT	telomerase reverse transcriptase
TOR	target of rapamycin
TTF-1	transcriptional termination factor 1
UAF	upstream activating factor
UBF	upstream binding factor
UCE	upstream control element
UV	Ultraviolet
V	volts
v/v	volume to volume
w/v	weight to volume
YFP	yellow fluorescent protein

Acknowledgements

I would firstly like to thank my supervisor Brian. Thank you for giving me the opportunity to carry out my PhD in your lab and for making the lab such an enjoyable place to work. I thank you for all your patience and help over the past 4 years, you are one the most patient men I know. Also thank you for lending a friendly ear and being so understanding.

To the members of the McStay lab, Jose-luis, Sofia and Mayo, thank you for the help and kind words that you have all expressed. Chelly thank you for all the help and kindness you have shared, you are a true lady. Ioanna, what can I say, the crazy Greek, thanks for everything, we've had some laughs and cries together. And Alice, thank you for all the times you have calmed me down when I started having my little TC panic attacks and all your help throughout the duration of my PhD.

To all the members of the centre for chromosome biology, thank you for making my PhD enjoyable and sharing many a Friday evening in the college bar. A special word of thanks to my TC1 girls, whom I have shared many tears and laughs.

To Karen and Lorna, thank you so much for everything, you both have been there to listen to my endless rants, and to all my friends at home who have been so supportive. To my extended family, of which there are many of you, thank you for all your love and support. To Mike, thank you so much for putting up with my craziness, especially the last few months, you have always been so supportive of everything I do, thank you.

To my Mum and Dad, thank you for all your love and support. Without you none of my achievements would have been possible. To my brother Noel, who is the strongest and most talented man I know, thanks for constantly trying to toughen me up. I love you all so much and you mean everything to me.

And to my beautiful sister Laura who I miss so much everyday, I know that you would be proud of me now, I just wish that you could be here with us to experience this. I would like to dedicate this thesis to my sister Laura, who was a wonderful, beautiful, intelligent and strong lady. I love you so much Laura.

"It matters not how strait the gate,
How charged with punishments the scroll,
I am the master of my fate;
I am the captain of my soul"

William Ernest Henley

Abstract

The nucleolus, the site of ribosome biogenesis, forms around arrays of ribosomal gene (rDNA) repeats termed nucleolar organiser regions (NORs). Transcriptionally active NORs appear as regions of under-condensed chromatin on metaphase chromosomes termed secondary constrictions. Silent NORs lose these chromosomal features and during interphase appear as foci of condensed chromatin dissociated from nucleoli. The architectural RNA polymerase I transcription factor, Upstream Binding Factor (UBF), has been shown to bind extensively over active rDNA repeats and we hypothesise that UBF is implicated in maintaining their open active chromatin state. Depletion of UBF in a variety of human cell lines, and in cells from the rat kangaroo *Potorous,* demonstrates that UBF is required for the maintenance of secondary constrictions on metaphase NORs. I also demonstrate that during interphase, UBF depletion induces rDNA condensation, with a proportion of NORs initially moving to the periphery and eventually dissociating from nucleoli. Thus I conclude that UBF levels set the proportion of NORs that are active.

Phylogenetic analyses reveal that UBF is not restricted to vertebrates as previously thought, but present across animal phyla even in the most primitive metazoans. Surprisingly, UBF from divergent species, including *Ciona intestinalis* can specifically recognise and bind to human NORs. UBF has low DNA sequence specificity, and rDNA regulatory sequences have diverged rapidly throughout evolution. Thus we speculated that UBF binding to rDNA involves recognition of a specific chromatin state and is not solely reliant on the underlying DNA sequence.

The SANT domain is a motif found in number of chromatin remodelling/binding complexes. A related domain present in the proto-oncogene *myb* functions as a histone tail interaction motif. SANT domains are characterised by the presence of three spatially conserved tryptophan residues. I have identified a SANT-like domain within the N-terminal dimerisation domain of UBF, that includes these conserved tryptophan residues. Mutational analysis reveals their critical nature for UBFs localisation. Future analysis of this novel SANT-like domain will provide insights into how UBF, a critical regulator of ribosome biogenesis, functions.

1 Introduction

1.1 History of the Nucleolus

The nucleolus is the most prominent sub-nuclear structure in all eukaryotic cells. Its primary function is ribosome biogenesis, which involves transcription of the ribosomal genes (rDNA) by the dedicated RNA polymerase I (RNA Pol I) machinery. Nucleoli form around active tandem arrays of rDNA repeats termed nucleolar organiser regions (NORs). Before going into the further detail of the nucleolus and ribosome biogenesis I would like to give a brief historical perspective as it highlights the main issues regarding NORs and nucleolar formation.

The nucleolus was documented as far back as the 1830's and in 1898 Montgomery published hand-drawn figures of nucleoli from a number of different species (Montgomery Jr, 1898). It took a further 30 years or more to discover that the nucleolus arises from specific chromosomal loci. These specific loci have a distinct appearance on metaphase chromosomes. Upon staining of chromosomes they are revealed as gaps or constrictions and were termed secondary constrictions, centromeres being the primary constrictions. Heitz discovered that the number of nucleoli that reformed at telophase correlated with the number of secondary constrictions present in metaphase (Figure 1.1) (Heitz, 1931). Around the same time McClintock independently observed this same phenomenon in *Zea mays* and went on and performed further analysis. She made use of a specific strain of *Zea mays* in which a single secondary constriction has been divided, by a reciprocal translocation, resulting in the appearance of two albeit smaller secondary constrictions. McClintock observed that instead of the single nucleolus usually present, there were now two nucleoli, indicating that nucleoli reform around these secondary constrictions (McClintock, 1934). McClintock therefore called these regions nucleolar organiser bodies, better known today as nucleolar organiser regions (NORs). Furthermore, McClintock concluded that the information required for nucleolar formation was redundant or repeated as each product of the reciprocal translocation could itself form a nucleolus. It would be a further 30 years before the composition of NORs and the function of the nucleolus would be revealed, but painstaking cell biology and remarkable intuition had established the connection between a chromosomal locus and formation of a sub-nuclear body.

The first indication of the function of the nucleolus was revealed in the mid 1960s when three individual groups discovered that NORs contained the genes encoding the 18S and 28S ribosomal RNAs (rRNAs). Two studies revealed the absence of rRNA synthesis and thus lack of ribosome biogenesis in *Xenopus* lacking nucleoli (Brown and Gurdon, 1964, Birnstiel et al., 1966). A study carried out in strains of *Drosophila* carrying different size NORs revealed that there was a direct correlation between the size of the NOR and the amount of rRNA (Ritossa and Spiegelman, 1965). Around the same period it was demonstrated that the rRNAs were initially transcribed as a single precursor rRNA before being processed to yield the 18S and 28S rRNAs (Liau and Perry, 1969, Scherrer et al., 1963). Another fundamental

advance in the understanding of the nucleolus came from the preparation of Miller spreads (Miller and Beatty, 1969), which enabled the visualisation of actively transcribed ribosomal genes and this will be discussed in section 1.3.

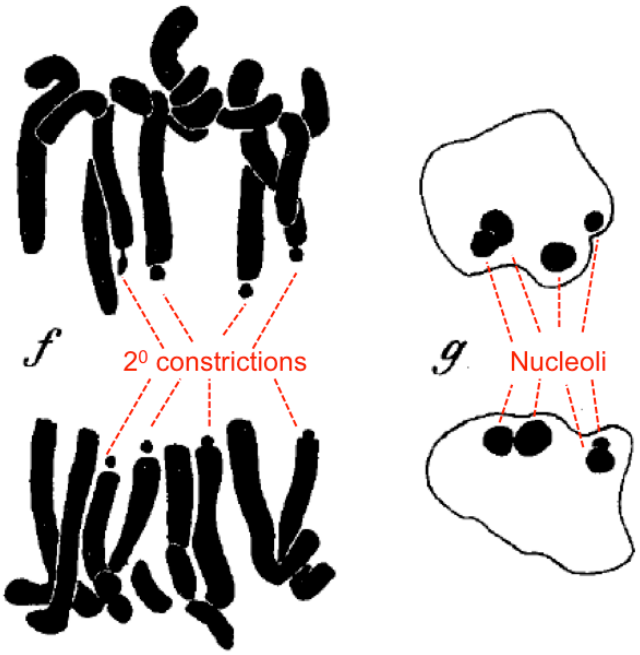

Figure 1.1 Heitz's conclusions
Heitz discovered in the early 1930s that the number of 2° constrictions (indicated on the left by red lines) corresponded to the number of nucleoli reformed in telophase (indicated by the red lines on the right). Figure adapted from (Heitz, 1931).

1.2 Characteristics and Organisation of ribosomal genes

NORs are composed of tandem arrays of rDNA repeats that are transcribed in a telomere to centromere direction (Worton et al., 1988). NORs are present in all eukaryotes, however the number of rDNA repeats varies greatly among eukaryotes, ranging from 100 to more than 10,000 in some animal cells and plant cells, respectively. One might assume that a larger number of rDNA repeats mirrors a higher demand for rRNA synthesis, however this does not seem to be the case. At any given time approximately 50% of the rDNA repeats are transcriptionally silent, suggesting that NORs can exist in an active or inactive state, which I will discuss in more detail in section 1.7. This also suggests that the number of rDNA repeats is in excess. Evidence that rDNA repeats are in excess comes from studying Robertsonian translocations, which are the most common form of translocations in humans, approximately 1/1,000 newborns (Hamerton et al., 1975). These translocation occurs as a result of the fusion of NOR bearing chromosomes, resulting in the loss of 2 out of the 10 NORs (Therman et al., 1989). Individuals carrying this type of translocation have no phenotype indicating that rDNA repeats are in excess. Further evidence indicating that rDNA repeats are in excess comes from work done in the yeast *Saccharomyces cerevisiae*, which contain approximately 150 rDNA

repeats on a single chromosome XII. Reduction of the total number of rDNA repeats to approximately 40 has no impact on cell growth or the rate of rRNA synthesis (Kobayashi et al., 1998), indicating that not only are the rDNA repeats in excess but that the rate of rRNA synthesis is not directly related to the number of rDNA repeats. Additionally plants, such as rye, have large NORs that allow the visualisation of both active and silent rRNA genes on a single NOR. The silent rRNA genes are located proximal to the centromere and are negative for silver staining, which is a diagnostic marker for active NORs (Caperta et al., 2002).

Another interesting feature of NORs is observed in some marsupial species, for instance in the rat-kangaroo (*Potorous*) model, where the NOR is located on the X chromosome. This means that female marsupials have two NORs and therefore twice the number of rDNA repeats in comparison to male marsupials (Robins et al., 1984). To balance the number of rDNA repeats between male and female marsupials one might expect some dosage compensation, however this is not the case. Both NORs in the female have been shown to be transcriptionally active by silver staining suggesting that NORs escape X-inactivation (Merry et al., 1983, Dhaliwal et al., 1988). We have also demonstrated, by silver staining, that NORs escape X-inactivation in the female *Potorous tridactylis* (PtK_1) cell line (Colleran and McStay unpublished data).

The organisation of rDNA repeats is similar among human and mouse with each repeat composed of an approximately 13kb transcribed region that codes for the 47S precursor rRNA (pre-rRNA) or 45S pre-rRNA in humans and mice, respectively. Transcribed regions are separated by intergenic spacers (IGS) of approximately 30kb (Gonzalez and Sylvester, 1995, Grozdanov et al., 2003, Sylvester et al., 2004). The mammalian IGS contains a number of regulatory elements including the gene promoter and transcription termination sites (Figure 1.2 (A)). In mouse and *Xenopus* rDNA repeats, spacer promoters and repetitive elements that function as transcriptional enhancers, are located within the IGS (Moss and Birnstiel, 1979, Kuhn and Grummt, 1987, Labhart and Reeder, 1984, Pikaard et al., 1990). Curiously, enhancer elements and spacer promoters are either absent or not yet characterised in the human rDNA repeat.

In the mouse, NORs are located on chromosomes 12, 15, 16, 17, 18 and 19 (Figure 1.2 (B)) (Dev et al., 1977). Humans have approximately 300-400 copies of the rDNA repeat (Schmickel, 1973) and these are distributed among the short arms of the five human acrocentric chromosomes, 13, 14, 15, 21 and 22 (Figure 1.2 (B)) (Henderson et al., 1972). The majority of rDNA arrays were detected as a 3Mb fragment that was released by digesting genomic DNA with an enzyme that does not cut in the human rDNA repeats, such as EcoRV, with some less obvious bands of about 1 and 2Mb (Sakai et al., 1995). This would suggest that the majority of NORs have approximately 70 rDNA repeats. A more recent study using peripheral blood lymphocyte samples from a number of healthy humans has revealed that the size of NORs can range between 50kb and 6Mb (Stults et al., 2008).

In the plant *Arabidopsis thaliana* the approximately 1200-1500 rDNA repeats, which encode the 18S, 5.8S and 25S, are arranged in tandem at NORs located on chromosome 2 and 4. The NORs are similar in size and composed of approximately 370 rRNA repeats, each repeat approximately 10-10.5 kb in size (Copenhaver and Pikaard, 1996). In *S. cervisiae* the tandem array of approximately 150 rDNA repeats is located on a single chromosome, chromosome XII. Each individual rDNA repeat consists of the 35S rRNA coding region to generate the 18S, 5.8S and 25S rRNAs, as well as the 5S rRNA coding regions and two nontranscribed regions, NTS1 and NTS2 (Figure 1.2 (C)). The presence of the 5S rRNA coding region within the rDNA repeat differs to that observed in higher eukaryotes. In humans, mice and *Xenopus*, the 5S rRNA genes are arranged in repeat arrays, separate from the nucleolar rDNA repeats (Nomura et al., 2004).

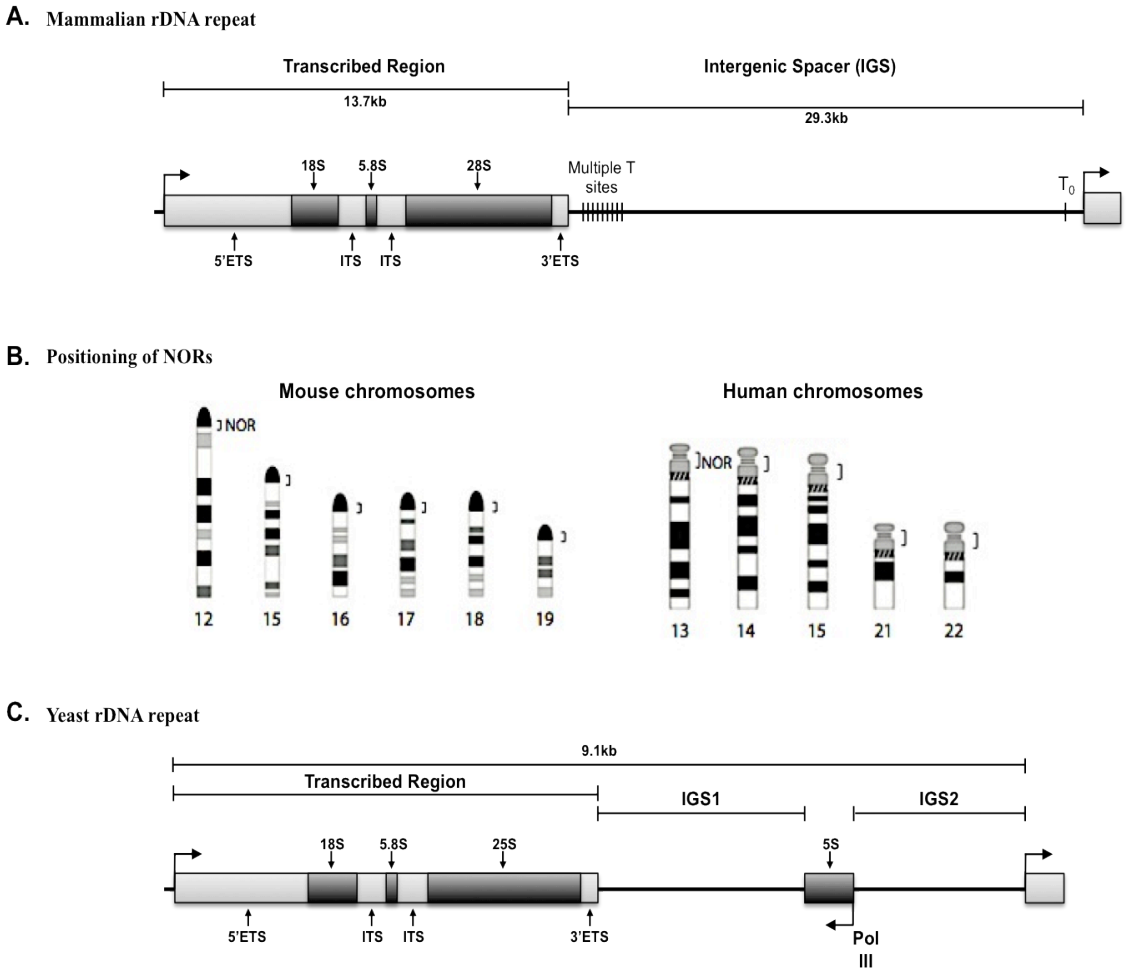

Figure 1.2 Positioning and organisation of nucleolar organiser regions (NORs)
(A) Schematic representation of mammalian rRNA genes. The 13kb transcribed region is processed to generate the final mature 18S, 5.8S and 28S ribosomal RNAs. These transcribed regions are separated by 30kb intergenic spacer (IGS) region.
(B) The location of NORs on human and mouse chromosomes indicated by brackets. Figure adapted from (McStay and Grummt, 2008)
(C) Schematic representation of yeast rRNA genes. In addition to containing the coding region for the 18S, 5.8S and 25S rRNAs, the 5S rRNA coding region is also located within each of the rDNA repeats. The 5S gene is independently transcribed by RNA polymerase III

The complexity of NORs is now starting to be appreciated. To date only a single mouse rDNA repeat has been fully sequenced (Grozdanov et al., 2003). Furthermore the original simplistic view that NORs are uniform arrays of identical rDNA units is now being revised. Molecular combing has revealed that human NORs are a mixture of canonical and non-canonical rDNA repeats, with as many as one-third of the non-canonical nature (Caburet et al., 2005). This complexity in NORs has prevented successful sequencing and therefore acrocentric short arms are absent from even the most current 2009 draft of the human genome (hg19). This lack of information on the sequences surrounding NORs extends to all vertebrates.

A 3Mb NOR is thought to represent between one-third and one-quarter of the DNA on the short arms of each human acrocentric chromosome. The positioning of NORs on the short arms of acrocentric chromosomes isolates them from other genes that are transcribed by RNA Pol II and III. Isolation of NORs is reinforced by the heterochromatic nature of the surrounding acrocentric short arm chromatin (Choo et al., 1990, Tagarro et al., 1994, Shiels et al., 1997).

1.3 Ribosomal gene transcription

The genetic isolation of NORs is reinforced by the fact that in all eukaryotes a dedicated RNA polymerase, RNA polymerase I (RNA Pol I) and its associated machinery transcribe ribosomal genes. In all eukaryotes there are three nuclear RNA polymerases, with each performing specific functions. The notion that more than one RNA polymerase was present was fuelled by the observation that transcription in the nucleolus occurs in the presence of low Mg^{2+}, whereas transcription in the nucleus occurs in the presence of high Mn^{2+}. Ion exchange chromatography on DEAE (diethylaminothanol)-Sephadex identified the presence of three different RNA polymerases, RNA Pol I, II, III (Roeder and Rutter, 1969). Another nomenclature system for the RNA polymerases was coined by Pierre Chambon, RNA polymerases A, B, C instead of I, II and III (Chambon, 1975). This nomenclature has been used for the naming of RNA polymerase sub-units, for example RPA43, which is an RNA Pol I subunit.

RNA Pol I transcribes only the 18S, 5.8S and 25S rRNAs, RNA Pol II transcribes protein-encoding genes and the majority of small nuclear RNAs (snRNAs) and finally RNA Pol III transcribes the remaining snRNAs and the 5S rRNA. It was work from the Nomura lab which proved that the function of RNA Pol I is solely transcription of rRNA genes. In yeast they demonstrated that by positioning the coding sequences for the 35S pre-rRNA gene downstream of a GAL7 promoter the resulting RNA pol II derived transcript could produce functional ribosomes. Yeast strains with defective RNA pol I were viable in this genetic background, revealing that ribosomal genes are the only essential genes transcribed by RNA pol I (Nogi et al., 1991).

For the purpose of my thesis I will describe only the mechanism of rDNA transcription by the dedicated RNA Pol I machinery. Transcription of rDNA in mammals generates a pre-rRNA transcript, which undergoes a number of modifications, including RNA processing, methylation and pseudo-uridylation to produce the mature 18S, 5.8S and 28S rRNAs (25S rRNA in yeast). These mature rRNAs together with the RNA Pol III transcribed 5S rRNA and ribosomal proteins constitute the large and small ribosomal subunits (Figure 1.3).

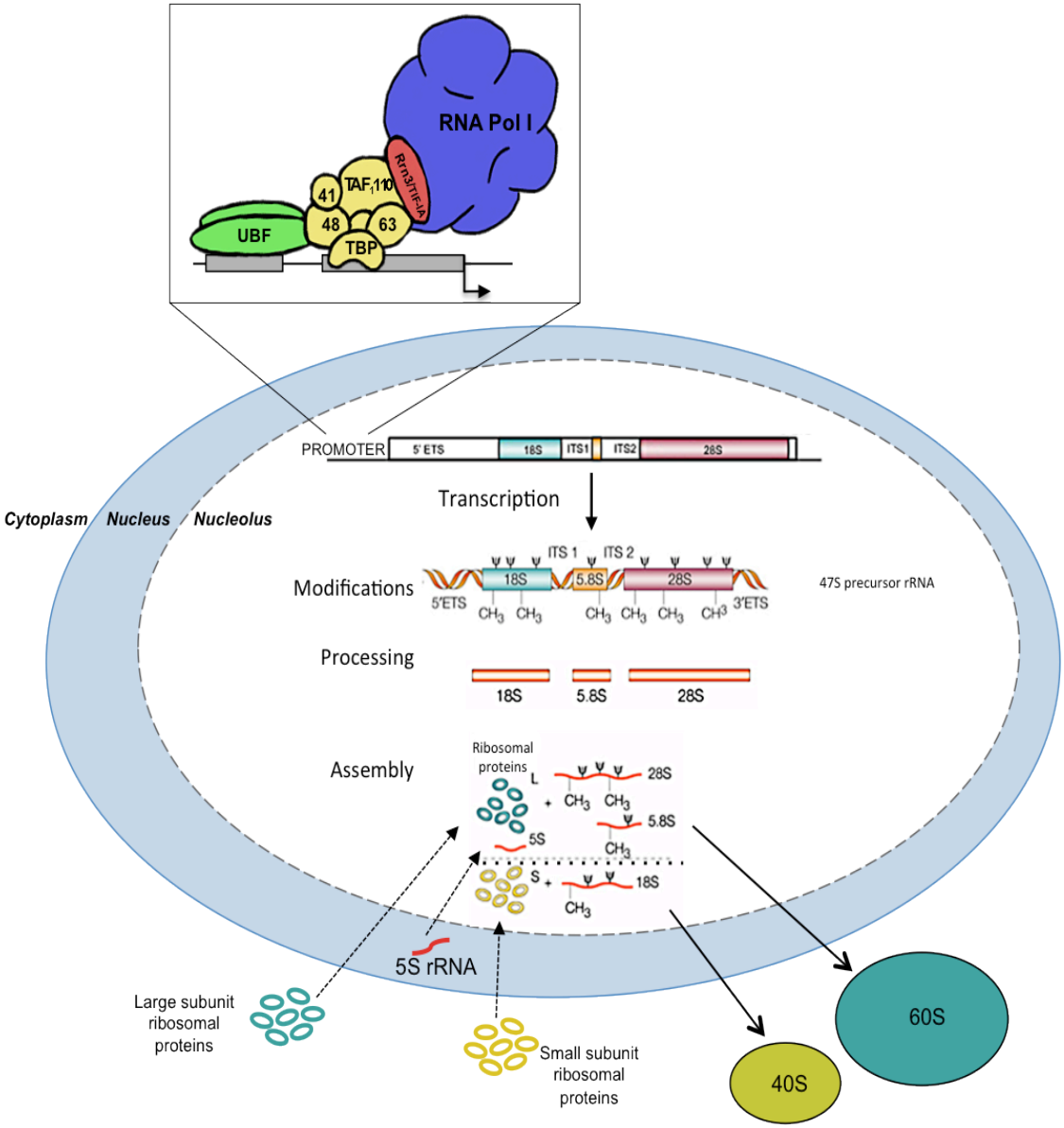

Figure 1.3 Schematic of ribosome biogenesis in mammalian cells
The diagram represents the main steps in ribosome biogenesis. The components of the pre-initiation complex (PIC), which binds to the rDNA promoter to initiate transcription, are shown in the inset. The 47S pre-rRNA transcript is modified (Ψ=pseudouridylation and CH_3= 2-*O*' ribose methylation), processed with the 18S rRNA assembling with small ribosomal proteins to generate the small 40S ribosome subunit, while the 5.8S and 28S rRNAs are assembled with the 5S rRNA and large ribosomal proteins to generate the large 60S ribosome subunit. The 40S and 60S ribosome subunits are exported to the cytoplasm where they bind to messenger RNA (mRNA) to form a functional ribosome.

The majority of ongoing transcription in the cell, up to 60%, is from rDNA. Miller spreads are the best way of visualising how heavily transcribed ribosomal genes are, appearing as structures reminiscent of a Christmas tree (Miller and Beatty, 1969). Miller spreads were first prepared from amphibian oocytes by Miller and co-workers. Generating Miller spreads involves subjecting the cells to low ionic strength buffers and detergents resulting in the release and dispersion of chromatin. The chromatin is centrifuged onto a carbon-coated grid and images taken by electron microscopy (EM). The trunk of the tree indicates the path of the ribosomal gene, while the approximately 100 nascent pre-rRNAs radiating away from the gene are the branches of the tree (Figure 1.4). Structures termed terminal knobs, evident at the 5' end of pre-rRNA transcripts (indicated by arrowheads, Figure 1.4), contain the Small Sub-Unit (SSU) processome, which will be discussed in the following section, 1.4. Miller spreads prepared from yeast reveal the high density of RNA Pol I loading on rRNA genes, that is one RNA Pol I complex every ~100 nucleotides (French et al., 2003). I will describe in more detail the transcription machinery and mechanisms that are required to achieve these high levels of rDNA transcription.

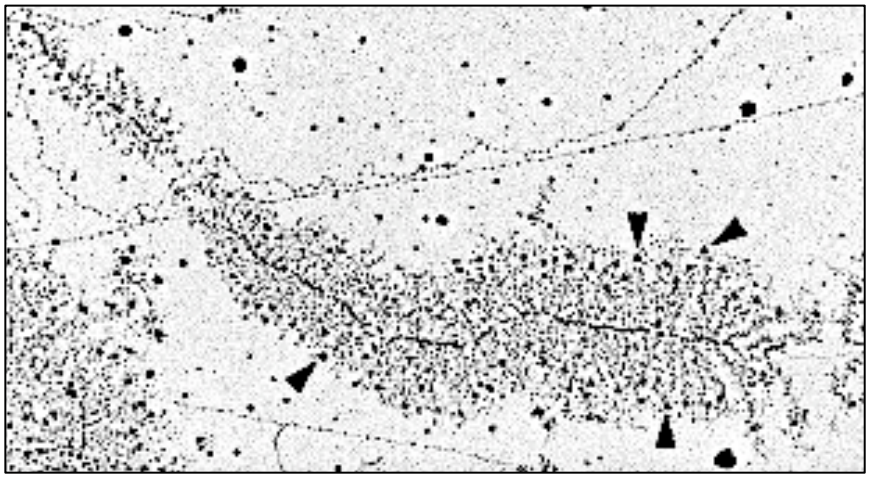

Figure 1.4 Electron microscopic image of a Miller spread prepared from mouse nucleolar chromatin
Miller spreads reveal the rDNA transcription unit, which is reminiscent of a Christmas tree. In this Christmas tree structure the rRNA genes occupy the trunk with the pre-rRNA nascent transcripts radiating away as the branches. The arrowheads indicate the 5' end terminal knobs structure, which contain the SSU processome. Figure from (Raška, 2003).

1.3.1 The basal RNA polymerase I factors for transcription initiation

A feature of rDNA promoters is their sequence divergence throughout evolution. This divergence is mirrored by changes in the basal RNA Pol I transcription machinery and consequently rDNA transcription is extremely species specific. This is exemplified by the fact that human rDNA cannot be transcribed, *in vivo* or *in vitro*, by mouse RNA Pol I machinery and vice versa (Miesfeld and Arnheim, 1984, Grummt et al., 1982, Mishima et al., 1982). This rapid evolutionary divergence is due to the fact that the RNA pol I transcription machinery transcribes

a single albeit repeated gene class. Alterations in the transcription machinery can be matched by compensatory changes in the rDNA promoter and vice versa. Note that alterations in the promoter sequence can be fixed throughout NORs by gene conversion or unequal crossing over, resulting in concerted evolution (Ganley and Kobayashi, 2007). Evolution of RNA Pol II and RNA Pol III machineries is constrained by the diverse array of gene classes that they transcribe.

Despite divergence in DNA sequence, the overall organisation of the rDNA promoter is comparable between species (Heix and Grummt, 1995). The rDNA promoter is bipartite, consisting of a CORE element that spans the transcriptional start site and an upstream control element (UCE) approximately 100 nucleotides further upstream. The human CORE element is required for accurate transcription initiation and behaves in a similar manner both *in vitro* and *in vivo*. In contrast the human UCE, which has a modulatory role, appears to function differently in *in vitro* and *in vivo* systems. Mutational analysis in the UCE region has very little impact on rDNA transcription *in vitro* suggesting that the UCE may be dispensable, however *in vivo* these same mutational analysis reveal that UCE is required for maximal transcription (Jones et al., 1988, Haltiner et al., 1986). The UCE of the *Xenopus* promoter is essential *in vitro* and *in vivo* (Moss, 1982, Sollner-Webb et al., 1983). In human and *Xenopus* the spatial arrangement and orientation of the CORE element and UCE is critical, as any changes in spacing between the two elements has been shown to drastically decrease the level of rDNA transcription (Windle and Sollner-Webb, 1986, Jones et al., 1988).

In mammals, assembly of the pre-initiation complex (PIC) at the rDNA promoter is required for rDNA transcription. Formation of the PIC requires the synergistic action of two RNA Pol I specific factors, the upstream binding factor (UBF) (Jantzen et al., 1990) and the promoter selectivity factor 1 (SL1) (Learned et al., 1985) or TIF-IB in mouse (Clos et al., 1986). UBF consists of an amino-terminal (N-terminal) dimerisation domain, multiple HMG (high mobility group) boxes and a carboxy-terminal (C-terminal) acidic tail (Jantzen et al., 1990, McStay et al., 1991, Jantzen et al., 1992) (Figure 1.5). Mammalian UBF exists as two splice variants, UBF1 and UBF2, as a result of alternative splicing of a single transcript, with UBF2 missing 37 amino acids from the second HMG box (O'Mahony and Rothblum, 1991). By western blotting both UBF1 and UBF2 have comparable intensity, yet UBF2 is incapable of supporting robust rDNA transcription compared to UBF1 and therefore has been rendered non-functional at the rDNA promoter (Hannan et al., 1996, Kuhn et al., 1994). Evidence as to why the activity of UBF2, at the level of rDNA transcription, is so poor is still unclear.

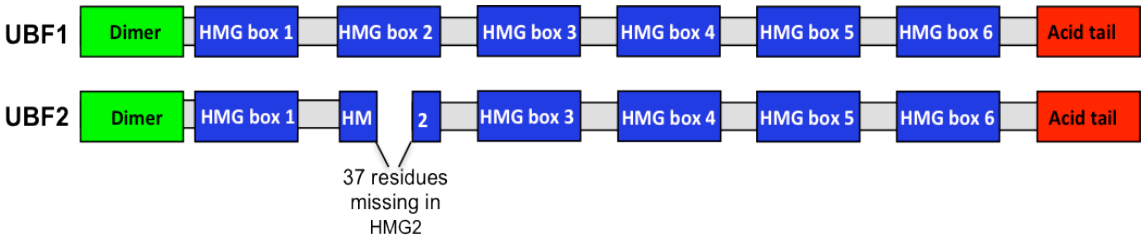

Figure 1.5 Upstream Binding Factor (UBF) structure
Structural organisation of the two splice variants of UBF. Both consist of N-terminal dimerisation, six HMG box domains and an acidic C-terminal tail. As a result of splicing UBF2 is missing 37 residues from the second HMG box.

UBF has been shown to form dimers in solution through its N-terminal dimerisation domain (McStay et al., 1991). UBF dimers bind to the rDNA promoter via their HMG boxes, so called because of their similarity in sequence and structure to the DNA binding domains present in the non-histone chromosomal architectural HMGB (high mobility group box) proteins (Jantzen et al., 1990). The C-terminal domain of UBF is comprised predominantly of acidic glutamic and aspartic residues, but also contains of a high abundance of serine residues. Phosphorylation of this acidic domain plays a critical role for UBFs functioning in transcriptional activation and is necessary for the recruitment of the SL1/TIF-IB complex to the promoter via direct protein-protein interaction (Jantzen et al., 1992, Voit et al., 1992, Tuan et al., 1999). Furthermore phosphorylation gives an overall negative charge to the C-terminal domain of UBF and this negative charge contributes to the silver staining associated with active NORs, which is described in section 1.7.

Promoter selectivity, as well as species specificity, is driven by SL1/TIF-IB. SL1/TIF-IB is a multi-protein complex made up of the TATA-binding protein (TBP) and five RNA Pol I specific TBP-associated factors (TAF_1s), TAF_1110, TAF_163, TAF_148, TAF_141 and $TAF_{11}12$ (Comai et al., 1992, Zomerdijk et al., 1994, Heix et al., 1997, Gorski et al., 2007, Denissov et al., 2007). SL1/TIF-IB binds to the CORE element and facilitates transcription complex assembly. SL1/TIF-IB, though TAF_148, interacts with the C-terminus of UBF, which subsequently results in the recruitment of the initiation-competent subpopulation of RNA Pol I defined by the presence of Rrn3 in humans and TIF-IA in mouse. Rrn3/TIF-IA acts as a link between RNA Pol I and SL1/TIF-IB and this is mediated by interactions of Rrn3/TIF-IA with the SL1/TIF-IB subunits TAF_1110 and TAF_163 (Miller et al., 2001, Yuan et al., 2002), as well as with the RNA Pol I specific subunit, RPA43 (Cavanaugh et al., 2002). Furthermore, UBF has been shown to interact directly with some of the RNA Pol I complex subunits, such as PAF53 and PAF49 (Hanada et al., 1996, Panov et al., 2006b). Once the PIC complex along with RNA Pol I is situated at the rDNA promoter, efficient rDNA transcription can occur (Figure 1.6 (A)).

In *S. cerevisiae*, rDNA transcription requires TBP, Rrn3p, the yeast homolog of Rrn3/TIF-IA and three multiprotein complexes, upstream activating factor (UAF), core factor (CF) and RNA

Pol I. Formation of the PIC at the rDNA promoter requires UAF binding to the upstream element followed by the recruitment of CF and the RNA Pol I/Rrn3p complex. RNA Pol I is necessary for stable association of CF at the promoter. TBP is required for efficient rDNA transcription, yet its exact function is still unknown (Grummt, 2003, Nomura et al., 2004, Aprikian et al., 2001). The UAF is a multi-protein complex composed of Rrn5p, Rrn9p, Rrn10p, Uaf30p and histones H3 and H4 (Keys et al., 1996, Keener et al., 1997). The CF consists of three proteins Rrn6p, Rrn7p and Rrn11p (Lalo et al., 1996, Keys et al., 1994).

There is evidence to suggest that the SL1/TIF-IB is the functional counterpart of CF in yeast. For example the interaction of Rrn3/TIF-IA with SL1/TIF-IB through TAF_1110 and TAF_163 appears to correspond with the interaction of Rrn3p with CF through its Rrn6p subunit (Nomura et al., 2004).

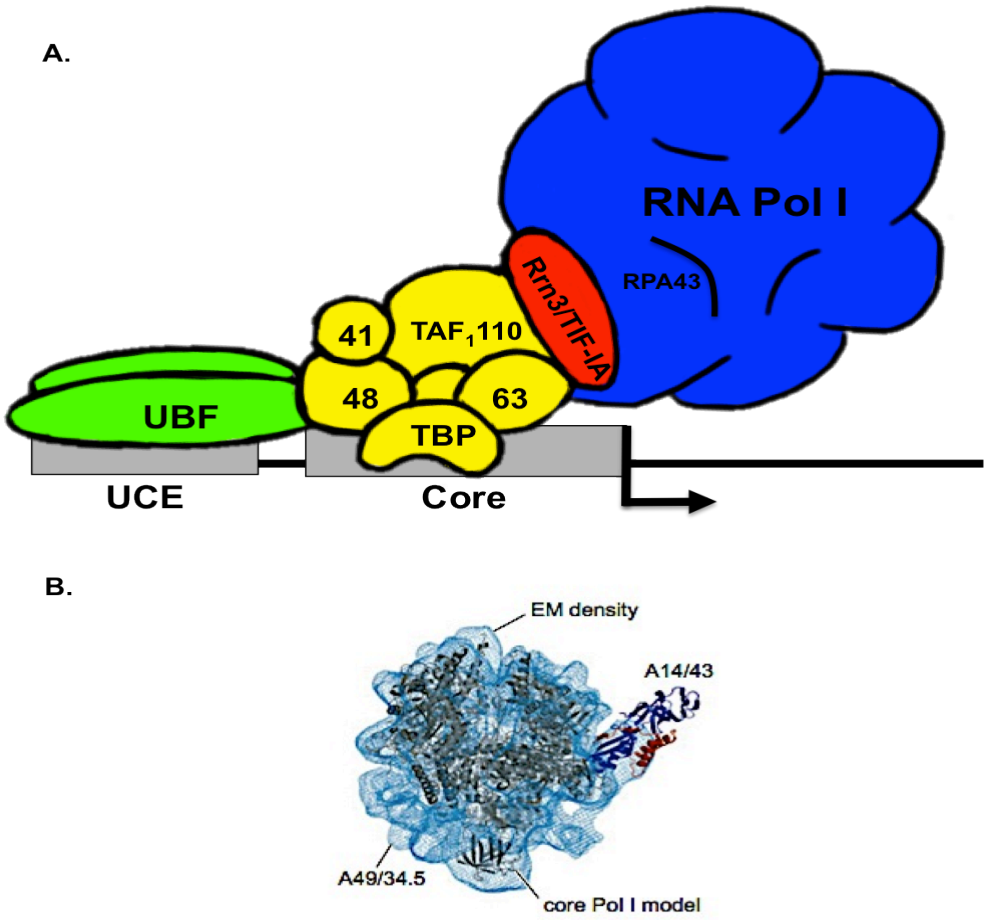

Figure 1.6 RNA polymerase I pre-initiation complex (PIC) and structure of RNA Polymerase I
(A) A dimer of UBF (green) binds to the rDNA promoter, which in turn recruits SL1/TIF-IB (yellow). SL1/TIF-IB is composed of TBP and five Pol I specific TBP-associated factors (TAF_1s). The initiation-competent form of RNA Pol I, which is associated with Rrn3/TIF-IA, is recruited and transcription commences. Protein-protein interactions involved in stabilising the PIC include:

I. TAF_148 interacts with the C-terminus of UBF
II. Rrn3/TIF-IA interacts with TAF_1110 and TAF_163
III. Rrn3/TIF-IA interacts with the RNA polymerase I subunit RPA43
IV. Additional UBF interacts with the RNA polymerase I subunit PAF49 and PAF53.

(B) Structure of RNA Pol I highlights the catalytic core, the A14/43 polymerase stalk and the RNA Pol I specific A49/34.5 structure. Figure from (Cramer et al., 2008).

These parallels between SL1-TIF-IA and CF might explain why it was initially assumed that UAF and UBF were performing the same function, however now we know that this is not the case. UBF is a nucleolar HMG box protein whereas UAF is a multi-protein complex. Instead a yeast nucleolar HMG box protein, Hmo1, which is required for efficient rDNA transcription, has been identified as performing the same functional role as UBF (Gadal et al., 2002). I will discuss this protein in more detail in chapter 5 and provide more parallels between Hmo1 and UBF.

Of the three eukaryotic RNA polymerases, RNA Pol I is the most divergent and this is most likely due to its exclusive role in rDNA transcription. Despite this divergence the complex RNA Pol I protein, is highly conserved from yeast to human. Analysis of the yeast RNA Pol I complex has been key to our understanding of what subunits constitute the human RNA Pol I complex. The yeast RNA Pol I complex, which is ~600kDa, consists of 14 subunits, 13 of which have mammalian orthologues. Five of these subunits are shared among the three eukaryotic RNA polymerases, two are shared between RNA Pol I and III while seven are RNA Pol I specific. RPA14 is the only subunit discovered in yeast that has no known identified mammalian orthologue (Panov et al., 2006b, Russell and Zomerdijk, 2005). The known composition of both yeast and mammalian RNA Pol I is outlined in table 1.1.

Yeast RNA Pol I subunits	Human RNA Pol I subunits	Unique/Shared Subunits among RNA Pols	
A190	RPA195	I	
A135	RPA135	I	
AC40	RPA40	I, III	
ABC27	RBP25	I, II, III	
ABC23	RBP14.4	I, II, III	
AC19	RPA16	I, III	Catalytic Core
ABC14.5	RPB17	I, II, III	
A12.2	RPA12.2	I	
ABC10α	RPB10α	I, II, III	
ABC10β	RPB10β	I, II, III	
A14	Not Identified	I	Polymerase Stalk
A43	RPA43	I	
A49	PAF53	I	RNA Pol I specific subcomplex
A34.5	PAF49	I	

Table 1.1 RNA Polymerase I subunits

Extensive structural analysis of RNA Pol I, carried out in the Cramer lab, has begun to facilitate our understanding of how RNA Pol I functions. Comparing the structures of the three RNA polymerases has revealed specific-structural characteristics that are conserved among RNA Pol I, II and III. All three have a 10 subunit catalytic core of homologous or shared subunits, outlined in table 1.1. Also conserved among the three polymerases is a heterodimeric subcomplex structure, termed A14/43, Rb4/7 and C17/25 in RNA Pol I, II and III, respectively, which forms the polymerase stalk (Peyroche et al., 2002, Armache et al., 2005, Jasiak et al., 2006, Kuhn et al., 2007). RNA Pol I has an additional specific heterodimeric subcomplex A49/34.5 (Figure 1.6 (B)) (Kuhn et al., 2007). When compared to RNA Pol II, the RNA Pol I has a distinct structure allowing specific interactions with Rrn3/TIF-I and recruitment of RNA Pol I. Furthermore, the RNA Pol I specific subunits A49 and A34.5 form heterodimers that function in stimulating elongation (Kuhn et al., 2007).

1.3.2 Elongation and Termination

In contrast to RNA Pol I transcription and termination, the mechanism by which RNA Pol I elongates is still poorly understood. Elongation proceeds *in vitro* upon promoter escape on a naked DNA template, however the precise mechanism by which elongation of RNA Pol I occurs at a chromatin level has yet to be established. One of the major drawbacks to understanding the process of elongation is the fact that it is still unclear as to whether or not rRNA genes are actively transcribed in the presence or absence of nucleosomes. A number of studies have suggested a functional role for UBF in facilitating RNA Pol I elongation. ERK dependent phosphorylations of UBF at threonine 117 (Thr117) and Thr201 residues, which are situated in the first and second HMG boxes, have been shown to enhance the rate of elongation (Figure 1.7). ERK phosphorylation enhances elongation by altering the first and second HMG boxes' affinity for linear DNA and inducing chromatin remodelling (Stefanovsky et al., 2006a, Stefanovsky et al., 2006b). UBF has also been demonstrated to stimulate promoter escape and clearance of RNA Pol I, thereby facilitating conversion of RNA Pol I from a static complex to a stable elongation complex (Panov et al., 2006a)

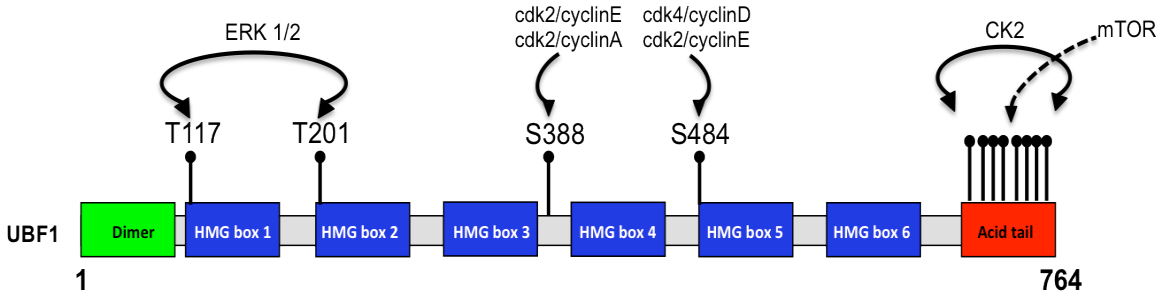

Figure 1.7 UBF modifications
UBF1 is a 764 amino-acid protein, which undergoes multiple post-translational modifications to modulate its activity. ERK can phosphorylate UBF at Threonine 117 in the first HMG box and Threonine 201 in the second HMG box (Stefanovsky et al., 2006b). During the cell cycle UBF is regulated by CDK-dependent phosphorylations at Serine 388 and Serine 484. The mTOR pathway and Casein kinase 2 have been shown to direct phosphorylations in the acidic C-terminal tail (Hannan et al., 2003a).

A recent study has found that TFIIH, which is primarily a transcription factor for RNA Pol II, is also essential for efficient rDNA transcription by functioning as a elongation factor of RNA Pol I (Assfalg et al., 2012). Mutations in the XPB and XPD subunits of TFIIH impair TFIIH of interacting with the rDNA and severely reduces RNA Pol I transcription by impeding elongation of RNA Pol I (Assfalg et al., 2012). The mutation of XPB and XPD subunits, which are known to play a role in nucleotide excision repair (NER), causes Cockayne syndrome (CS). This leads me to another factor speculated to be involved in stimulating RNA Pol I elongation. The chromatin remodeller CSB (Cockayne syndrome protein B) and the histone methyltransferase, G9a, have been suggested to imprint a specific chromatin mark, which in turn recruits chromatin remodelling enzymes or elongation factors thereby enabling transcription through chromatin (McStay and Grummt, 2008). Mutations in the CSB protein result in the aforementioned Cockayne syndrome, characterised by sunlight sensitivity, growth retardation, neurological and skeletal abnormalities, and a reduction in rDNA transcription levels (Bradsher et al., 2002).

Transcription termination is a multistep process. It involves halting RNA Pol I, release of both RNA Pol I and the pre-rRNA transcript, as well as the 3'end processing of the primary RNA transcript. The mechanism of RNA Pol I termination appears to be conserved from humans to yeast. In mouse multiple transcription termination sites (T) are located just downstream of the 28S rRNA coding region, that can bind the transcription termination factor 1 (TTF-1) and terminate transcription (Bartsch et al., 1988, Grummt et al., 1985). Binding of TTF-1 forces RNA Pol I to halt, resulting in a conformational change in RNA Pol I that then interacts with PTRF (Pol I and Transcript Release Factor). This RNA Pol I/PTRF interaction combined with a T-rich DNA sequence upstream of the terminator sites mediates transcription termination by releasing the RNA Pol I and rRNA transcripts (Mason et al., 1997, Jansa et al., 1998). Immediately upstream of the transcription initiation site, a single termination site (T_0) has been conserved in mouse, rat, human and *Xenopus*. This T_0 has been shown to stimulate and stabilise

transcription *in vivo*, suggesting a dual functioning for TTF-1 (Grummt et al., 1986, McStay and Reeder, 1986, Henderson and Sollner-Webb, 1986).

Similar to the mammalian terminator, the yeast terminator contains two elements: a T-rich DNA stretch, which encodes the last 10-12 nucleotides of the transcript that is being terminated (Lang and Reeder, 1995), and a specific termination factor. Despite *in vitro* evidence suggesting that Reb1 is the required termination factor, its role in RNA Pol I termination *in vivo* is unclear. A recent study has revealed that it is not Reb1, but the Myb-like protein Ydr026c/Nsi1, that is required for efficient rDNA transcription termination *in vivo* (Reiter et al., 2012).

1.4 Pre-rRNA processing

Ribosome biogenesis is a highly complex and coordinated process, which occurs primarily in the nucleolus, but also in the nucleus and cytoplasm. The initial step in ribosome biogenesis is rDNA transcription and this accounts for up to 60% of the total cellular transcription activity, indicating that this process is a major metabolic event in all cells (Warner, 1999). The complex series of events involves synthesis, processing and modifications of pre-rRNA, assembly with ribosomal proteins and transient interactions with non-ribosomal proteins. Although an extremely complex process, the ribosomal proteins and non-ribosomal factors that associate with the pre-rRNA transcript are highly conserved from yeast to human. Also the pre-rRNA processing and assembly pathways are closely related, but not identical, between yeast and human.

The complexity of ribosome synthesis is highlighted by the abundance of proteins utilised in this process. Multiple nucleolar proteomic studies has revealed a dramatic increase in the number of proteins associated with nucleoli, from an initial ~700 to a staggering ~5000 proteins (Andersen et al., 2002, Andersen et al., 2005, Scherl et al., 2002, Boisvert et al., 2010, Ahmad et al., 2009, Lam et al., 2010). Of these 5000 proteins, ~30% are known to be involved in the production of the ribosomal subunits, however this number is probably an underestimate. Nucleolar proteomic analyses also reveal that the nucleolus is involved in other processes besides ribosome biogenesis, including cell cycle control, stress responses and the biogenesis of other functional ribonucleoproteins (RNPs). Given that ribosome biogenesis is a metabolically demanding process, it is only logical that it is stringently regulated. Hence key components of the RNA Pol I machinery are targets for regulating rDNA transcription during the cell cycle and in response to growth factors, stress and differentiation and this will be discussed in the following section.

Each eukaryotic 80S ribosome is composed of a small 40S subunit and large 60S subunit. The small 40S subunit contains the 18S rRNA and a subset of ribosomal proteins. The large 60S subunit contains the 5.8S, 28S/25S rRNAs and the imported RNA Pol III transcribed 5S rRNA,

as well as ribosomal proteins. Biogenesis of these ribosomal subunits begins with the synthesis of the 45S and 35S pre-rRNA transcripts in mammals and yeast, respectively, by the RNA Pol I machinery. This pre-rRNA undergoes processing and modifications, directed by a number of small nucleolar ribonucleoproteins (snoRNPs) complexes, to generate the mature 18S, 5.8S and 28S or 25S, in mammals and yeast respectively.

The snoRNP complexes consist of non-coding RNA, called small nucleolar RNA (snoRNA), associated with a number of different proteins. There are two classes of snoRNAs, the box C/D snoRNAs and H/ACA snoRNAs, which direct 2'-*O*-ribose methylation and pseudouridylation, respectively (Ganot and Bortolin, 1997, Kiss-László et al., 1996, Ni et al., 1997, Tycowski et al., 1996). The box C/D snoRNAs associate with 4 core proteins, NOP58, NOP56, 15.5K and the methyltransferase fibrillarin (yeast homolog Nop1) (Watkins et al., 2000). The H/ACA snoRNAs associate with Nop10, Gar1, Nhp2 and the pseudouridylase Nap57, also known as dyskerin (Meier, 2005). Pseudouridylation and 2'-*O*-ribose methylation are extremely abundant modifications carried out by hundreds of snoRNAs. Approximately 100 modified sites are evident in the *S. cerevisiae* ribosome and up to approximately 200 modified sites in vertebrate ribosomes, further illustrating the complexity of pre-rRNA processing.(Bleichert and Baserga, 2011)

Several of the box C/D snoRNAs are essential for pre-rRNA cleavage, these include U3, U8 and U14 snoRNAs. For example U3 snoRNA is key to the biogenesis of the 40S subunit. U3 snoRNA acts as a chaperone and facilitates pre-rRNA folding and subsequent cleavage at the A0, A1 and A2 cleavage sites, which result in the release of 18S rRNA (Kass et al., 1990). U8 and U22 snoRNAs, which are only present in higher eukaryotes, are also required for pre-rRNA cleavage. U22 snoRNA is involved in 18S pre-rRNA processing (Tycowski et al., 1994), whereas U8 snoRNA is the only identified snoRNA that is essential for processing of the 60S subunit 5.8S and 28S rRNAs (Peculis and Steitz, 1993).

In yeast the U3 snoRNA is found in the 90S pre-ribosome complex, along with the 35S pre-rRNA, small subunit ribosomal proteins, t-UTPs (U three proteins) and other factors involved in the biogenesis of the 40S subunit (Dragon et al., 2002, Grandi et al., 2002). This 90S pre-ribosome complex predominately lacked 60S subunit synthesis factors and hence was termed the SSU (Small Sub-Unit) processome. On Miller spreads, which were described in the previous section 1.3, the structures termed terminal knobs at the 5' end of nascent pre-rRNA transcripts contain the SSU processome. This was confirmed by depleting SSU processome components, which resulted in the loss of the terminal knob structures (Miller and Beatty, 1969, Mougey et al., 1993, Dragon et al., 2002).

The t-UTPs function by linking transcription and pre-rRNA processing and have been demonstrated to be required for efficient rDNA transcription and pre-rRNA processing (Gallagher et al., 2004, Prieto and McStay, 2007). t-UTPs function is conserved from yeast to

human. Human orthologs for six of the seven yeast t-Utps have been identified. These include human UTP4, UTP5, UTP10, UTP15 and UTP17 (Prieto and McStay, 2007) and a recent study demonstrates that the human nucleolar protein (NOL11) is a t-UTP and most likely an ortholog of Utp8 in yeast (Freed et al., 2012). To date no ortholog has been identified for yeast Utp9. The t-UTPs were originally identified as factors co-purified with the SSU processome (Dragon et al., 2002) and shortly after this the t-UTPs were shown to function as a subcomplex of the SSU processome (Gallagher et al., 2004, Krogan et al., 2004). The t-UTP subcompex can bind to ribosomal chromatin in the absence of U3 snoRNA, suggesting that t-UTP association may be the initial step for the assembly of the rest of the SSU processome (Gallagher et al., 2004). Additionally t-UTP recruitment to rDNA is UBF-dependent and independent of transcription (Prieto and McStay, 2007). The t-UTPs reveal the highly coordinated linking of rDNA transcription to processing events, reinforcing the complexity associated with ribosome biogenesis.

The mature ribosome subunits do not contain snoRNAs, therefore after successfully performing their functions the snoRNAs and their associated proteins need to be released from the pre-rRNA transcript. RNA helicases are believed to play an important role in this process by directly unwinding the snoRNA-pre-rRNA duplex. Although no evidence for direct unwinding has been shown to date, studies supporting this theory are emerging. It has been shown that depletion of RNA helicases results in some of the snoRNAs remaining associated with pre-ribosomes (Bohnsack et al., 2008, Liang and Fournier, 2006, Srivastava et al., 2010). Other predicted models for release of snoRNAs have been suggested, such as conformational changes that the pre-rRNAs undergo during processing could weaken their association for snoRNAs. Also the binding of ribosomal proteins and/or nonhelicase processing factors could displace snoRNA from the pre-rRNA. In yeast ~100 snoRNAs are thought to act on the pre-rRNA transcript throughout biogenesis, however there are only 20 nucleolar RNA helicases. It is unlikely that these nucleolar RNA helicases alone release all the snoRNAs and it is more probable that a combination of RNA helicases and other indirect mechanisms contribute to the release of snoRNAs from pre-rRNAs (Bleichert and Baserga, 2011).

Only the initial events of pre-rRNA processing are described as the more in-depth events are beyond the scope of this thesis. Nevertheless, the resulting mature 40S and 60S ribosome subunits are exported to the cytoplasm, where they bind to messenger RNA (mRNA) to form a functional 80S ribosome.

1.5 Regulation of rDNA transcription

As mentioned above rRNA synthesis, which is the rate-limiting step of ribosome biogenesis, is a metabolically demanding process that is tightly regulated. The rate of rDNA transcription

fluctuates in response to growth factors, nutrient availability, stress and differentiation. Modulating the rate rDNA transcription is achieved by both short- and long-term regulation. Short-term regulation involves altering the rate of transcription from active rDNA repeats by regulating key components of RNA Pol I machinery such as SL1/TIF-IB and UBF and in particular Rrn3/TIF-IA. In contrast, long-term regulation requires changing the ratio of active to inactive rDNA repeats by epigenetic alteration of rDNA chromatin.

In this section I will discuss the regulation of RNA Pol I during the cell cycle, in which UBF and SL1/TIF-IB are the major targets, and also the regulation of Rrn3/TIF-IA in response to growth factor and nutrient availability. The effect of stress and cancer on the rate of rDNA transcription, as well as tissue-specific regulation of rDNA transcription will also be discussed.

1.5.1 Cell Cycle regulation of rDNA transcription

Mammalian rDNA transcription is a cell cycle regulated process. Transcription ceases during mitosis, gradually increases during G1, and reaches maximum levels during S and G2 (Klein and Grummt, 1999). Mitotic rDNA transcriptional inhibition, as well as the reactivation of transcription, is regulated primarily by posttranslational modifications of key factors of the RNA Pol I machinery. Inactivation of rDNA transcription occurs as a result of cyclin dependent kinase (cdk) 1/ cyclin B phosphorylation of the SL1/TIF-IB subunit TAF_I110 at threonine 852 (Thr852). This phosphorylation inhibits SL1/TIF-IB interacting with UBF, thereby preventing PIC formation and consequently rDNA transcription (Heix et al., 1998, Kuhn et al., 1998). UBF is also inactivated during mitosis. This is caused by mitotic-specific inhibitory phosphorylations of UBF (Klein and Grummt, 1999) and possibly due to the loss of essential phosphorylations required for UBF activity (Grummt, 2003). Upon mitotic exit and as cells progress though G1- and S-phase rDNA transcription is gradually restored to its maximum level. Reestablishing transcription requires the action of Cdc14B phosphatase, which dephosphorylates Thr852, thereby recovering SL1/TIF-IB activity and its ability to interact with UBF (Drygin et al., 2010). Reactivation also correlates with the phosphorylation of UBF by the G1 specific kinases cdk4/cyclin D and cdk2/cyclin E at serine 484 (Ser484), and later during S phase by cdk2/cyclin E and cdk2/cyclin A at Ser388 (Figure 1.7). Phosphorylation at the latter site increases the interaction between UBF and the RNA Pol I subunit PAF53 (Voit et al., 1999, Voit and Grummt, 2001). UBF/PAF53 interaction is further enhanced by PCAF-dependent acetylation of UBF (Meraner et al., 2006).

1.5.2 Growth dependent regulation of rDNA transcription

The rate of rDNA transcription fluctuates in response to mitogenic stimuli and the availability of nutrients. For instance, the MAPK (mitogen-activated protein kinase) signalling pathway has

been demonstrated to regulate RNA Pol I transcription. In response to extracellular stimuli, such as EGF (epidermal growth factor), the EGFR (EGF receptor) is activated and initiates the MAPK cascade event, which includes Raf, MEK1/2 and ERK1/2. Once activated, ERK1/2 phosphorylates and activates ribosomal S6 kinase (RSK). RSK and ERK1/2 phosphorylate Rrn3/TIF-IA at Ser649 and Ser633, respectively, which results in up-regulation of rDNA transcription and cell proliferation (Zhao et al., 2003, Wang et al., 2001).

The rate of rDNA transcription is also regulated in response to nutrient availability by the TOR (target of rapamycin) kinase pathway. The TOR proteins, which are members of the phosphatidylinositol 3-kinase (PI3K) family, have been associated with nutrient-dependent regulation of proliferation and cell growth in both humans and yeast. Nutrient starvation or rapamycin inhibition of TOR pathway results in reduced rRNA synthesis and as a result reduced ribosome production. In mammals, Rrn3/TIF-IA is the primary target for mammalian TOR (mTOR) (Mayer et al., 2004), with inhibition of the mTOR pathway triggering inactivation of Rrn3/TIF-IA. The protein phosphatase 2A (PP2A) is activated and causes dephosphorylation of Rrn3/TIF-IA at Ser44. This dephosphorylation of Ser44 correlates with increased phosphorylation at Ser199 by an unknown kinase, resulting in deactivation of Rrn3/TIF-IA. The inactive form of Rrn3/TIF-IA cannot interact with SL1/TIF-IB or RNA Pol I, thereby obstructing PIC formation, resulting in transcription inhibition (Mayer et al., 2004). Phosphorylation of Rrn3/TIF-IA at Ser44 and Ser199 results in opposite activity status, indicating that balancing these antagonising phosphorylation sites is important in regulating rDNA transcription (Mayer et al., 2004). The effect of both these signalling pathways on UBF will be discussed in section 1.9.

1.5.3 RNA Pol I transcription responds to genotoxic stress

The nucleolus has also been shown to play a role in response to cellular stresses. A well-known phenomenon due to genotoxic stress, such as UV irradiation, and inhibition of RNA Pol I transcription by actinomycin D (Act D) treatment, is nucleolar segregation. Nucleolar segregation occurs as a result of the segregation of the three sub-compartments of the nucleolus, the fibrillar centre (FC), the dense fibrillar compartment (DFC) and the granular component (GC), into three distinct but juxtaposed domains at the periphery of the nucleolus, termed nucleolar caps (Shav-Tal et al., 2005). Furthermore the nucleolar proteome changes dramatically in response to Act D treatment and DNA damage (Andersen et al., 2005, Boisvert et al., 2010).

The nucleolar stress response correlates with the activation and stabilisation of the tumour suppressor protein, p53. Cellular levels of p53 are kept low due to interactions with the E3 ubiquitin ligase, MDM2/HDM2, which directs p53 for degradation. Cellular stress causes the

redistribution of both large (L) and small (S) ribosomal proteins, such as L5, L11, L23 and S7, from the nucleolus to the nucleoplasm (Boulon et al., 2010, Zhang and Lu, 2009). Here these proteins can interact with MDM2/HDM2, preventing degradation of p53, thereby resulting in p53-dependent cell cycle arrest. p14ARF (alternate reading frame) also plays a role in triggering p53-dependent cell cycle arrest in response to cellular stress, however the mechanism by which this occurs is more complex. Convincing work has shown that p14ARF, which is predominantly a nucleolar protein, can bind to MDM2/HDM2 and sequester it to the nucleolus, thereby stabilise p53 (Weber et al., 1999). Equally compelling work has shown that nucleoplasmic p14ARF is sufficient to directly inhibit ubiquitin ligase activity of MDM2/HMD2 and stabilise p53 (Llanos et al., 2001). The accumulation of activated p53 reduces RNA Pol I transcription, with the general consensus among most researchers in the field that this is an indirect effect. However one study has suggested that this down-regulation of rDNA transcription is a direct effect. This study proposes that accumulation of p53 interferes with SLI/TIF-IB and UBF interactions *in vitro* and thus prevents PIC formation at the rDNA promoter by (Zhai and Comai, 2000).

Another mechanism, by which RNA Pol I is inhibited in response to stress, requires a series of intracellular signals through JNK2 (c-jun N-terminal protein kinase 2). JNK2, a member of the JNK family, is activated in response to multiple different cellular stresses. Activated JNK2 targets Rrn3/TIF-IA and triggers phosphorylation at a single residue, Thr200. This phosphorylation prevents Rrn3/TIF-IA interacting with SL1/TIF-IB, as well as with RNA Pol I, thereby inhibiting rDNA transcription (Mayer et al., 2005).

1.5.4 Cancer and regulation of DNA transcription

Up-regulation of rRNA synthesis is a hallmark of cancer (Ruggero and Pandolfi, 2003). Oncogenes and tumour suppressors have been shown to regulate rDNA transcription by targeting key RNA Pol I factors. The proto-oncogene, c-Myc, has been demonstrated to up-regulate rDNA transcription by up-regulating the cellular levels of UBF, while Mad1, the c-Myc antagonist, down-regulates UBF expression and rDNA transcription (Poortinga et al., 2004). The ability of c-Myc to interact directly with rDNA and the RNA Pol I specific factor, SL1/TIF-IB, further demonstrates a role for c-Myc in modulating rRNA synthesis (Grandori et al., 2005, Arabi et al., 2005). During differentiation, loss of c-Myc is required for down-regulation of rDNA transcription. This down-regulation of rDNA transcription is orchestrated by down-regulating expression of UBF, Rrn3/TIF-IA and the RNA Pol I subunits, which have been demonstrated to be direct targets of c-Myc (Poortinga et al., 2004, Poortinga et al., 2011). In contrast, the hyper-activation of rDNA transcription evident in c-Myc driven cancers is most

likely caused by the up-regulation of the c-Myc target genes, UBF, Rrn3/TIF-IA and RNA Pol I.

Tumour suppressors limit the growth of tumours. This growth inhibition coincides with tumour suppressor's ability to repress RNA Pol I transcription. The tumour suppressor pRb (retinoblastoma protein) and related pocket proteins, p107 and p130, can restrict cell growth and proliferation. pRb accumulates in nucleoli as a result of cell confluence, cell cycle arrest or differentiation and induces repression of rRNA synthesis (Cavanaugh et al., 1995, Hannan et al., 2000b). This down-regulation in rDNA transcription appears to involve pRb-UBF interactions, however the precise mechanism is unclear. One study demonstrates that the interaction between pRb and UBF results in the dissociation of UBF from rDNA (Voit et al., 1997). The other study shows that pRb/UBF interactions inhibit UBF's ability to interact with SL1/TIF-IB, thereby preventing PIC formation (Hannan et al., 2000a). The latter study also demonstrated that the pRb related pocket protein p130, but not p107, can bind to UBF and repress RNA Pol I transcription (Hannan et al., 2000a).

1.5.5 Tissue-specific regulation of rDNA transcription

In a multicellular organism, cells differ in their need for rRNAs and therefore the rate of rRNA synthesis varies upon cell types. An example of this cell-type-specific regulation is observed in developing mouse oocytes, whereby the rate of RNA Pol I transcription doubles without increasing the number of rRNA genes. To increase rDNA transcription these cells use basonuclin, a transcription regulator expressed primarily in keratinocytes and gametogenic cells of testis and ovary. Basonuclin not only affects RNA Pol I transcription but has also been shown to localise to the nucleolus, as well as remaining bound to rDNA throughout the cell cycle (Tian et al., 2001, Zhang et al., 2007, Tseng et al., 1999).

Another example of a cell-type-specific regulator of rDNA transcription is the Runt-related transcription factor, Runx2. Runx2 is implicated in establishing and maintaining cell identity and a key factor in osteoblast differentiation. Runx2 regulates rRNA synthesis by repressing RNA Pol I transcription (Young et al., 2007). Similar to basonuclin, Ruxn2 localises to the nucleolus and remains bound to mitotic NORs. These examples indicate that at least a subset of rDNA repeats are regulated by tissue-specific factors according to the cell's requirements.

1.6 The Nucleolus

In the previous sections I have discussed the biochemistry of ribosome biogenesis and stressed how it is a costly, coordinated process that is tightly regulated. I will now concentrate on the ultrastructure of the nucleolus and how the different compartments facilitate the various steps in ribosome biogenesis. The nucleolus is the most prominent sub-nuclear compartment. Typically

nucleoli stain poorly with DAPI and are surrounded by an intensely stained heterochromatic shell. At the ultrastructural level nucleoli are composed of three sub-compartments. These compartments are revealed by electron microscopy and termed the fibrillar centre (FC), the dense fibrillar compartment (DFC) and the granular component (GC) (Figure 1.8). The FCs are visualised as clear regions that are surrounded by the DFC, which appears as a highly contrasted region due to tightly packed fibrils. The GC consists of small granules of 15-20nm in diameter, which forms a meshwork thereby embedding the FC and DFC (Sirri et al., 2008). The FCs are characterised by the enrichment of rDNA, RNA Pol I subunits and UBF (Goessens, 1984, Scheer and Rose, 1984, Jordan, 1991). FCs are believed to be the interphasic counterparts of mitotic NORs due to the fact that UBF is present at both interphasic FCs and mitotic NORs. There has been a lot of debate as to the intra-nucleolar localisation of ribosomal genes. The general consensus now is that rDNA transcription occurs at the DFC and the FC/DFC interface, which was exemplified by mapping the incorporation of modified nucleotides, such as bromouridine (BrU) or the drug 5-flurouridine (5-FU), into nascent rRNA transcripts (Casafont et al., 2006, Koberna et al., 2002, Raška et al., 1995). Processing of the nascent rRNA transcripts occurs largely in the DFC where snoRNPs and processing proteins such as fibrillarin and nucleolin are found to accumulate (Azum-Gelade et al., 1994, Dragon et al., 2002, Grandi et al., 2002, Puvion-Dutilleul et al., 1997). In the GC mature rRNA and ribosomal protein assembly is completed before export of the subunits into the cytoplasm via the nuclear pores. Some of the proteins associated with the GC compartment include nucleophosmin/B23, Nop52 and nucleostemin (Orrick et al., 1973, Savino et al., 1999, Tsai and McKay, 2002).

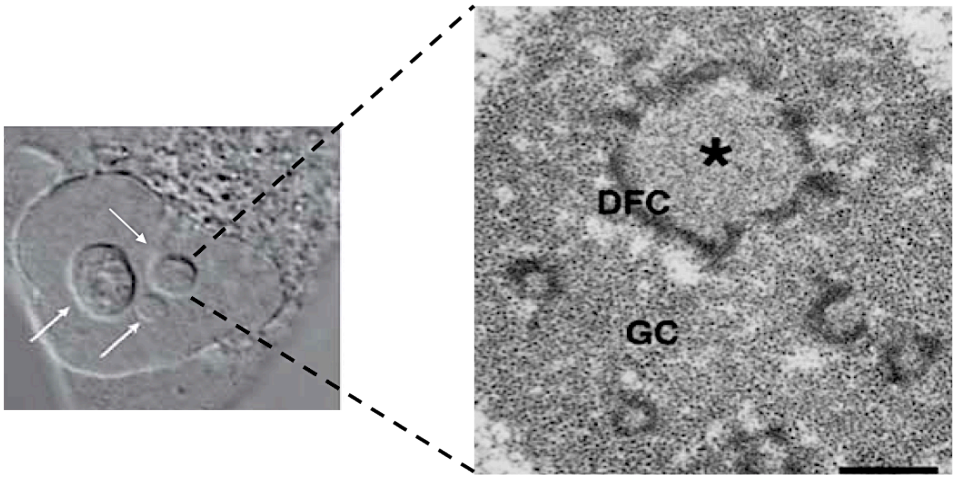

Figure 1.8 Sub-compartments of the Nucleolus
(A). Differential interference contrast (DIC) image of a HeLa cell. White arrows indicate the three prominent nucleoli. Figure adapted from (Boisvert et al., 2007)
(B). Transmission EM revealing the three sub-compartments of HeLa nucleoli. Asterisk indicates the FC that is surrounded by the DFC and embedded in the GC. Figure from (Sirri et al., 2008).

Nucleolar assembly and disassembly is regulated by the cell cycle in higher eukaryotes. At the onset of mitosis rDNA transcription is inhibited. In late prophase the nuclear envelope breaks

down, chromatin condenses into chromosomes and the nucleolus is no longer visible (Figure 1.9). Disassembly of the nucleolus correlates with the redistribution of many of the nucleolar proteins to the surface of the chromosome, forming a perichromosomal layer during mitosis (Gautier et al., 1992). Interestingly UBF, SL1/TIF-IB, TTF-I and Treacle remain bound to rDNA repeats during mitosis. The maintenance of some of the key components of RNA Pol I machinery enables the rapid resumption of rDNA transcription upon mitotic exit. There is some debate as to the fraction of RNA Pol I subunits that remain bound to mitotic NORs (Scheer and Rose, 1984, Valdez et al., 2004, Jordan et al., 1996, Roussel et al., 1993, Roussel et al., 1996, Leung et al., 2004). In the McStay lab the routine immunostaining of human cells using a number of RNA Pol I subunit antibodies reveals that mitotic NORs are devoid of any RNA Pol I subunits (unpublished work from McStay lab).

Reassembly of nucleoli occurs in early telophase. It requires the coordination between reactivation of rDNA transcription and the recruitment of pre-nucleolar bodies (PNBs). Partially processed rRNA transcripts along with their associated processing factors are assembled into PNBs in telophase, which then interact with the rDNA to translocate the components to the NORs (Savino et al., 2001, Hernandez-Verdun et al., 2002, Jimenez-Garcia et al., 1994, Dundr et al., 2000). The resumption of rDNA transcription occurs simultaneously from each NOR associated with components of RNA Pol I machinery. This results in the formation of a small nucleolus around each individual NOR. These small nucleoli coalesce to form large nucleoli incorporating multiple NORs (Savino et al., 2001). The nucleolar cycle for higher eukaryotes is depicted in (Figure 1.9). In yeast rDNA transcriptional inhibition is initiated during anaphase by Cdc14 phosphatase, and interestingly the nucleolus remains intact throughout mitosis in these lower eukaryotes (Clemente-Blanco et al., 2009).

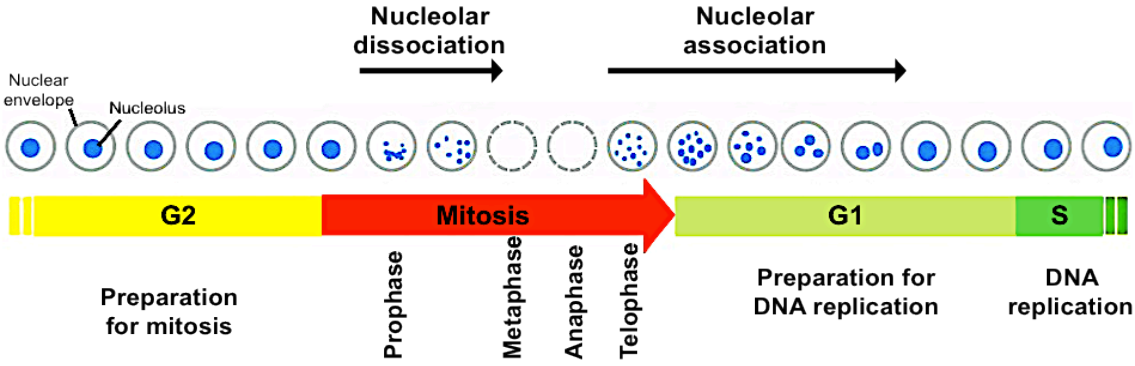

Figure 1.9 The nucleolar cell cycle for higher eukaryotes
At the onset of mitosis rDNA transcription ceases. The nuclear envelope is disrupted and the nucleolus is no longer visible at late prophase. In telophase rDNA transcription is reactivated from each NOR associated with RNA Pol I machinery. This results in the presence of multiple small nucleoli that form around each transcriptionally competent NOR. The reassembly of the nuclear envelope also begins in telophase. In G1 the individual small nucleoli coalesce to form a single large nucleolus or 2-3 nucleoli, the number of nucleoli is dependent on the cell line. This figure was adapted from Molecular Biology of the Cell 5th Edition.

Over the past decade much work has been done to establish the nucleolar proteome. To date approximately 5000 proteins have been identified to associate with the human nucleolus (Andersen et al., 2005, Andersen et al., 2002, Scherl et al., 2002, Ahmad et al., 2009, Lam et al., 2010, Boisvert et al., 2010), revealing additional functions for the nucleolus aside from its primary function in ribosome biogenesis. These functions include cellular processes such as stress responses and cell cycle regulation, which were discussed in the previous section. Furthermore the nucleolus has been linked with processing and maturation of RNAs other than rRNA. For examples transfer RNA (tRNA), RNase P RNA and the U6 spliceosomal small nuclear (sn)RNA are all transcribed in the nucleus by RNA Pol III, transported to the nucleolus where they undergo processing and maturation. This is similar to the 5S rRNA, which is also transcribed by RNA Pol III in the nucleus and processed in the nucleolus, suggesting that the maturation of Pol III transcripts occurs at a common location, the nucleolus (Boisvert et al., 2007). Interestingly when compared to the nucleolar proteome of yeast, 90% of the proteins identified in yeast have human homologs indicating that the nucleolar proteome is highly conserved through evolution (Andersen et al., 2005). Proteome studies have also revealed that viral infections can alter the nucleolar proteome. A number of viruses have been shown to target the nucleolus and interrupt the host cells functioning by recruiting cellular proteins to enhance viral replication (Hiscox, 2007, Lam et al., 2010).

These recent advances in nucleolar proteome analysis reveal just how complex and dynamic this organelle is, as well as shedding light on additional functions of the nucleolus.

1.7 Ribosomal gene chromatin

Eukaryotic DNA is packaged with proteins to form chromatin. The basic repeating unit of chromatin is the nucleosome, which consists of ~145-147bp of DNA wrapped around a histone octomer made up of two of each of the histones H2A, H2B, H3 and H4 (Luger et al., 1997). The linker histone H1 binds to the linker DNA, resulting in two complete turns around the octomer and stabilising a higher chromatin structure such as the 30-nanometer fibres. These 30nm fibres undergo sequential chromatin condensation steps, with each step resulting in a more compact state with the final chromatin structure visualised as metaphase chromosomes (Luger et al., 2012). In cells two different states of chromatin structure are evident, silent heterochromatin and active euchromatin. These two different chromatin states can be distinguished by different histone post-translational modifications and differences in rDNA methylation status. Ribosomal genes can exist in either one of these chromatin states depending on their activity status. Inactive NORs adopt a closed heterochromatin state, in contrast active NORs adopt an open euchromatin state enabling RNA Pol I and other key component of the transcription machinery to associate with the rDNA promoter and thereby facilitate rDNA transcription.

1.7.1 DNA methylation, histone modifications and mechanisms for silencing ribosomal genes

In mammalian cells indirect methods have been employed to distinguish active from silent rDNA repeats. These methods include determining the DNA methylation status of rDNA sequences and identifying specific histone modifications associated with rDNA chromatin. Chromatin immunoprecipitation (ChIP) combined with digesting DNA with methylation-sensitive restriction enzymes revealed that active rDNA genes are associated with hypomethylated DNA, acetylated histones H4 and H3, together with histone H3 trimethylated at lysine residue 4 (H3K4me3). In contrast, silent rDNA repeats have hypermethylated DNA and are associated with methylated H3K9, H3K20 and H3K27 (Bird et al., 1981, Lawrence et al., 2004, Earley et al., 2006, Santoro et al., 2002, Zhou et al., 2002). The current view is that histone modifications can recruit effector proteins, for example the heterochromatic protein 1 (HP1), which facilitates condensation of the chromatin and silencing of the ribosomal gene. However there is not always a strict division between active and silent histone modifications. For example, H3K9me3 modifications occur at the transcribed regions of all mammalian RNA Pol II genes (McStay and Grummt, 2008, Pikaard and Lawrence, 2002, Santoro and Grummt, 2005).

A mechanism that directs silencing of ribosomal genes has been proposed for the mouse model. This model suggests that TTF-1 binding to the promoter proximal terminator site (T_0) results in the recruitment of the ATP-dependent nucleolar remodelling complex (NoRC). NoRC is composed of two subunits, ATPase SNF2h and TIP5 (TTF-1 interacting protein 5), and has also been identified in humans (Strohner et al., 2001). NoRC in turn recruits the DNA methyltransferases Dnmt1 and Dnmt3b as well as histone deacetylases (HDAC1), which results in de novo DNA methylation and histone deacetylation. The resulting DNA methylation of a single CpG dinucleotide positioned upstream of the transcriptional start site, at -133, has been demonstrated to be sufficient to interfere with UBF binding to the promoter thereby preventing rDNA transcription. Demonstrating this model in human has proved difficult as the human rDNA is much more complex containing 25 CpGs. Studies have been able to reveal that the human rDNA promoter is neither fully methylated nor unmethylated, however human cancer cell lines do exhibit hypomethylation at the promoter when compared to normal cells (Ghoshal et al., 2004, Majumder et al., 2006).

Although it has been well documented in the literature that silent rDNA is associated with hypermethylation, recent studies are starting to debate this theory. In eukaryotic cells approximately half of the rDNA genes are transcriptionally silent, yet the Svoboda lab have shown in a recent study that with the exception of transformed cell lines, DNA hypermethylation is rarely observed in primary tissues or cells (Sinkkonen et al., 2010). This study, in parallel with other studies suggest that rDNA methylation accumulates in established

transformed cell lines, such as HeLa, human embryonic kidney (HEK) 293 or mouse NIH 3T3 (Németh et al., 2008, Brown and Szyf, 2007, Sinkkonen et al., 2010), in aged cells (Oakes et al., 2003) and non-dividing neuronal cells (McGowan et al., 2008). This suggests that methylation of rDNA may confer stability rather than be involved in establishing the silent state.

1.7.2 Active and inactive NORs

Actively transcribed ribosomal genes adopt an open chromatin state. During mitosis rDNA transcription is shut down, the nucleolus disassembles and the chromatin becomes fully condensed appearing as chromosomes. One defining characteristic of active NORs in all eukaryotes is their appearance as secondary constrictions on metaphase chromosomes, the primary constriction being the centromere. Appearance of active NORs as secondary constrictions is due to the chromatin at this region being approximately ten-fold less condensed than the adjacent α-satellite DNA (Heliot et al., 1997). This decondensed chromatin state gives rise to reduced DAPI binding resulting in an apparent gap in the chromosome (Figure 1.10 (A)). Often, an axis of condensed DNA, thought to be AT-rich, is found within the secondary constriction (Saitoh and Laemmli, 1994).

In organisms containing multiple NORs, the secondary constrictions associated with active NORs are usually small and difficult to visualise. Therefore, a more reliable and common technique for identifying and counting the number of active NORs is staining metaphase chromosomes with silver nitrate (Bloom and Goodpasture, 1976) (Figure 1.10 (B)). The success of silver staining is driven by the fact that a number of the components of the RNA Pol I machinery, which have an acidic/argyophilic domain, remain bound to active NORs during mitosis. These proteins include UBF, SL1/TIF-IB, TTF-I and Treacle (Scheer and Rose, 1984, Roussel et al., 1993, Roussel et al., 1996, Jordan et al., 1996, Valdez et al., 2004). For certain human cell lines the number of active NORs has been established by silver staining. In human lymphocytes on average 8 out of the 10 NORs are active (Heliot et al., 2000) and in the cancer cell line HeLa, 7 of the 10 NORs are active (Roussel et al., 1993).

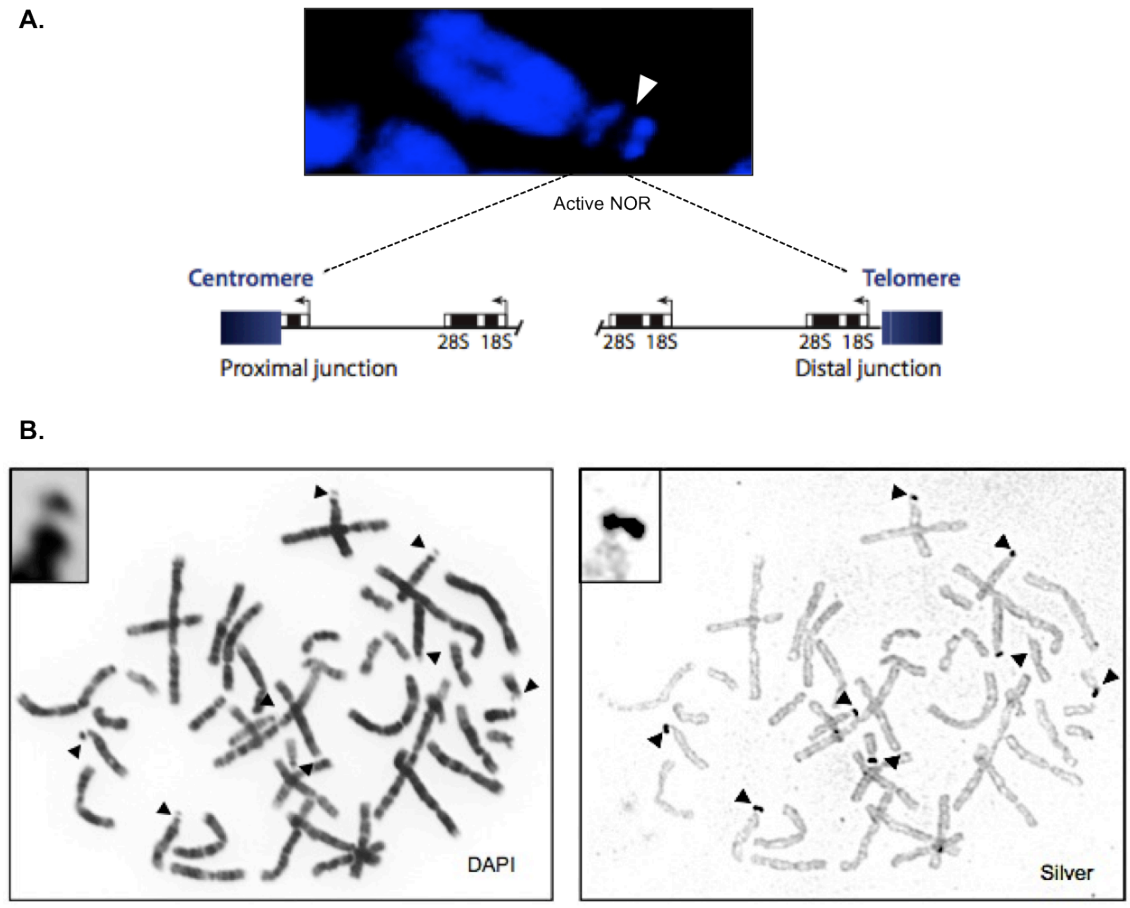

Figure 1.10 Characteristics of active NORs
(A) The secondary constriction (indicated by the white arrowhead) is visualised on a DAPI stained metaphase chromosome as a gap in the chromosome. The organisation and orientation of rDNA within the NOR is illustrated below. Figure adapted from (McStay and Grummt, 2008).
(B) Active NORs (arrowheads) are revealed by the presence of secondary constriction by DAPI staining (left) and these secondary constrictions are also positive for silver staining (right). These metaphase chromosomes were prepared from human blood lymphocytes. Figure from (Grob et al., 2011).

In contrast to active NORs, the rDNA chromatin of silent NORs is heterochromatic. Hence silent NORs do not form secondary constrictions, are not positive for silver staining and lack association of any of the RNA Pol I machinery. In human cells silent NORs appear as condensed foci during interphase, which are dissociated from nucleoli and are not bound by nucleolar proteins such as UBF (McStay and Grummt, 2008). Interestingly, studies performed in mouse>human somatic cell hybrids show that silent human NORs associate with mouse nucleoli (Sullivan et al., 2001). The human NOR is transcriptionally inactive due to the species specificity of ribosomal gene transcription (see section 1.3). It should be pointed out that all mouse chromosomes are acrocentric, with their short arms aggregating in so-called chromocentres. Thus the organisation of silent NORs in mouse cells may be expected to be somewhat different to that observed in human cells.

1.7.3 The proportion of active rDNA repeats

Although silver staining is a powerful technique to establish if a NOR is transcriptionally silent or active, it cannot resolve the proportion of rDNA repeats that are active. Instead the proportion of rDNA repeats that are transcriptionally active can be determined by biochemical studies using a DNA cross-linking reagent, psoralen. Active rRNA genes are free of regularly spaced nucleosomes and obtain a euchromatic state that is accessible to psoralen. In contrast inactive rRNA genes adopt a heterochromatic state that is inaccessible to psoralen (Conconi et al., 1989, Dammann et al., 1993). After psoralen cross-linking, active and inactive rRNA genes can be distinguished on an agarose gel due the cross-linked DNA, that is the open active rRNA genes migrate slower than the non-cross-linked DNA. Based on numerous studies it is now generally agreed that only approximately half of the rDNA repeats are transcriptionally active at any one given time for most cell types (Conconi et al., 1989, Grummt and Pikaard, 2003, McStay and Grummt, 2008).

Yeast have a single NOR and similar to higher eukaryotes approximately half the rDNA repeats are inactive at any one given time. This indicates that active and inactive rDNA repeats can be intermingled among a single NOR (Carmo-Fonseca et al., 2000). In higher eukaryotes, the 50% of silent rDNA repeats, determined by biochemical assays, is at odds with the number of silent NORs observed at the chromosomal level. This suggests that similar to yeast, human NORs are a mosaic of active and silent rDNA repeats. Another layer of complexity is added by the fact that up to one-third of human rDNA repeats demonstrate noncanonical arrangement (Caburet et al., 2005), which could account for a significant fraction of silent rDNA repeats (Figure 1.11).

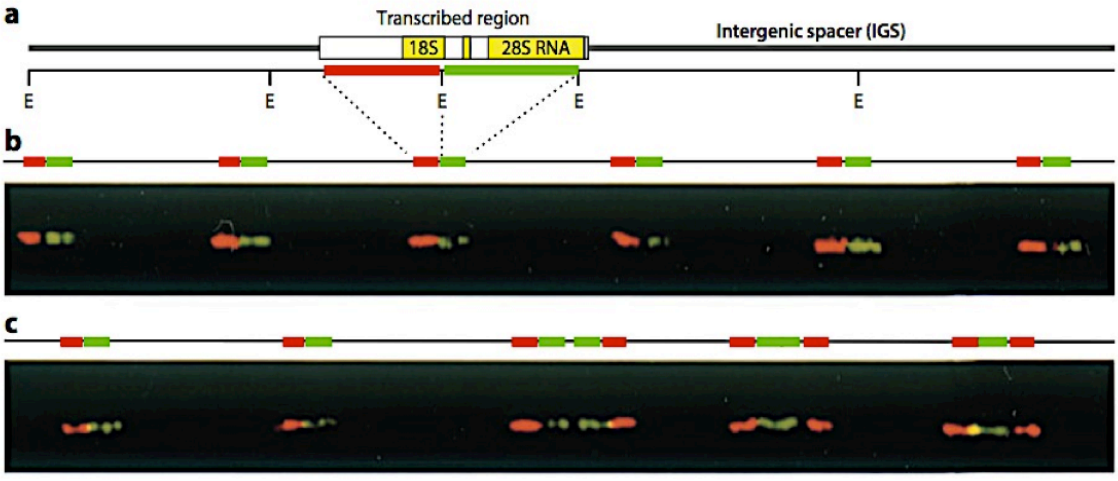

Figure 1.11 Molecular combing of the human rDNA locus.
(A) Schematic of the position of the two molecular probes used to detect the rDNA transcription units. The red probe and the green probe hybridises to the 5' part and 3' part of the pre-rRNA coding, respectively. (B) Canonical rDNA repeats in tandem, each repeat is composed of a dual fluorescent signal and the adjacent IGS. (C) This image shows two canonical rDNA repeats followed by three non-canonical rDNA repeats. Figure from (McStay and Grummt, 2008) which was originally adapted from (Caburet et al., 2005).

1.8 UBF binding and architectural role

UBF consists of a N-terminal dimerisation domain, multiple HMG boxes and a C-terminal acidic tail (Jantzen et al., 1990, McStay et al., 1991, Jantzen et al., 1992). Mammalian UBF exists as two splice variants, UBF1 and UBF2. As a consequence of alternative splicing UBF2 is missing 37 amino acids from the second HMG box (O'Mahony and Rothblum, 1991) (Figure 1.5)). In solution UBF has been shown to form dimers through its N-terminal dimerisation domain (McStay et al., 1991). A dimer of UBF binds to rDNA via its HMG boxes. As mentioned previously, these HMG boxes are so called due to their similarity in sequence and structure to the DNA binding domain present in the non-histone chromosomal architectural HMGB proteins (Jantzen et al., 1990).

HMG box proteins can be classified into two subclasses based on their DNA binding differences. The first subclass is highly diverse and is made up of HMG proteins containing a single HMG box with no C-terminal acidic tail. This subclass of HMG proteins confers sequence specificity for AT-rich DNA, examples include the mammalian testis-determining factor SRY (Sinclair et al., 1990) and the T cell factor TCF1 (van de Wetering et al., 1991). The second subclass of HMG box proteins lacks any sequence specificity for binding and contains two or more HMG boxes and a C-terminal acidic tail. Examples of proteins in this second subclass include the HMGB proteins, HMGB1 and HMGB2, which bind DNA with no sequence specificity, but instead recognise DNA structural features (Travers, 2003). UBF falls into the latter subclass of HMG box proteins. Of the multiple HMG boxes present in UBF the first HMG box is sufficient for rDNA binding, with the remaining HMG boxes enhancing this UBF-rDNA interaction (Jantzen et al., 1992, Jantzen et al., 1990, McStay et al., 1991). *In vitro* experiments have failed to identify any DNA binding specificity for UBF other than a preference for GC-rich DNA (Copenhaver et al., 1994). UBF's lack of sequence specificity is in conflict with UBFs specificity for binding rDNA throughout the cell cycle (Roussel et al., 1993).

Similar to the HMG boxes in HMGB proteins, the first HMG box in UBF has been shown *in vitro* to adopt a twisted L-shape consisting of three α-helices (Xu et al., 2002), which can introduce bends into DNA. Electron spectroscopic imaging has revealed that a dimer of *Xenopus* UBF is able to bend 180bp of nucleosomal free rDNA promoter into a 360° loop *in vitro* (Putnam et al., 1994, Bazett-Jones et al., 1994). This results in a structure that resembles the core nucleosome and therefore has been termed the "enhancesome" (Stefanovsky et al., 2001a). It is probable that UBF binds to a nucleosomal template and I will discuss this below in the latter part of the section.

UBF is an extremely abundant protein with up to 10^6 molecules of UBF in *Xenopus* and human cells (Sullivan et al., 2001, McStay et al., 1997). The abundance of UBF and its concentration within nucleoli is at odds with the notion that UBF binding is restricted to the rDNA promoter.

Nucleolar ChIP assays have revealed that UBF binds across the entire rDNA repeat including both the transcribed region and the intergenic spacer (IGS) in *Xenopus*, human and mouse cells (O'Sullivan et al., 2002). The specificity of UBF binding to rDNA is reemphasised by the lack of any UBF binding to satellite DNA adjacent to the rDNA (O'Sullivan et al., 2002).

The *in vivo* localisation of UBF and the fact it remains bound to rDNA throughout the cell cycle, including the secondary constrictions associated with mitotic NORs, support an architectural role for UBF (Roussel et al., 1996, Roussel et al., 1993). Further evidence suggesting an architectural role for UBF is supported by UBFs ability to compete with linker histone H1 *in vitro* (Kermekchiev et al., 1997). Linker histone H1 is required for establishing and maintaining compact higher-order chromatin structures. Binding of UBF and histone H1 is mutually exclusive, with the two proteins implicating opposite effects on chromatin. UBF can displace histone H1 *in vitro*, resulting in chromatin decompacting (Kermekchiev et al., 1997).

The generation of pseudo-NORs has provided the most compelling evidence to date that UBF has an architectural function. Pseudo-NORs were generated by integrating megabase arrays of *Xenopus* enhancer (XEn) elements into a non-acrocentric chromosome (Mais et al., 2005). These integrated XEn elements are blocks of 60 or 81bp repeats located in the IGS of *Xenopus* rDNA repeat whose transcriptional enhancer function is solely dependent on UBF binding (McStay et al., 1997, Pikaard et al., 1989). As mentioned before a feature of RNA Pol I machinery and rDNA itself is their rapid evolutionary divergence such that human RNA Pol I machinery cannot functionally support rDNA transcription in mouse and vice versa. Regardless of this human UBF displays high affinity for these XEn elements, despite the lack of sequence similarity to the human rDNA repeat and this binding has been shown *in vitro* to support enhancer function (Bell et al., 1989, McStay et al., 1997). These XEn arrays ranged in size from 0.1Mb to 2.Mb, which is comparable in size to endogenous NORs. Recruitment of human UBF to the XEn arrays is observed throughout the entire cell cycle and results in the formation of novel bodies outside the nucleolus (Figure 1.12 (A)) (Mais et al., 2005). The most striking feature of extensive UBF binding at these ectopic arrays was the formation of a novel secondary constriction on metaphase chromosomes that mimics endogenous NORs, that is lacks DAPI staining and is positive for silver staining (Figure 1.12 (B)). Unlike endogenous NORs, the pseudo-NORs are transcriptionally inactive due to the lack of any functional promoter in the XEn arrays, yet are still capable of recruiting the RNA Pol I machinery (Mais et al., 2005). UBF depletion by siRNA in the pseudo-NOR cell line results in loss of the RNA Pol I machinery and t-UTPs recruitment, as well as loss of silver staining from the novel nuclear bodies, indicating that recruitment of these factors is UBF-dependent (Prieto and McStay, 2007). The pseudo-NORs provide evidence that UBF plays a role in defining the open chromatin state associated with active NORs.

UBF has been demonstrated *in vivo* to bind across the entire rDNA repeat in human, mouse and *Xenopus* revealing that UBF binding is not restricted to regulatory elements such as promoters or enhancers (Mais et al., 2005). How does UBF, a protein that lacks any sequence specificity for binding, spread from rDNA promoters and enhancers and bind across the entire rDNA with high specificity. This raises the long debated question as to whether or not UBF can bind to a nucleosomal DNA template. *In vitro* UBF has can bind to DNA packaged as a nucleosome and displace linker histone H1 (Kermekchiev et al., 1997). Additionally, DNA that is assembled into chromatin can be transcribed in a UBF-dependent manner *in vitro* (Langst et al., 1997). The most recent evidence suggesting that UBF can interact with nucleosome comes from a SILAC based proteomic study (Bartke et al., 2010). Pseudo-NORs not only provide evidence that UBF has an architectural function, but also provide evidence for UBF binding to a nucleosomal template *in vivo*. Micrococcal nuclease digestion of nuclei prepared from the pseudo-NOR cell line reveals that the XEn DNA arrays are packaged as nucleosomes. The fact that these arrays are extensively loaded with UBF allows one to conclude that UBF is capable of binding to nucleosomes (Wright et al., 2006).

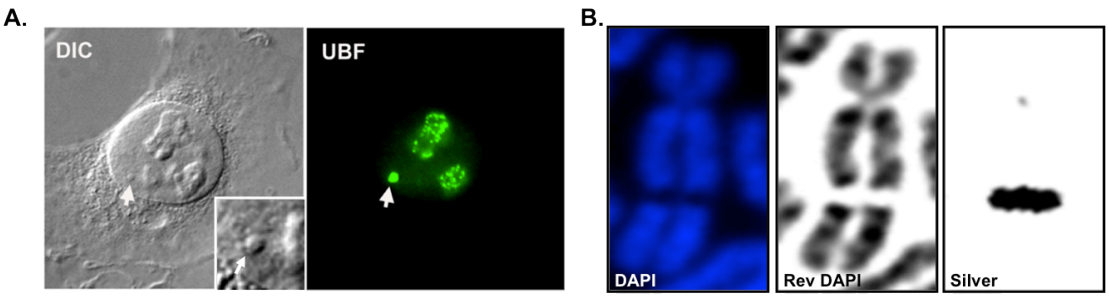

Figure 1.12 Extensive UBF binding can generate novel nuclear bodies and novel secondary constrictions
(A). DIC image and immunofluorescence staining, using anti-UBF antibodies, show the pseudo-NOR as a novel nuclear body (see inset) associated with UBF (white arrows indicates the pseudo-NOR). Figure from (Prieto and McStay, 2008)
(B). Pseudo-NORs mimic endogenous NORs by inducing a secondary constriction, visualised by DAPI (far left and middle box), as well as being positive for silver staining far right box.

1.9 UBF and regulation of ribosome biogenesis

As mentioned in section 1.5 the rate of rDNA transcription fluctuates throughout the cell cycle and in response to growth factors, stress and when cells undergo differentiation. Fluctuation in the rate of rDNA transcription occurs by regulating key components of the RNA Pol I machinery and can be categorised into long- or short-term regulation. Long-term regulation is achieved by regulating the number of active rDNA repeats and the major targets for this type of regulation are NoRC and TTF-1. Short-term regulation is achieved by controlling the rate of rDNA transcription from the active rDNA repeats. As described in section 1.5, Rrn3/TIF-IA is a key target for this short-term regulation. In this section I will focus on UBF and how it is

subjected to posttranslational modifications for short-term regulation of transcription, as well as altering absolute UBF levels for long-term regulation.

UBF is modulated during the cell cycle by G1 cdk4-cyclinD and cdk2-cyclinE dependent phosphorylations resulting in rDNA transcription (Voit et al., 1999). Acetylation is an additional cell cycle dependent modification of UBF. Acetylation of UBF peaks during G1/S-phase, which results in the association of UBF with the RNA Pol I subunit PAF53 (Meraner et al., 2006). The availability of nutrients and growth factors has a direct role on the rate of rDNA transcription. EGF activation of the MAPK signalling pathway results in ERK1/2 dependent phosphorylation of UBF at Thr117 and Thr201 situated in the first and second HMG boxes (Figure 1.7) (Stefanovsky et al., 2001b). Phosphorylation of UBF at these sites results in up-regulation of rDNA transcription by enhancing RNA Pol I elongation (Stefanovsky et al., 2001b), as well as altering the first and second HMG boxes affinity for linear DNA, which again facilitates elongation (Stefanovsky et al., 2006a, Stefanovsky et al., 2006b). Furthermore the mTOR pathway regulates transcription by S6-kinase dependent phosphorylation at the C-terminal tail of UBF (Figure 1.7), which enhances rDNA transcription by promoting the interacting between SL1/TIF-IB and UBF (Hannan et al., 2003b). In addition, the insulin growth factor 1 (IGF1) causes the insulin receptor substrate-1 (IRS-1) to bind to phosphoinositide 3-kinase (PI3K), which directly phosphorylates UBF, resulting in up-regulation of rDNA transcription (Drakas et al., 2004).

The absolute levels of UBF are altered in response to long-term cellular demands such as differentiation and cancer. Up-regulation of rDNA transcription has been linked to hypertrophic growth in neonatal and adult cardiomyocytes, which correlates with increased expression of UBF (Brandenburger et al., 2003). The contrary is observed in cells under-going differentiation. In these cells the rate of rDNA transcription is down regulated and this correlates with a significant decrease in cellular UBF levels. This reduction in UBF expression had been observed in a number of differentiation models, including differentiation of L6 myoblasts to myotubes (Larson et al., 1993), F9 embryonal carcinoma cells to primitive endoderm cells (Datta et al., 1997, Alzuherri and White, 1999), 3T3-L1 preadipocyte cells to adipocytes (Li et al., 2006b) and during murine granulocytic differentiation (Poortinga et al., 2004, Poortinga et al., 2011, Sanij et al., 2008, Liu et al., 2007).

1.10 UBF provides a platform for the recruitment of other factors

The RNA Pol I machinery is in excess. Live cell imaging experiments have shown that only a minor fraction, 7-10%, of RNA Pol I molecules are engaged in rDNA transcription (Dundr et al., 2002). In higher eukaryotes an estimated 30,000 to 40,000 RNA Pol I molecules are engaged at any one time, that is 100-130 RNA Pol I molecules per active repeat and ~300 active

repeats (Puvion-Dutilleul, 1983, Miller Jr and Bakken, 1972). By quantitating western blots in the McStay lab, HeLa cells were found to contain ~ 1 million molecules of the RNA Pol I subunit, RPA194, and a >100 fold excess of SL1/TIF-IB when compared to the number of active rDNA promoters (Wright and McStay, unpublished data). The vast excess of unengaged RNA Pol I molecules and SL1/TIF-IB still colocalise to nucleoli. However, this excess of RNA Pol I machinery in the nucleoli is at odds with recruitment based solely on PIC formation at the rDNA promoter. So the question arises as to how these proteins are recruited to active NORs. Nucleolar ChIP has revealed that RNA Pol I and SL1/TIF-IB are associated with both the transcribed region and non-transcribed IGS of rDNA repeats (Mais et al., 2005). This combined with the fact that UBF binds across the entire rDNA repeat, suggests that recruitment of excess RNA Pol I machinery to the IGS is dependent on protein-protein interactions with UBF. The pseudo-NORs have provided persuasive evidence for this theory.

During interphase, pseudo-NORs form novel nuclear bodies that are not only associated with UBF, but virtually all components of the RNA Pol I machinery (Mais et al., 2005). These include RNA Pol I subunits analysed to date (PAF53, RPA43, RPA195, RPA135), the SL1/TIF-IB subunits (TBP, TAF_1110) as well as Rrn3/TIF-IA (Mais et al., 2005). Pseudo-NORs are transcriptionally inactive due to the lack of promoter sequence, however the recruitment of Rrn3/TIF-IA to pseudo-NORs suggests that the RNA Pol I subunits sequestered are transcriptional competent. Additionally factors involved in processing and maturation of pre-rRNA transcripts also associate with pseudo-NORs (Prieto and McStay, 2007). These factors include the t-UTPs, which function by linking transcription and pre-rRNA processing and the nucleolar phosphoproteins Nopp140 and Treacle. Nopp140 associates with box H/ACA snoRNPs (Meier and Blobel, 1994) and the RNA Pol I subunit RPA194 (Chen et al., 1999), whereas Treacle interacts with box C/D snoRNPs (Hayano et al., 2003). UBF has also been demonstrated to directly interact with proteins involved in rDNA transcription and pre-rRNA processing (see table 1.2).

The pseudo-NOR model provides evidence that UBF binding to the IGS of endogenous NORs can create a platform that recruits most of the RNA Pol I machinery, as well as key factors involved in ribosomes biogenesis. The recruitment of all these factors, in a UBF-dependent manner, ensures the rapid onset of rDNA transcription and nucleolar reformation upon mitotic exit.

UBF Interactor	Function	Experimental evidence	Reference
PAF53	Pol I subunit	*In vitro* interaction and co-immunoprecipitation	(Hanada et al., 1996); (Meraner et al., 2006)
PAF49	Pol I subunit	*In vitro* interaction	(Panov et al., 2006b)
TAF_I48	SL1 subunit	*In vitro* interaction	(Beckmann et al., 1995)
TBP	SL1 subunit	*In vitro* interaction	(Kwon and Green, 1994)
Treacle	Interacts with box C/D snoRNPs	Yeast 2 hybrid and co-immunoprecipitation	(Valdez et al., 2004)

Table 1.2 Proteins involved in Ribosome Biogenesis that directly interact with UBF
Table adapted from (Grob et al., 2011).

1.11 Thesis Aims

Work in this thesis is aimed at testing our hypothesis that UBF is fundamental to organising the decondensed rDNA chromatin of active NORs, thereby retaining key factors to facilitate the rapid reactivation of rDNA transcription upon mitotic exit. I set out specific questions to test our hypothesis, these included:

1. Is UBF the fundamental factor required to maintain the open chromatin state associated with active NORs? I analysed the effect on the rDNA chromatin state, at interphase and metaphase, as a consequence of UBF depletion in a number of cell models.
2. UBF was thought to be restricted to vertebrates, yet secondary constrictions are a common feature of all eukaryotes. Therefore is UBF evolutionarily conserved and more prevalent than previously thought? Making use of the availability of both genomic DNA and complementary DNA (cDNA) sequence I performed multiple tBLASTn searches to identify the presence of open reading frames (orfs) similar to UBF.
3. UBF, a protein that has little sequence specificity in DNA binding, yet targets rDNA chromatin with high specificity. I sought to determine if UBF contains a so far unrecognised chromatin interaction motif that could be responsible for this specificity.

2 Material and methods

2.1 DNA Manipulation

The majority of the work and results presented in this thesis involves shuttling the UBF open reading frame between vectors and manipulating certain regions of UBF. Virtually all the UBF cloning done for my thesis proved problematic. UBF appears to be selected against when grown in Escherichia coli (*E.coli*) and point mutations readily occurred. Therefore sequencing was critical after performing cloning using UBF.

2.1.1 Plasmid DNA Purification from small cultures

Single colonies were picked and grown in 10mls LB medium plus appropriate antibiotic selection O/N shaking at 37°C**.** Cells were centrifuged at 4000xg for 15min, 4°C. DNA was extracted and purified from cells using NucleoSpin® Plasmid kit (Machery-Nagel Cat No. 740588.250) following manufacturer's protocol.

2.1.2 Plasmid DNA Purification from large cultures

Starter culture of 10mls LB media plus appropriate antibiotic was inoculated with a single colony and grown for 8-9h shaking at 37°C**.** This culture was then transferred to 400ml LB medium plus appropriate antibiotic and grown O/N shaking at 37°C**.** Cells were centrifuged at 4000xg for 15min, 4°C. Plasmid DNA was extracted and purified using NucleoBound® Xtra Maxi (Machery-Nagel Cat No. 740414.50) following manufacturer's protocol.

2.1.3 Glycerol Stocks

800µl of an O/N culture added to screw cap tube containing 200µl of pre-warmed Glycerol (100%) to give final concentration of 20% Glycerol. Tubes were vortexed and sample stored at -80°C.

2.1.4 Determining Concentration and Purity of Nucleic acid

DNA samples were diluted in TE and absorption measured at 260nm using Picodrop (Picodrop Limited). Measured concentration was then multiplied by dilution factor. Pure DNA is indicated by sharp single peak and a A260/A280 ratio reading between 1.8 and 1.9.

2.1.5 DNA sequencing

DNA samples were sent to Source BioScience (LifeScience) where automated DNA sequencing is performed. Sequence traces were visualised using 4peaks (mekentosj.com) and sequence

contigs were assembled and checked using DNA Strider 1.4 or Serial Cloner 2.5 (serial-cloner.en.softonic.com) when using Lion operating system on Macintosh.

2.1.6 Agarose Gel Electrophoresis

Agarose gels were prepared by dissolving agarose at concentrations from 0.8%-1% (w/v) in 1xTAE (0.04M Tris-acetate, 1mM EDTA) and heating in a microwave oven. EtBr was added to melted agarose (0.5µg/ml) and gel was poured into gel cast with well comb and allowed to set at RT. One-tenth volume of gel loading buffer (40% sucrose (w/v), 0.25% bromophenol blue (w/v) or 0.25% Xylene cyanol (w/v) in distilled H_2O) was added and the samples were electrophoresed alongside a DNA ladder (HyperLadder Bioline) at 80-100 V. DNA was visualised on UV transilluminator (Gbox imager Syngene) and images were captured using GeneSnap software from Syngene.

2.1.7 Restriction Digests

Diagnostic digests were carried out using restriction enzymes, purchased from NEB (New England BioLabs®) or Roche. At least 2 units of enzyme was used per 1µg DNA and incubated at 37°C (or optimum temperature for required enzyme) for at least 1 hour in the appropriate buffer.

2.1.8 Extraction of DNA from Agarose gels

Appropriate restriction digests were performed and DNA bands visualised on bench top UV transilluminator (Benchtop 3UV™ UVP) at 302nm. The selected bands were extracted from the gel using a scalpel and transferred to an eppendorf. DNA was purified from extracted bands using NucleoBound® Extract II (Machery-Nagel Cat No. 740609.50) according to manufacturer's protocol.

2.1.9 Purification of PCR products

PCR products were purified using NucleoBound® Extract II (Machery-Nagel Cat No. 740609.50) according to manufacturer's protocol.

2.1.10 Ligation of DNA fragments to generate constructs

Standard 20µl ligation reactions typically contained 2µl 10x ligation buffer, 1-2µl T4 DNA ligase, ~70ng of vector DNA and 3-5 fold molar excess of insert DNA. Reactions were incubated at RT from 2h to O/N.

Commercial constructs used for cloning and resulting generated constructs are outlined in table 2.1 and 2.2, respectively.

Plasmid	Description	Use
pBluescript SK- (Stratagene)	Amp^r, fl(-) origin of ss-DNA replication, LacZ	Performing mutagenesis on N-terminal fragment of UBF
pENTR™/D-TOPO® (Invitrogen)	Kan^r, Gateway™ Entry vector with attL sites for site specific recombination, pUC origin	Rapid and efficient directional cloning of blunt ended PCR products.
pENTR4 (Invitrogen)	Kan^r, Gateway™ Entry vector, pUC origin	attL sites for site specific recombination with Gateway™ Destination vector
pcDNA-DEST40 (Invitrogen)	Amp^r for *E.coli*, Neo^r for mammalian cells, Gateway™ Destination vector for C-terminal fusion of V5-6xHIS tag, CMV promoter, pUC origin for *E.coli*, SV40 promoter and origin for mammalian cells	attR sites for site specific recombination with Gateway™ Entry vector to generate expression construct for expression in mammalian cells
pT-Rex-DEST30 (Invitrogen)	Amp^r for *E.coli*, Neo^r for mammalian cells, hybrid promoter comprising of a CMV promoter and two tetracycline operator sites ($TetO_2$) for tetracycline regulated expression	attR sites for site specific recombination with Gateway™ Entry vector to generate a vector that permits tetracycline-regulated expression of gene of interest in mammalian cells that already express Tet repressor protein,

Table 2.1 Commercial constructs used

Construct	How construct was generated	Use
pENTR/D-TOPO_hUBF1Δstop **(Brian McStay)**		This entry vector enables hUBF1 to be transferred, by an LR site specific recombination reaction, to any destination vector. This construct is suitable for C-terminal fusion.
pENTR4_*Ciona*UBF **(C.Colleran)**	PCR to amplify CionaUBF orf was performed on image clone Acc No.AB210737. Primers used introduced a 5'Nco1 and 3'EcoRV sites. Digested PCR fragment was cloned into Nco1 EcoRV digested pENTR4.	This entry vector enables *Ciona*UBF to be transferred, by an LR site specific recombination reaction, to any destination vector.
pcDNA_DEST40_ *Ciona*UBF **(C.Colleran)**	LR recombination reaction between pENTR4_*Ciona*UBF and pcDNA_DEST40	Expressing *Ciona*UBF-V5 6xHis C-terminal fusion protein in mammalian cells
pENTR201_Hmo1Δstop **(Olivier Gadal)**	Kind gift from Olivier Gadal	This entry vector enables Hmo1 to be transferred, by an LR site specific recombination reaction, to any destination vector. This construct is suitable for C-terminal fusion.
pcDNA_DEST40_Hmo1Δstop **(C.Colleran)**	LR recombination reaction between pENTR201_Hmo1Δstop and pcDNA_DEST40	Transfecting Hmo1 into mammalian cells
pT-REx-DEST30_Hmo1 **(C.Colleran)**	LR recombination reaction between pENTR201_Hmo1Δstop and pT-REx-DEST30	Tetracycline regulated expression of Hmo1 in mammalian cells
DEST40-GFP-C-term **(McStay Lab)**	Modification of pcDNA-DEST40 Gateway™ Destination vector, V5-6xHIS tag replaced with GFP	attR sites for site specific recombination with Gateway™ Entry vector to generate expression construct for expression in mammalian cells
DEST_hUBFwt_GFP_Cterm **(C.Colleran)**	LR recombination reaction between pENTR/D-TOPO_hUBF1Δstop and DEST_GFP	Expressing hUBF1wt-GFP C-terminal fusion protein in mammalian cells
DEST_hUBF_*W1A*_GFP_Cterm DEST_hUBF_*W3A*_GFP_Cterm DEST_hUBF_*W1AW2AW3A*_GFP_Cterm **(C.Colleran)**	pBluescript (SK-)_hUBF1(Not1Xho1) mutants were Not1 Xho1 digested and cloned into Not1 Xho1 digested pDEST_hUBFwt_GFP_Cterm.	Expressing hUBF1-tryptophan mutants-GFP C-terminal fusion protein in mammalian cells to analyze the effect of mutating the conserved tryptophans on UBF localization

Table 2.2 Constructs generated

2.1.11 Transformation into competent cells

An aliquot of competent cells (50µl) was allowed to thaw on ice and plasmid DNA or 10µl of ligation mix was added to cells and incubated on ice for 15-20 min. Cells were heat shocked at 42°C for 30 seconds and then chilled on ice for 2 min. 1ml of LB media (10g/L Bacto tryptone, 5g/L Bacto yeast extract, 170mM NaCl pH7.0) was added to cells and cells were incubated at 37°C while shaking at 1200rpm for 1h. One-tenth of the transformation was plated out on agar plate, containing appropriate antibiotic, and the remaining volume was centrifuged at 4000 rpm for 5min. The cell pellet was resuspended in small volume of LB media and plated out on agar plate containing appropriate antibiotic.

2.1.12 Preparing competent cells

A single colony was used to inoculate 10ml LB and incubated in a 37°C shaker until OD_{600} was 0.5. This 10ml culture was then used to inoculate a 200ml culture and grown until OD_{600} was 0.5. The culture was chilled on ice for 5min and centrifuged at 4000xg for 5min, 4°C. The cell pellet was resuspended 80ml TFB I (30mM Potassium acetate, 100mM $RbCl_2$, 10mM $CaCl_2.2H_2O$, 50mM $MnCl_2.4H_2O$, 15% Glyverol (v/v), pH5.8 with acetic acid) and chilled on ice for 15min. Cells were pelleted at 4000xg for 10min, 4°C**.** The cell pellet was resuspended in 8ml TFB II (10mM Mops, 75mM $CaCl_2.2H_2O$, 10mM $RbCl_2$, 15% Glycerol (v/v), pH6.5 with 1M KOH) and chilled on ice for 30min. Cells were aliquoted into eppendorfs, snap frozen in liquid nitrogen and stored at -80°C.

2.1.13 Bacterial Strains

Strain	Genotype	Special Characteristics	Use
DH10B	F– mcrA Δ(mrr-hsdRMS-mcrBC) Φ80lacZΔM15 ΔlacX74 recA1 endA1 araD139 Δ(ara leu) 7697 galU galK rpsL nupG λ–	Endonuclease deficient (endA) to prevent non-specific digestion thereby yielding cleaner DNA and recombinase deficient (recA) to reduce unwanted recombination and improve insert stability	Standard Cloning
JM109	endA1 glnV44 thi-1 relA1 gyrA96 recA1 $mcrB^+$ Δ(lac-proAB) e14- [F' traD36 $proAB^+$ $lacI^q$ lacZΔM15] hsdR17($r_K^-m_K^+$)	Endonuclease deficient (endA) and Recombinase deficient (recA) as well as HsdR for effiecient transformation of cloned unmethylated DNA from PCR	Cloning repetitive DNA
$T1^R$	F^- *mcr*A Δ(*mrr-hsd*RMS-*mcr*BC) Φ80*lac*ZΔM15 Δ*lac*X74 *rec*A1 *ara*Δ139 Δ(*ara-leu*)7697 *gal*U *gal*K *rps*L (Str^R) *end*A1 *nup*G *fhu*A::*IS2*	Resistant to ccdB gene product and resistant to T1 and T5 phage (tonA)	Propagate ccdB Gateway vectors

Table 2.3 Bacterial Strains

2.1.14 PCR

DNA products for cloning, generally into a Gateway® (Invitrogen) vector, were generated using the proofreading DNA polymerase *Pfu*. This polymerase is isolated and prepared in the lab by Brian McStay. A typical PCR reaction using *Pfu* contained ~50ng of DNA template, 0.2mM dNTPs, 0.2µM of each primer, 1M Betaine and a 1:10 dilution of 10x*Pfu* Buffer (200mM Tris-HCl pH8.8, 20mM $MgSO_4$, 100mM KCl, 100mM $(NH_4)_2SO_4$, 1% Triton X-100, 1mg/ml BSA nuclease free).

The PCR conditions were generally 30 cycles as follows:

Denature- 95°C 30 seconds

Anneal- temperature gradient of 50-70°C for 30 seconds

Extension- 72°C 2min/kb.

Mastercycler® Gradient (Eppendorf) was used to perform all PCR reactions.

2.1.15 Mutagenesis

All mutagenesis was performed using QuikChange® Lightning kit (Stratagene) according to manufacturer's specifications, except annealing temperature in PCR cycle was increased from 60°C to 68°C to improve stringency of reaction. Also PCR reactions were incubated with Dpn1 for a minimum of 20mins and then transformed into JM109 competent cells. The resulting products were routinely verified by DNA sequencing. This was to confirm that the correct mutation had been inserted and furthermore to ensure no unwanted mutations had been generated.

Sequences of primers used for mutagenesis reactions are outlined in table 2.4. The initial construct used for mutagenesis reaction and the resulting mutated constructs are outlined in table 2.5.

Oligonucleotide Name	Sequence
UBF1 W1A *forward*	5' CAAAGGCCAAGACCGTGCGTCCCAGGAAGACATG 3'
UBF1 W1A *reverse*	5' CATGTCTTCCTGGGACGCACGGTCTTGGCCTTTG 3'
UBF1 W2A *forward*	5' GAA TCA CAC ATC GAC GCG GAA AAA GTA GCA TTT AAA G 3'
UBF1 W2A *reverse*	5' CTT TAA ATG CTA CTT TTT CCG CGT CGA TGT GTG ATT C 3'
UBF1 W3A *forward*	5' CATGTGCAAGCTCAAAGCGGTGGAGATTTCTAATG 3'
UBF1 W3A *reverse*	5' CATTAGAAATCTCCACCGCTTTGAGCTTGCACATG 3'

Table 2.4 Primers used for mutagenesis reactions

Construct	How construct was generated	Use
pBluescript (SK-)_hUBF1wt(Not1Xho1) **(C.Colleran)**	Digested pENTR/D-TOPO_hUBF with Not1 and Xho1 and cloned fragment into Xho1 Not1 site in pBluescript (SK-)	This construct was used as the DNA template in mutagenesis reactions to generate the individual tryptophan mutations in the predicted SANT domain in the N-terminus off UBF.
pBluescript(SK-)hUBF(Not1Xho1)*W1A* pBluescript(SK-)hUBF(Not1Xho1)*W2A* pBluescript(SK-)hUBF(Not1Xho1)*W3A* pBluescript(SK-)hUBF(Not1Xho1)*W1AW2A* pBluescript(SK-)hUBF(Not1Xho1)*W1AW3A* pBluescript(SK-)hUBF(Not1Xho1)*W1AW2AW3A* **(C.Colleran)**	QuikChange® Lightning kit (Stratagene) was used to generate the tryptophan mutations. pBluescript (SK-)_hUBF1 (Not1Xho1) was used as template in reaction. For double tryptophan mutations pBluescript(SK-)hUBF(Not1Xho1)*W1A* was used as DNA template. For triple tryptophan mutations pBluescript(SK-) hUBF(Not1Xho1) *W1AW2A* was used as DNA template.	The Not Xho fragment from each of the individual constructs was used to clone into Not1 Xho1 digested pDEST_hUBFwt_GFP_Cterm, thereby replacing the wt SANT domain with the tryptophan mutations

Table 2.5 Starting construct for mutagenesis reactions and mutated constructs generated

2.1.16 Extraction of genomic DNA from cultured human cells

Cells were grown in T175 flask until ~90% confluent, media was removed and cells are washed twice with 10ml PBS. Add 5ml TE (20mM Tris pH8, 2mM EDTA) to flask followed by addition of SDS to a final concentration of 0.5% and proteinase K to a final concentration of 0.3mg/ml. The flask was incubated overnight at 37°C. Solution was transferred to 15ml tube and $1/10^{th}$ volume 3M Sodium Acetate was added. Then an equal volume of Phenol/Chloroform was added and the tube rotated at RT for 20mins. Sample was centrifuged at 4000g for 10min and aqueous layer transferred to fresh tube. 500ug RNase I was added to sample and incubated at 37°C for 30min to degrade any RNA. The phenol/chloroform extraction was repeated, i.e an equal volume of phenol/chloroform was added and sample rotated at RT for 20mins. Sample was centrifuged at 4000g for 10min and aqueous layer transferred to a fresh tube. 2½ volumes 100% ethanol was added and sample incubated at -20°C for 20min to precipitate DNA. DNA was collected with Pasteur pipette and washed by dipping into 70% ethanol (v/v). DNA was finally resuspended in appropriate volume of TE (10mM Tris pH8, 0.1mM EDTA) depending on amount of DNA precipitated.

2.2 RNA

2.2.1 RNA extraction

Cells were grown in T175 flask until ~90% confluent and harvested by scraping in ice-cold PBS. Cells are pelleted at 1200rpm for 5mins. The cell pellet is resuspended in 1ml TRIsure™ (Bioline) and incubated at RT for 5mins. 0.2ml of chloroform is added per 1ml of TRIsure™ and shaking vigorously for 15 seconds. Sample is incubated at RT for 15mins, then centrifuged at 12000g for 15min at 4°C. Aqueous phase is recovered and transferred to clean eppendorf and 0.5ml isopropanol is added per 1ml TRIsure™. Sample incubated at RT for 10min and centrifuged at 12000g for 10min at 4°C. Supernatant is removed with pipette and RNA pellet is washed with 1ml ice-cold 70% ethanol. RNA pellet is centrifuged at 12000g for 5min at 4°C. The RNA pellet is then air-dried and dissolved in 50-100µl Hyclone H_2O. RNA sample is stored at -20°C.

2.2.2 S1 nuclease protection assays

The probes used in S1 nuclease protection assays were HYPUR gel-purified 60-mer oligonucleotide supplied by MWG, 5'end (TTGGGCCGCCGGGTTATTGCTGACACGCTGTCCTCTGGCGACCTGTCGCTGGAGAG GTTG) and A' cleavage probe (5'-CGGACCCGGCCCGGGAGAGCACGACGTCACCACATCGATCACGAAGAGCCCCCCG GGAGC-3'). These probes were designed to determine the levels of 47S pre-rRNA and the efficiency of cleavage at the primary cleavage site respectively. Oligonucleotides (200 ng) were 5' end-labeled with γ-32P ATP and T4 polynucleotide kinase. Due to secondary structure within the probe, it was denatured in a boiling water bath prior to labeling. For each S1 nuclease protection assay, a 10-µg sample of RNA is resuspended in 27 µL of H_2O together with 3 µL of 10× Hybridisation buffer (3 M NaCl, 0.1 M Tris pH 7.9, 10 mM EDTA) and 1 µL (2 ng) of labeled probe. Hybridisations were incubated for 3 h at 65°C and then placed on ice. 270 µL of chilled S1 nuclease buffer (1 mM ZnSO4, 30 mM Na acetate pH 5.4, 50 mM NaCl) containing 50 units of S1 nuclease (Worthington) was added and the reaction incubated for 30 min at 37°C. Nuclease digestion was stopped by the addition of 50 µL of 5 M ammonium acetate, 5 µL of 0.5 M EDTA, and 10 µL of 10% SDS. Following ethanol precipitation and washing with 70% ethanol, pellets were resuspended in 6 µL of loading buffer (80% deionised formamide, 0.01% xylene cyanol and bromophenol blue dyes in 1× TBE). Denatured samples were electro-phoresed on 8% denaturing (7 M urea) polyacrylamide gels run in 1× TBE, and signals were visualised and quantified using a Fuji scanner (FujiFilm FLA-5100).

2.3 Tissue Culture

2.3.1 Cell Lines

The male human fibrosarcoma cell line, HT1080 were grown in Dulbeco's MEM+GlutaMAX-1 (+ 4.5 g/L glucose; GIBCO) supplemented with 10% fetal bovine serum (v/v) (BioSera) and 5U/mL (100µg/ml) of penicillin/streptomycin (Sigma). Generated stable cell lines, derived from HT1080 were all cultured in above media but also 5µg/mL blasticidinS (Melford) and/or 300µg/ml G418 Sulfate (Melford) and/or 200µg/ml Zeocin (Melford) supplemented as required. The 3D-1 pseudo-NOR containing cell line (Mais et al 2005), derived from the HT1080 cell line, was cultured in DMEM supplemented with 5µg/mL blasticidinS (Melford). HT1080 TetR10 cell were also cultured in DMEM supplemented with 5µg/mL blasticidinS (Melford).
The UBFKD cells, again derived from HT1080 cell line, were cultured in DMEM and pen/strep but supplemented with 10% Tetracycline free fetal bovine serum (BioSera) and 5µg/mL blasticidinS and 200µg/ml Zeocin. Generated stable cell lines, derived from UBFKD were cultured in above media supplemented with 300µg/ml G418 Sulfate.

The karyotypically normal non-transformed female human hTERT-immortalised retinal pigment epithelial (hTERT-RPE-1) cell line was grown DMEM/Nutrient Mixture F-12 Ham (+ 15mM HEPES, sodium bicarbonate, without L-Glutamine, (Sigma)) supplemented with 10% fetal bovine serum (v/v) (BioSera), 1% L-Glutamine 200mM (v/v)(Sigma), 4.5% Sodium bicarbonate (v/v)(Sigma) and 5U/mL (100µg/ml) of penicillin/streptomycin (Sigma).

The rat-kangaroo marsupial *Potorous tridactylis* cells, PtK_1 (female) and PtK_2 (male) were derived from kidney tissue of a normal adult female and male respectively. Both PtK_1 and PtK_2 were cultured in Minimum Essential Medium (MEM) Eagle (+ Earles salts, reduced $NaHCO_3$, without L-Glutamine, (Sigma)) supplemented with 10% fetal bovine serum (v/v) (BioSera), 2% L-Glutamine 200mM (v/v) (Sigma), 1% MEM Non-Essential amino acid (v/v) (Sigma) and 5U/mL (100µg/ml) of penicillin/streptomycin (Sigma).

2.3.2 Maintaining cell lines

Cells were cultured in T75 or T175 culture flasks. The media was removed from flask and cells were washed with (Phosphate Buffered Saline) PBS. The cells were trypsinised with a final concentration of 1xTrypsin (Sigma) at RT or 37°C between 2-5min depending on cell type. The flask was gently tapped to detach cells and an equal volume of media was added to inhibit trypsin. Single cell suspension was achieved by pipetting up and down and cells were re-seeded at required dilution into new flask containing media.

For the *Potorous tridactylis* cell line the cells were trypsinised using 1 volume 1xTrypsin (Sigma)/ 2 volume 1x Versene (Gibco) and incubated at 37°C for 5min.

2.3.3 Generating the UBF KD stable cell line

Transfections were performed using a standard calcium phosphate protocol in 150mmx20mm plates. HT1080 cells were transfected with 20µg of the Tetracycline repressor protein expressing plasmid pcDNA6/TR (Invitrogen) and selection was carried out using DMEM medium supplemented with 5µg/mL blasticidin (GIBCO). Colonies were picked approximately 12 days later using cloning discs (SIGMA) and transferred to 6-well plates. The clones were maintained in blasticidin containing media and screened by determining their ability to repress expression of proteins dependent on Tetracycline operator (TetO). A positive clone was selected, HT1080 TetR10, and transfected with pTER+ plasmid containing human UBF shRNA sequence (sequence of UBFshRNA kindly given by Ross Hannon).
Human UBF shRNA oligonucleotides:

GATCCCGGAGATCATGAGAGACTATATTTCAAGAGAATATAGTCTCTCATGATCTCCTTTTTGGAAA
GGCCTCTAGTACTCTCTGATATAAAGTTCTCTTATATCAGAGAGTACTAGAGGAAAAACCTTTTCGA

Selection was carried out using DMEM medium supplemented with blasticidin and Zeocin. Resistant colonies were picked and tested for their ability to downregulate UBF levels upon induction of expression of UBF shRNA upon addition of 1µg/mL Doxycycline. A positive clone, termed 8iii, was selected. Additional cloning of the 8iii cell line resulted in a more homogenous population of cells and the final cell line was called UBFKD.

2.3.4 Long Term Storage and Recovery of Cell Lines from Liquid N_2

Cells from T175 culture flask were trypsinised and pelleted at 1200 rpm for 5min. The cell pellet was resuspended in 3-4mls of freezing medium (10% DMSO (v/v) 90% FBS (v/v)). 1ml cell suspension aliquots were transferred to cryotubes then placed in Nalgene Cryo 1°C and stored at -80°C overnight. Cells were then transferred to liquid nitrogen tanks.
For recovery of cell from liquid N_2, the cryotube containing frozen cells was thawed quickly by placing tube in a 37°C water bath. The cells were transferred to 15ml tube containing 5mls media and centrifuged at 1200rpm for 5min. The cell pellet was resuspended in 12mls media and transferred to T75 flask.

2.3.5 Trypan Blue Exclusion Test of Cell Viability

Cells were harvested by trypsinisation, centrifuged at 1200rpm for 5min and the cell pellet was resuspended in PBS. An equal volume (~10µl) of cell suspension and trypan blue (0.4 % trypan

blue, 0.81% NaCl and 0.06% K_2HPO_4) (Sigma) were mixed and incubated at RT for 5-10mins. Viable cells, based on dye exclusion, were counted using hemacytometer (Kovac) for each sample.

2.3.6 Flow Cytometry

Cells were harvested by trypsinisation, centrifuged at 1200rpm for 5min and the cell pellet was resuspended in PBS. The cells were fixed by adding cold 70% Ethanol in a dropwise manner and incubated at 4°C for 30mins or the samples were stored at -20°C. Fixed cells were pelleted at 3000rpm for 7mins and the cell pellet was incubated with 500µl Propidium Iodide (PI)–RNAse (BD Pharmingen™) for 20mins at RT in the dark. Samples were analyzed on FACS Canto II (BD Bioscience).

2.3.7 Transfections

To generate stable cell lines transfections were performed using a standard calcium phosphate protocol in 150mm x20mm plates. Cells were seeded the day before so that the cell density is approximately 40-50% confluent for transfection. 2xHEBS (270mM NaCl, 10mM KCl, 1.4mM Na_2HPO_4, 10mM Dextrose, 42mM HEPES pH 7.05) and $CaCl_2$ (2.5M in 10mM HEPES pH 7.2) were thawed at RT. TE (pH 7.15) was also allowed to warm to RT. For each 15cm plate, 800µl 2xHEBS was placed in sterile 15ml tube. 16-33µg of DNA was added to an eppendorf and volume brought up to 720µl with TE (pH 7.15). Eppendorf was vortexed briefly and 80µl of 2.5M $CaCl_2$ was added. The DNA and $CaCl_2$ were mixed by pipetting up and down and then added dropwise to 800µl 2xHEBS in 15ml tube. DNA/$CaPO_4$ solution was incubated at RT for no longer than 10min before adding to cells in a dropwise manner. The dish was agitated to ensure good mix and placed back in incubator (37°C/5% CO_2). After 5-7 hours a fine precipitate should be visible under light microscope. The media was removed and cells washed with PBS until precipitate is no longer visible. Fresh warm media is added to dish and replaced in incubator.

Appropriate selection marker (BlasticidinS and/or G418 Sulfate) is added to media 24hr after transfection, initially at high concentration (e.g. 10µg/mL blasticidinS and/or 1000µg/ml G418 Sulfate). Concentration of selective markers decreased gradually as cell death became evident. Colonies were picked approximately 12 days later using cloning discs (SIGMA) and transferred to 6-well plate containing appropriate media (5µg/mL blasticidinS and/or 300µg/ml G418 Sulfate).

Transient transfections were performed using TransIT reagent (Mirus Bio Corp) following manufacturers protocol or by standard calcium phosphate as described above except in a 10cm

dish (500µl 2xHEBS, 10-20µg DNA, 459µl TE, 50µl $CaCl_2$). Cells were analyzed 24-48hr after transfection by immunostaining or western blotting.

2.3.8 siRNA transfections

TransMessenger™ transfection reagent (Qiagen) was used to transfect siRNA oligos into the hTERT-RPE-1 cell line following manufacturers protocol using 1:5 ratio of siRNA oligo (µg) to TransMessenger reagent (µl), respectively. hTERT-RPE-1 cells were seeded out in 6-well plate and transfected with UBFsiRNA oligos 24 and 72 hours after seeding and harvested 24 hours after second round of siRNA transfection. The control siRNA used for the in these siRNA transfections is a scrambled sequence of the human nucleolar protein RNA helicase II/Guα, which was originally described in (Henning et al., 2003).

si-934Scr: GUA ACA AUG AGA GCA CGG C

Potorous tridactylis (PtK) UBF siRNA duplexes were purchased as Smartpools from Dharmacon. siRNA duplexes were transfected using a final concentration 20 nM with DharmaFECT 1 reagent (Thermo Scientific) according to manufacturers protocol 24 and 72-h after seeding. The cells were harvested 24 hours after second round of siRNA transfection.

Target	Sequences in Smartpool
Human UBF	Sequence 1: UAACCAAGAUUCUGUCCAAUU Sequence 2: GGACCGUGCAGCAUAUAAAUU Sequence 3: CCAAUAAACGUAAGAGCAUUU Sequence 4: GAAGUUCCGUACAUUGACAUU
Potorous tridactylus (PtK) UBF1	Sequence 1: GAAAUUAGCAGAAGAGCAAUU Sequence 2: GGACAAAUUUGAUGGGCGAUU Sequence 3: GAAGUAACCUGGAACAAUAUU

Table 2.6 Sequence of siRNA oligonucleotides

2.3.9 Electron Microscopy

Cells were grown in T75 or T175 culture flasks to ~90% confluency. The media was removed and cells were fixed with 4% PFA/1% Glutaraldehyde EM grade (Agar Scientific) at 4°C for 20 min. The cell were washed once briefly with 10mM Ammonium Chloride in 1xPBS, followed by 45min incubation at 4°C in 12-25mls 10mM Ammonium Chloride in 1xPBS. The cell were

washed 3x 5 min with 1xPBS at 4°C. Cells were dehydrated with a series of ethanol washes, first 30% Ethanol for 15min at 4°C, followed by 50% ethanol for 15mins at 4°C, then 70% ethanol for 15mins or store O/N at 4°C. Following 70% ethanol incubation the cells were incubated with 90% ethanol for 15mins at 4°C. The cells were harvested by scraping in the 90% ethanol and centrifuged at 1200 rpm for 5mins at 4°C to obtain a cell pellet. The cell pellet was resuspended in 100% ethanol and incubated 3x15min at RT. After final ethanol wash the embedding process was started. It is critical that all components to prepare Agar 100 resin (Agar Scientific) and mixing vessels are pre-warmed at 60°C before use. Agar 100 expoxy resin, DDSA, MNA and BDMA were all mixed according to manufacturers protocol to create a medium block. The cell pellet was resuspended in 3:1 (v/v) ethanol 100%/Agar 100 Resin and incubated at RT for 2h with rotation. Cells were pelleted at 1200 rpm for 5mins at 4°C. The cell pellet was resuspended in 1:1 (v/v) ethanol 100%/Agar 100 and incubated at RT for 2h with rotation. Cells were pelleted again at 1200 rpm for 5mins at 4°C. The cell pellet was resuspend in 1:3 (v/v) ethanol 100%/ Agar 100 and incubated O/N with rotation. Cells were pelleted at 4000g for 15mins, resuspended in 100% Agar 100 and transferred to a BEEM capsule (Agar Scientific). The cells were then pelleted to the bottom of the BEEM at 4000g for 30min. The capsule was filled to capacity with Agar 100 and the block was incubated with BEEM capsule lid open for 48hr-72hr in 60°C oven containing silica gel.
The block was sent to Valentina Sirri in the Pierre and Marie Curie institute Paris for analysis.

2.3.10 Immunofluorescent Staining of Cells

Cells were grown on glass coverslips or Superfrost® Plus microscopic slides (Scientific Laboratory Supplies) for at least 24hr. The media was removed and cells were fixed with 4% paraformaldehyde (PFA) (w/v) in PBS for 10min at RT. The cells were then rinsed with PBS 3x10min and permeabilised with 0.5% Saponin (w/v) and 0.5% Triton X-100 (v/v) in PBS for 10min at RT. Antibodies were diluted from 1:100 to 1:200 in 1% bovine serum albumin (BSA) (w/v) in PBS. Between 100-150µl of primary unconjugated antibody was applied to coverslip/slide (table 2.7) and incubated for 60min in humidity chamber at 37°C. The coverslip/slide was rinsed 3x10min with PBS followed by incubation with 100-150µl of conjugated secondary antibody (table 2.8) for 45-60min in humidity chamber. The cells were rinsed 3x10min with PBS and coverslips/slides mounted in Vectashield plus DAPI (Vector Laboratories).

2.3.11 Combined Immunofluoresence and FISH on 3D Preserved Nuclei

Cells were grown on Superfrost® Plus microscopic slides (Scientific Laboratory Supplies). The media was removed and the cells were fixed with 4% paraformaldehyde (PFA) (w/v) in PBS for

10min at RT. The cells were washed 3x10min with PBS and then permeabilised with 0.5% Saponin (w/v) and 0.5% Triton X-100 (v/v) in PBS for 10min at RT. The cells were washed 3x10min with PBS before incubating slides in 20% glycerol/PBS (v/v) for 2 hours. The slides were snap frozen in liquid N_2 and stored at -80°C. Hybridisation probes were labeled with spectrum green or red dUTP using Nick Translation kit (Vysis) following manufacturers protocol. Prior to hybridisation the slides were thawed in PBS with an additional wash in fresh PBS. The slides were then depurinated in 0.1M HCl for 5min and washed 2x5min with PBS. Prior to denaturation, the cells were equilibrated with 50% deionised formamide/2xSSC for 15min in humidity chamber at 37°C. The precipitated DNA probe (50ng/slide) was resuspended in Hybrisol VII (Qbiogene) (25µl/slide) and applied to a coverslip on 37°C block. The probe was then applied to cells and sealed with rubber cement (Marabu-Fixogum). Both probe and cells were denatured at 73°C for 12mins and then allowed to hybridise for at least 18h in humidity chamber at 37°C. Post hybridisation washes consisted of 3x5min in 50% formamide/2xSSC at 42°C and 3x5min in 0.1 SSC at 60°C. The slides were then washed in PBS and subjected to antibody staining as outlined in section 2.3.10.

When using Fibrillarin monoclonal antibody the antibody staining was performed with primary and secondary antibodies, followed by fixation with 2% PFA in PBS for 10min, prior to depurination and hybridisation.

2.3.12 Preparing Metaphase spreads

Cells were grown in T175 culture flask to ~60-70% confluence and treated with Demecolcine (Sigma), at a final concentration of 0.1µg/ml, for between 1-2 hrs depending on cell line (eg HT1080 1hr, PtK_2 2hrs). Mitotic cells were recovered by mitotic shake off and transferred to a 50ml tube. Mitotic cells were centrifuged at 1200rpm for 5mins and the cell pellet was washed in PBS. Mitotic cells were centrifuged again at 1200rpm for 5mins. The cell pellet was resuspended in 5-10mls of hypotonic solution (75mM KCl) and incubated at 37°C for 20mins. The volume hypotonic solution used depends on the size of the cell pellet. The cells are centrifuged at 1200rpm for 5mins, and the cell pellet was resuspended in freshly prepared Carnoy's fixative solution (3:1 (v/v) methanol/glacial acetic acid). Cells were incubated in Carnoy's fixative solution for 10min at RT before being centrifuged at 1200rpm for 5mins. The cell pellet was resuspended in a small volume of the fixative solution. Mitotic cells were then dropped using a Pasteur pipette from a height onto superfrost slides and allowed air dry before being subjected to immunostaining or hybridisation.

2.3.13 Combined immunofluorescence and FISH on metaphase spreads

Once metaphase spreads had air-dried they were briefly incubated in PBS prior to antibody staining. Following immunostaining the metaphase spreads are fixed with 1% PFA and then depurinated with 0.1M HCl for 2min. Prior to denaturation, cells were equilibrated with 50% deionised formamide/2xSSC for 15min in humidity chamber at 37°C. The precipitated DNA probe (50ng/slide) was resuspended in Hybrisol VII (Qbiogene) (25µl/slide) and applied to coverslip on 37°C block. The probe was then applied to cells and sealed with rubber cement (Marabu-Fixogum). Both probe and chromosomal DNA were denatured at 73°C for 12mins and then allowed to hybridise for at least 18h in humidity chamber at 37°C. The post hybridisation washes consisted of 0.4xSSC/0.3% NP-40 for 2mins at 73°C followed by 2xSSC/0.3% NP-40 at RT. The slides were mounted in Vectashield plus DAPI (Vector Laboratories).

2.3.14 Combined FISH and Silver staining on metaphase spreads

Metaphase spreads were subjected to FISH as outlined in section 2.3.13. After post hybridisation washes the slides were rinsed briefly in PBS and then allowed to air dry. 2% Gelatine solution supplemented with 0.1% formic acid was added to the slide followed by the addition an equal volume of 50% silver nitrate solution. A coverslip was applied and the slide was incubated on a 60°C block until the solution had turned dark brown. The slide was then subjected to a quick wash in water, allowed to air dry and mounted in Vectashield plus DAPI (Vector Laboratories).

2.3.15 Imaging of fixed cells

Z-stacks of fluorescent images were captured and merged using a Photometric Coolsnap HQ camera and Volocity 5 imaging software (Improvision) with a 63x Plan Apochromat Zeiss objective mounted on a Zeiss Axioplan2 imaging microscope. The number and the depth of Z-stacks taking per an image were calculated by establishing the depth of the cell first. The midpoint of the cell was established by moving the microscopes focus drive until the cell was in focus. This point was set as zero using Velocity 5 imaging software. The upper and lower limit of a cell are set by moving the focus drive up and down, respectively, until the cell is just out of focus. The averaging depth for an interphase cell was ~4µm and ~8µm for a metaphase cell. The limit for the depth of each Z-stack was 0.2µm, with the preferred depth being 0.15µm. By changing the number of Z-stacks taking I could obtain the desired Z-stack depth, hence for interphase cells ~30 Z-stacks were taking and for metaphase cells ~50 Z-stacks. Once the correct number and depth of Z-stacks was established the required channels for imaging were selected, DAPI, FITC and Rhodamine and the image was captured using Volocity 5.

Selected images were then deconvolved using the Volocity 5 software. Specific parameters are set to determine when the deconvolution will end. These parameters include a confidence limit set at 95% and an iteration limit set at 50. The deconvolution will continue until the confidence limit has exceeded the 95% set or the number of iterations set is reached.

2.3.16 Live cell imaging

Cells were grown in MatTek Corp Glass bottom 35mm uncoated culture dishes (product code: P35G-1.5-10-C). Once cells had grown to 70-80% confluence a final concentration of 20mmol/L HEPES (pH 7.2) was added immediately prior to analysis. Dishes were transferred to heated chamber (37°C). Live cell microscopy was conducted using a DeltaVision Core system (Applied Precision) controlling an interline charge-coupled device camera (Coolsnap HQ^2; Roper) mounted on an inverted microscope (IX-71; Olympus). Images were collected every 10 minutes at 2×binning using a 63×oil objective and 0.2 µm Z-stacks sections. Images were deconvolved and maximum intensity projected using SoftWoRx (Applied Precision).

Antibody	Clone Number	Species raised in	Antigen	Source	Dilution for Immunofluorescence (IF)/Western Blot(WB)
α-hUBF1/2		Sheep	Full-length baculovirus expressed recombinant protein (J.Wright)	McStay Lab and Diagnostic Scotland Edinburgh	IF: 1/200 WB: 1/1500
α-hPAF49		Sheep	Full-length baculovirus expressed recombinant protein (C.Mais)	McStay Lab and Diagnostic Scotland Edinburgh	IF: 1/200 WB: 1/2000
α-hRPA43		Sheep	Full-length baculovirus expressed recombinant protein (C.Mais)	McStay Lab and Diagnostic Scotland Edinburgh	IF: 1/200 WB: 1/2000
α-Fibrillarin	72B9	Mouse		Provided by U Scheer, Wuerzburg	IF: 1/200
α-Cleaved PARP (Asp214) (19F4)	9546	Mouse		Cell Signaling Technology	WB: 1/2000
α-V5 epitope	SV5-Pk1	Mouse monoclonal	V5 epitope Pk mca1360	Serotec α	IF: 1/100
α-Hmo1		Rabbit		Provided by Olivier Gadal	IF: 1/200 WB: 1/2000

Table 2.7 Primary antibodies

Antibody	Species raised in	Catalogue Number	Source	Dilution for Immunofluorescence (IF)/ Western Blot(WB)
Rhodamine α-rabbit	Donkey	711-025-152	Jackson ImmunoResearch	IF: 1/200
Rhodamine α-sheep	Donkey	713-025-147	Jackson ImmunoResearch	IF: 1/200
Rhodamine α-mouse	Donkey	715-025-150	Jackson ImmunoResearch	IF: 1/200
Rhodamine α-human	Donkey	709-025-149	Jackson ImmunoResearch	IF: 1/200
FITC α-mouse	Donkey	717-095-150	Jackson ImmunoResearch	IF: 1/200
FITC α-human	Donkey	709-095-149	Jackson ImmunoResearch	IF: 1/200
FITC α-sheep	Donkey	713-095-147	Jackson ImmunoResearch	IF: 1/200
Cy2 α-rabbit	Donkey	711-225-152	Jackson ImmunoResearch	IF: 1/200
α-sheep HRP	Mouse monoclonal	A9452	SIGMA-ALDRICH	WB: 1/2000
α-rabbit HRP	Donkey	711-035-152	Jackson ImmunoResearch	WB: 1/5000

Table 2.8 Secondary Antibodies

2.4 Protein

2.4.1 Harvesting Protein Samples

Cells were grown in 10cm dishes, harvested by trypsinisation and the cells were counted using a heamocytometer. The cells were centrifuged at 1200rpm for 5mins, 4°C, and the cell pellet was washed with PBS. The cells were centrifuged again at 1200rpm for 5mins, 4°C. The final cell pellet was resuspended in an appropriate volume of Laemmli Buffer to give a volume concentration of $1x10^4$ cells/μL. The samples were boiled for 10mins at 95°C followed by sonication in Bioruptor waterbath sonicator for 3x30sec bursts at the highest magnitude.

2.4.2 Western Blotting

Electrophoresis of proteins was performed on NuPAGE® Novex 4-12% Bis-Tris gels (Invitrogen™) using Xcell *SureLock*™ Mini-cell (Invitrogen™) and NuPAGE® running buffer (Invitrogen™) following manufacturer's protocol. The gels were either subjected to staining using Coomassie brilliant blue (PhastGel® BlueR (Sigma), 10% acetic acif, 40% Methanol) or transferred to Hybond™ECL™ nitrocellulose membrane (Amersham) using xCell II™blot module (Invitrogen™) and NuPAGE® transfer buffer (Invitrogen™) following manufacturer's protocol. The membranes were blocked in 5% Marvel (w/v) in PBS at RT for 2h or overnight at

4°C. Membranes were then incubated with the chosen primary antibody (table 2.7), that has been diluted in 5% Marvel (w/v), for 1h at RT or O/N at 4°C. Following incubation with the primary antibody, the membrane was washed 3x10min in PBS at RT. Specific secondary antibody coupled to HRP (horseradish peroxidase) (table 2.8) was diluted in 5% Marvel (w/v) before incubation with the membrane for 1h at RT. The membrane was washed 3x10min in PBS at RT. Equal volumes of Western Lightning™ *Plus*-ECL Enhanced Luminol Reagent and the Oxidising Reagent (PerkinElmer) were mixed and applied to membrane for 2-3min. Chemiluminescence signals were detected with CCD Syngene G-Box chemi XT16 camera and images captured using GeneSnap software from Syngene and quantification was done using GeneTools software from Syngene.

3 Characterisation of the inducible UBF shRNA human cell line, UBFKD

3.1 Background

UBF is an extremely abundant protein with the number of UBF molecules quantified in *Xenopus* and human fibroblast cells at approximately 10^6 UBF molecules per cell (McStay et al., 1997, Sullivan et al., 2001). The absolute levels of UBF are regulated in response to changes in cellular demands, for instance UBF levels are up regulated in cancer cells and decreased during differentiation. Several differentiating models have shown this reduction in UBF levels, such as differentiation of L6 myoblasts to myotubes (Larson et al., 1993), F9 embryonal carcinoma cells to primitive endoderm cells (Alzuherri and White, 1999, Datta et al., 1997), 3T3-L1 pre-adipocyte cells to adipocytes (Li et al., 2006a) and during murine granulocyte differentiation (Sanij et al., 2008, Poortinga et al., 2004, Poortinga et al., 2011, Liu et al., 2007).

Active NORs adopt an open chromatin state and UBF has been demonstrated to remain bound to active NORs throughout the cell cycle. The ability to construct pseudo-NORs by integrating UBF binding site arrays into human chromosomes has provided evidence that UBF binding is required for the formation of secondary constrictions (Mais et al., 2005). Hence we hypothesise that UBF is essential for maintaining the open chromatin state associated with active NORs. This thesis aims to analyse the effect of UBF depletion on the rDNA chromatin state *in vivo*, both in interphase cells and also on metaphase chromosomes.

To understand the biological relevance of a specific gene, in our case UBF, one should analyse the consequence of altering the function of that gene in cells or organisms. RNA interference (RNAi) is a powerful technique that enables us to look specifically at the consequence of depleting UBF and aid our understanding of UBFs functioning in the cell. RNAi can be applied to cells by two types of molecules, chemically synthesised double-stranded small interfering RNA (siRNA) or vector based short hairpin RNA (shRNA). Synthesised siRNAs are generally 21-base pair double stranded RNA molecules that are incorporated into the multi-protein RNA-induced silencing complex (RISC). Argonaute 2 (Ago-2), one of the main components of the RISC, cleaves and releases the sense strand of the siRNA duplex resulting in an activated form of RISC. The remaining antisense strand serves as a guide strand that directs the RISC to the complementary mRNA, resulting in the cleavage and subsequent degradation of the target mRNA (Aagaard and Rossi, 2007). In contrast to siRNA, the shRNA-containing vector is transcribed in the nucleus. The primary transcript, which contains a hairpin structure, is initially processed in the nucleus to form the pre-shRNA transcript by a complex that contains the RNA III enzyme Drosha and the RNA binding domain protein DGCR8. The pre-shRNA transcript is exported to the cytoplasm and loaded onto another complex, which contains the RNase III protein DICER, where the loop of the hairpin is cleaved off resulting in mature shRNA (Rao et al., 2009). The mature shRNA associates with RISC and mediates gene silencing as described above for the siRNAs.

From personal communications with Professor Tom Moss we know that UBF is an essential gene. Unpublished studies from the Moss lab have shown that UBF knockout experiments in mouse result in embryotic lethality. In the McStay lab an inducible UBF shRNA human cell line has been generated to enable us to analyse the consequences of UBF depletion. The sequence for the UBF shRNA, which were kindly given by Professor Ross Hannan, specifically targets the UBF open reading frame just after the splicing region, thereby targeting both isoforms of UBF, UBF1 and UBF2 (Figure 3.1 (A)). shRNA mediated interference has some important advantages over siRNAs. Transiently transfecting siRNAs into cells is only short lived whereas shRNA-expressing vectors can be stably introduced into cells with the opportunity of making stable cell lines. shRNAs are endogenously expressed *in vivo* from RNA Pol III promoters and as mentioned above are processed *in vivo* by the RNAse III enzyme Dicer and RISC, thereby ensuring stable suppression of the targeted gene (Paddison et al., 2002). Using the inducible UBF shRNA cell line we can control the levels at which we deplete UBF. This will allow us to analyse the consequences that lowering UBF levels has on the ribosomal chromatin.

In this chapter I will describe the characterisation of the UBFKD cell line containing an inducible shRNA that targets UBF1 and UBF2. I first established that depleting endogenous UBF using high concentrations of the shRNA induction reagent, doxycycline, resulted in redistribution of nucleolar proteins, nucleolar morphological changes, growth arrest and cell death. I then established conditions at which we could substantially reduce levels of endogenous UBF without inducing cell death or growth arrest. These conditions will allow us to analyse the effect on the rDNA chromatin in the presence of reduced UBF levels.

3.2 Results

3.2.1 Characterise the effect of depleting UBF in the UBFKD cell line

The HT1080 human fibrosarcoma cell line was chosen to make the UBF shRNA stable cell line (UBFKD). A characteristic of HT1080 cells is that the nucleoli are dispersed, irregular in shape and often nucleoli are indistinguishable from one another. Interestingly in the HT1080 cell line all the NORs appear to be active, this is in contrast to HeLa cells where 3-4 silent NORs are always evident as condensed foci dissociated from nucleoli (McStay and Grummt, 2008). The fact that all the NORs are active may be due to the presence of mutant *ras* and constitutive signalling through the MAP (mitogen-activated protein) kinase pathway. In the lab a DNA probe, which hybridises to a sequence distal to each human NOR, provides a powerful tool for counting individual NORs. This distal junction (DJ) probe will prove invaluable in the proceeding chapter when determining the effect on rDNA chromatin at individual NORs as a result of depleting UBF levels.

The initial UBF shRNA cell line, termed 8iii, was generated in the lab by a co-worker, Jose-Luis Prieto. Preliminary experiments in which I subjected doxycycline treated 8iii cells to immunostaining with α-hUBF antibodies revealed that only a sub-population of the cells were sensitive to the UBF shRNA. In order to fully establish the consequence of UBF depletion by shRNA induction I decided that a single population of cells was required. Therefore I re-cloned 8iii cells to generate a cell line in which the effect of inducing expression of UBF shRNA is homogenous in all cells. This resulting cell line was termed UBFKD, full details as to how it was generated is described in section 2.3.3.

The Tet-inducible RNAi plasmid (pTER) utilised in the UBFKD cell line was constructed by modifying the pcDNA™3.1/Zeo to include the RNA Pol III H1 promoter with a Tet-operator (TetO) sequence (Brummelkamp et al., 2002, Van De Wetering et al., 2003). The H1 promoter is exploited because it gives rise to a 21-22 nucleotide shRNA in which the complementary strands are separated by a short loop sequence (Brummelkamp et al., 2002). Additionally the H1 promoter transcriptional start site and terminal signal, a row of five thymidine residues, are well defined (Baer et al., 1990). shRNA expression is suppressed due to the binding of the Tet repressor (TetR) protein to the TetO sequences. The TetR protein is expressed from the pcDNA™6/TR construct, which is stably expressed in the UBFKD cells. As a consequence of its increased stability over tetracycline, the derivative doxycycline is used in cell culture media as the inducing agent. When doxycycline is added it binds to TetR proteins, thereby preventing binding to the TetO sequence and enabling the induction of UBF shRNA expression (Figure 3.1 (B)).

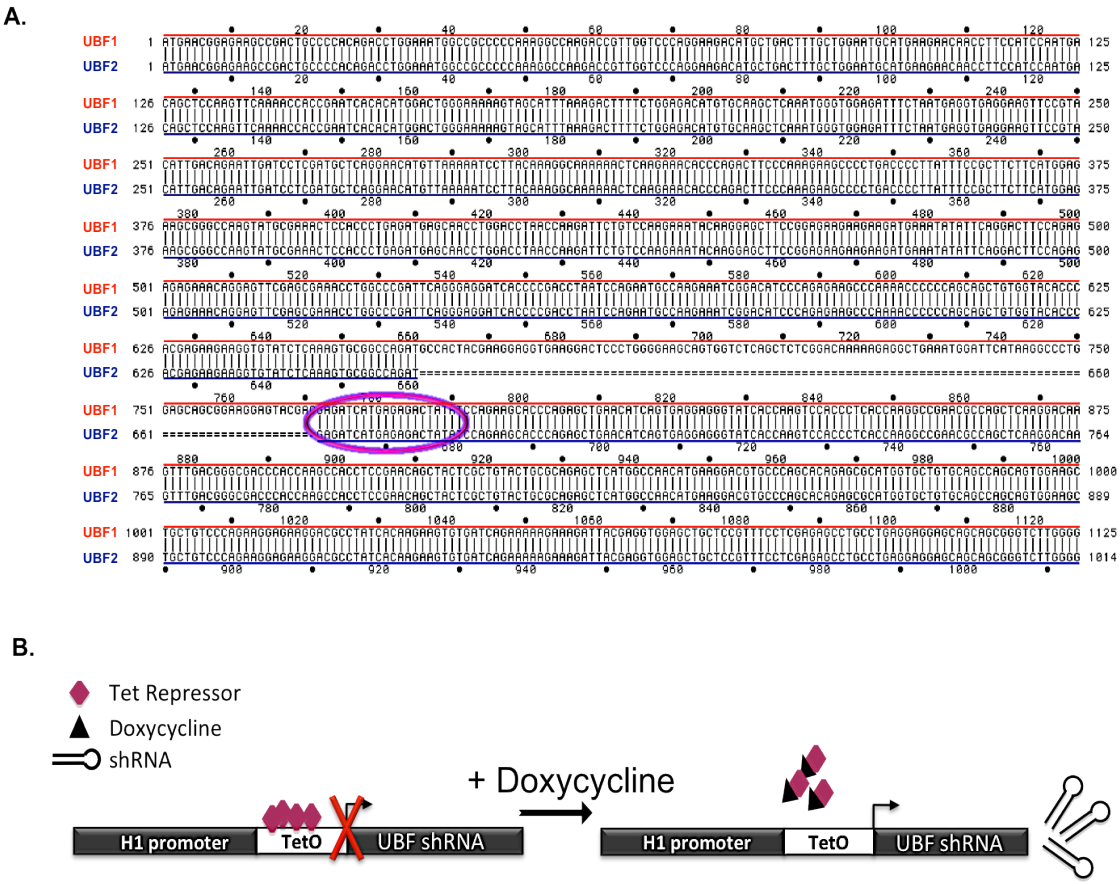

Figure 3.1 Schematic of targeted region of human UBF by shRNA and UBF shRNA induction
(A) Alignment of hUBF1 and hUBF2 orfs reveals the region targeted by UBF shRNA (pink circle). The shRNA targets both splice variants of hUBF, immediately after the deleted 111 nucleotides from the second HMG box in hUBF2.
(B) This illustration demonstrates how the UBFKD cell line functions. In the absence of doxycycline the Tet Repressor (TetR) binds to the Tet Operator (TetO) inhibiting shRNA induction. Addition of doxycycline obstructs TetR binding and initiates induction of hUBF shRNA expression.

To determine the effects of inducing UBF shRNA expression, the UBFKD cells were treated with a final concentration of 1µg/ml doxycycline. This concentration was chosen as it was previously shown as the optimal concentration for induction of shRNAs using the pTER+ vector (Van De Wetering et al., 2003). UBFKD cells were seeded out and subjected to doxycycline treatment (1µg/ml) for different time intervals and the effect of this higher concentration was carefully monitored. Firstly cells were harvested from different time points (48, 96 and 144 hours), lysed in Laemmli sample buffer and loaded by equal cell number ($5x10^5$cells/lane) on NuPAGE gels. HT1080 parental cell lysate ($5x10^5$cells) was loaded in parallel as a control to indicate the total quantity of cellular UBF. All protein samples were loaded in duplicate and stained with coomassie blue to ensure equal loading. Additionally, detection of the RNA Pol I subunit RPA43, using α-hRPA43 antibodies, was employed to ensure no overall global change in levels of nucleolar proteins as a consequence of UBF depletion. Immunoblotting with the α-hUBF antibody reveals that the UBF levels in UBFKD cells treated with 1µg/ml doxycycline are

reduced by greater than 10-fold after 48hrs. Quantification of western blots was performed by capturing the chemiluminescent signal with CCD (charged couple device) camera of Syngene G:Box and quantifying signal using GeneTools software (Syngene). 144hrs after the initial induction of shRNA expression, UBF is virtually undetectable by western blotting (Figure 3.2 (A)). Monitoring the UBFKD cells treated with 1μg/ml doxycycline for 144hrs by phase microscope reveals a noticeable change in nucleolar structure with the presence of vacuoles in the cytoplasm. These changes in nucleolar structure as a consequence of UBF depletion will be discussed below.

To analyse the effect of UBF depletion on growth and cell cycle profile I performed trypan blue exclusion assays and FACS analysis on UBFKD cells treated with doxycycline for 24, 48, 72 and 96hr. UBFKD cells, in the presence and absence of doxycycline were harvested for each timepoint in duplicate, as were parental HT1080 cells as a control. The resulting growth curves reveal a severe growth defect in UBFKD cells treated with 1μg/ml doxycycline. 48hr after induction of UBF shRNA the UBFKD cells cease to proliferate (Figure 3.2 (B)). To analyse what impact this growth inhibition has on the cell cycle profile FACS analysis was performed. Asynchronous cells were harvested, fixed, stained with Propidium Iodine (PI) and analysed on FACS Canto II. Asynchronous cells from the parental HT1080 cell line were again used as a control to indicate normal cell cycle profile for these cells. In the 24 and 48hr profiles there is no obvious deviation from the control HT1080 cell cycle profile. In contrast, the 72 and 96 hr cell cycle profiles show a reduction in G2/M cells indicating that cells have started to withdraw from the cell cycle and hence stopped proliferating (Figure 3.2 (C)). Also evident at the 72 and 96 hr timepoints is an accumulation of cells sub-G1 indicative of cell death possibly due to apoptosis (Figure 3.2 (C)). Trypan blue assays and FACS analysis were performed on three independent occasions, each reproducing the same results.

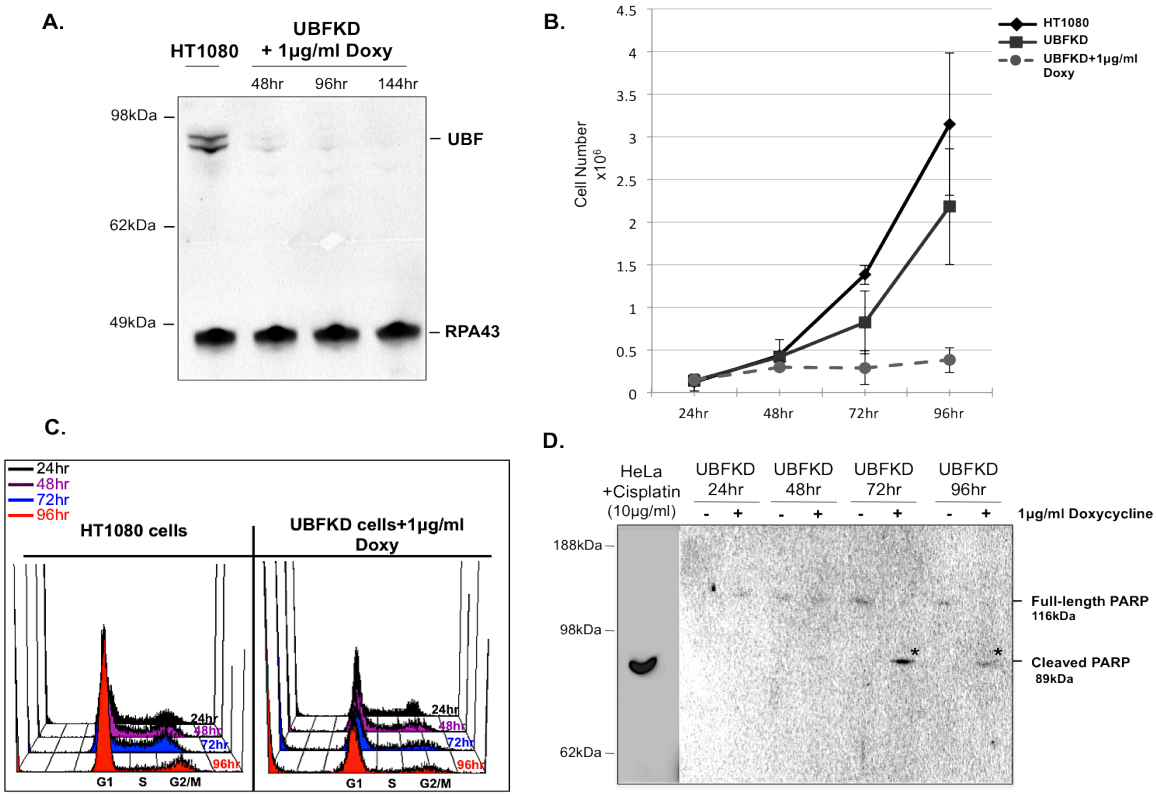

Figure 3.2 UBF depletion induces a severe growth defect and cell death
(A). UBFKD cells treated with 1µg/ml Doxycycline for 48, 96 and 144 hrs were harvested and lysed directly in appropriate volume of Laemmli sample buffer to give $1x10^4$ cells/µl. HT1080 cell lysate was used as a control. 10µl of each sample was loaded on NuPAGE gel and membrane probed with α-hUBF antibodies, to indicate level of UBF depleted, and α-hRPA43 antibodies.
(B). Equal cell number ($1x10^5$) was seeded into T25 flasks in duplicate for UBFKD and UBFKD+1µg/ml Doxycycline. HT1080 cells were used as an additional control. Cells were harvested in duplicate at 24, 48, 72, and 96hr time points. An aliquot of each cell suspension was mixed with an equal volume of trypan blue and viable cells were counted. Error bars are formulated from three independent repeats.
(C). Similar to the trypan blue assay, equal cell number were seeded out ($1x10^5$) for HT1080 and UBFKD+1µg/ml Doxycycline. Asynchronous cells were harvested at 24, 48, 72 and 96hr timepoints and fixed with cold 70% ethanol before incubating with PI, as outlined in section 2.3.6. Samples were then analysed on FACS Canto II.
(D). Cell lysate was harvested from UBFKD cells treated with 1µg/ml Doxycycline for 24, 48, 72 and 96hrs. Lysate from HeLa cells treated with 10µg/ml cisplatin, which induces apoptotic death, was used as a control to detect cleaved PARP. Samples were loaded on NuPAGE gel and membrane probed with α-PARP antibodies. Asterisks (*) indicate cleaved PARP bands in UBFKD+1µg/ml Doxycycline 72 and 96 hr samples.

To determine if the sub-G1 peak observed by FACS is as a result of apoptosis I performed western blot analysis with a α-cleaved PARP (poly (ADP-ribose) polymerase) antibody. During programmed cell death PARP is cleaved, by caspase-3 and caspase-7, thereby preventing it functioning in DNA repair and facilitating cells commitment to undergo apoptosis. Protein samples from UBFKD cells cultured in the presence and absence of doxycycline at 24, 48, 72 and 96hr were loaded in parallel with a positive control, HeLa cells treated with 10µg/ml cisplatin (kindly given by Dr. Severine Hennequart). Cisplatin is a platinum-containing anti-cancer drug that interferes with cell proliferation and thereby induces apoptosis. Full-length PARP appears as

a band of 116kDa whereas cleaved PARP, signifying apoptotic death, appears as an 89kDa band. Western blot analysis provides evidence that the sub-G1 peak observed by FACS is due to apoptotic cell death. Low intensity bands, indicated by asterisks in (Figure 3.2 (D)), are observed at ~89kDa in the UBFKD+1μg/ml doxycycline 72 and 96hr samples. These bands relate in size with the cleaved PARP in the control sample in (lane 1, Figure 3.2 (D)). Furthermore, the cleaved PARP bands are only detected in the timepoints in which sub-G1 peaks are evident by FACS.

I have established that the UBFKD cell line, upon doxycycline treatment, induces expression of shRNA that targets both splice variants of UBF resulting in efficient depletion of UBF. Using the standard concentration of 1μg/ml doxycycline induces a severe growth arrest and cell death, with evidence suggesting cell death is due to apoptosis.

3.2.2 UBF depletion causes redistribution of nucleolar proteins

I next wanted to examine if depleting UBF effects the localisation of nucleolar proteins. The first protein I examined was fibrillarin, a protein component of C/D box snoRNPs that directs 2'-*O*-ribose methylation during pre-rRNA processing (Niewmierzycka and Clarke, 1999, Tollervey et al., 1993) that is highly conserved in eukaryotes (Aris and Blobel, 1991, Henriquez et al., 1990). The effect of UBF depletion on fibrillarin localisation was investigated by immunofluorescence. In non-treated UBFKD cells, α-hUBF antibodies reveal the characteristic punctate staining associated with UBF in the nucleolus. Fibrillarin staining, revealed using α-fibrillarin antibodies, co-localises with UBF in nucleoli (top row, Figure 3.3). As UBF levels are depleted in UBFKD cells treated with 1μg/ml doxycycline, the UBF staining becomes less intense when compared to non-treated cells. UBF depletion correlates with changes in the pattern of fibrillarin staining, becoming more circular in comparison to non-treated UBFKD cells (second panel in third row, Figure 3.3). Also observed in UBFKD cells treated with 1μg/ml doxycycline is that any remaining endogenous UBF is redistributed from the nucleolus to the nucleoplasm. These effects are most obvious 72hr after induction of UBF shRNA and this timepoint also correlates with the first signs of fibrillarin dispersing from the nucleolus (second panel in bottom row, Figure 3.3).

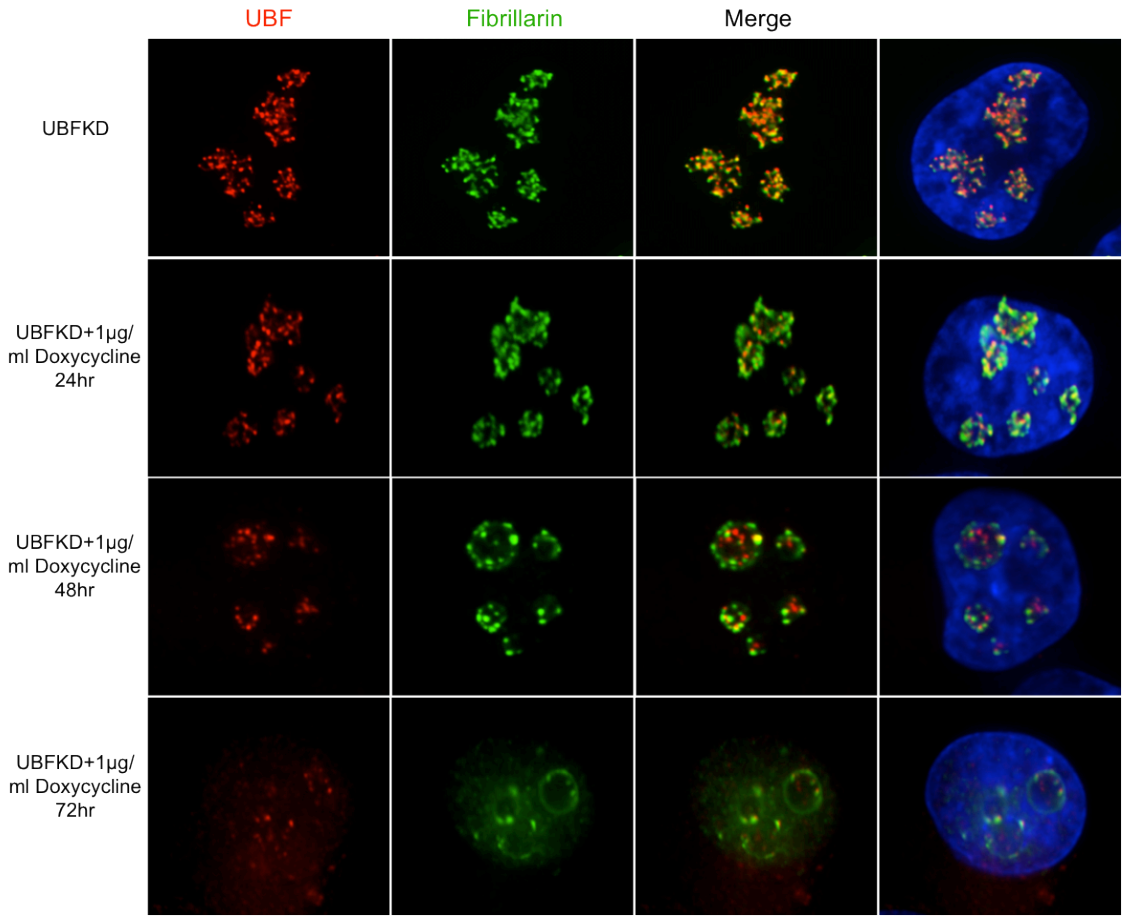

Figure 3.3 UBF depletion results in the redistribution of the early maturation protein, Fibrillarin
UBFKD cells were treated with 1µg/ml doxycycline for 24, 48 and 72hrs, untreated UBFKD cells were used as a control (top row). Cells were fixed, permeabilised and subjected to immunostaining, outlined 2.3.10. hUBF is visualised using α-hUBF antibodies followed by incubation with rhodamine coupled α-sheep antibody (first panel) and fibrillarin visualised with α-fibrillarin antibodies followed by incubation with FITC coupled α-mouse antibody (second panel). Merge of both signals and both signals plus DAPI are shown in the third and fourth panels, respectively.

I then went on to examine the effect of UBF depletion on the RNA Pol I specific subunits, PAF49 and RPA43. PAF49 interacts with PAF53 and the SL1 subunit TAF_I48 through its N-terminal region (Yamamoto et al., 2004). Evidence that PAF49 plays a role in rDNA transcription comes from *in vivo* studies in which overexpression of a PAF49 deletion mutant reduces the synthesis of pre-rRNA transcripts (Yamamoto et al., 2004). In yeast, mutations or deletions in the Pol I subunit RPA43 results in the failure to synthesise pre-rRNA transcripts *in vivo,* suggesting that RPA43 is an essential component of yeast RNA Pol I (Thuriaux et al., 1995). In the non-treated UBFKD cells, both α-hPAF49 and α-hRPA43 antibodies reveal punctate staining that co-localises with fibrillarin in the nucleolus (top row, Figure 3.4 (A) & (B), respectively). As a consequence of UBF depletion the RNA Pol I specific subunits, PAF49 and RPA43, begin to disperse from the nucleolus to the nucleoplasm (bottom row, Figure 3.4 (A) & (B), respectively).

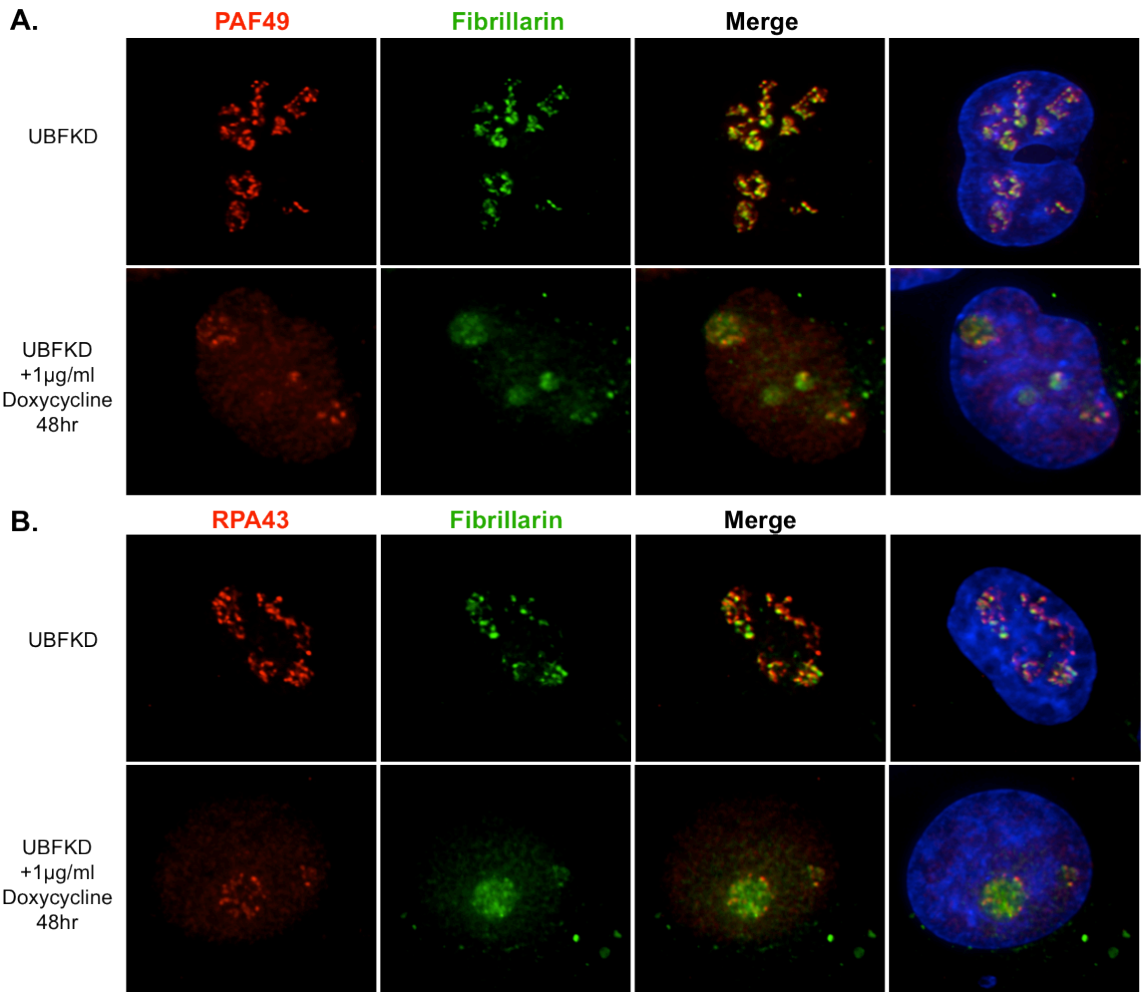

Figure 3.4 UBF depletion results in the redistribution of the specific RNA Polymerase I subunits
UBFKD cells were treated with 1µg/ml doxycycline for 48hrs, fixed, permeabilised and subjected to immunostaining as outlined 2.3.10. Untreated UBFKD cells were used as a control.
(A) hPAF49 and (B) hRPA43 are visualised using α-hPAF49 and α-hRPA43 antibodies, respectively, followed by incubation with rhodamine coupled α-sheep antibody (first panel). Fibrillarin was used as nucleolar marker and visualised with α-Fibrillarin antibodies followed by incubation FITC coupled α-mouse antibody (second panel). Merge of both signals and both signals plus DAPI are shown in the third and fourth panels, respectively.

3.2.3 Establishing conditions that deplete endogenous UBF levels sufficiently without impacting on cell growth

I have demonstrated that depleting a significant proportion of endogenous UBF, using 1µg/ml doxycycline, induces a severe growth arrest and triggers apoptotic cell death. While this confirms that UBF is essential, it provides little information on its *in vivo* role. Therefore the main aim of this chapter is to generate conditions in the UBFKD cell line in which UBF levels are substantially reduced without impacting on cell growth. This resulting cell line will allow us to analyse the effect that reducing cellular levels of UBF has on the rDNA chromatin state *in vivo*.

To determine the concentration of doxycycline required to create such conditions the UBFKD cells were seeded out in T75 culturing flasks and treated with varying concentrations of doxycycline. The initial concentrations of doxycycline ranged from 1ng/ml to the extreme 1μg/ml, which included 10ng/ml and 100ng/ml. Within 7 days changes in nucleolar morphology were evident in 10ng/ml, 100ng/ml and 1μg/ml doxycycline treated UBFKD cells. Nucleoli were now apparent as prominent circular structures, in contrast to the dispersed, irregular shaped nucleoli associated with non-treated UBFKD cells. Additionally these cells had ceased proliferating and cell death was evident by the presence of floating cells. In contrast the 1ng/ml doxycycline treated cells showed no evidence of a defect in cell proliferation and no changes to nucleolar morphology were evident.

I therefore seeded out new T75 flasks of equal cell density and treated the cells with 1ng/ml, 2ng/ml, 5ng/ml and 10ng/ml doxycycline. The cells were monitored daily to identify any defect in cell proliferation. Within 7 days the UBFKD cells cultured in 5ng/ml and 10ng/ml doxycycline were proliferating at a slower rate and cell death was evident. In contrast the 2ng/ml doxycycline treated UBFKD cells, were growing marginally slower than non-treated UBFKD cells, however by phase contrast there was evidence of changes in nucleolar morphology. These changes were analysed and are discussed in the following section.

I decided to fully characterise these UBFKD cells cultured in 2ng/ml doxycycline, from here on in termed 2ng UBFKD cells, to determine the level of UBF depleted and analyse if this reduction in UBF levels has an impact on cell growth. Cell lysates were prepared from 2ng UBFKD cells and an equal cell number ($5x10^5$ cells) of 2ng UBFKD and control HT1080 cells were loaded. The protein samples were loaded in duplicate so that the samples could be stained with coomassie blue to ensure equal loading. The membrane was probed with α-hUBF antibodies to reveal the amount of UBF depleted and α-hRPA43 antibodies to ensure no global change in total levels of RNA Pol I subunits. The western blot was quantified using GeneTools (Syngene) and a 4.5-fold reduction in endogenous levels of UBF determined for these 2ng UBFKD cells (Figure 3.5 (A)).

To analyse if this 4.5-fold reduction in UBF levels observed in the 2ng UBFKD cells has any impact on cell proliferation growth curves were generated. HT1080, UBFKD, 2ng UBFKD and UBFKD+1μg/ml doxycycline cells were seeded out in duplicate. Cells were harvested at 24, 48, 72 and 96hr time points for each cell line and subjected to trypan blue staining. Growth curves generated indicate that there is no impact on cell proliferation in the 2ng UBFKD cells, interestingly these cells proliferate at much the same rate as the HT1080 parental line and the non-treated UBFKD cells (Figure 3.5 (B)). The growth defect is observed again for UBFKD+1μg/ml doxycycline cells. Three independent trypan blue assays were performed, as described above, with each resulting growth curve producing the same trend.

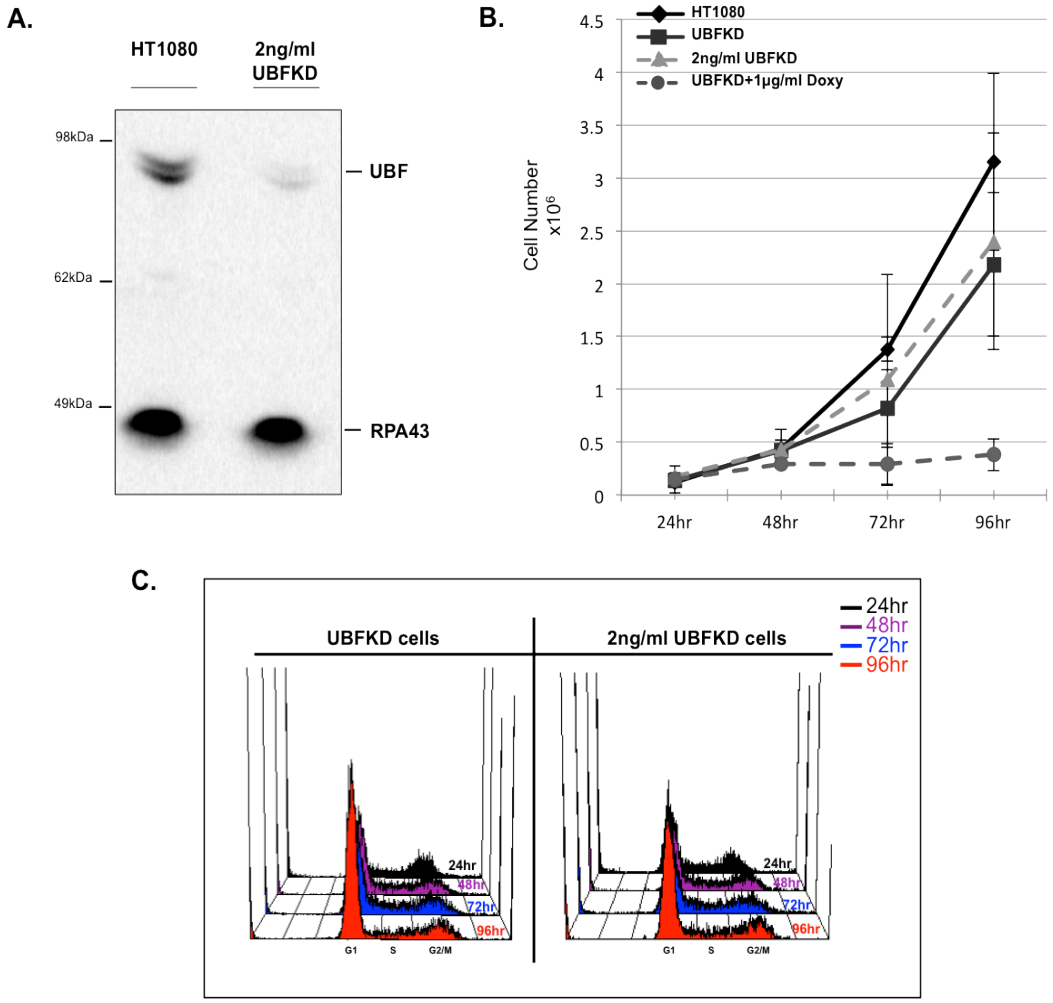

Figure 3.5 Characterisation of 2ng UBFKD cells
(A). UBFKD cells that were cultured in 2ng/ml doxycycline for an extended period were harvested and lysed directly in an appropriate volume of Laemmli sample buffer to give $1x10^4$ cells/µl. HT1080 cell lysate was used as a control. 10µl of each sample was loaded on NuPAGE gel and membrane probed with α-hUBF antibodies to indicate depletion of UBF and α-hRPA43 antibodies as a loading control.
(B). Equal cell number ($1x10^5$) was seeded out in T25 flasks in duplicate for UBFKD, 2ng UBFKD and UBFKD+1µg/ml doxycycline. HT1080 cells were used as an additional control. Cells were harvested in duplicate at 24, 48, 72 and 96hr time points. An aliquot of each cell suspension was mixed with an equal volume of trypan blue and viable cells were counted. Error bars are formulated from three independent repeats.
(C). Similar to the trypan blue assay, equal cell number were seeded out ($1x10^5$) for UBFKD and 2ng UBFKD. Asynchronous cells were harvested at 24, 48, 72 and 96hr timepoints and fixed with cold 70% ethanol before incubating with PI, as outlined in section 2.3.6. Samples were analysed on FACS Canto II.

Having established that there is no growth defect associated with the 2ng UBFKD cells, I performed FACS analysis to ensure that this 4.5-fold reduction in UBF levels did not alter the cell cycle profile of the 2ng UBFKD cells. UBFKD and 2ngUBFKD asynchronous cells were harvested at 24, 48, 72 and 96hrs in duplicate and samples were fixed and stained with PI. The DNA content profile in (Figure 3.5 (C)) demonstrated that the 2ng UBFKD cell cycle profile does not deviate from the control non-treated UBFKD cell cycle profile. As was the case for the trypan

blue cell viability assays, FACS analysis was performed on samples harvested from three independent experiments.

Combining cell viability assays and FACS analysis I have demonstrated that we can create conditions in which we can reduce UBF levels 4.5-fold without impacting severely on cell growth. The 2ng UBFKD cells can sustain the 4.5-fold reduction in UBF levels for an extended period of time (9-10 weeks). After ~10 weeks, cells cultured in the presence of 2ng/ml doxycycline start to lose the silencing effects, most likely by becoming resistant to the shRNA. All the work conducted using these 2ng UBFKD cells is carried out within 6 weeks of the initial induction of UBF shRNA using 2ng/ml doxycycline. These 2ng UBFKD cells will be used in the next chapter to analyse the effect that reducing cellular levels of endogenous UBF has on human rDNA chromatin state.

3.2.4 Effect on nucleolar structure upon UBF depletion

The changes in nucleolar morphology as a consequence of UBF depletion were very distinctive. These changes to nucleolar morphology were initially observed in UBFKD cells treated with 1µg/ml doxycycline, however the same changes were also evident in the 2ng UBFKD cells. By phase contrast UBFKD control cells were directly compared to UBFKD+1µg/ml doxycycline and the 2ng UBFKD cells. In UBFKD untreated cells the nucleoli are dispersed and irregular in shape and frequently the nucleoli are indistinguishable from each other (Figure 3.6). The appearance of UBFKD nucleoli is similar to nucleoli observed in the parental HT1080 cell line. In contrast, UBFKD+1µg/ml doxycycline and 2ng UBFKD nucleoli appear as distinct circular nucleoli. A common feature of UBF+1µg/ml doxycycline and 2ng UBFKD cells is the presence of a single or two large nucleoli (indicated by arrowheads, Figure 3.6). Additionally in the UBFKD+1µg/ml doxycycline cells, the presence of vacuoles in the cytoplasm was commonly observed.

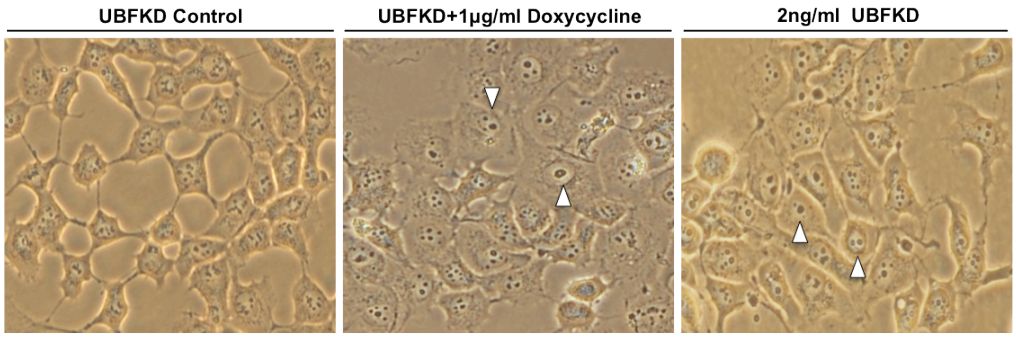

Figure 3.6 UBF depletion induces changes in nucleolar morphology
Phase contrast images were taking of UBFKD, UBFKD+1µg/ml and 2ng UBFKD doxycycline using Olympus inverted microscope CKX41) and Olympus E-420 digital SLR camera. White arrowheads indicate cells with a single or two nucleoli.

To analyse more in depth the changes that occur in nucleolar structure as a consequence of UBF depletion we performed transmission electron microscopy (TEM). TEM employs energetic electrons to produce high-resolution images and provide morphologic and compositional information. TEM is a common technique used to visualise the fibrillar centre (FC), dense fibrillar component (DFC) and granular component (GC) regions of the nucleolus, which were described in the introduction. Samples were prepared as described in section 2.3.9 for 2ng UBFKD and UBFKD+1µg/ml doxycycline cells. HT1080 cells were used as a control. Once embedded and polymerised in Agar 100 the cells were sent to Valentina Sirri at the Pierre and Marie Curie institute in Paris. Here the blocks of cells were thinly sliced, stained with thionin blue and analysed.

Directly comparing TEM images from HT1080 control and 2ng UBFKD cells it is difficult to decipher any major changes in the nucleolar sub-compartments (Figure 3.7 (A(ii)(iii)) & (B(ii)(iii)), respectively). The proportion of FCs, which are visualised as the lighter areas, appears to be equivalent in both HT1080 and 2ng UBFKD nucleoli. However, TEM imaging of 2ng UBFKD cells reveals the changes in nucleolar shape that is observed by phase microscopy. Unlike the dispersed and irregular shaped HT1080 nucleoli, the 2ng UBFKD nucleoli appear as prominent circular structures similar to that observed in HeLa cells or HT1080 cells treated with the protein kinase A agonist 8-chloro-cAMP (Krystosek, 1998). Chronic knockdown of UBF in UBFKD+1µg/ml doxycycline cells, results in changes in nucleolar shape similar to those observed in the 2ng UBFKD cells (Figure 3.7 (C)). Additionally, the appearance of structures reminiscent of nucleolar caps is observed in the 1µg/ml doxycycline nucleoli (indicated by red arrowhead, Figure 3.7 (C (ii))). Nucleolar cap formation is characteristic of cells treated with actinomycin D (Act D), which is a drug that can specifically inhibit RNA Pol I transcription at low concentrations and cause segregation of nucleolar sub-compartments (indicated by red arrowhead, Figure 3.7 (D)). However the nucleolar caps observed in UBFKD+1µg/ml doxycycline nucleoli cannot be due to rDNA transcription inhibition and I will provide evidence for this in the next section.

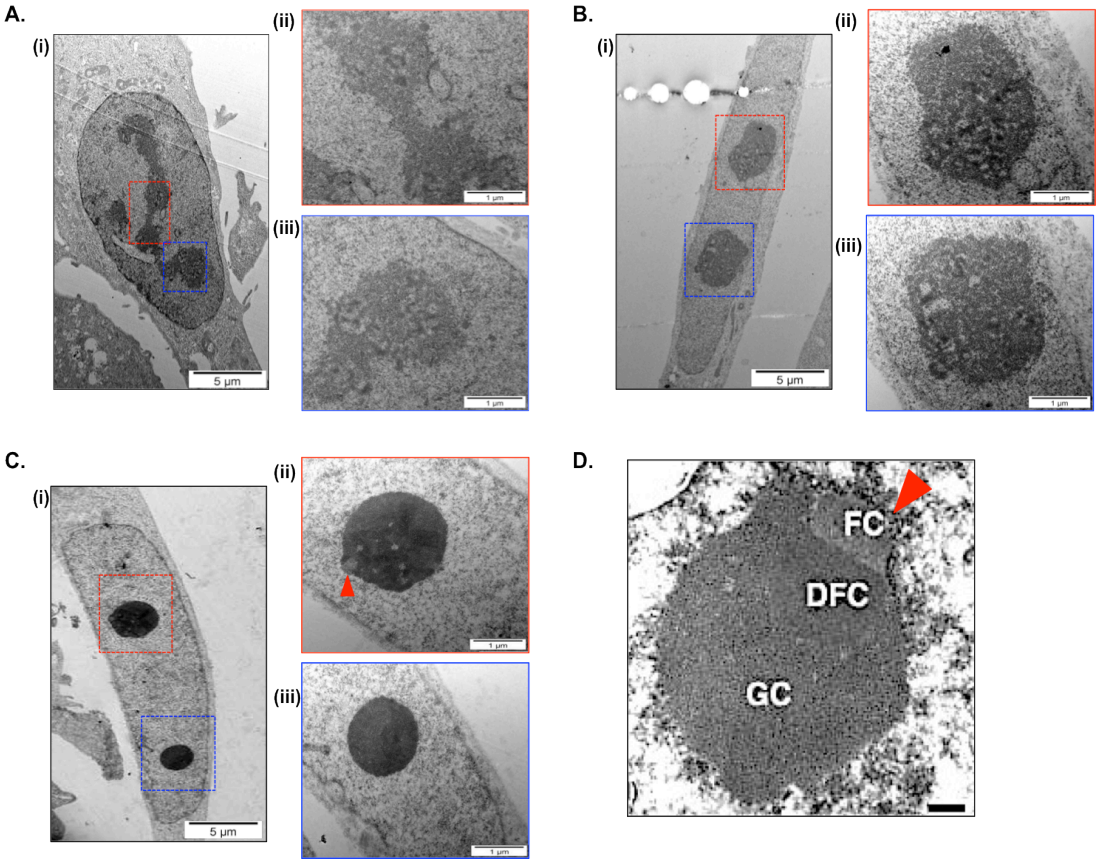

Figure 3.7 Electron microscopy images of UBF depletion cells
Electron microscopy images of (A) HT1080, (B) 2ng UBFKD and (C) UBFKD+1µg/ml Doxycycline cells. All cells were fixed in PFA and Glutaraldehyde, embedded in Agar 100 resin, sliced and stained with thionin blue. The FC is observed as the whitest areas, which is surrounded by DFC, visible as more intense staining, and is embedded in the GC. In UBFKD+1µg/ml Doxycycline nucleoli, structures reminiscent of a nucleolar cap are evident (indicated by arrowhead (C)(ii)). (E) Human nucleolar segregation following Act D treatment. The three sub-compartments are labelled and the arrowhead indicates the nucleolar cap formed due to inhibition of RNA Pol I transcription. Figure adapted from (Hernandez-Verdun et al., 2010).

3.2.5 Depletion of UBF does not have a significant impact on rDNA transcription

The S1 nuclease protection assay is a powerful technique used to detect and quantify specific RNAs in a total cellular RNA extract (outlined in Figure 3.8 (A)). We took advantage of this technique to analyse if reducing UBF levels has an effect on the rate of rDNA transcription and rRNA processing. The 47S pre-rRNA transcript is a very short-lived RNA species. It is rapidly cleaved in the 5' ETS at the A' cleavage site and the resulting 5' portion of the ETS is rapidly degraded. Thus performing S1 nuclease protection assays with a 5' end P^{32} labelled oligo (Figure 3.8 (B)) and measuring the levels of the 5' end of the 47S pre-rRNA is often used as a direct measure of the levels of on-going transcription. Prof. Brian McStay performed the S1 nuclease protection assays on the RNA samples that I prepared.

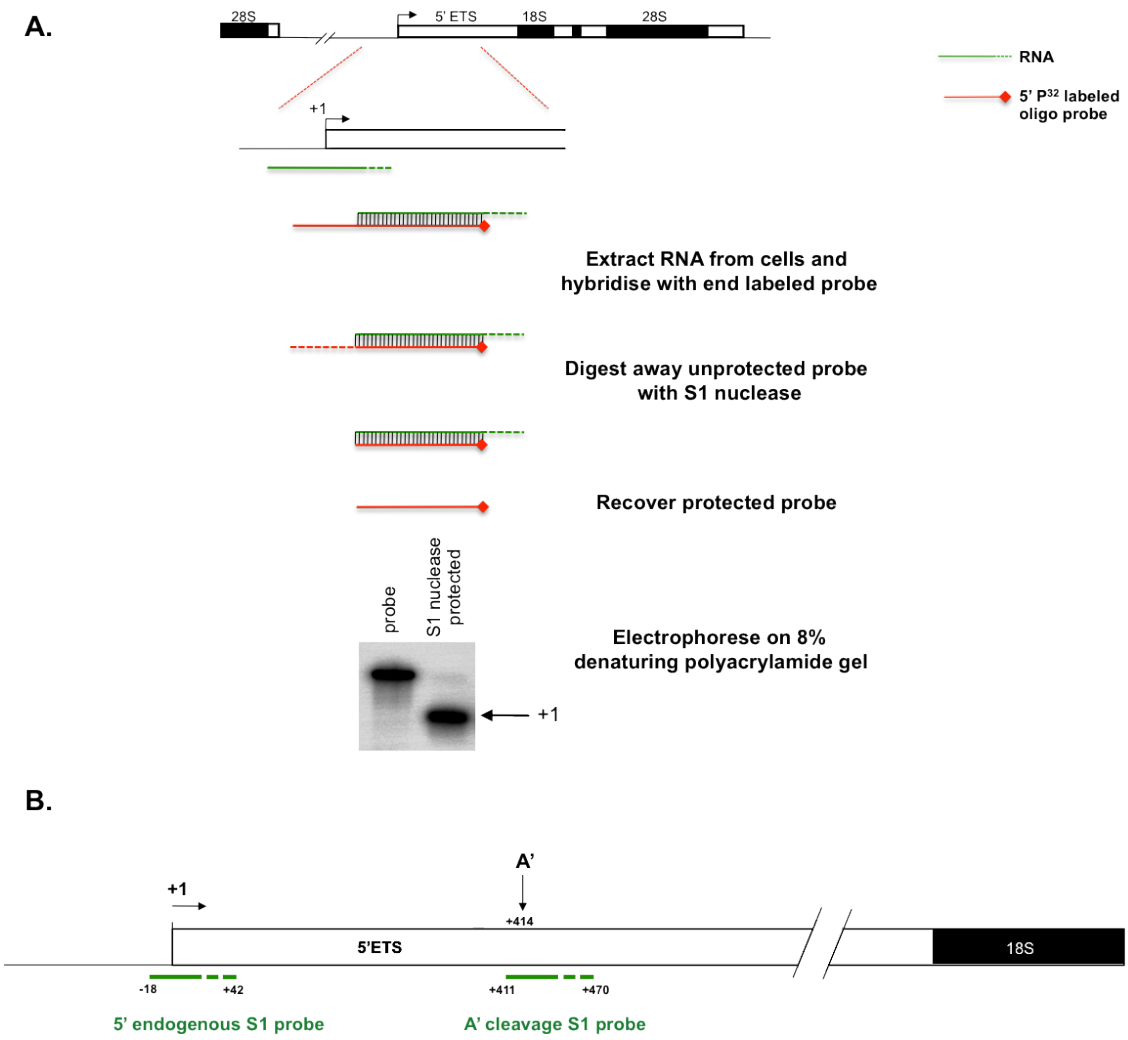

Figure 3.8 Schematic of S1 protection assay and location of the relative S1 probes used
(A) RNA is extracted from mammalian cells outlined in 2.2.1 and hybridised with specific 5' end labelled probe. After hybridisation, unbound/unprotected probe is digested with S1 nuclease. The protected probe is recovered, run on 8% denaturing polyacrylamide gel and signals visualised using a Molecular Imager (BioRad). (B) Illustration of the 5' endogenous S1 probe, the A' cleavage site and the A' cleavage S1 probe.

Both the 2ng UBFKD and UBFKD+1µg/ml doxycycline treated cells were analysed for defects in rDNA transcription. By analysing both states of UBF reduction, a 4.5-fold and greater than 10-fold reduction in 2ng UBF KD and UBFKD+1µg/ml doxycycline cells, respectively, we can determine if different UBF cellular levels correlate with different effects on rDNA transcription. RNA was extracted from HT1080 and 2ng UBFKD as described in section 2.2.1. For the UBFKD+1µg/ml doxycycline cells, RNA was extracted 2, 4 and 6 days after induction of UBF shRNA. Total RNA (10µg) was prepared in a final volume of 27µl and the probe was hybridised, isolated and detected as described in section 2.2.2. It should be noted that RNA was only extracted from those cells surviving in the presence of a greater than 10-fold reduction in UBF levels. Before RNA was extracted the cells were washed multiple times to remove any dead floating cells to ensure that only RNA from surviving cells was analysed.

We initially tested RNA from UBFKD cells treated with 1µg/ml doxycycline for 48, 96 and 144 hours, to determine if almost complete abolition of UBF levels impacted on the rate of rDNA transcription. HT1080 and *E.coli* RNA were used a controls to demonstrate normal rDNA transcription levels and complete digestion of non-hybridised probe, respectively, under the assay conditions used. Using the 5' end probe we were able to reveal that depleting UBF by greater than 10-fold had no impact on the levels of on-going transcription (Figure 3.9 (A)). We then analysed if there was any effect on the rate of rDNA transcription in the 2ng UBFKD cells, which we know are proliferating at a similar rate to the parental cell line except the endogenous UBF levels are down 4.5-fold. The S1 nuclease protection assay was performed using RNA extracted from the 2ng UBFKD cells and the 5' end probe, with HT1080 and *E.coli* RNA as controls again. The S1 assay reveals that there is no impact on efficient rDNA transcription when UBF levels are reduced 4.5-fold (Figure 3.9 (B)).

Having established that there is no impact on the rate of rDNA transcription as a consequence of UBF depletion we then wanted to determine if there was any effect on pre-rRNA processing. It is important to analyse the efficiency of pre-rRNA processing as defects could result in the accumulation or stabilisation of uncleaved 47S pre-rRNA transcripts, thereby giving an apparent increase in the rate of rDNA transcription. To assess the impact of UBF depletion on pre-rRNA processing, the efficiency of processing at the A' primary cleavage site was determined by S1 nuclease protection assays (Figure 3.8 (B)). Cleavage at the A' site, at nucleotide +414 of the pre-rRNA transcript (Kass et al., 1987), is the earliest U3-snoRNP-dependent cleavage event in pre-rRNA processing.

RNA samples from UBFKD+1µg/ml doxycycline cells and the 2ng UBFKD cells were used again and hybridised with the A' cleavage probe. The full-length hybridised probe and the truncated probe represent the uncleaved and A' cleaved transcripts, respectively. The ratio of these signals provides a measure of the efficiency of cleavage and the combined signal can be used as a measure of the level of on-going rDNA transcription. In the HT1080 control we observe that the majority of transcripts are cleaved. Interestingly, depleting cellular levels of UBF by greater than 10-fold or by 4.5-fold does not affect the ratio of uncleaved to cleaved when compared to control (Figure 3.9 (C) & (D), respectively). This suggests that not only does lowering UBF levels not impact on the rate of rDNA transcription, but also has no effect on the efficiency of pre-rRNA processing.

These S1 assays also confirm that the structures, reminiscent of Act D nucleolar caps, observed by EM in UBF+1µg/ml doxycycline nucleoli are not due to rDNA transcription inhibition.

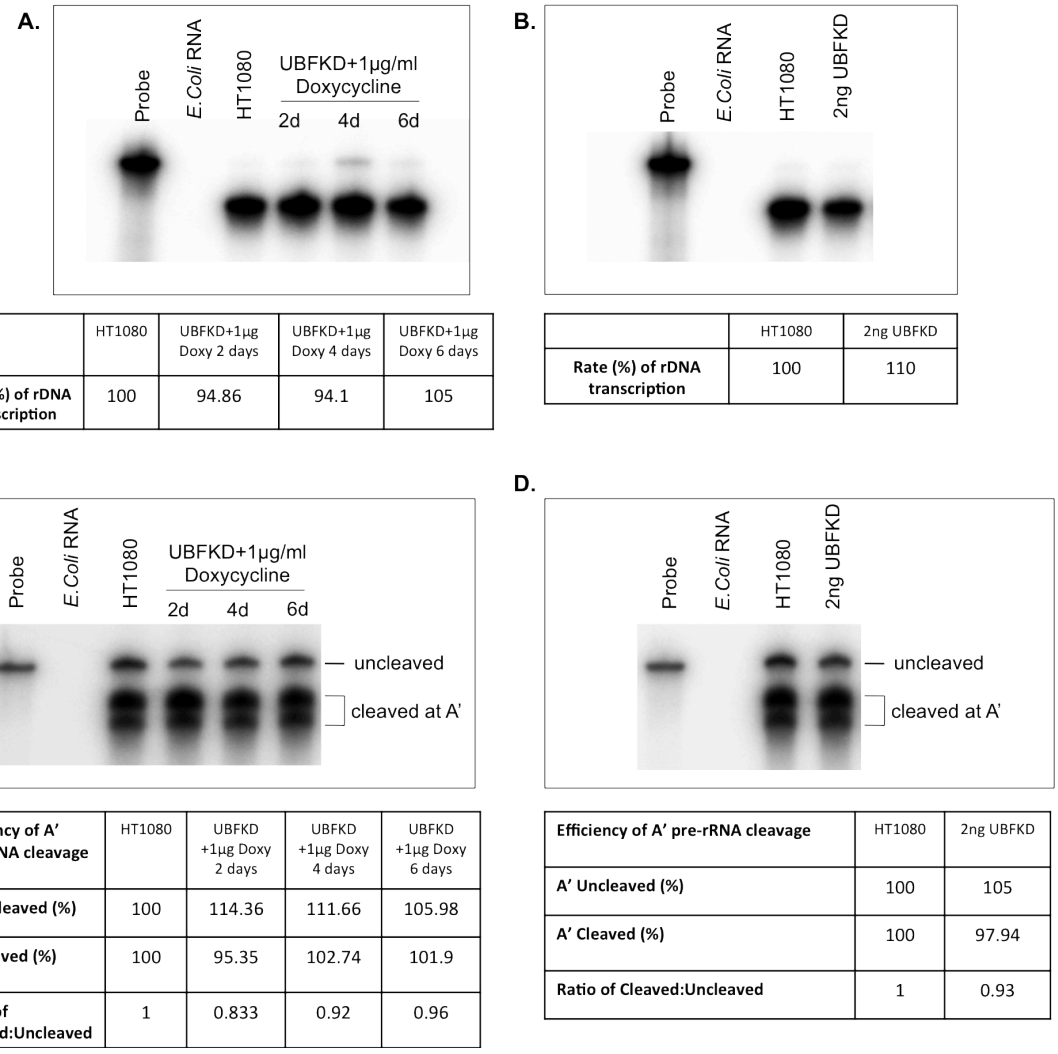

	HT1080	UBFKD+1µg Doxy 2 days	UBFKD+1µg Doxy 4 days	UBFKD+1µg Doxy 6 days
Rate (%) of rDNA transcription	100	94.86	94.1	105

	HT1080	2ng UBFKD
Rate (%) of rDNA transcription	100	110

Efficiency of A' pre-rRNA cleavage	HT1080	UBFKD +1µg Doxy 2 days	UBFKD +1µg Doxy 4 days	UBFKD +1µg Doxy 6 days
A' Uncleaved (%)	100	114.36	111.66	105.98
A' Cleaved (%)	100	95.35	102.74	101.9
Ratio of Cleaved:Uncleaved	1	0.833	0.92	0.96

Efficiency of A' pre-rRNA cleavage	HT1080	2ng UBFKD
A' Uncleaved (%)	100	105
A' Cleaved (%)	100	97.94
Ratio of Cleaved:Uncleaved	1	0.93

Figure 3.9 S1 protection assays reveal that depleting UBF has no significant impact on rDNA transcription and pre-rRNA processing

(A) & (B) S1 assays were performed with the 5'-endogenous probe and RNA was extracted from UBFKD cells treated with 1µg/ml Doxycycline for 2, 4 and 6 days (A) and 2ng UBFKD cells (B) as outlined in section 2.2.1. RNA from HT1080 was used as a control to indicate complete cellular rDNA transcription levels. *E.coli* RNA was used as an addition control to demonstrate complete digestion of non-hybridised probe. The initial starting 5' endogenous labelled probe was run in parallel (first lane in (A) & (B)).
(C) & (D) S1 assays were performed using the A' cleavage probe and RNA was extracted from UBFKD cells treated with 1µg/ml Doxycycline for 2, 4 and 6 days (C) and 2ng UBFKD cells (D) and the same controls were used as described above. The initial starting A' cleavage labelled probe was run in parallel (first lane in (C) & (D)). Uncleaved or cleaved transcripts at the A' site are labelled.

3.3 Discussion

The open chromatin state of active NORs on metaphase chromosomes correlates with the presence of a secondary constriction and extensive UBF binding. Work in the pseudo-NOR cell line has demonstrated that UBF binding can induce an open chromatin state, visualised as a novel secondary constriction on metaphase chromosomes (Mais et al., 2005). I hypothesise that UBF is causal in the formation of secondary constrictions. To test this hypothesis I made use of an inducible UBF shRNA human cell line, UBFKD. The main objective of the work described in this chapter was to characterise this UBFKD cell line and establish conditions whereby I can deplete a significant proportion of endogenous UBF without inducing severe growth defects. By generating such conditions I will be able to utilise these cells in the following chapter and analyse the effect that reduced UBF levels have on the rDNA chromatin state.

Chronic knockdown of UBF in the UBFKD cell line, using 1μg/ml doxycycline, resulted in the redistribution of nucleolar proteins, changes in nucleolar morphology, growth arrest and apoptotic cell death. In contrast I have demonstrated that a 4.5-fold reduction in UBF levels, using 2ng/ml doxycycline, does not impact severely on cell growth, in fact these 2ng UBFKD cells proliferate at a similar rate to the UBFKD and parental HT1080 cell lines. Moreover the 2ng UBFKD can be maintained with this 4.5-fold reduction in cellular UBF for an extended period. The 2ng UBFKD cells are not a stable cell line and after ~10 weeks of culturing in 2ng/ml doxycycline the cells show signs of becoming resistant to the effects of the UBF shRNA. However the extended time at which these 2ng UBFKD cells can sustain lower cellular levels of UBF is sufficient for us to conduct the experiments required. These 2ng UBFKD cells provide an ideal model for analysing the effect of reduced UBF levels on the rDNA chromatin state, which is analysed in the following chapter.

By characterising the UBFKD cell line I observed interesting consequences as a result of UBF depletion. Firstly chronic depletion of UBF, using 1μg/ml doxycycline, resulted in the *in vivo* redistribution of the nucleolar proteins, fibrillarin, RAF49 and RPA43, from the nucleolus to nucleoplasm. The redistribution of the RNA Pol I specific subunits, RAF49 and RPA43, may be explained by the fact that recruitment of these proteins has been demonstrated in the pseudo-NOR cell line to be UBF-dependent (Mais et al., 2005, Prieto and McStay, 2007). Additionally PAF49 has been shown to directly interact with UBF (Hanada et al., 1996, Meraner et al., 2006). There is no evidence for UBF-dependent recruitment of fibrillarin or a direct interaction between these proteins, yet redistribution of fibrillarin from the nucleolus is evident as a result of UBF depletion. The pattern for fibrillarin redistribution is somewhat different to that of the RNA Pol I subunits. Fibrillarin accumulates at the periphery of the nucleolus initially before diffusing out to the nucleoplasm. The time point at which I have detected apoptotic cell death in UBFKD cells treated with 1μg/ml doxycycline, that is 72hrs after UBF shRNA induction, correlates with the

same time point that fibrillarin is observed to diffuse from the nucleolus. This suggests that redistribution of fibrillarin may be as a result of the nucleolus falling apart, which leads to cell death. In the literature it has been demonstrated that the irreversible disassembly of nucleoli during apoptosis correlates with the redistribution of fibrillarin from the nucleolus (Soldani et al., 2009).

A second finding, as a result of lowering cellular UBF levels, was changes to the nucleolar morphology. Parental HT1080 and non-treated UBFKD cells have dispersed irregular shaped nucleoli and often the nucleoli are indistinguishable from each other. In contrast nucleoli from UBFKD cells, with either a 4.5-fold or greater than 10-fold reduction in UBF levels, appeared as prominent, circular shaped structures. These morphological changes are reminiscent of HT1080 cells treated with the protein kinase A agonist 8-chloro-cAMP (Krystosek, 1998). Krystosek observed that the reverse transformation of the HT1080 malignant cell line with 8-chloro-cAMP correlated with growth inhibition and formation of prominent nucleoli. This 8-chloro-cAMP study compares with what we are observing in the 1µg/ml doxycycline treated UBFKD cells, that is growth arrest correlating with the formation of prominent nucleoli. However it does not explain why we observe changes in nucleolar morphology in the 2ng UBFKD cells, which have a 4.5-fold reduction in UBF levels, but proliferate at the same rate as parental cells. TEM experiments did not reveal any obvious changes in the nucleolar sub-compartments of the 2ng UBFKD nucleoli when compared to HT1080 nucleoli. TEM images did reveal the present of cap-like structures, reminiscent of ActD nucleolar caps, in UBF+1µg/ml doxycycline nucleoli. ActD treatment induces rDNA transcription inhibition, however I have demonstrated, and discuss below, that these cap-like structures observed in the UBFKD+1µg/ml doxycycline nucleoli cannot be due to transcription inhibition.

One of the most striking observations was that there was no impact on the rate of rDNA transcription or the efficiency of pre-rRNA processing in the 2ng UBFKD cells or the UBFKD+1µg/ml doxycycline cells. These findings are consistent with work published from the Hannan lab. They demonstrate that RNAi-mediated depletion of UBF in the mouse NIH3T3 cells resulted in only a minor decrease in the rate of rDNA transcription despite the fact that the number of active rDNA repeats had decreased significantly (Sanij et al., 2008). This implies that the remaining active repeats must be hyper-activated to sustain normal transcription levels.

In the UBFKD+1µg/ml doxycycline cells the endogenous UBF is reduced by greater than 10-fold, the cells arrest and eventually die by apoptosis, yet the rate of rDNA transcription is sustained at normal levels. This observation can be explained by the fact that we take care to only extract RNA from surviving cells. This is achieved by washing the cells multiple times to remove any dead cells, with only attached cells remaining when conducting the RNA extraction. The normal levels of transcription are sustained in these surviving cells depleted of UBF most likely by hyper-activation of remaining active repeats as described in (Sanij et al., 2008).

I have demonstrated that chronic depletion of UBF results in apoptotic cell death, but how and when apoptosis is triggered is unknown. One theory is that the hyper-activation of rDNA transcription from the remaining active rDNA repeats in UBF depleted cells, as discussed above, cannot be sustained indefinitely. Eventually ribosome production goes below a critical threshold and apoptotic death is triggered. The second theory takes into account our knowledge that UBF remains bound to NORs during mitosis. Hence, this implies that UBF is necessary to propagate the activity status of an NOR faithfully through cell division, thereby acting as a memory marker for the reactivation of NORs in daughter cells when rDNA transcription resumes. Therefore it may be the case that UBFKD+1μg/ml doxycycline cells do not have the required levels of UBF to propagate the activity status of NORs through mitosis to daughter cells. Hence in the absence of UBF, reactivation of rDNA transcription cannot occur at these daughter NORs and the cells die because ribosome biogenesis is compromised.

Work in this chapter and that from the UBF knockout mouse model in Tom Moss's lab has demonstrated that UBF is an essential protein. I will make use of the 2ng UBFKD cells, which sustain a 4.5-fold reduction in UBF levels for an extended period of time, to investigate the consequence of reduced UBF levels on the rDNA chromatin *in vivo*.

4 UBF is required to maintain the open chromatin state associated with active NORs

4.1 Background

Only approximately half of the rRNA genes are transcriptionally active at any given time. This is at odds with the number of silent NORs observed at the chromosomal level, suggesting the NORs are a mixture of active and silent rDNA repeats. Based on the transcriptional activity of rRNA genes, rDNA chromatin can exist in one of two states. Psoralen cross-linking experiments have revealed that the transcribed regions active rDNA repeats adopt a euchromatic state devoid of regularly spaced nucleosomes. Inactive genes on the other hand are inaccessible to psoralen, display regularly spaced nucleosomes and associated with a heterochromatic state (Conconi et al., 1989). Psoralen crosslinking experiments performed in a number of different organisms reveal that the two classes of rDNA chromatin co-exist in growing cells.

On metaphase chromosomes active NORs appear as gaps in the chromosomes and are termed secondary constrictions. The rDNA chromatin at these secondary constrictions is approximately ten-fold less condensed than the adjacent satellite DNA, resulting in reduced dye binding and hence giving rise to the apparent gap in the chromosome (Heliot et al., 1997). Often an axis of DNA, which is thought to be AT-rich DNA is found within the secondary constriction (Saitoh and Laemmli, 1994). Active NORs are associated with specific RNA Pol I factors, such as UBF, SL1/TIF-IB, TTF1 and Treacle (Jordan et al., 1996, Leung et al., 2004, Roussel et al., 1996, Roussel et al., 1993, Scheer and Rose, 1984, Valdez et al., 2004), providing compelling evidence that secondary constrictions are transcriptionally competent upon mitotic exit. The RNA Pol I components that remain bound to active NORs contain an acidic/argyophilic domain allowing the detection of active NORs by silver nitrate staining (Bloom and Goodpasture, 1976).

The rDNA of inactive NORs is packaged in a heterochromatic state and therefore indistinguishable from the adjacent satellite DNA, hence silent NORs do not form secondary constrictions on metaphase chromosomes. Furthermore, silent NORs are not positive for silver staining and this is due to the absence of components of the RNA Pol I machinery. During interphase silent NORs are visualised as condensed foci, which lack the association of any of the RNA Pol I machinery (Figure 4.1) (McStay and Grummt, 2008).

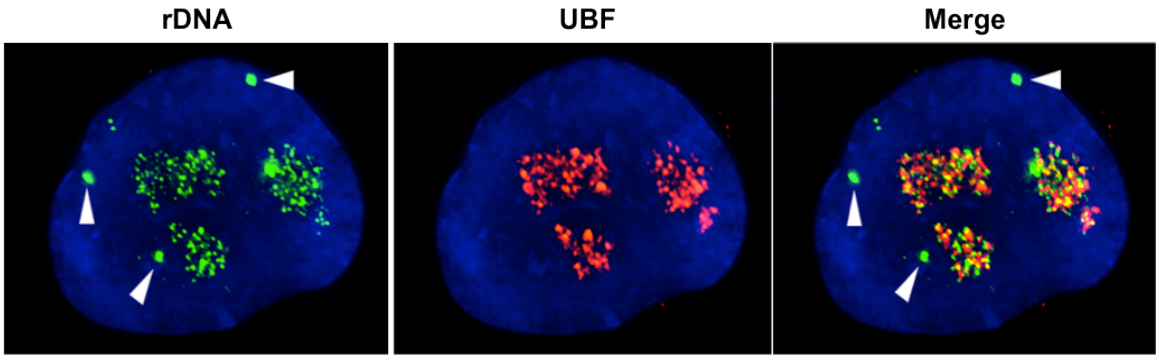

Figure 4.1 Silent NORs are visualised as condensed rDNA foci devoid of UBF
An interphase HeLa cell was subjected to 3D-immunoFISH to reveal the localisation of rDNA and UBF. The 11.9-kb rDNA probe labelled spectrum green is used to visualise the rDNA and UBF is visualised using α-hUBF antibodies followed by incubation with rhodamine coupled α-human antibodies (red). Silent NORs, indicated by arrowheads, appear as condensed rDNA foci dissociated from nucleoli and devoid of UBF. Figure from (McStay and Grummt, 2008).

The fact that UBF binds across the entire rDNA repeat (O'Sullivan et al., 2002) and remains associated with secondary constrictions on mitotic NORs (Roussel et al., 1993) suggests that it may be involved in inducing the open chromatin state of active NORs. The pseudo-NORs have provided compelling evidence that extensive UBF binding can induce the formation of secondary constrictions (Mais et al., 2005). The formation of secondary constrictions, as a result of extensive UBF binding, may be due to the fact that UBF and linker histone H1 binding is mutually exclusive. Linker histone H1 binds to nucleosomes and is involved in stabilising the compact higher order chromatin structures. UBF has been shown to displace linker histone H1 *in vitro* suggesting that it plays a role in promoting decompaction of chromatin *in vivo* (Kermekchiev et al., 1997). In support of this theory, *in vivo* biochemical studies in mouse have demonstrated that RNAi-mediated depletion of UBF results in an increase in the levels of linker histone H1 on rDNA (Sanij et al., 2008).

The decompaction of chromatin as a consequence of extensive UBF binding in the pseudo-NOR cell line led us to hypothesise that UBF is required to maintain the open chromatin state associated with active NORs throughout the cell cycle. To test this hypothesis I analysed the effect on rDNA chromatin *in vivo* in the 2ng UBFKD cells, which have a 4.5-fold reduction in UBF cellular levels. Additionally I analysed the effect *in vivo* of RNAi-mediated depletion of UBF in the karyotypically normal human cell line hTERT RPE-1.

The most defining feature of active NORs is their appearance as secondary constrictions on metaphase chromosomes. To establish if UBF is required to maintain the decondensed chromatin state associated with secondary constrictions I analysed the consequence of UBF depletion at the chromosomal level. To study changes in the chromosomal features of secondary constrictions I employed the rat kangaroo *Potorous tridactylus* (PtK) cell line. The reasoning for selecting this marsupial PtK cell line is due to their secondary constriction being larger and

easier to visualise on metaphase chromosomes than those of human cells. Therefore these cells provide a more convenient model system to study the effect of UBF depletion on the maintenance of the open chromatin state associated with secondary constriction.

4.2 Results

4.2.1 Reduction in cellular levels of UBF results in rDNA chromatin condensation *in vivo*

In the previous chapter I established conditions in which I could deplete endogenous UBF levels by 4.5-fold without impacting on cell growth or the efficiency of rDNA transcription and processing when compared to parental HT1080 cell line. These 2ng UBFKD cells provide an ideal cell model to analyse the rDNA chromatin state of cells that survive with minimum cellular levels of UBF. To analyse the effect on rDNA chromatin *in vivo*, as a consequence of reduced UBF levels, 3D-immunoFISH (fluorescence in situ hybridisation) experiments were performed on cells fixed with 4% paraformaldehyde (PFA) from 2ng UBFKD cells and the parental HT1080 cells. In contrast to fixation with organic solvents, which dehydrate the cell, fixation with the cross-linking reagent PFA forms molecular bridges, thereby preserving the cells structure. Human rDNA was visualised using an 11.9-kb Eco-RI restriction fragment, labelled with spectrum green, that contains human intergenic spacer sequence immediately upstream of the promoter. Nucleoli were visualised using antibodies against the nucleolar protein fibrillarin.

A characteristic of the HT1080 human cell line is that all the NORs appear to be active. In the control HT1080 cells the rDNA is observed as punctate staining dispersed throughout the nucleolus (top row, Figure 4.2). The dispersed pattern for rDNA staining is indicative of active decondensed rRNA genes. The pattern of rDNA staining observed in the 2ng UBFKD cells is strikingly different (bottom row, Figure 4.2). The 4.5-fold reduction in the levels of cellular UBF in the 2ng UBFKD cells results in the rDNA chromatin now appearing as large condensed foci on the periphery of the nucleolus. Moreover, silent NORs dissociated from nucleoli are evident. These silent NORs are reminiscent of the condensed foci associated with silent NORs in HeLa cells (Figure 4.1). Despite the fact that both the HT1080 control cells and the 2ng UBFKD cells are proliferating at a similar rate there is a definite contrast in the organisation of their rDNA chromatin.

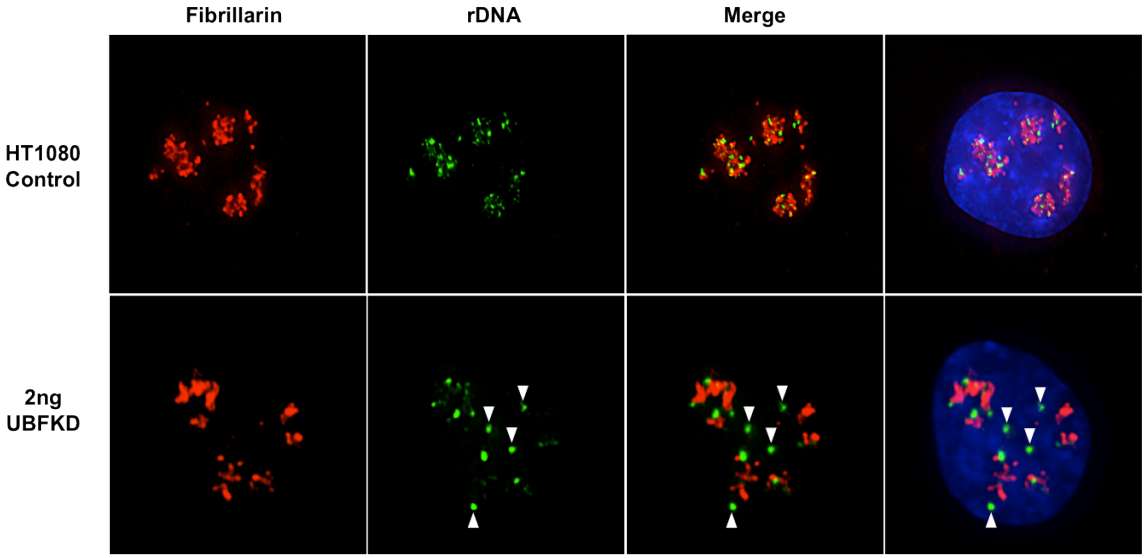

Figure 4.2 3D-immunoFISH reveals that depletion of UBF results in rDNA chromatin condensation *in vivo*
HT1080 and 2ng UBFKD cells were subjected to 3D-immunoFISH as outlined in section 2.3.11. Nucleoli were revealed using α-fibrillarin antibodies followed by incubation with rhodamine coupled α-mouse antibodies (red). The rDNA was visualised by hybridisation with the 11.9-kb EcoRI fragment, which contains the intergenic spacer region immediately upstream of the promoter, labelled with spectrum green. In HT1080 control cells (top row) the rDNA is visualised as punctate staining dispersed within the nucleolus. Reduced UBF levels cause the rDNA chromatin to condense (bottom row) and appear as large foci. Silent NORs are also evident as condensed rDNA foci dissociated from nucleoli (arrowheads indicate silent NORs).

4.2.2 Reduction in UBF levels results in an increase in the proportion of silent NORs *in vivo* in the karyotypically normal human hTERT RPE-1 cell line

To reinforce the findings in the 2ng UBFKD cells, that UBF is required for maintaining the open chromatin state of rDNA *in vivo*, I decided to analyse the consequences of UBF depletion in a different cell model. I selected the hTERT RPE-1 (retinal pigment epithelial) human cell line because it is a non-transformed cell line and karyotypically normal, thus contains 10 NORs. Furthermore, checkpoints such as p53 are intact.

UBF is an extremely abundant protein, therefore time was invested in generating optimal conditions to deplete a significant proportion of endogenous UBF by siRNA. I established that the most efficient transfection conditions for RPE-1 cells are performed in a 6-well plate using a 1:5 ratio of smartpool duplex human UBF siRNAs (μg) to TransMessenger (Qiagen) reagent (μl). Due to the abundance and stability of UBF two rounds of siRNA transfections were performed. RPE-1 cells were seeded out at low density and the initial transfection was performed on cells at approximately 50-60% confluence. A second round of transfection was performed 48hrs later and the cells were analysed 24hr after the second transfection. The efficiency of UBF knockdown was determined by western blotting. The cells were harvested, resuspended in Laemmli buffer and loaded onto NuPAGE gels. In parallel protein samples were prepared from cells that were transfected with control siRNA under the same conditions used

for the UBF siRNAs. The control siRNA, si934Scr, was originally described in (Henning et al., 2003) and its sequence corresponds to a scrambled sequence of the mouse and human nucleolar protein, RNA helicase II/Guα.

To ensure equal loading the electrophoresed protein samples were stained with coomaisse blue or the membrane was stained with Ponceau after transfer to visualise the intensity of protein bands (Figure 4.3 (A)). The membrane was incubated with α-hUBF antibodies and α-hRPA43 antibodies. The RPA43 band intensity reveals that there is no overall global change in the RNA Pol I subunits as a consequence of RNAi-mediated depletion of UBF (Figure 4.3 (B)). Comparing the band intensity for UBF between the control siRNA and the UBF siRNA, using GeneTools software (Syngene), suggests that UBF levels have been depleted 5.3-fold (Figure 4.3 (B)).

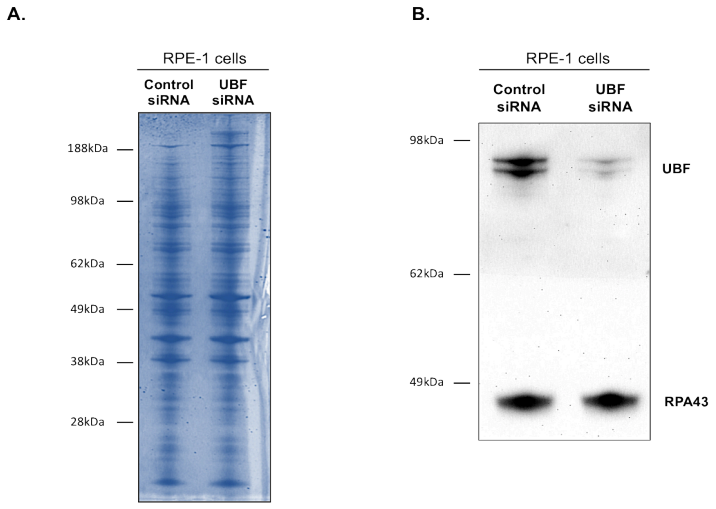

Figure 4.3 RNAi-mediated depletion of UBF in RPE-1 human cells
RPE-1 cells were treated with control si934Scr or human UBF siRNAs. Transfections were performed in a 6-well plate using a 1:5 ratio of siRNA(μg) to TransMessenger reagent (μl). Two rounds of siRNA transfections were performed 24hrs and 72hrs after cells were seeded. Cells were harvested 24hrs after second transfection and lysed in Laemmli sample buffer. Samples were loaded on NuPAGE gel in duplicate and stained with coomassie blue (A) or transferred to membrane and probed with α-hUBF antibodies and α-RPA43 antibodies (B). The protein gel (A) reveals that an equal quantity of protein was loaded for the control and UBF depleted samples. Immunoblotting with α-hUBF antibodies reveals that the UBF siRNA transfection efficiently reduced cellular UBF levels (B). The RPA43 bands indicate that depletion of UBF has no impact in global levels of RNA Pol I subunits (B).

To analyse the consequence of UBF depletion on the rDNA chromatin state of these karyotypically normal cells I repeated the siRNA transfections using the control and UBF siRNA oligonucleotides and the same conditions described above. 6hrs after the second siRNA transfection was added the cells were trypsinised and seeded out on Superfrost® Plus microscopy slides. 3D-immunoFISH was carried out on preserved nuclei from RPE-1 cells treated with control and UBF siRNAs using the 11.9-kb rDNA probe spectrum labelled red and antibodies against the nucleolar protein fibrillarin. In control cells the rDNA is visualised as punctate staining within the nucleolus, which is indicative of active decondensed rRNA genes

(Figure 4.4 (A)). From our experience, all the NORs of RPE-1 cells appear to be active and are located within nucleoli.

Upon RNAi-mediated UBF depletion we observe the same change in the pattern of rDNA staining that was observed in the 2ng UBFKD cells. The rDNA chromatin has become more condensed, appearing as large rDNA foci, some of which have dissociated from nucleoli (silent NORs indicated by arrowheads in Figure 4.4 (B)). Changes in nucleolar morphology are also evident in RPE-1 cells with reduced UBF levels. In contrast to control nucleoli, which are dispersed and irregular in shape (Figure 4.4 (A)), the nucleoli in UBF siRNA treated cells are more circular. In some transfected cells not only has the nucleolar morphology changed but also the pattern for fibrillarin staining (bottom row, Figure 4.4 (B)). Fibrillarin staining in these cells is somewhat reminiscent of cells that have been treated with ActD, suggestive that rDNA transcription is shutting down and this is discussed more in the latter part of this chapter.

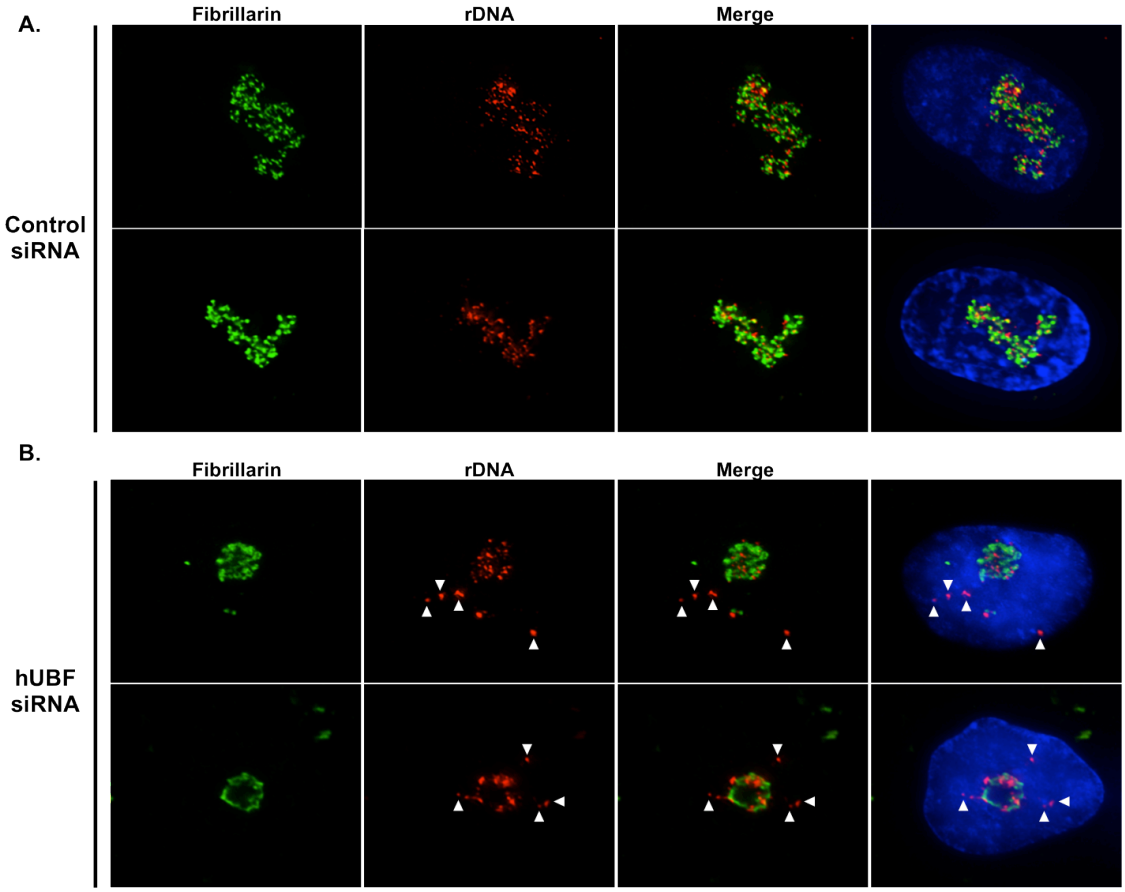

Figure 4.4 Reducing cellular levels of UBF results in rDNA chromatin condensation in RPE-1 human cells

RPE-1 cells were treated with control si934Scr or human UBF siRNAs, using conditions described in figure legend 4.3, were subjected to 3D-immunoFISH as outlined in section 2.3.11. Nucleoli were revealed using α-fibrillarin antibodies followed by incubation with FITC coupled α-mouse antibodies (green). rDNA was visualises by hybridisation with the 11.9-kb EcoRI rDNA fragment labelled with spectrum red. (A) Control RPE-1 cells reveal the characteristic punctate staining for rDNA indicative of open active rDNA chromatin (red). All the rDNA is localised within nucleoli. (B) RPE-1 cells transfected with human UBF siRNAs results in condensation of the rDNA chromatin. Silent NORs are now apparent as condensed rDNA foci dissociated from nucleoli. Arrowheads indicate silent NORs.

Using the 11.9-kb rDNA probe we observed an increase in the number of silent NORs as a consequence of UBF depletion. However this probe does not allow us to discriminate between individual NORs preventing us from counting the number of NORs that become silenced as a consequence of UBF depletion. The most logical method of overcoming this problem is to use a marker that is adjacent to the NOR. In the lab Prof. Brian McStay has identified a sequence distal to the NOR, meaning between the NOR and the telomere. He has demonstrated that this sequence is shared among all the human acrocentric chromosomes (Figure 4.5) (unpublished data from Brian McStay). This DNA probe that hybridises to this distal junction (DJ) provides a powerful tool to distinguish and count individual NORs. The NORs in human cells are located on the short arms of the five acrocentric chromosomes, hence in a karyotypically normal human diploid cell, like RPE-1 cells, one would expect to observe 10 DJ foci.

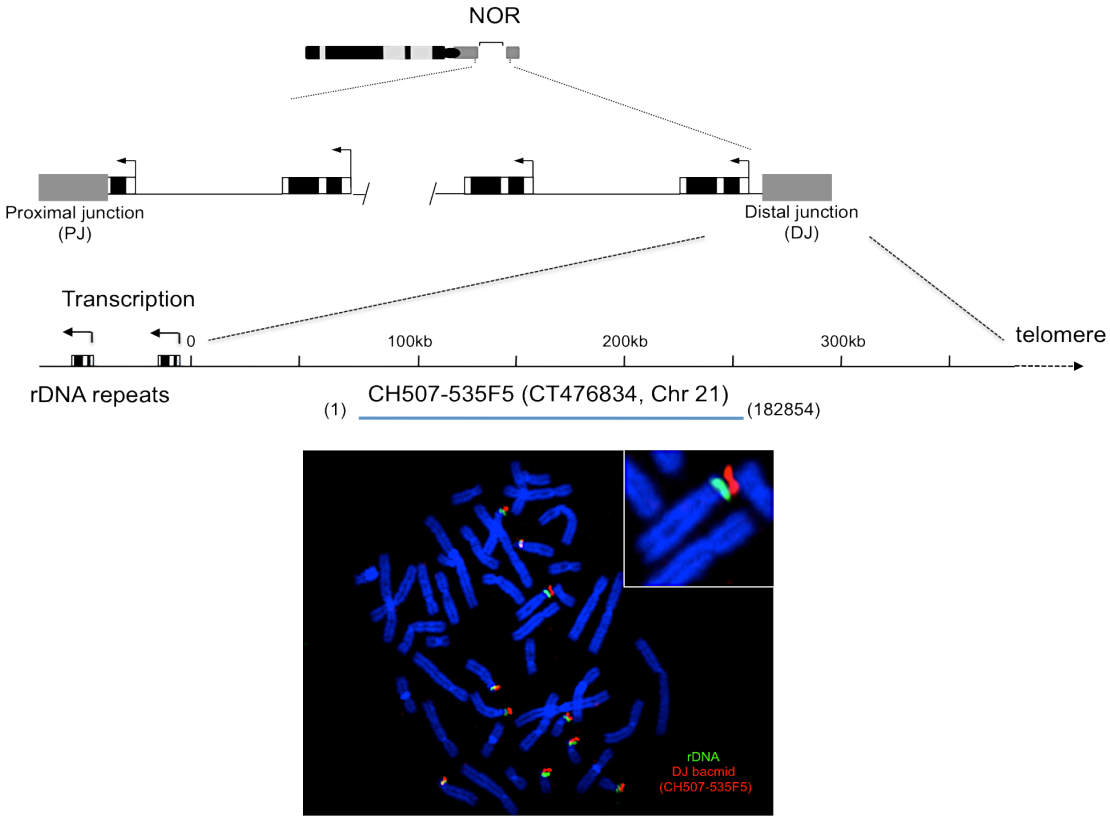

Figure 4.5 Location of the Distal Junction
The schematic at the top indicates the positioning of the distal junction (DJ), that is between the NOR and the telomere. The DJ region is enlarged to show the location of the sequence from DJ bacmid CH507-535F5. The sequence of the DJ is shared among all human acrocentric chromosomes. The chromosome spread depicts this fact, in which human chromosomes are hybridised with the 11.9-kb rDNA probe and the DJ bacmid. rDNA is detected on the 10 acrocentric chromosomes, as is the DJ probe. In the inset image one of the acrocentric chromosomes from the spread is enlarged to demonstrate that this DJ region is located at the telomere end of the NOR (B. McStay generated this figure from his own unpublished work).

3D-immunoFISH was performed on control and UBF siRNA treated cells as described above, except the DJ probe labelled with spectrum red was employed instead of the 11.9-kb rDNA probe. As expected 10 DJ spots were identified in all the control and UBF siRNA treated RPE-1 cells (Figure 4.6). In control cells all the DJ spots are observed at the periphery of the nucleolus, which is visualised using antibodies against fibrillarin (Figure 4. 6 (A)). Cells depleted of UBF show the characteristic change in nucleolar morphology to a more circular shape as a result of reduced UBF levels (Figure 4. 6 (B)). This is in contrast to the irregular shape nucleoli observed in control cells. The DJ probe reveals that cells depleted of UBF have a number of silent NORs dissociated from nucleoli and more importantly this probe enables us to count the number of NORs that become silenced (arrowheads indicate silent NORs, Figure 4. 6 (B)). The average number of silent NORs was shifted from zero in control cells to three in UBF depletion cells (table 4.1). Again in some cells depleted of UBF the fibrillarin pattern for staining is similar to cap like structures observed in cells treated with ActD (Figure 4. 6 (C)). Why some UBF depleted cells have this pattern for fibrillarin staining is discussed later.

Probe	Control siRNA	hUBF siRNA
DJ Foci	0.2 (+/- 0.42) n=10	2.9 (+/- 0.87) n=10

Table 4.1 Increase in number of silent NORs upon UBF depletion in RPE-1 cells
The proportion of silent NORs was calculated by counting the number of dissociated NORs from nucleoli using the DJ probe in 10 RPE-1 control cells and 10 RPE-1 UBF depleted cells.

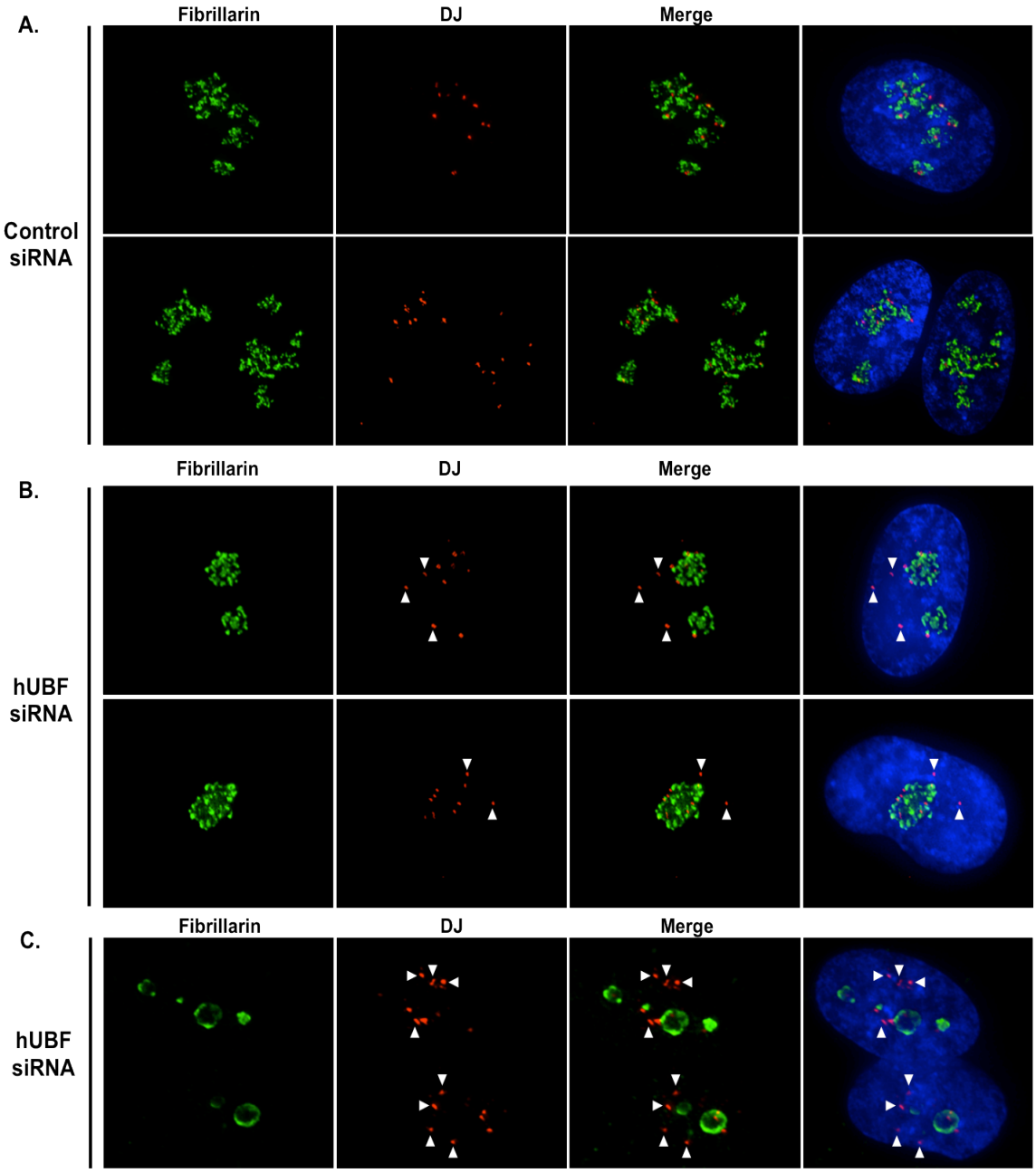

Figure 4.6 3D-immunoFISH reveals *in vivo* that reduced UBF levels in human RPE-1 cells correlates with an increase in the number of silent NORs
3D-immunoFISH was performed on RPE-1 cells treated with control si934Scr or human UBF siRNAs. Nucleoli visualised using α-fibrillarin antibodies followed by incubation with FITC coupled α-mouse antibodies (green). The DJ sequence was revealed by hybridisation with the DJ probe labelled with spectrum red. (A) Control RPE-1 cells reveal the 10 DJ foci located at the periphery of nucleoli, indication that all the NORs are active. (B) RNAi-mediated depletion of UBF in RPE-1 cells results in an increase in the number of DJ foci dissociated from nucleoli. These dissociated DJ foci represent silent NORs, indicated by arrowheads.(C) In some instances UBF siRNA treated cells display dramatic changes in the pattern of fibrillatin staining. Arrowheads indicate silent NORs.

4.2.3 UBF is required for maintaining the open rDNA chromatin state of secondary constrictions on metaphase chromosomes in the *Potorous tridactylus* male cell line

In the context of an interphase cell I have established that a reduction in UBF levels results in rDNA chromatin condensation and an increase in the number of silent NORs dissociated from nucleoli. I now wanted to analyse the effect of UBF depletion on the secondary constriction at the chromosomal level. The RPE-1 would prove a logical cell model to use, due to their normal karyotype and the fact that I have§ established efficient siRNA transfection conditions for these cells. However preparation of chromosomes from these human cells cells reveals that the secondary constrictions of active NORs cannot be reliably detected by DAPI staining. This is due to the secondary constrictions being located near the end of the acrocentric chromosomes making it difficult to distinguish if we are visualising a secondary constriction or just the end of the chromosome. The only reliable method of detecting active NORs in human cells is by silver staining.

Analysing the consequence of UBF depletion on the rDNA chromatin state associated with secondary constrictions requires a cell model in which the secondary constrictions are easily detectable on metaphase chromosomes due to the lack of DAPI staining. The rat kangaroo marsupial cell line, *Potorous tridactylis* (PtK), was chosen for these chromosomal studies. PtK_1 and PtK_2 cells are derived from the kidney tissue of a normal female and male adult *Potorous tridactylis*, respectively. These cells prove an ideal model for studying changes in chromosomal features, as their chromosomes are large in size. Additionally, all the rRNA genes in PtK cells are located on the X-chromosome, hence males have a single large NOR and females have two large NORs (Figure 4.7). The large size of the NOR in this marsupial cell line and its location in the middle of the X chromosome should provide easier visualisation of secondary constrictions in comparison to human cell lines.

A summer student in the lab, Marc Chenut, successfully cloned and sequenced both splice variants of PtK UBF. In order to visualise nucleoli in PtK cells I analysed if the nucleolar antibodies we had available in the lab would cross-react and detect the corresponding proteins in the PtK cells. α-hUBF antibodies and α-fibrillarin antibodies were both detectable in the nucleolus of PtK cells as punctate staining characteristic to that observed in human cells. Using these antibodies revealed two nucleoli in female PtK_1 cells and a single nucleolus in the male PtK_2 cells (Figure 4.8). The reason for observing a single nucleolus in male PtK cells and two in female PtK cells is due to the location of the PtK rRNA genes on the X-chromosome. The α-hUBF antibodies were also capable of detecting both splice variants of PtK UBF by western blotting.

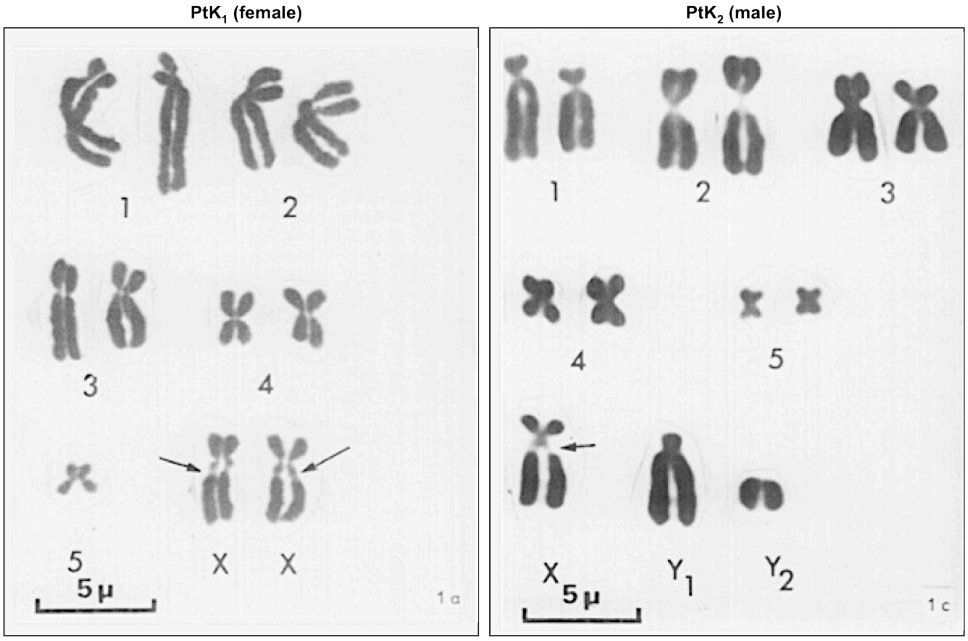

Figure 4.7 Karyotype of PtK_1 and PtK_2 cells
On the left is the female PtK_1 karyotype. The two X-chromosomes, each with a secondary constriction, are indicated by arrows. On the right the male PtK_2 karyotype. The single X-chromosome with a secondary constriction is indicated by an arrow. Figure adapted from (Berns et al., 1972).

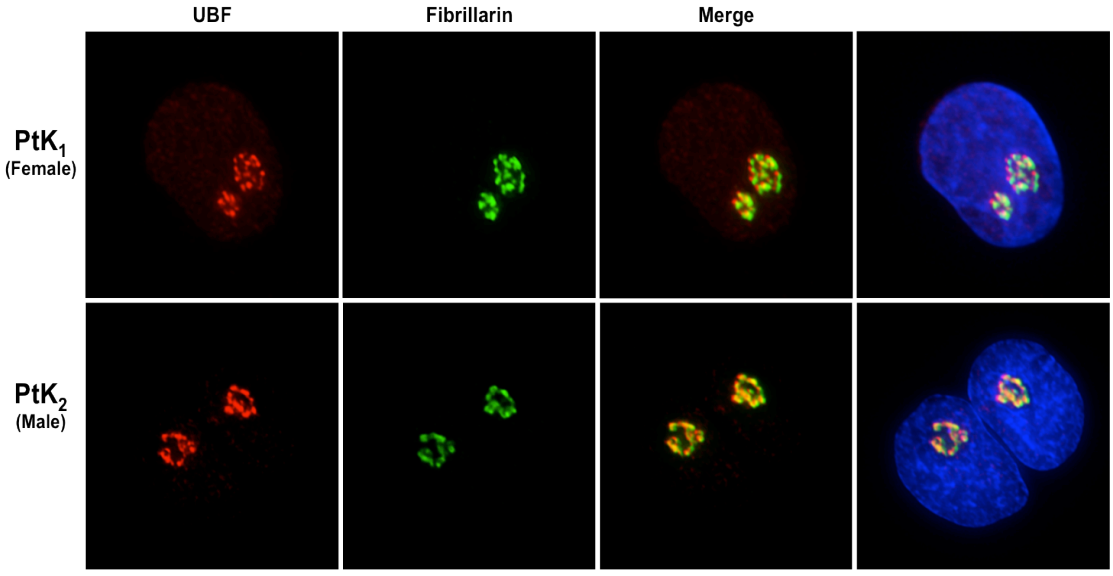

Figure 4.8 Nucleoli in the marsupial *Potorous tridactylus* (PtK) cell line are revealed using antibodies against human UBF and mouse fibrillarin
PtK_1 and PtK_2 cells were fixed, permeabilised and subjecting to immunostaining as outlined 2.3.10. PtK UBF is visualised by incubation with α-hUBF antibodies followed by incubation with rhodamine coupled α-sheep antibody and fibrillarin visualised with α-fibrillarin antibodies followed by incubation with FITC coupled α-mouse antibody. The female PtK_1 cells (top row) reveal two nucleoli, whereas the male PtK_2 cells (bottom row) have a single nucleolus.

In order to analyse the effect of UBF depletion on the chromatin state of secondary constrictions I needed to establish optimal conditions for preparing metaphase spreads. After 1hr incubation with 0.1µg/ml colchicine a relatively small proportion of the cells had arrested in mitosis. Therefore I tried 2hr incubation with 0.1µg/ml colchicine, however this longer colchicine block resulted in shorter and over condensed chromosomes, which prevented the visualisation of the large secondary constriction. I reverted back to 1hr colchicine block using a final concentration 0.1µg/ml colchicine and metaphase spreads were prepared as described in section 2.3.12, except the colchicine treated cells were harvested by scraping. Colchicine causes mitotic arrest of dividing cells by interfering with microtubule organisation, in particular the microtubules of the mitotic spindle. The prepared metaphase spreads were subjected to silver staining before mounting in DAPI.

For the male PtK_2 metaphase spreads the secondary constriction was easily identified due to the appearance of a gap in the X chromosome and this gap correlated with being positive for silver staining (arrowheads indicate NOR, Figure 4.9). Upon analysis of the female PtK_1 metaphase spreads it was clear to us that there was a dramatic variation among the spreads. Between spreads there were differences in the morphology of the chromosomes and the number of chromosomes, suggesting that the PtK_1 cells were contaminated with different cell lines. Upon studying the literature I discovered that this variation in chromosome number among metaphase spreads is a common feature of PtK_1 cells with a passage number greater than 100 (Levan, 1970). In this paper they observed that over 50% of the metaphase spreads from PtK_1 cells with a passage number greater than 100 had deviated from the normal karyotype of the PtK_1 cells (2n=11). Despite the high frequency of deviation I was able to identify PtK_1 spreads with 11 chromosomes (Figure 4.9). In these spreads two secondary constrictions were observed, both of which are associated with silver staining (arrowheads indicate NOR, Figure 4.9). Due to the variation observed among the PtK_1 chromosome spreads I conducted the rest of my experiments using the male PtK_2 cell line.

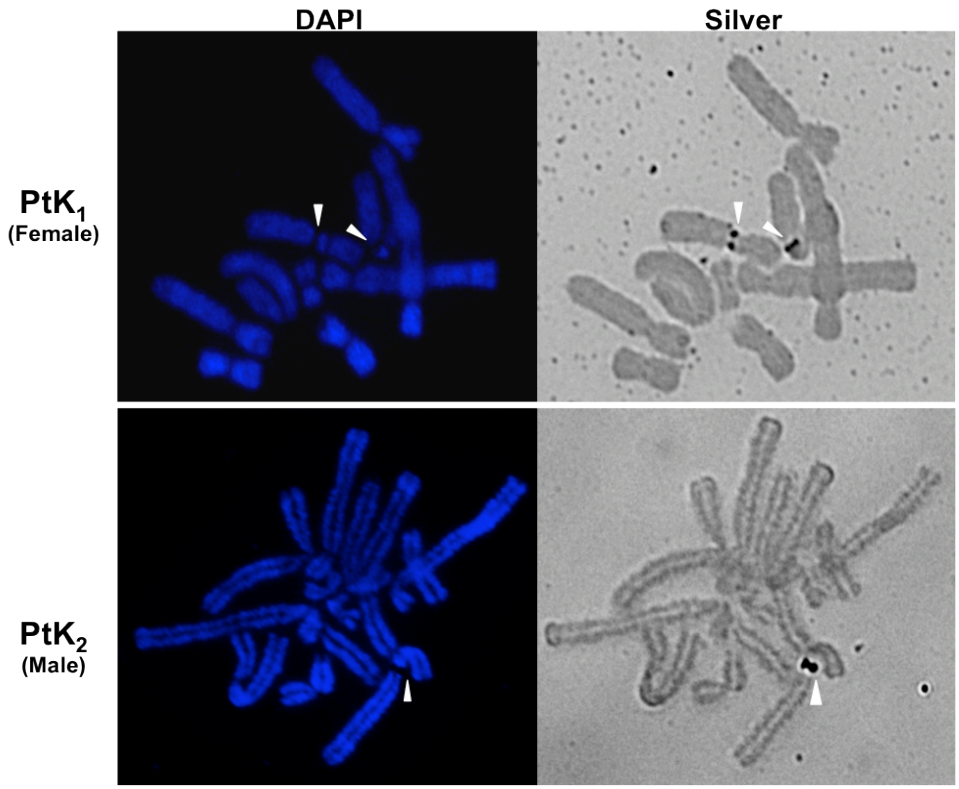

Figure 4.9 Secondary constrictions are visualised on metaphase spreads from PtK_1 and PtK_2
PtK_1 and PtK_2 cells were treated with a final concentration of 0.1µg/ml colchicine for 1hr and metaphase spreads were prepared as outlined in section 2.3.12, except mitotic cells were harvested by scraping rather than mitotic shake off. Prepared spreads were subjected to silver staining (section 2.3.14) before mounting in DAPI. In the female PtK_1 metaphase spreads (top row) the two secondary constrictions are visualised as gaps in the X-chromosomes and these secondary constrictions are positive for silver staining (indicated by arrowheads). Similarly in the male PtK_2 metaphase spread (bottom row) the single secondary constriction is observed on the X-chromosome due to lack of DAPI staining and this secondary constriction is positive for silver staining (indicated by arrowheads).

Having established that I can detect PtK_2 nucleoli using antibodies and visualise the single secondary constriction on metaphase chromosomes, I could then address the consequence of UBF depletion on the rDNA chromatin of secondary constrictions. Three siRNA oligonucleotide duplexes were ordered from Dharmacon based on the PtK UBF sequence established by Marc Chenut. As was the case for the RPE-1 cells, the generation of optimal conditions for efficient transfection of the UBF siRNA was required. Successful depletion of PtK UBF required two rounds of siRNA transfections using DharmaFECT 1 reagent and a final concentration of 20nM PtK UBF siRNA duplexes pooled together. The second round of siRNA transfection was performed 48hr after the first transfection. Transfected cells were harvested for analysis by western blotting 24hrs after second transfection. In parallel PtK_2 cells were mock transfected as a control. This mock transfection was conducted using the same conditions as for the UBF siRNA transfection, except lacked any siRNA oligonucleotides. Mock-transfected cells were harvested, lysed in sample buffer and run in parallel with UBF siRNA transfected PtK_2

cells. To ensure equal loading protein samples were loaded in duplicate and half the NuPAGE gel was stained with coomassie blue, while the remaining half was transferred to membrane and incubated with α-hUBF antibodies. The protein gel reveals that the samples harvested from the mock and UBF siRNA treated cells contained comparable levels of protein (Figure 4.10 (A)). Western blotting reveals that PtK_2 cells treated with UBF siRNAs results in a significant reduction in the endogenous levels of PtK UBF, which was quantified using GeneTools software (Syngene) to be a 50-fold reduction (Figure 4.10 (B)).

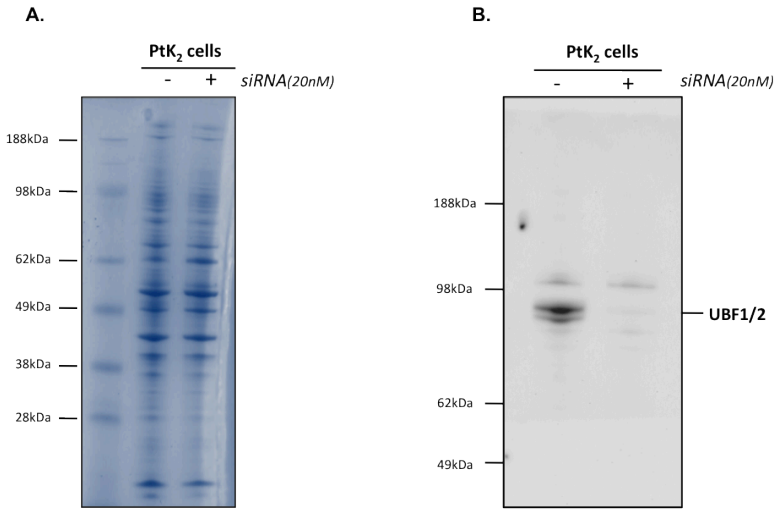

Figure 4.10 RNAi-mediated depletion of PtK UBF in PtK_2 cells
PtK_2 cells were mock transfected or transfected with PtK UBF siRNAs. Transfections were performed in 6-well plates using DharmaFECT 1 reagent and a final concentration of 20nM PtK UBF siRNAs. Two rounds of siRNA transfections were performed 24hrs and 72hrs after cells were seeded. Mock treated cells and PtK UBF siRNA transfected cells were harvested 24hrs after second transfection and lysed in Laemmli sample buffer. Samples were loaded on NuPAGE gel in duplicate and stained with coomassie blue (A) or transferred to membrane and probed with α-hUBF antibodies (B). The protein gel (A) reveals equal quantity of protein loaded for control and UBF depleted samples. Immunoblotting with α-hUBF antibodies reveals that the UBF siRNA transfection efficiently reduced cellular levels of PtK UBF (B).

The efficiency of the UBF siRNA transfection was also monitored by immunostaining. Control and UBF depleted PtK_2 cells were subjected to immunostaining using α-hUBF antibodies and α-fibrillarin antibodies. A single nucleolus is observed in the PtK_2 control cells to which both UBF and fibrillarin localise (Figure 4.11 (A)). The UBF staining is extremely faint in cells treated with PtK UBF siRNA confirming that the transfection conditions are efficiently depletion endogenous PtK UBF (Figure 4.11 (B)). Also evident in the UBF siRNA treated PtK_2 cells is a change in fibrillarin staining. The nucleolar protein appears to localise to one area of the nucleolus rather than dispersing throughout the nucleolus as seen in the control PtK_2 cells (Figure 4.11 (B)).

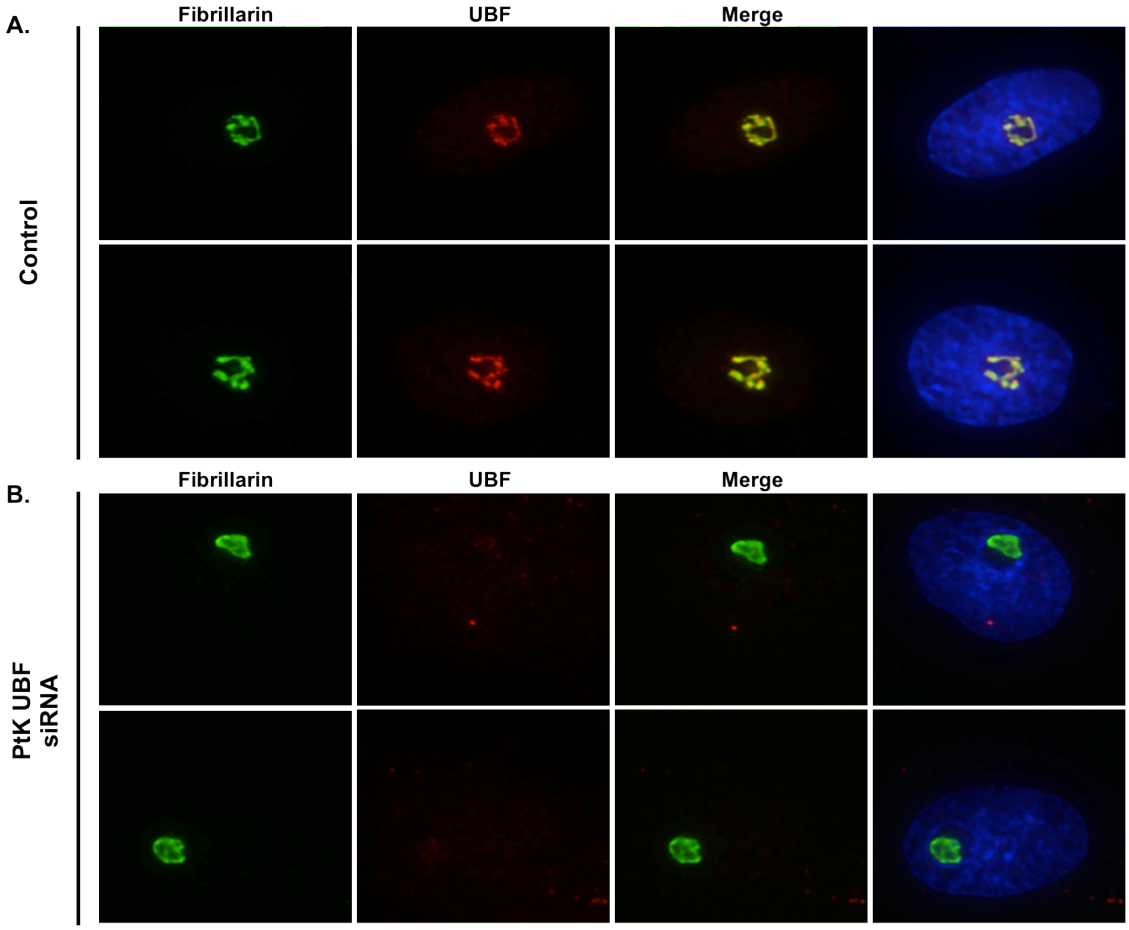

Figure 4.11 Immunostaining of UBF depleted PtK_2 cells reveals loss of PtK UBF in nucleoli
Mock and PtK UBF siRNA transfected PtK_2 cells were fixed, permeabilised and subjected to immunostaining as outlined 2.3.10. PtK UBF is visualised by incubation with α-hUBF antibodies followed by incubation with rhodamine coupled α-sheep antibody and fibrillarin visualised with α-fibrillarin antibodies followed by incubation with FITC coupled α-mouse antibody. (A) In control PtK_2 cells UBF (red) and fibrillarin (green) co-localise within the single nucleolus. (B) UBF staining is undetectable in PtK_2 cells transfected with PtK UBF siRNA. Furthermore there is a noticeable change in the distribution of fibrillarin in cells depleted of UBF. Fibrillarin appears to localise to one area of the nucleolus, this is in contrast to its localisation throughout the nucleolus in control cells.

The primary purpose for choosing the PtK model was to determine the effect that reduced UBF levels have on the rDNA chromatin state of secondary constrictions. To analyse this I repeated the siRNA transfections using the conditions described above. 24hrs after second transfection cells were harvested for protein samples or treated with colchicine to generate metaphase spreads from mock treated and UBF depleted PtK_2 cells. Metaphase spreads were examined for loss of the secondary constriction as well as loss of silver staining as a consequence of UBF depletion. The secondary constriction was easily distinguished in metaphase spreads from control cells as a gap in the X-chromosome and this gap was also positive for silver staining (arrowhead indicated NOR, Figure 4.12). The metaphase spreads analysed from PtK_2 cells depleted of UBF were negative for silver staining and there was no evidence of secondary constrictions (Figure 4.12). These results support our hypothesis that UBF depletion results in

the loss of secondary constriction, however we needed an approach to detect PtK rDNA to ensure that the spreads we were analysing contained the X-chromosome.

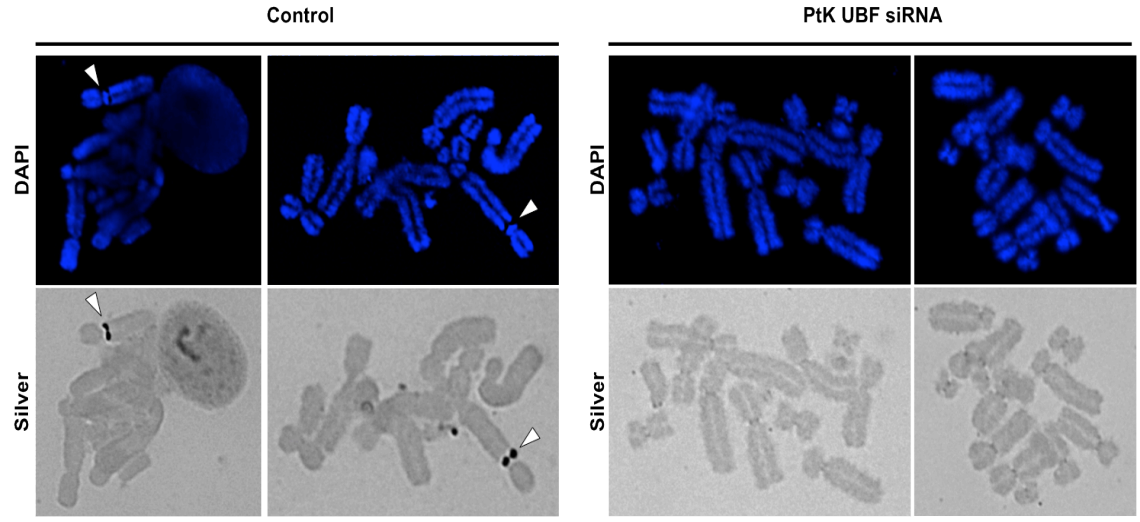

Figure 4.12 Loss of the secondary constriction and silver staining in PtK_2 cells depleted of UBF
Mock and UBF siRNA transfected PtK_2 cells were treated with a final concentration of 0.1µg/ml colchicine for 1hr and metaphase spreads were prepared from as outlined in section 2.3.12 except mitotic cells were harvested by scraping. Metaphase spreads were subjected to silver staining (section 2.3.14) before mounting in DAPI. In control PtK_2 spreads the secondary constrictions are revealed due to lack of DAPI staining, as well as being positive for silver staining (arrowheads indicate secondary constrictions). In the metaphase spreads prepared from PtK UBF siRNA treated cells there is no evidence of secondary constrictions. Additionally, silver staining does not detect any positive NORs in these UBF depleted spreads.

To identify the PtK rDNA and hence the X-chromosome in chromosome spreads we made a DNA probe that recognises a sequence within the transcribed region of PtK rDNA and labelled it with spectrum red. FISH was performed on both control and UBF depleted PtK_2 metaphase spreads. The PtK rDNA probe visualised in control metaphase chromosomes was observed to co-localise with the secondary constriction on the X-chromosome (Figure 4.13). In metaphase spreads prepared from UBF depleted PtK_2 cells the PtK rDNA probe identifies the rDNA repeats on the X-chromosome. However the region that is hybridised with the PtK rDNA probe lacks any evidence of a secondary constriction by DAPI staining. These results indicate that UBF is required for maintaining the open rDNA chromatin state associated with secondary constrictions on metaphase chromosomes.

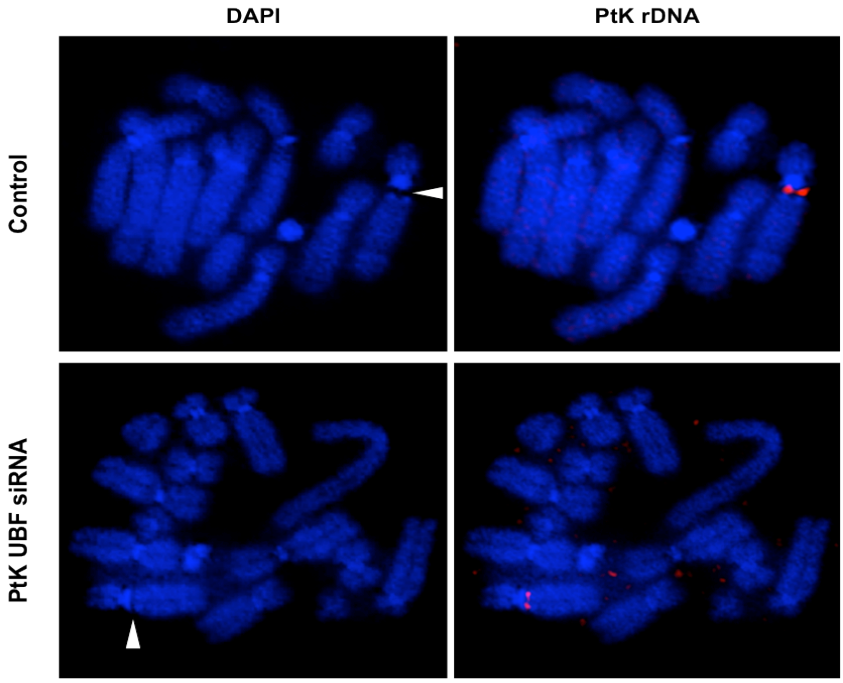

Figure 4.13 Reduction in endogenous UBF levels in PtK_2 cells results in the loss of the single secondary constriction
FISH was performed on metaphase spreads prepared from mock and UBF siRNA transfected PtK_2 cells using PtK rDNA probe labelled with spectrum red (outlined in section 2.3.14). In control metaphase spreads (top row) the secondary constriction is revealed by a gap in the X-chromosome with which the PtK rDNA probe co-localises (arrowhead indicates secondary constriction). In the metaphase spreads prepared from the PtK UBF siRNA treated cells the PtK rDNA probe indicates the positioning of the rDNA repeats on the X-chromosome, however no secondary constriction is observed to correlate with the NOR.

4.3 Discussion

At the outset we hypothesised that UBF plays a fundamental role in maintaining the open chromatin state associated with active NORs. Combining our 3D-immunoFISH and chromosomal studies we now provide convincing evidence in support of our hypothesis. In the HT1080 cell line, from which the 2ng UBFKD cells were derived, and RPE-1 cells all the NORs are associated with nucleoli and therefore appear to be active. In both cell lines we demonstrate that a reduction in UBF levels results in the condensation of rDNA chromatin and the appearance of silent NORs. It appears that when NORs become fully silenced they dissociate from the nucleolus and appear like those silent NORs observed in cell lines such as Hela (Figure 4.1). Making use of the DJ probe, which allows us to count individual NORs, we have been able to determine that on average three NORs become silenced in the RPE-1 cells as a consequence of a 5.3-fold reduction in UBF levels.

To analyse the effect of UBF depletion on the appearance of secondary constrictions we choose the PtK rat kangaroo cell model. In this marsupial cell line we observe that UBF depletion results in the loss of the decondensed chromatin state associated with secondary constrictions. Similar findings have also been demonstrated in the pseudo-NOR cell line. The pseudo-NORs

have provided one of the most valuable models for studying UBFs functioning in human cells. Published work from the pseudo-NOR model has shown that extensive UBF binding induces the formation of a large novel secondary constriction on a non-acrocentric chromosome (Mais et al., 2005). RNAi-mediated depletion of UBF in the pseudo-NOR cell line results in the loss of the novel secondary constriction, which is shown in (Figure 4.14). This result combined with the results presented in this chapter indicates that UBF binding induces the formation of secondary constrictions.

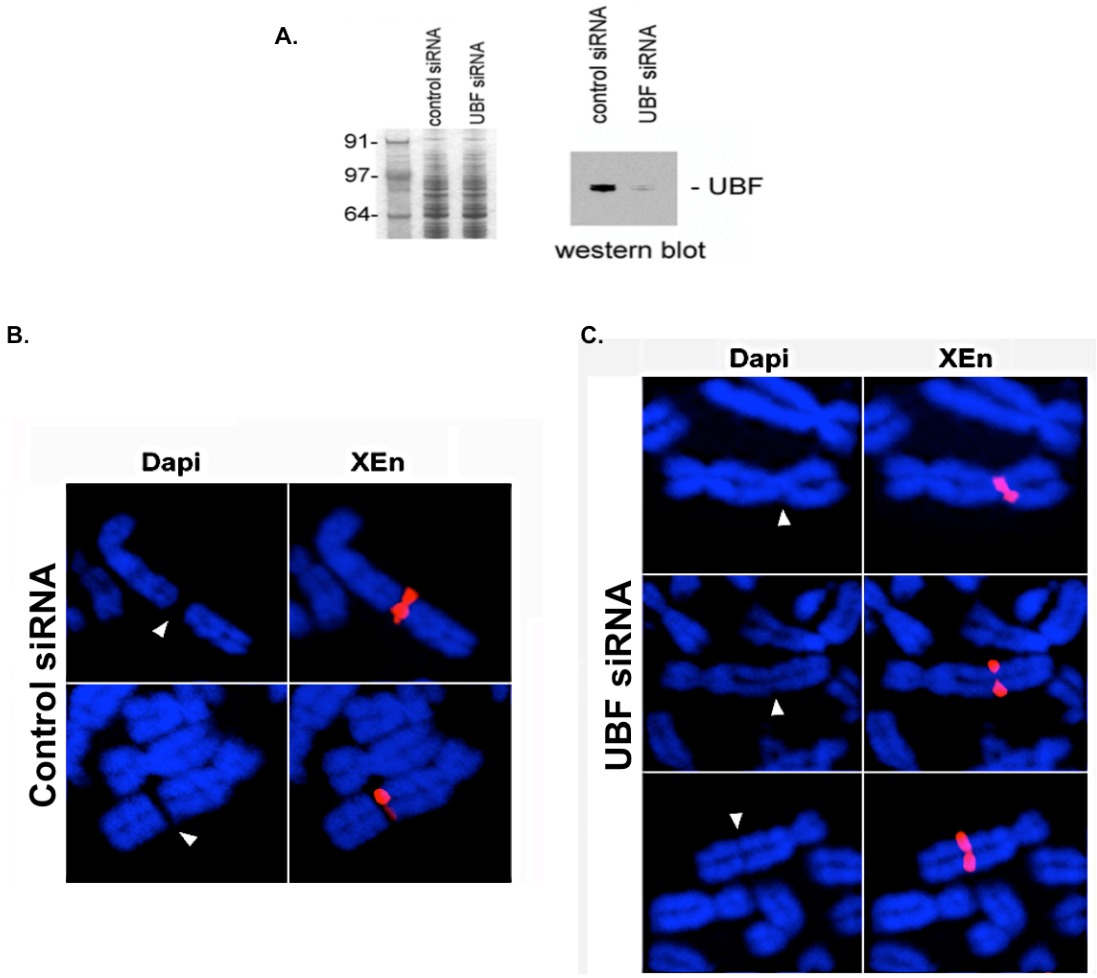

Figure 4.14 Depletion of UBF in the pseudo-NOR cell line results in the loss of the novel secondary constriction
(A) Pseudo-NOR cell line was transfected with control si934Scr or human UBF siRNAs. Transfections were performed using DharmaFECT1 reagent and a final concentration of 20nM siRNAs. Two rounds of siRNA transfections were performed 24hrs and 72hrs after cells were seeded. Protein samples from control and UBF depleted cells were loaded on NuPAGE gel. Coomassie staining indicates an equal quantity of protein was loaded for each sample and immunoblotting with α-hUBF antibodies reveals that the UBF siRNA transfection efficiently reduced cellular levels of UBF in the pseudo-NOR cell line.
(B)&(C) FISH was performed on metaphase spreads prepared from pseudo-NOR cells treated with control and UBF siRNAs using XEn DNA probe labelled with spectrum red. (A) In the control metaphase spreads the large novel secondary constriction is observed as a gap, due to lack of DAPI staining, in the non-acrocentric chromosome that is co-localised with the XEn probe (arrowheads indicate pseudo-NOR). (B) The XEn probe identifies the pseudo-NOR in the metaphase spreads prepared from UBF depleted cell. Reduction in UBF levels results in the loss of the novel secondary constriction (arrowheads indicate the loss of the novel secondary constriction). Unpublished data from José-Luis Prieto and Brian McStay.

A further interesting finding while studying chromosomal spreads from the PtK cells was that both the NORs from PtK_1 (female) cells were active. This reveals that NORs escape X-inactivation by resisting the spread of heterochromatin. This resistance to the spreading of heterochromatin of the NOR on the X-chromosome is not surprising as active NORs are also resistant to chromatin condensation, evident by their appearance as secondary constrictions on metaphase chromosomes. This suggests that there is some factor or mechanism preventing the spreading of heterochromatin over rRNA genes. Our work provides strong evidence that UBF is key for preventing the spreading of heterochromatin.

Having established that UBF maintains the open chromatin state associated with active NORs there are still major outstanding questions. We know from the work presented in this chapter that a decrease in UBF cellular levels results in the presence of silent NORs. Therefore is there a hierarchy among the acrocentric chromosomes for the silencing of NOR or is it completely random? Demonstrating which NORs are silenced is extremely difficult as we do not have short arm probes for each acrocentric chromosome allowing us to distinguish between NORs. In the lab we have DNA probes that can identify the long arms of acrocentric chromosomes, however these probes hybridise at regions that are some distance from the rDNA. Hence performing FISH using the rDNA and long arm acrocentric probes would not be worthwhile as the distance between each probe would prevent us confidently matching a silent rDNA foci to a specific acrocentric chromosome.

In higher eukaryotes only approximately half of the rDNA repeats are active at any given time (Conconi et al., 1989, Dammann et al., 1993). This is at odds with the number of silent NORs observed at the chromosomal level suggesting that the NORs are a mosaic of active and inactive rDNA repeats. Therefore when it comes to silencing an entire NOR, as is the case in human cells with reduced UBF levels, one could speculate that NORs with a higher ratio of silent to active rDNA repeats would be silenced first. Furthermore, human NORs vary in size from 50kb to 6Mb (Stults et al., 2008) and hence vary in their number of rDNA repeats. The number of rDNA repeats within an NOR may play a role in determining if that NOR is silenced first. For example one might assume that NORs with fewer rDNA repeats would be tilted towards silencing before those NORs with a larger number of repeats. Arguably the rDNA repeats of smaller NORs may be all active instead of a mosaic of active and inactive repeats, therefore these smaller NORs may be the last to be silenced. There is no doubt that establishing whether or not NORs are silenced randomly or sequentially would prove beneficial to the field. If there is a hierarchy among the NORs this may indicate that some NORs are dispensable while others are critical for cell survival. If there is a hierarchy among the NORs is it the same among different cell lines? To establish this multiple karyotypically normal cell models would need to be analysed.

Another major question is the mechanism by which silent NORs become dissociated from the nucleolus. There are two possibilities, 1. does a silent NOR dissociate from the nucleolus sporadically during a cell cycle or 2. after mitosis the silent NOR is not transcribed, therefore does not form a small nucleolus capable of associating with other nucleoli. We believe that the second possibility is the more favourable. Therefore to recap on the nucleolar cycle (section 1.6 and Figure 1.9), during mitosis rDNA transcription is shut down and the nucleolus is disassembled. Nucleolar reassembly begins in telophase and is dependent on the resumption of rDNA transcription from each NOR associated with components of the RNA Pol I machinery, such as UBF. This results in the presence of numerous small nucleoli that form around each individual NOR. These small nucleoli coalesce to form a single nucleolus or a few large nucleoli (Ochs et al., 1985, Benavente et al., 1987). Considering the nucleolar cycle we hypothesise the following mechanism by which silent NORs become dissociated from nucleoli as a consequence of UBF depletion. The rDNA repeats initially condense and form foci at the periphery of the nucleolus. As the cell enters mitosis the nucleolus disassembles. Upon reassembly these newly silenced NORs that were at the periphery of the nucleolus in the previous cell cycle are incapable of forming a nucleolus as they lack the association of UBF and other components of the RNA Pol I machinery. As a result these silent NORs do not coalesce with the small nucleoli formed around transcriptionally competent NORs and thus become isolated from the final large nucleoli or single nucleolus (Figure 4.15).

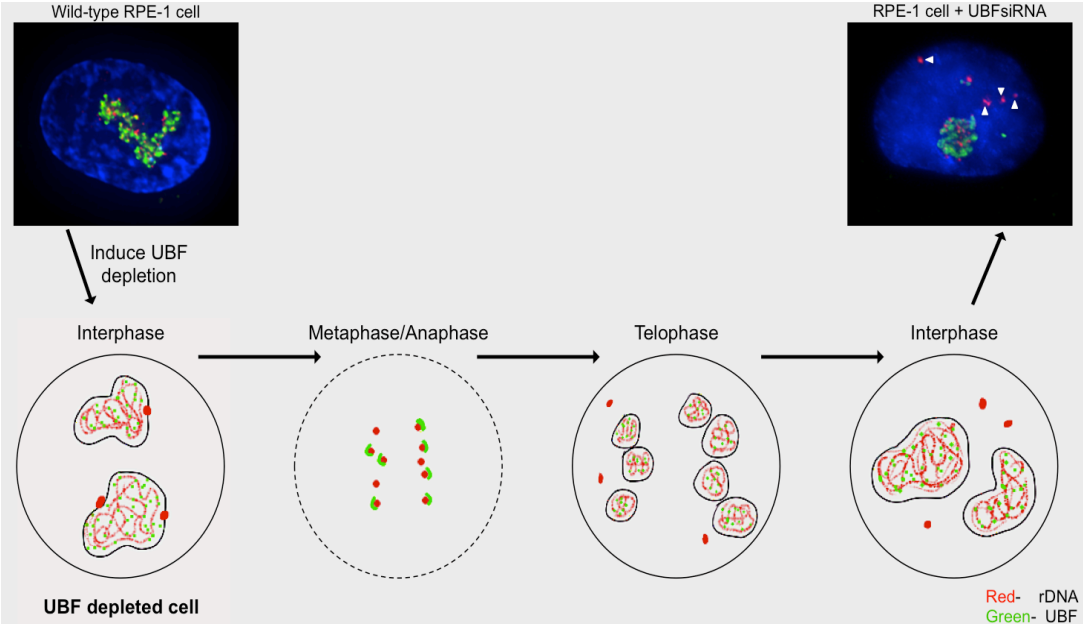

Figure 4.15 Schematic of our hypothesis as to how silent NORs become dissociated from nucleoli
On the top left is an image of a wild type RPE-1 cell in which all the rDNA is associated within the nucleolus, which is visualised using using α-fibrillarin antibodies. The depletion of UBF, by siRNA or shRNA, causes the rDNA (red) to condense back to the periphery of the nucleolus (indicated by red foci). As the cell enters mitosis the nucleolus disassembles (evident by dashed line). The condensed rDNA foci that were present at the periphery of the nucleolus in the interphase cell appear as silent NORs at metaphase/anaphase, evident by the lack of UBF binding (green). In telophase the nuclear envelope begins to reassemble. Nucleolar reassembly also begins in telophase, with individual nucleoli forming around each NOR that is associated with UBF. These small nucleoli coalesce to form larger nucleoli. In contrast those silent NORs lacking UBF are incapable of forming a nucleolus. These silent NORs cannot coalesce with the small nucleoli and thus become isolated from the final large nucleoli. The silent NORs appear as condensed rDNA foci (red) dissociated from nucleoli in interphase. On the top right is an image of a RPE-1 cell depleted of UBF in which large rDNA foci disassociated from the nucleolus (arrowheads) is observed.

The 2ng UBFKD cells are maintained for an extended time with a 4.5-fold reduction in UBF levels. Despite proliferating at much the same rate as parental HT1080 cells with no defects in rDNA transcription or processing the 2ng UBFKD rDNA chromatin is noticeably more condensed with the appearance of a number of silent NORs. The 2ng UBFKD cells are stable for an extended period of time, therefore the silent NORs observed in these cells are propagated through multiple cell divisions. One might assume that epigenetic marks such as DNA methylation or histone modifications may play a role in maintaining these silent NORs through cell divisions. However work from the Hannan lab has made us rethink this assumption. Our *in vivo* studies which demonstrate the condensation of rDNA chromatin and the presence of silent NORs due to a reduction in cellular UBF complements biochemical studies from the Hannan lab. They demonstrate by psoralen crosslinking and ChIP experiments that UBF depletion in mouse cells results in both an increase in the proportion of rDNA repeats that adopt a silent heterchromatic state and an increase in the association of linker histone H1 with rDNA (Sanij et al., 2008). Importantly they demonstrate that rRNA gene silencing resulting from UBF

depletion does not require NoRC-induced DNA methylation of the -133 CpG dinucleotide site (Sanij et al., 2008), which is contrary to previous work demonstrating that methylation at this site is required for silencing mouse rRNA genes (Santoro and Grummt, 2005, Santoro and Grummt, 2001). The correlation between DNA methylation and silencing of rRNA genes is further contradicted from studies conducted in a murine differentiation model. During differentiation the proportion of silent rDNA repeats increases and this correlates with a reduction in UBF levels and UBF binding to rDNA repeats, but no increase in rDNA methylation (Sanij et al., 2008). Demonstrating if the newly silenced NORs we observe upon UBF depletion are associated with increased DNA methylation would prove difficult as the human rDNA is much more complex containing 25 CpGs.

UBF is an essential player in maintaining the open chromatin state of active NORs, as we have clearly demonstrated that loss of UBF correlates with the loss of secondary constrictions. In turn the maintenance of this open rDNA chromatin state must be important as secondary constrictions, which were initially identified in plants (Heitz, 1931, McClintock, 1934), are present among all species.

5 UBF is evolutionarily conserved across animal phyla

5.1 Background

Work presented in this thesis and previously published work from pseudo-NORs (Mais et al., 2005) has provided compelling evidence that extensive UBF binding is required for the formation of secondary constrictions on metaphase chromosomes, and maintaining the open chromatin state of active NORs during interphase. Secondary constrictions are a common characteristic of most if not all eukaryotes, including plants where they were first described (Heitz, 1931, McClintock, 1934). For instance, NORs in rye plants are large and easily distinguished from the rest of the genome on metaphase spreads as regions lacking DAPI staining and positive for silver staining (Caperta et al., 2002). Despite the evidence for secondary constrictions in nearly all eukaryotes, UBF was thought to be restricted to vertebrates. This concept was fuelled by the lack of a UBF-like protein in model organisms such as *Drosophila*, *Caenorhabditis elegans*, yeast and *Arabidopsis*.

In yeast a distantly related HMG box protein, Hmo1, has been suggested to perform similar functions to UBF in yeast. Hmo1 is one of ten HMG-box proteins present in *S. cerevisiae*. Hmo1 is comprised of three domains, box A is a weakly conserved HMG box, box B is a canonical HMG box with close sequence similarity to four of the HMG boxes in human UBF, and box C is a charged motif involved in DNA bending (Figure 5.1 (A)) (Lu et al., 1996, Kamau et al., 2004). The divergent box A domain binds to DNA with low affinity and facilitates structure specific DNA binding of Hmo1, whereas box B domain directs most of the DNA binding with lower structural specificity (Kamau et al., 2004). The box B domain is closely related in sequence to four of the six HMG boxes in human UBF (Gadal et al., 2002) (Figure 5.1 (B)).

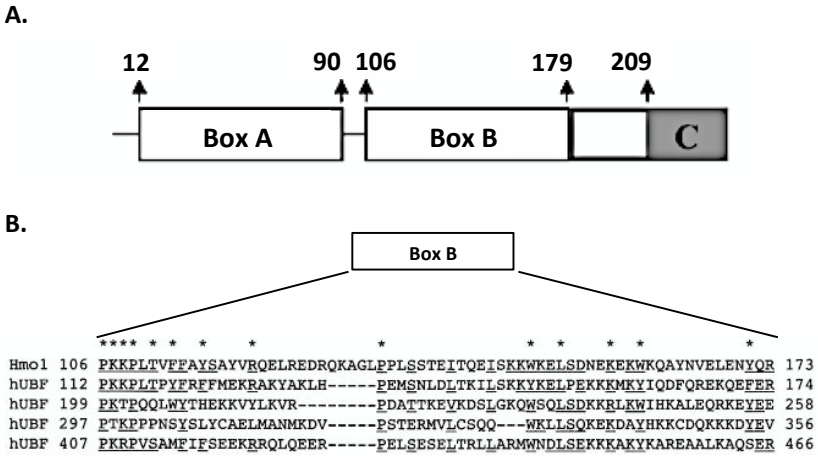

Figure 5.1 Organisation of Hmo1 domains
(A) Hmo1 is comprised of three domains, a weakly conserved HMG box (Box A), a canonical HMG box (Box B) and a lysine rich motif (Box C). Figure from (Bauerle et al., 2006).
(B) Hmo1 HMG box B sequence is aligned with the first four HMG boxes of human UBF. Identical or highly conserved residues are underlined. Asterisks denote the general HMG box consensus. Figure adapted from (Gadal et al., 2002).

Gadal's group was the first to determine that Hmo1 is required for efficient rDNA transcription in yeast (Gadal et al., 2002). They demonstrated that the cold sensitive growth defect associated with deleting the RNA Pol I specific sub-unit, Rpa49, is suppressed by overexpressing Hmo1 and this overexpression correlates with an increase in rRNA synthesis (Gadal et al., 2002). In the same study they further demonstrated that the combined deletion of Hmo1 and Rpa49 is lethal and this lethality is solely due to a RNA Pol I-dependent defect. This study reveals that not only is Hmo1 a *bona fide* RNA Pol I factor but that it also acts synergistically with Rpa49.

The suggestion that Hmo1 performs a UBF like role in yeast has come from a number of studies demonstrating functional similarities between UBF and Hmo1. For instance Hmo1 has been shown to concentrate primarily in the nucleolus where it co-localises with Fob-1, a known rDNA-binding factor (Gadal et al., 2002). Hmo1 binds across the entire *S. cerevisiae* rDNA repeat *in vivo* (Hall et al., 2006). Furthermore *in vivo* studies have demonstrated that actively transcribed yeast rRNA genes are associated with Hmo1 and largely deviod of histone molecules, revealing that Hmo1 and histone binding to rRNA genes is mutally exclusive in yeast also (Merz et al., 2008). A convincing new study has investigated the chromatin state of rRNA genes throughout the yeast cell cycle (Wittner et al., 2011). As is the case in all mammalian cells, the yeast rDNA chromatin exists in two states. These two states include an open active chromatin state devoid of regularly spaced nucleosomes and an inactive closed state associated with regularly spaced nucleosomes, with both forms co-existing throughout the cell cycle (Conconi et al., 1989). In yeast, newly replicated 35S rRNAs are assembled into nucleosomes, thus converting open rRNA genes to a closed chromatin state (Lucchini and Sogo, 1995, Lucchini et al., 2001, Wittner et al., 2011). RNA Pol I transcription is required for rRNA genes to re-establish an open chromatin state, however it does not play a role in maintaining the open chromatin state outside of S-phase. Hmo1 was identified as the factor necessary for stabilising and maintaining the open chromatin state by preventing replication independent nucleosomal assembly (Wittner et al., 2011). In yeast individual rRNA genes may change their transcription status randomly, such that in each new generation the set of rRNA genes that were active preceding S-phase may be different to the subset that are active post S-phase (Dammann et al., 1995). However in mammalian cells such a mechanism does not seem likely as the maintenance of silent rRNA genes is associated with epigenetic marks (McStay and Grummt, 2008).

Furthermore both UBF and Hmo1 have been linked to the TOR (target of rapamycin) pathway, connecting the regulation of RNA Pol I transcription to nutrient availability. In mouse cells the TOR pathway stimulates transcription through S6-kinase dependent phosphorylation of UBF at the C-terminal tail, which promotes UBF-SL1 interactions (Hannan et al., 2003a). In yeast, inhibition of the TOR pathway by rapamycin causes the dissociation of Hmo1 from the rDNA and from some of the ribosomal protein (RP) gene promoters (Berger et al., 2007). In the

absence of Hmo1 the TOR-dependent suppression on RP gene promoters is alleviated (Berger et al., 2007). This suggests that Hmo1 is directly involved in regulating RNA Pol I transcription and RP gene expression in response to the TOR pathway. A more recent study has demonstrated that Hmo1 expression is regulated by the TOR signalling pathway (Xiao et al., 2011). The Hmo1 promoter is negatively regulated by Hmo1, moreover Hmo1 promoter activity reduces by ~50% when TOR is inhibited by rapamycin, and this inhibition requires Hmo1 (Xiao et al., 2011). This study extends Hmo1 functioning in response to TOR signalling to include regulation of its own expression. Just to note that in contrast to TORs ability in yeast to regulate expression of RP genes, mammalian TOR controls the translation of mRNAs encoding RPs. mRNAs of all RPs contain an oligopyrimidine tract at their transcriptional start site (5'TOP) that confers translational control of their expression in response to mitogens. In the presence of rapamycin, mitogen induced 5'TOP translational of mRNAs is inhibited and this is controlled through inhibition of $p70^{S6K}$ (p70 ribosomal protein S6 kinase) (Jefferies et al., 1997).

The known functions of UBF to date are mainly restricted to RNA Pol I transcription, while Hmo1 is implicated in additional functions. Hmo1 binds strongly to most RP gene promoters and is involved in regulating their expression by RNA Pol II (Berger et al., 2007, Hall et al., 2006, Kasahara et al., 2007, Kasahara et al., 2008). Hmo1 may confer genome stability, for instance deletion of Hmo1 results in reduced plasmid stability and chromatin that is hypersensitive to micrococcal nuclease (Lu et al., 1996). Additionally, Hmo1 functionally interacts with DNA topoisomerase II (Top 2) during S-phase and together these factors have been suggested to prevent chromosome fragility, thereby maintaining genome stability (Bermejo et al., 2009).

The aim of this chapter was to revise the notion that UBF is restricted to vertebrates. We hypothesised that UBF may be more prevalent than previously thought or that there is UBF-like proteins performing functions similar to that of UBF. This hypothesis is driven by the fact that secondary constrictions are identified in all eukaryotes. Our findings reveal that UBF is not restricted to vertebrates but present throughout the animal phyla. The second aim of this chapter was to determine if the yeast nucleolar HMG box protein, Hmo1, is the functional counterpart of UBF. Hmo1 work presented in this chapter is from an on-going collaboration with Olivier Gadal. On my part I set out to determine if Hmo1 could recognise rDNA chromatin and have the capacity to fulfil the functions of UBF in human cells. These collaborate studies reveal that UBF, when expressed in yeast, can fulfil some of the functions of Hmo1, however in humans Hmo1 cannot recapitulate UBF functions.

5.2 Results

5.2.1 UBF is present across the animal phyla

In recent years there has been an explosion of sequence data from non-vertebrate organisms, both genomic DNA and complementary DNA (cDNA). To ascertain if UBF was present in non-vertebrate species we made use of DNA sequences available online and performed BLAST (Basic Local Alignment Search Tool) searches using the translated BLAST program (tblastn) (NCBI). A tblastn search enables one to compare a protein sequence, in our case UBF, to the translated NCBI nucleotide database. UBF is composed of an N-terminal dimerisation domain, six HMG boxes and a C-terminal acidic tail. In mammalian cells HMG box containing proteins are divided into two major groups. In the first group the HMG boxes mediate sequence-specific DNA binding, in contrast the HMG boxes in the second group bind DNA with little or no sequence specificity. UBF falls into the latter group. Due to the vast number of HMG box containing proteins and the fact that UBF contains six HMG boxes I set out strict criteria that newly identified orfs had to fulfil in order to be categorised as a UBF protein. The criteria set out meant that new UBF orfs had to contain a N-terminal dimerisation domain, multiple HMG boxes and a C-terminal acidic tail. Complying with this criterion we identified a number of species containing orfs with significant homology to human UBF. Interestingly these orfs were identified from species throughout the animal phyla (Figure 5.2).

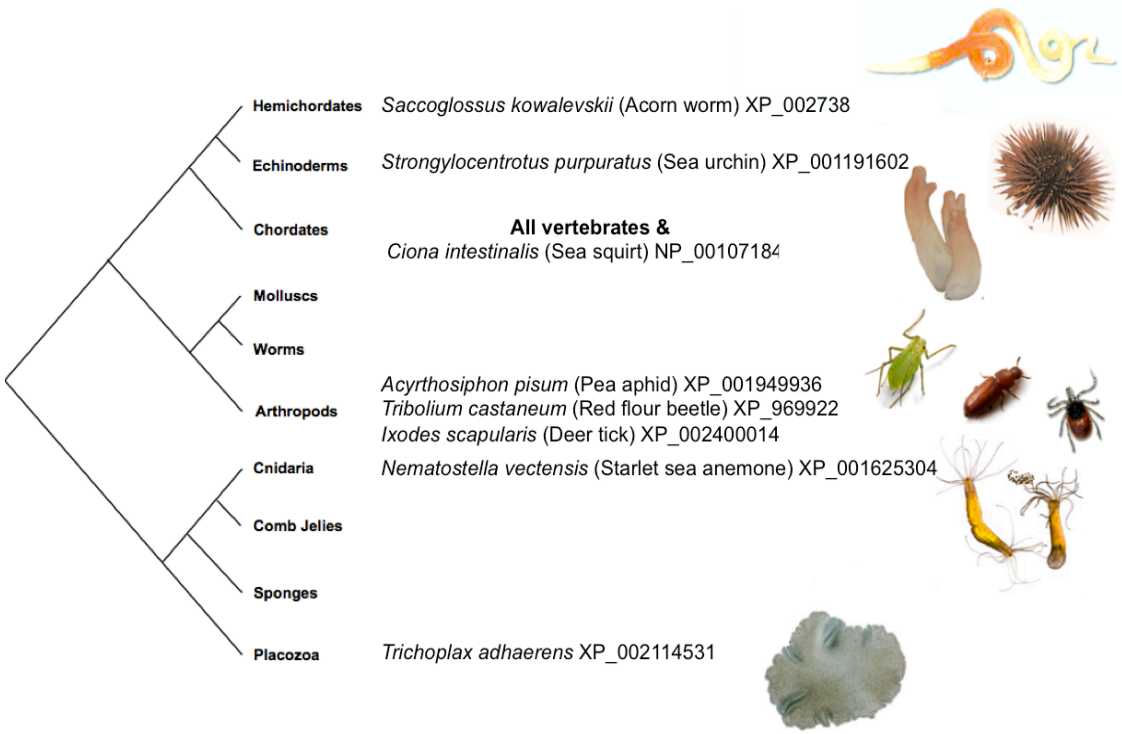

Figure 5.2 Phylogenetic tree of UBF containing species
tBLASTn searches reveal that UBF is present in non-vertebrates and more interestingly UBF is found throughout the animal phyla. The names of species containing open reading frames with significant homology to UBF are shown in the appropriate position alongside a phylogenetic tree. The accession number associated with each UBF homolog is also shown. Figure from (Grob et al., 2011).

For example UBF was found in other chordates such as *Ciona intestinalis*. Alignment of the protein sequences for human UBF and *Ciona* UBF using ClustalW2 (EMBL-EBI) reveals the sequence similarities between the two species (Figure 5.3). There is ~40% homology in the dimerisation domain and ~54% homology in the first HMG box. *Ciona* UBF obtains multiple HMG boxes as well as a C-terminal acidic tail, similar to human UBF. Moreover we also discovered UBF in acorn worms and sea urchins, which fall into the hemichordate and echinoderm phylum, respectively, which are considered the closest non-chordate relatives.

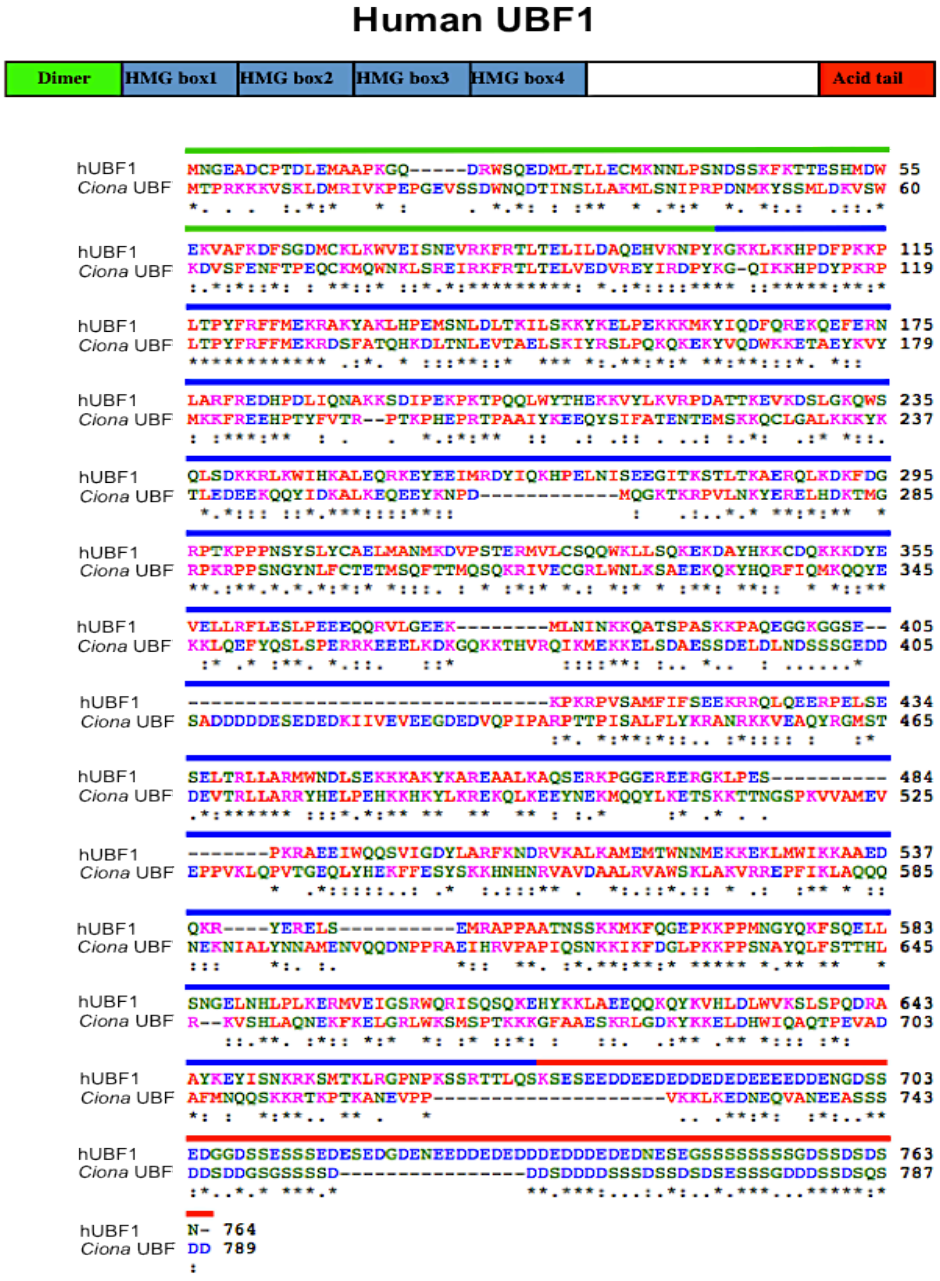

Figure 5.3 Alignment of Human UBF1 and *Ciona intestinalis* UBF
ClustalW2 alignment of human UBF1 and *Ciona intestinalis* UBF. A schematic of human UBF1 is shown above the alignment. The line above the sequence indicates the different domains of human UBF, the N-terminal dimerisation domain (green), HMG boxes (blue) and the C-terminal acidic tail (red). Fully conserved residues are denoted by (*), strongly conserved residues are denoted by (:) and weakly conserved residues are denoted by (.).

Interestingly our tblastn searches identified orfs similar to UBF in a number of insects such as pea-aphids, red flower beetles and deer ticks, despite the lack of UBF or a UBF-like protein in the model organism *Drosophila.* Alignment of the UBF protein sequence from each of these insects with human UBF reveals strong sequence similarities, particularly in the N-terminal dimerisation domain and the first four HMG boxes (Figure 5.4). Focusing first on the human UBF and pea aphid sequences, there is further sequence homology in the fifth and sixth HMG boxes and strong sequence homology in the C-terminal acidic tail. The red flower beetle and deer tick lack the fifth HMG box and most of the final HMG box when compared to human UBF. These two insects also have considerably shorter C-terminal acidic tails. Despite these differences the red flower beetle and deer tick, along with the pea-ahpid, fulfil the criteria to be categorised as a UBF protein. The fact that we have identified UBF in insects, which are more divergent from humans than *Ciona*, reinforces our findings that UBF is not restricted to vertebrates.

The most striking finding from the tblastn search was the evidence of an orf with considerable similarities to human UBF in the *Trichoplax adhaerans* genome. *Trichoplax,* the sole representative species of the Placozoa phyla, is considered to represent the most primitive metazoan with the smallest known animal genome, 50-Mbps (Srivastava et al., 2008). This *Trichoplax* orf, similar to human UBF, encodes multiple HMG boxes and an N-terminal dimerisation domain which shares ~30% identity with the same domain in *Ciona* UBF (Figure 5.5). The *Trichoplax* orf lacks any evidence of the characteristic C-terminal acidic tail, thus strictly speaking does not fulfil the criteria set out for identifying UBF in new species. However I will explain in the following chapter why we believe this identified orf from the *Trichoplax* genome is in actual fact *Trichoplax* UBF.

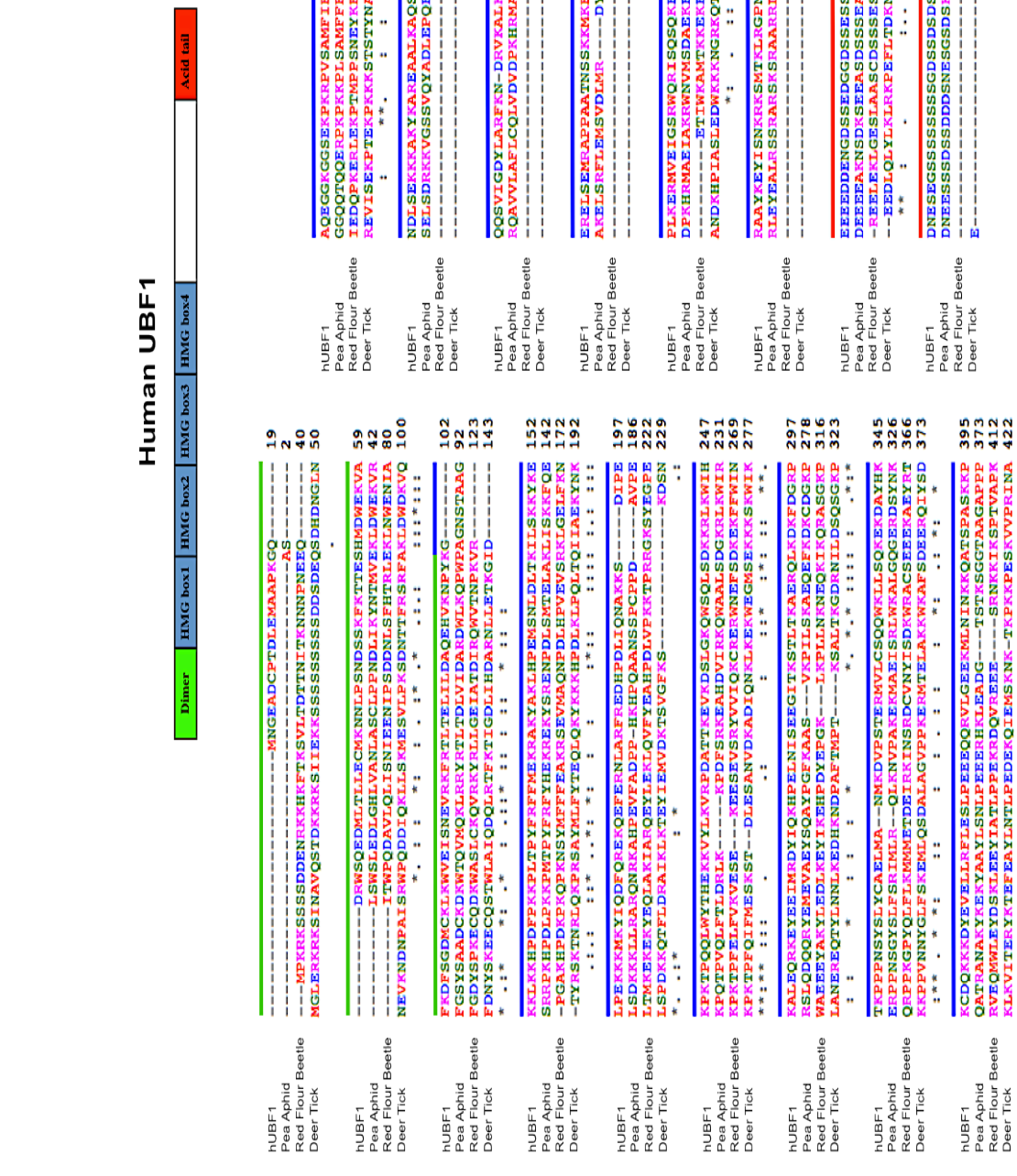

Figure 5.4 Alignment of Human UBF1, Pea Aphid UBF, Red Flour Beetle UBF and Deer Tick UBF
Alignment of human UBF1 and UBF from three insect species generated using ClustalW2. A schematic of human UBF1 is displayed above. The line above the sequence indicates the different domains of human UBF, the N-terminal dimerisation domain (green), HMG boxes (blue) and the C-terminal acidic tail (red). Fully conserved residues are denoted by (*), strongly conserved residues by (:) and weakly conserved residues by (.).

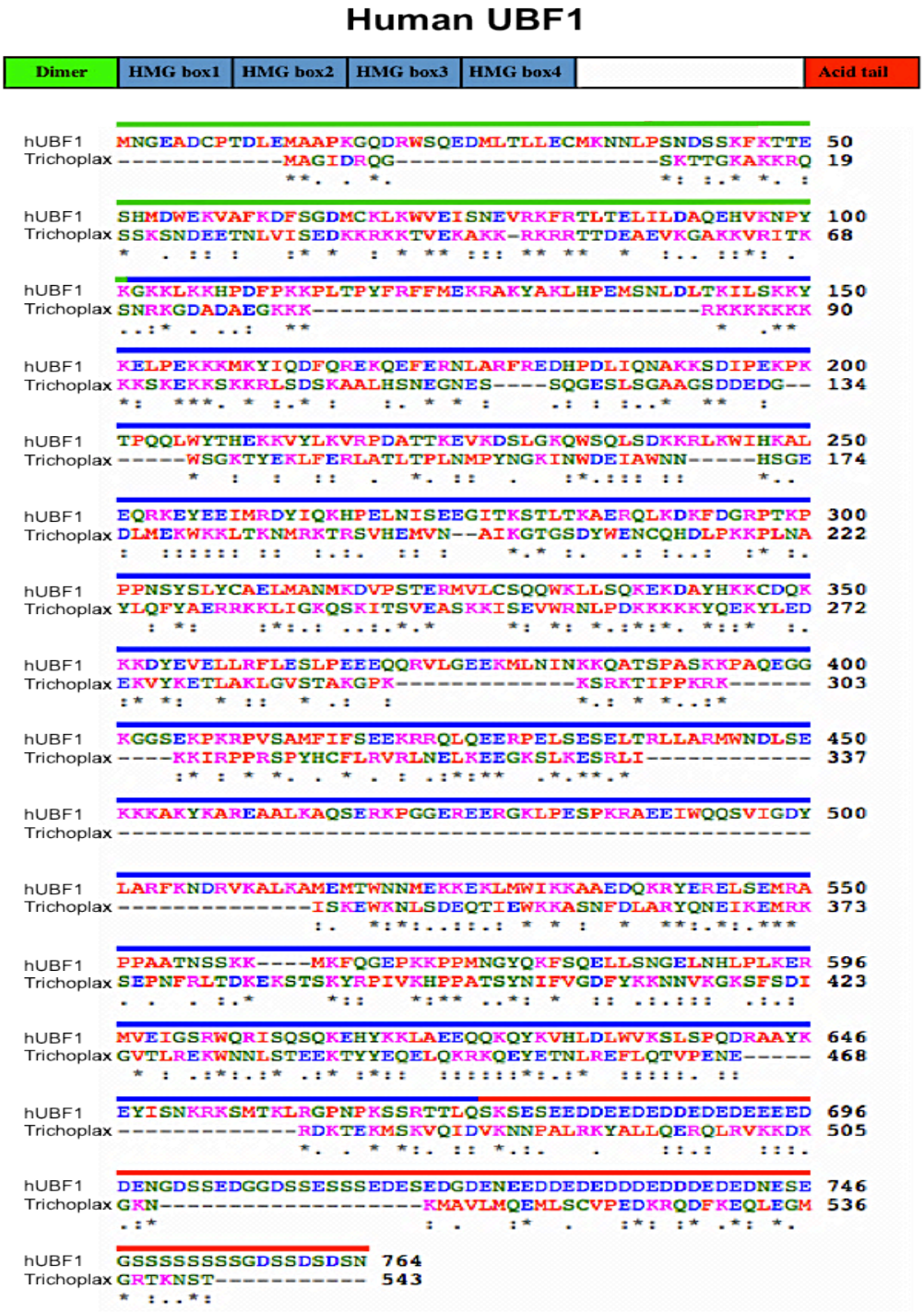

Figure 5.5 Alignment of Human UBF1 and *Trichoplax* UBF
Alignment of human UBF1 and *Trichoplax* UBF was generated using ClustalW2. A schematic of human UBF1 is displayed above. The line above the sequence indicates the different domains of human UBF, the N-terminal dimerisation domain (green), HMG boxes (blue) and the C-terminal acidic tail (red). Fully conserved residues are denoted by (*), strongly conserved residues by (:) and weakly conserved residues by (.).

5.2.2 *Ciona intestinalis* UBF co-localises with UBF at NORs in human cells

To establish if the newly identified UBF orfs from different species functions like human UBF I decided to analyse the localisation of *Ciona* UBF in human cells. We obtained an IMAGE clone for *Ciona intestinalis* cDNA (clone ID. ciem801a01-ciem854p24) from RIKEN BRC, Japan. The C*iona* UBF orf was amplified from the IMAGE clone with *Pfu* DNA polymerase using a 5' forward primer containing an NcoI restriction site. The PCR product was digested with NcoI restriction enzyme and the NcoI-blunt ended C*iona* UBF orf was subsequently cloned into the pENTR4™Gateway® entry vector, which was NcoI/EcoRV digested. Diagnostic restriction digests were performed to verify the correct pENTR4_*Ciona*UBF construct was generated. I then made use of the Gateway® technology (Invitrogen) to transfer *Ciona* UBF DNA from pENTR4_*Ciona*UBF to the pcDNA-DEST40™ destination vector by *in vitro* recombination. This destination vector contains a V-5 epitope tag that fuses to the C-terminus of *Ciona* UBF. The pcDNA-DEST40_CionaUBF expression construct was transfected into human cells to determine whether or not *Ciona* UBF can target rDNA chromatin.

The pseudo-NOR cell line (Mais et al., 2005) was used to analyse *Ciona* UBF targeting in human cells. Using the pseudo-NOR cell line enables us to address if *Ciona* UBF can target human NORs throughout the cell cycle as well as the pseudo-NORs. pcDNA-DEST40_*Ciona*UBF construct was transfected into cells using the TransIT reagent (Mirus Bio Corp). 24 hours after transfection was applied the cells were subjected to immunostaining using α-human UBF and α-V5 antibodies, conjugated to FITC coupled α-human and rhodamine coupled α-mouse antibodies, respectively. The punctate staining characteristic of endogenous UBF is in the nucleolus (Figure 5.6 (A)). UBF also concentrates at pseudo-NORs, appearing as large brightly stained UBF foci (arrowheads indicate pseudo-NORs, Figure 5.6 (A)). Interestingly those cells expressing *Ciona* UBF reveal that during interphase, *Ciona* UBF can target nucleoli as well as pseudo-NORs (Figure 5.6 (A)).

One of the defining characteristics of UBF is its ability to remain bound to mitotic NORs that were active in the previously cell cycle. I analyzed transfected metaphase cells to determine if *Ciona* UBF can target mitotic human NORs. α-human UBF antibodies reveal endogenous UBF at mitotic NORs (Figure 5.6 (B)). Surprisingly, *Ciona* UBF was found to co-localise with human UBF and target mitotic NORs. Our observations reveal that *Ciona* UBF is capable of targeting pseudo-NORs and NORs throughout the entire cell cycle. Furthermore, it confirms that the UBF orfs I identified in non-vertebrate species function like human UBF, reinforcing our findings that UBF is present across the animal phyla.

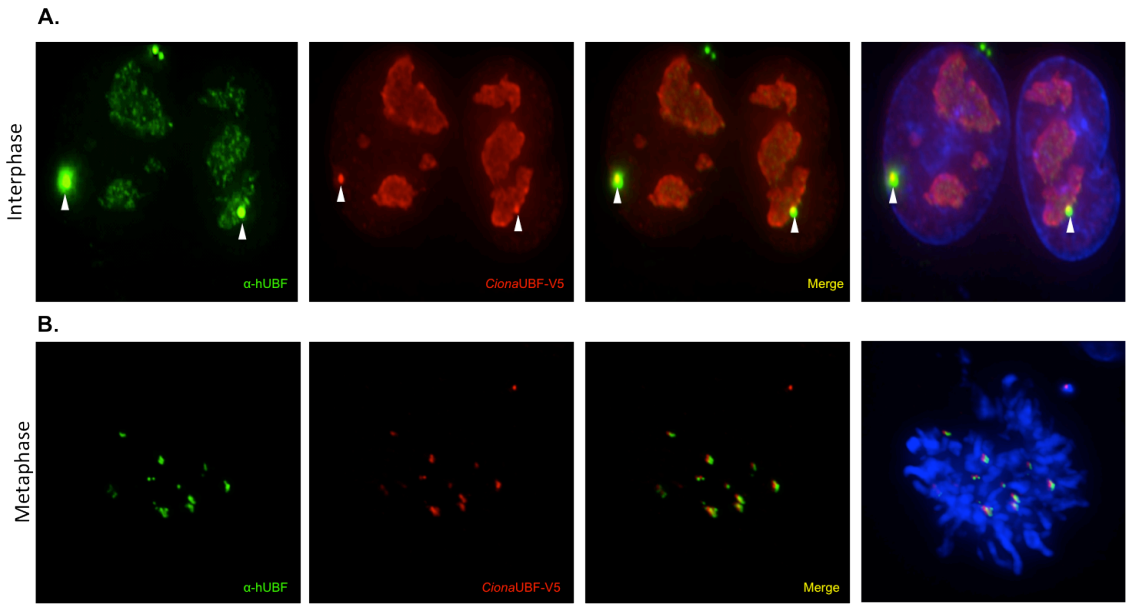

Figure 5.6 *Ciona* UBF co-localises with UBF at NORs in human cells throughout the cell cycle and at pseudo-NORs
(A) An interphase pseudo-NOR cell transiently transfected with pcDNA-DEST40_*Ciona*UBF as outlined 2.3.7. Cells were fixed, permeabilised and subjected to immunostaining as outlined 2.3.10. Human UBF is visualised by incubation with α-hUBF antibodies followed by incubation with FITC coupled α-human antibody (green) and *Ciona* UBF is visualised with α-V5 antibodies followed by incubation with rhodamine coupled α-mouse antibody (red). Merge of both signals and both signals plus DAPI are shown in the third and fourth panels, respectively. Pseudo-NORs are indicated by arrowheads.
(B) A metaphase cell transfected with pcDNA-DEST40_*Ciona*UBF as described above. hUBF and *Ciona* UBF were visualised as described above.

5.2.3 The yeast HMG box protein, Hmo1, co-localises with UBF at NORs throughout the cell cycle and is recruited to pseudo-NORs

There is no evidence of UBF in yeast, however there is a yeast nucleolar HMG box protein, Hmo1 that has been demonstrated to perform similar functions to UBF in yeast. Work from the Gadal lab provided the first evidence that Hmo1 targets nucleoli and is required for efficient rDNA transcription in yeast (Gadal et al., 2002). In our collaborative work with Olivier Gadal we wanted to ask a key question, whether UBF can functionally substitute for Hmo1 in yeast and can Hmo1 functionally substitute for UBF in humans.

Work carried out in Gadals lab found that YFP-UBF1 expressed in yeast co-localises with Hmo1 and the known yeast nucleolar protein Nop1 at the nucleolus (Figure 5.7 (A)). YFP-UBF2 also targets nucleoli in yeast, co-localising with Hmo1 and Nop1 (personal communication with O. Gadal). In the absence of Hmo1, yeast cells show a growth defect at 25°C. Gadals lab revealed that expression of untagged UBF1 or UBF2 could not rescue this growth defect in this hmo1Δ background, suggesting that neither UBF1 nor UBF2 can fully substitute for Hmo1 *in vivo*. Deletion of Hmo1 combined with the deletion of the yeast RNA Pol I subunit Rpa49 is lethal. This lethality is repressed and growth restored upon overexpression of Hmo1 and UBF1, but not UBF2 in this *hmo1*Δ*rpa49*Δ background (Figure

5.7 (B)). Interestingly, the YFP-UBF1 could not rescue the growth phenotype in hmo1Δrpa49Δ yeast cells. This suggests that tagging UBF at the N-terminus interferes with its ability to function correctly, therefore when generating tagged UBF constructs I made sure that the tag was at the C-terminus. In the following chapter I will discuss why we believe tagging the N-terminus of UBF interferes with its functioning.

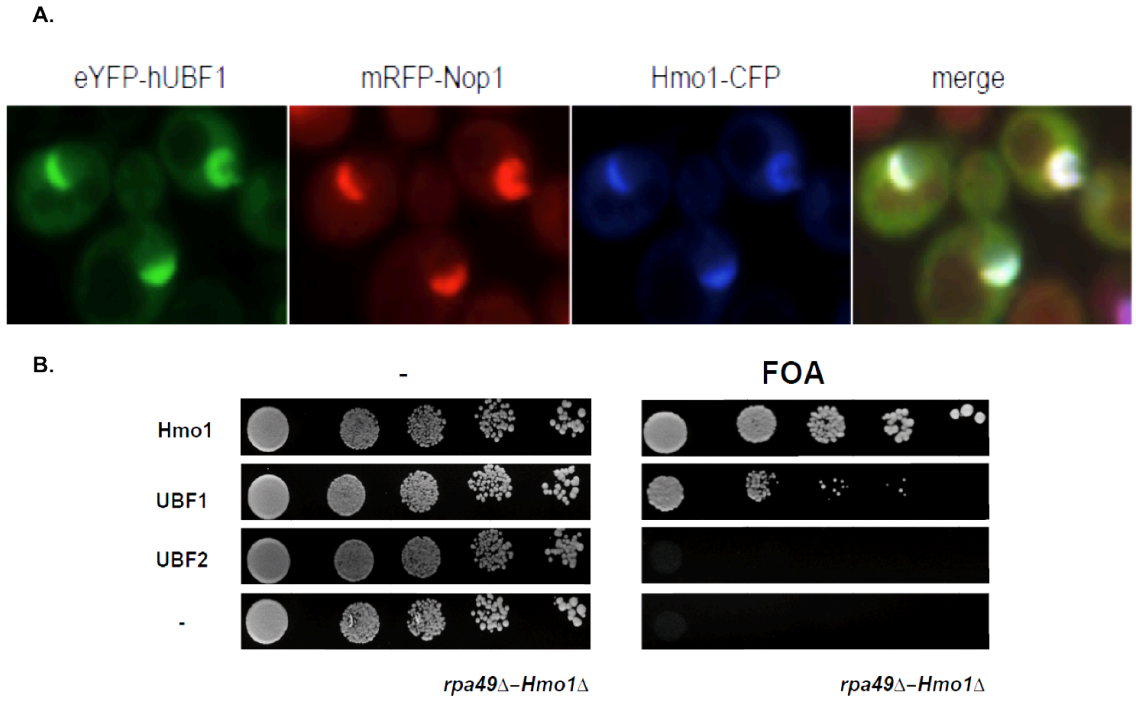

Figure 5.7 UBF1 is nucleolar in yeast and can substitute for Hmo1 in *rpa49ΔHmo1Δ* strain
(A) The eYFP-UBF1 construct (green) was transfected into a yeast strain expressing mRFP-Nop1 and Hmo1-CFP (blue). The co-localisation of the three fusion proteins is observed in the merge image (last panel).
(B) Tenfold serial dilutions of the *rpa49ΔHmo1Δ* stain expressing Hmo1, UBF1, UBF2 and an empty vector (-) were spotted on plates containing 5-FOA (fluroorotic acid) to test for complementation. Plates lacking 5-FOA were used as a control to confirm that similar numbers of cells were spotted.
The Gadal lab generated this figure.

Based on the above findings from the Gadal lab I set out to perform the reciprocal experiments in human cells. I first wanted to determine if Hmo1 can target NORs in human cells and then address if Hmo1 can functionally substitute for human UBF. α-Hmo1 antibodies and pENTR201_Hmo1 construct, in which the Hmo1 lacks a stop codon, were received from Olivier Gadal. To address whether Hmo1 could target NORs in human cells I made use of the Gateway® technology and cloned the Hmo1 orf from pENTR201_Hmo1 into pcDNA-DEST40™ destination vector. I decided to adopt the same policy for generating a tagged Hmo1 construct as for human UBF, that is ensure tag is at the C-terminus of the Hmo1 orf. The pcDNA-DEST40 is an ideal destination vector because the V-5 tag is fused to the C-terminus of Hmo1. To ensure the resulting pcDNA-DEST40_Hmo1 expression construct was correct restriction digests were performed. The pcDNA-DEST40_Hmo1 construct was transfected into

HT1080 human cells using TransIT reagent (Mirus Bio Corp). 24 hours after transfection was added the cells and subjected to antibody staining using α-human UBF and α-Hmo1 antibodies, conjugated to FITC coupled α-human and rhodamine coupled α-rabbit antibodies, respectively. Immunostaining reveals that in Hmo1 expressing cells Hmo1 co-localises with UBF in the nucleolus, appearing as punctate staining similar to that observed for UBF (Figure 5.8, top row). There is evidence of a small fraction of Hmo1 in the nucleoplasm, however the majority is targeted to the nucleolus. Moreover, upon analysis of metaphase cells it was clear that Hmo1 was also capable of co-localising with UBF on mitotic NORs (Figure 5.8, middle row). Also observed was that high levels of Hmo1 expression triggered the redistribution of a significant proportion of the endogenous UBF from the nucleolus into the nucleoplasm (Figure 5.8, bottom row). Additionally, nucleolar localisation of Hmo1 is non-existent in these Hmo1 overexpressing cells.

The fact the Hmo1 co-localises with UBF on mitotic NORs indicates that Hmo1 recruitment is independent of transcription. To validate this I made use of the pseudo-NORs which lack any promoter sequence and are therefore transcriptionally silent (Mais et al., 2005). The pcDNA-DEST40_Hmo1 construct was transfected into the pseudo-NOR bearing cell line with TransIT reagent (Mirus Bio Corp) and cells were subjected to immunostaining with α-human UBF and α-Hmo1 antibodies as described above. Hmo1 was observed to be recruited to pseudo-NORs, moreover the majority of Hmo1 expressed in the cell was enriched at the pseudo-NOR (arrowheads indicate pseudo-NORs, Figure 5.9). This enrichment at the pseudo-NOR correlates with the absence of Hmo1 in the nucleolus.

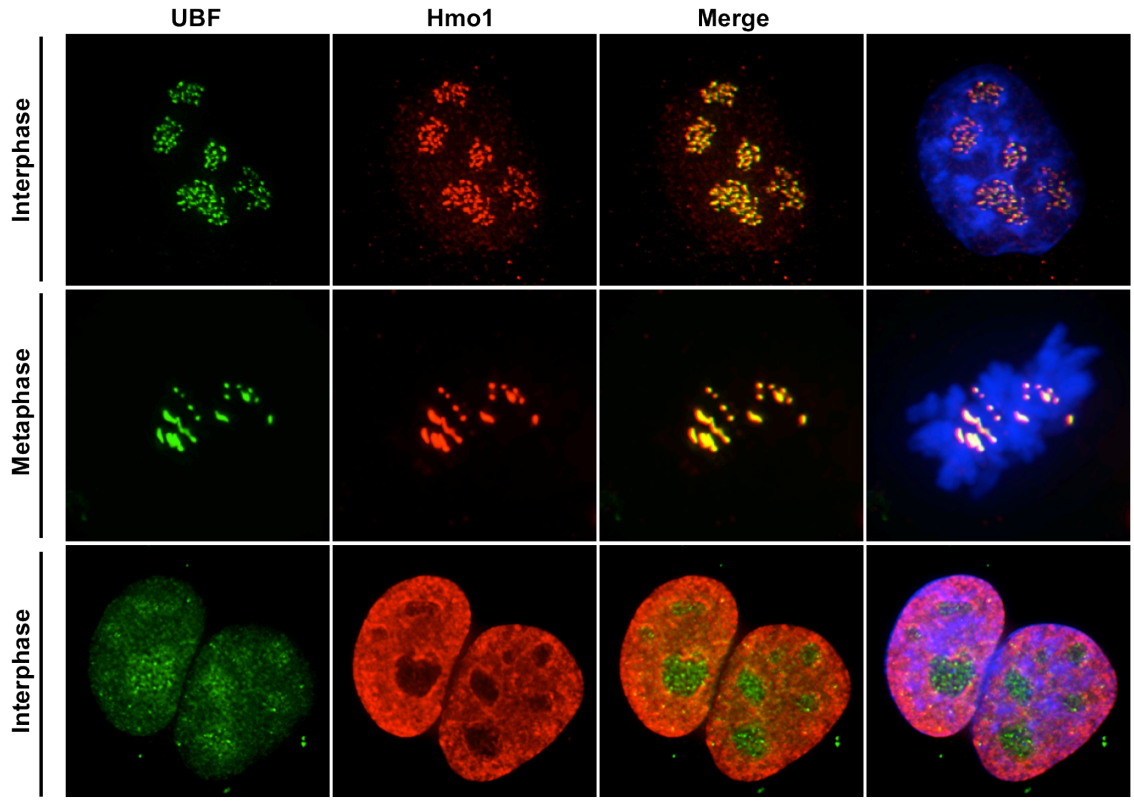

Figure 5.8 Hmo1 co-localises with UBF at NORs in human cells throughout the cell cycle
HT1080 cells were transiently transfected with pcDNA-DEST40_Hmo1 as outlined 2.3.7. Cells were fixed, permeabilised and subjected to immunostaining as outlined 2.3.10. Human UBF is revealed using α-hUBF antibodies followed by incubation with FITC coupled α-human antibody (green) and Hmo1 is visualised with α-Hmo1 antibodies followed by incubation with rhodamine coupled α-rabbit antibody (red). Hmo1 co-localises with UBF at nucleoli and mitotic NORs shown in an interphase and metaphase cell, respectively (top and middle row). Overexpression of Hmo1 causes the redistribution of UBF (bottom row, first panel) and the absence of Hmo1 in nucleoli (bottom row, second panel).

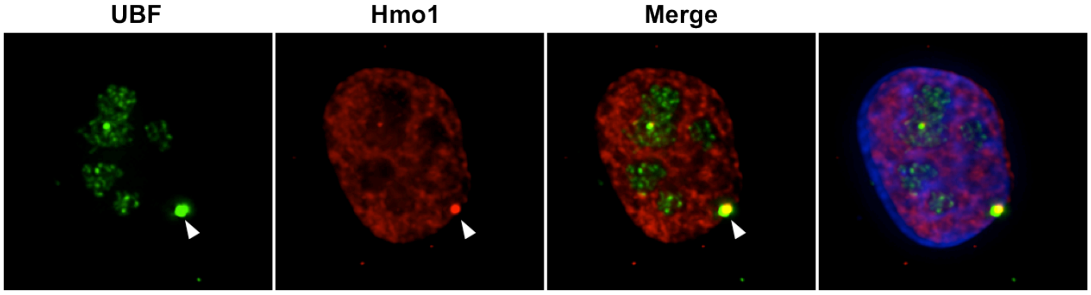

Figure 5.9 Hmo1 co-localises with UBF at pseudo-NORs
The pseudo-NOR cell line was transiently transfected with pcDNA-DEST40_Hmo1 as outlined 2.3.7. Cells were fixed, permeabilised and subjected to immunostaining as outlined 2.3.10. Human UBF is visualised using α-hUBF antibodies followed by incubation with FITC coupled α-human antibody (green). Hmo1 is visualised with α-Hmo1 antibodies followed by incubation with rhodamine coupled α-rabbit antibody (red). Arrowheads indicate pseudo-NORs.

5.2.4 Hmo1 is not sufficient to rescue cell growth upon UBF depletion

Our results clearly indicate that Hmo1, when transiently transfected into human cells, targets NORs throughout the cell cycle as well as targeting pseudo-NORs. From our collaborative work with Olivier Gadal we know that human UBF1, not UBF 2, can rescue the lethality observed in the *hmo1*Δ*rpa49*Δ yeast strain. Therefore to test the functionality of Hmo1 in human cells I designed an experimental approach in which we can deplete UBF levels and induce expression of Hmo1 simultaneously. From characterisation of the UBFKD cell line in chapter 3, I know that induction of UBFshRNA using a high concentration of doxycycline (1µg/ml) results in a severe growth arrest after 48hrs. Therefore I can make use of these conditions in the UBFKD cell line to address if Hmo1 expression can rescue this growth defect. I utilised the UBFKD cell line to generate a human cell line in which I could simultaneously deplete endogenous UBF and turn on Hmo1 expression.

Generation of such a cell line requires a construct in which I can induce the expression of Hmo1 in mammalian cells. Making use of the Gateway® technology I cloned the Hmo1 orf into the pT-REx-DEST30 destination vector. This destination vector contain two tetracycline operator 2 ($TetO_2$) sites within the human CMV promoter for tetracycline-regulated expression of your gene of interest, in our case Hmo1 (Yao et al., 1998). Expression of the gene is suppressed due to the binding of Tet repressor (TetR), which is expressed from the pcDNA™6/TR construct, to the $TetO_2$ sequences. Addition of doxycycline prevents Tet repressor binding to $TetO_2$ sequences thereby allowing expression of Hmo1.

The resulting pT-REx-DEST30_Hmo1 construct was transfected into the HT1080 TetR human cell line. The HT1080 TetR cell line, generated in the McStay lab, contains the pcDNA™6/TR construct that constitutively expresses the TetR protein. HT1080 TetR cells were seeded in 150mm dishes, transfected with pT-REx-DEST30_Hmo1 construct using the standard Calcium Phosphate method and stable cell lines were generated as outlined in 2.3.7. To verify that the HT1080 TetR_pT-REx_DEST30_Hmo1 stable clone of cells was expressing Hmo1 upon doxycycline treatment I harvested cells that were cultured in the presence and absence of doxycycline at a final concentration of 1µg/mL. Cells were lysed in Laemmli sample buffer and an equal cell number ($5x10^4$ cell/lane) was loaded for each sample on NuPAGE gels. HT1080 parental cells were also loaded as an extra control. Expression of Hmo1 is evident only when HT1080 TetR_pT-REx_DEST30_Hmo1 cells are cultured in the presence of doxycycline (Figure 5.10 (A)). This indicates that the Hmo1 construct can efficiently express Hmo1 upon doxycycline treatment, but also reveals that the construct is tightly regulated, i.e. there is no Hmo1 expression in the absence of doxycycline.

The pT-REx-DEST30_Hmo1 construct was subsequently transfected into the UBFKD cells, as described above, to generate a stable pool of cells. This stable pool of cells enables us to deplete

endogenous UBF by inducing UBFshRNA expression, while simultaneously turning on expression of Hmo1. Protein samples were harvested from UBFKD_pT-REx_DEST30_Hmo1 cells that were cultured in the presence and absence of 1μg/mL doxycycline. Equal cell number was loaded for each protein sample and UBFKD parental cell lysate was loaded as an extra control. Immnuoblotting with α-UBF and α-Hmo1 antibodies reveals that upon doxycycline treatment UBF levels are depleted and Hmo1 expression is induced (Figure 5.10 (B)). Western blotting also reveals that this cell line is tightly regulated with no effect on UBF levels or expression of Hmo1 in the absence of doxycycline.

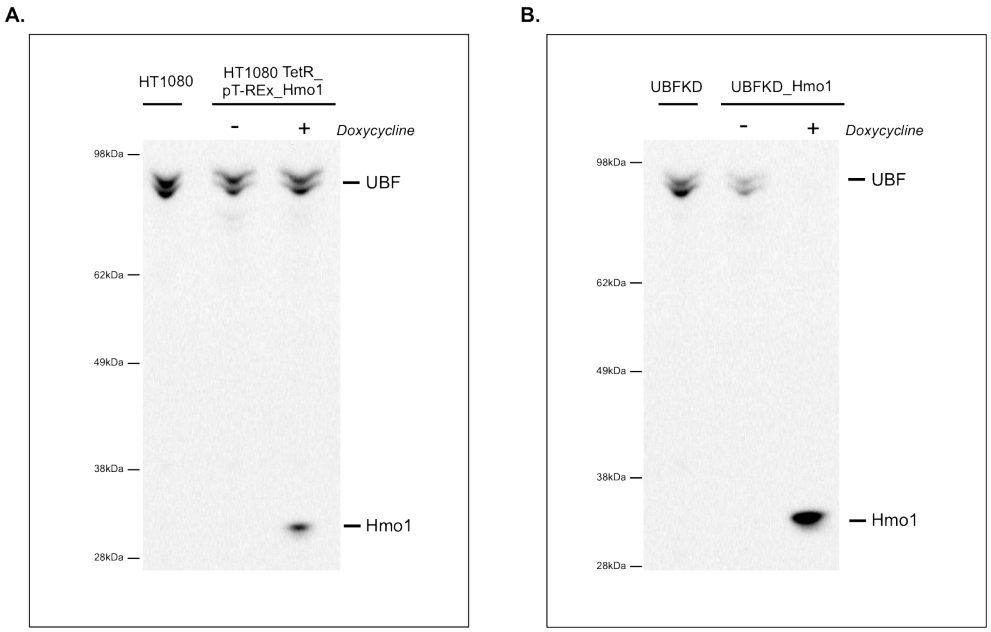

Figure 5.10 Inducible expression of Hmo1 and UBF shRNA simultaneously in human cells
(A). HT1080 TetR_pT-Rex_Hmo1 cells were cultured in absence and presence of 1μg/ml doxycycline for 48hours. Cells were harvested and lysed directly in an appropriate volume of Laemmli sample buffer to give $1x10^4$ cells/μl. HT1080 cell lysate was used as a control. 10μl of each sample was loaded on NuPAGE gel and membrane probed with α-hUBF antibodies and α-Hmo1 antibodies to reveal expression of Hmo1.
(B). UBFKD_Hmo1 cells were cultured in absence and presence of 1μg/ml doxycycline for 48hours. Cells were harvested and lysed directly in appropriate volume of Laemmli sample buffer to give $1x10^4$ cells/μl. 10μl of each sample was loaded on NuPAGE gel and membrane probed with α-hUBF antibodies to reveal reduction in UBF levels and α-Hmo1 antibodies to reveal expression of Hmo1.

I can now use the UBFKD_pT-REx_DEST30_Hmo1 cells, termed UBFKD_Hmo1, to ascertain if Hmo1 can substitute for UBF in human cells. UBFKD _Hmo1 and UBFKD cells were cultured in the presence and absence of 1μg/mL doxycycline, and assayed for cell viability. Protein samples were harvested in parallel for each time point to monitor UBF depletion and Hmo1 expression. Growth curves demonstrate that in the absence of doxycycline both UBFKD and UBFKD_Hmo1 cells proliferate at the same rate, duplicating approximately every 28 hours (Figure 5.11 (A)). Western blotting indicates just how tightly regulated the UBFKD_Hmo1 cell line is with no induction of UBF shRNA or Hmo1 expression in the absence of doxycycline

(third lane, Figure 5.11 (B)). The previously documented growth arrest observed in UBFKD cells treated with 1µg/mL doxycycline is observed, with western blotting confirming the depletion of cellular UBF levels (Figure 5.11 (A) & (B)). Western blotting reveals that the addition of doxycycline to the UBFKD_Hmo1 cell line results in a gradual depletion of endogenous UBF with a simultaneous increase in expression of Hmo1 from the 24 to 96 hr time point (fourth lane, Figure 5.11 (B)). Growth curves reveal that the induction of Hmo1 expression is not sufficient to relieve the growth arrest resulting from UBF depletion (Figure 5.11 (A)). In the UBFKD_Hmo1 cells treated with 1µg/mL doxycycline a severe growth defect is evident at 48hrs, similar to that observed in the UBFKD cells treated with high concentrations of doxycycline. These experiments reveal that Hmo1 cannot substitute for UBF in human cells. The growth curves were generated based on two independent experiments.

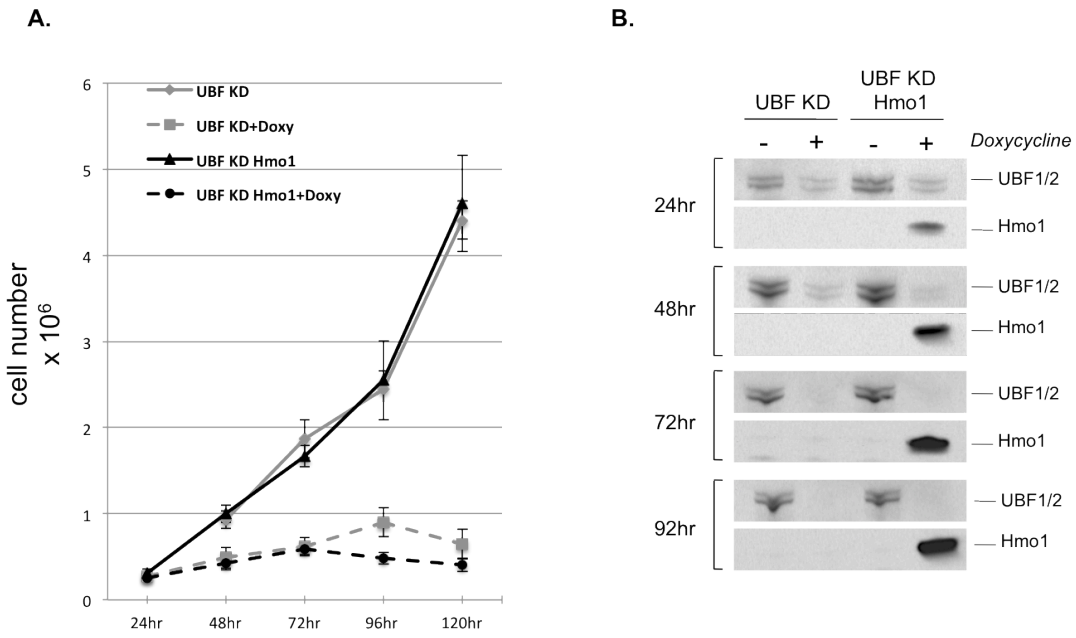

Figure 5.11 Hmo1 cannot substitute for UBF in human cells
(A). Equal cell number ($1x10^5$) was seeded out in T25 flasks in duplicate for UBFKD and UBFKD_Hmo1 in the presence and absence of 1µg/ml doxycycline. Cells were harvested in duplicate at 24, 48, 72, 96 and 120hr time points. An aliquot of each cell suspension was mixed with an equal volume of trypan blue and viable cells were counted. Error bars were formulated based on two independent repeats of the experiments
(B). UBFKD and UBFKD_Hmo1 cells were harvested in the presence and absence of 1µg/ml doxycycline for the 24, 48, 72 and 96hr time points, and lysed in an appropriate volume of Laemmli sample buffer to give $1x10^4$ cells/µl. 10µl of each sample was loaded on NuPAGE gel and membrane probed with α-hUBF antibodies to indicate depletion of UBF and α-Hmo1 antibodies to reveal Hmo1 expression.

5.3 Discussion

UBF was thought to be restricted to vertebrates, yet secondary constrictions are a common characteristic among nearly all eukaryotes. Furthermore I have demonstrated that UBF is causal for the formation of these secondary constrictions, so what is driving the formation of secondary constrictions in non-vertebrates? We hypothesise that UBF is more prevalent than previously thought or that a UBF-like protein is present in these non-vertebrates. By performing tblastn searches I reveal for the first time that UBF is not restricted to vertebrates but is present in species across the animal phyla, such as *Ciona Intestinalis*, insects and *Trichoplax adhaerans*, which is considered the most primitive metazoan. All the newly identified UBF orfs, with the exception of *Trichoplax* UBF, have the three main characteristics of UBF, a N-terminal dimerisation domain, multiple HMG boxes and a C-terminal acidic tail. *Trichoplax* UBF lacks an obvious C-terminal acidic tail, however in the following chapter I will describe a novel domain within UBF, which is conserved within the predicted *Trichoplax* UBF, that we believe is critical for UBF functioning.

The notion of UBF being restricted to vertebrate is fuelled by the fact that no UBF has been identified in model organisms such as *C.elegans*, yeast, and *Arabidopsis*. No UBF has been identified in *Drosophila*, yet I have demonstrated that UBF is present in insects, such as pea-aphid. One reason for the absence of UBF in model organisms, such as *Drosophila*, is that gene loss appears to have been more prevalent in these model systems than previously thought (Kortschak et al., 2003). Hence, UBF and a number of other proteins that are thought to be vertebrate innovations are actually present in more primitive metazoans.

To ensure the newly identified UBF orfs are functioning like human UBF I demonstrated that *Ciona* UBF is capable of targeting human NORs throughout the cell cycle. *Ciona* UBFs ability to target mitotic NORs suggests that its recruitment is independent of transcription. Transcription-independent recruitment of *Ciona* UBF to NORs is supported by ability of *Ciona* UBF to target pseudo-NORs, which are known to be transcriptionally silent due to the lack of a promoter (Mais et al., 2005). An observation in human cells transiently transfected with *Ciona* UBF, was that the intensity of endogenous human UBF staining in nucleoli was much weaker in those cells positive for *Ciona* UBF expression. This apparent reduction in human UBF levels at nucleoli may be due to *Ciona* UBF recognising the same chromatin or underlying DNA sequence as human UBF and therefore competing for the same binding site. Another concept is that, due to the high sequence similarity within the dimerisation domain, human UBF and *Ciona* UBF form heterodimers that target NORs.

Despite demonstrating that UBF is more prevalent than previously thought, there is still the need to identify what factor is driving the formation of secondary constrictions in plants. A 58kDa polypeptide in the onion plant *Allium cepa* was identified as a potential UBF candidate

(Rodrigo et al., 1992), however genomic evidence revealed that this 58kDa protein was just an artefact.

The HMG box protein, Hmo1, has been suggested to perform a similar role to UBF in yeast. Despite the lack of sequence similarity between UBF and Hmo1 multiple studies have provided support for UBF and Hmo1 performing similar functions in humans and yeast, respectively (Gadal et al., 2002, Hall et al., 2006, Merz et al., 2008). In collaboration with Olivier Gadal, we set out to address if UBF and Hmo1 are functional counterparts. Studies conducted by Gadals group found YFP-UBF1 and YFP-UBF2 co-localised with Hmo1 at the single crescent shaped nucleolus of a yeast cell. Deletion of Hmo1 results in a growth defect that cannot be rescued by overexpressing human UBF1 or UBF2. Deletion of Hmo1 and the yeast RNA Pol I subunit, Rpa49, is lethal, however overexpression of human UBF1, but not UBF2, can restore growth in this double mutant. These studies reveal that human UBF1 cannot fully substitute for Hmo1 but can partially fulfil some of Hmo1 functions in yeast. Interestingly Gadals group found that only untagged human UBF1 was capable of rescue, as the lethality observed in *hmo1*Δ*rpa49*Δ mutant was not relieved using N-terminal tagged UBF1. I will discuss in the following chapter why tagging at the N-terminus of UBF may be interfering with its ability to function correctly.

In human cells I demonstrated that Hmo1 targets NORs throughout the entire cell cycle. Hmo1 appears as punctate staining in the nucleolus, similar to that observed for human UBF, with a low nucleoplasmic signal. Hmo1 targets mitotic NORs and pseudo-NORs revealing that Hmo1 recruitment is independent of transcription. To address if Hmo1 can functionally substitute for UBF I made use of the UBFKD cell line in which I can induce the expression of UBF shRNA. Exploiting the UBFKD cells I generated a stable pool of cells in which I deplete UBF and turn on expression of Hmo1 simultaneously. Growth curves reveal that Hmo1 expression cannot rescue the growth defect associated with UBF depletion.

We speculate that there may be a number of reasons for the inability of Hmo1 and UBF to functionally substitute for each other. Firstly, failure of UBF1 to fully recapitulate Hmo1 functions in yeast could be due to the fact that UBF functions are restricted to RNA Pol I whereas Hmo1 performs additional functions. For instance Hmo1 binds strongly to most ribosomal protein (RP) gene promoters and therefore is involved in regulating RP gene expression by RNA Pol II (Berger et al., 2007, Hall et al., 2006, Kasahara et al., 2007, Kasahara et al., 2008). Hence UBF1 can only fulfil the RNA Pol I functions associated with Hmo1. This then raises a question, is human UBF2 capable of fulfilling the additional functions that Hmo1 performs in yeast, that is regulate RP gene expression in humans? UBF2 is rendered non-functional at the rDNA promoter and to this day has no known function, yet by western blotting UBF2 represents 50% of total cellular UBF. Additionally by western blotting I observe that the levels of UBF1 are higher than UBF2 in isolated nucleoli, indicating that a proportion of cellular UBF2 is located in the nucleoplasm (data not shown). Therefore, is the UBF2 present in

the nucleoplasm binding to RP gene promoters? In the literature UBF2 has been suggested to function as an RNA Pol II transcription factor (Grueneberg et al., 2003), however the evidence supporting this is not strong.

The inability of Hmo1 to rescue the growth defect as a consequence of UBF depletion in human cells might be due to the mechanism by which Hmo1 is recruited to human NORs. We cannot say whether or not Hmo1 is directly interacting with human rDNA or rDNA chromatin or if Hmo1 recruitment to NORs is dependent on protein-protein interactions with UBF. High level of Hmo1 expression in human cells results in the loss of Hmo1 targeting to nucleoli and the redistribution of UBF from the nucleolus to the nucleoplasm. Is this redistribution a reflection of UBF-Hmo1 interactions or a toxic effect to the cell? I have tried to determine whether Hmo1 recognises and binds the underlying rDNA sequence/rDNA chromatin or if Hmo1 binding is UBF dependent. I attempted an RNAi-mediated approach to deplete UBF and then transiently transfect Hmo1 in the pseudo-NOR cell line. This experimental approach did not work because UBF is an essential gene and the cells begin to die upon UBF depletion.

I have shown that UBF is evolutionarily conserved across animal phyla and that UBF's ability to target NORs is also conserved, demonstrated by *Ciona* UBF targeting human NORs. How UBF directs this specificity for binding to rDNA is unknown. However we speculate that the mechanism driving UBF specificity for rDNA is also evolutionarily conserved.

6 Identification of a novel SANT-like domain in the N-terminal region of UBF

6.1 Background

UBF binds specifically to rDNA repeats throughout the cell cycle, however this is at odds with UBFs lack of sequence specificity for DNA binding. In mammalian cells HMG-box containing proteins fall into two major groups. The first group is highly diverse and consists of proteins that contain a single HMG-box with no acidic C-terminal tail. This group confers sequence specificity for DNA binding, an example of such a protein is the mammalian testis-determining factor SRY (Sinclair et al., 1990). The second group consists of HMGB-type non-sequence specific DNA binding proteins that contain two or more HMG boxes and a C-terminal acidic tail. UBF falls into this latter group with *in vitro* experiments failing to identify any DNA binding specificity for UBF other than a preference for GC-rich DNA (Copenhaver et al., 1994). UBF specifically targets NORs and binds across the entire rDNA repeat *in vivo* (O'Sullivan et al., 2002). This specificity for UBF binding is reinforced by the lack of any UBF binding to the adjacent satellite DNA (O'Sullivan et al., 2002) and by immunostaining. What is driving UBF's ability to specifically recognise rDNA is still a major question in the field to this day.

A feature of the RNA Pol I machinery, and the rDNA itself, is their rapid evolutionary divergence. This is exemplified by the inability of human RNA Pol I machinery to support rDNA transcription in mouse and vice versa. Despite this evolutionary divergence UBFs ability to recognise and bind to rDNA is highly conserved, suggesting that UBFs ability to target rDNA is not solely dependent on the underlying DNA sequence, leading us to speculate that there may be an unidentified chromatin interaction motif within UBF. There are some studies in the literature suggesting that UBF is capable of binding to a nucleosomal template. *In vitro* UBF has been shown to bind to DNA packaged as a nucleosome and displace linker histone H1, suggesting that UBF and H1 binding are mutually exclusive (Kermekchiev et al., 1997). Also DNA assembled into chromatin can be transcribed in a UBF-dependent manner *in vitro* (Langst et al., 1997). A recent SILAC based proteomic study has identified UBF as a nucleosomal interactor (Bartke et al., 2010). In this study, a SILAC nucleosome affinity purification (SNAP) approach was used to identify proteins that are influenced by certain histone modifications in the context of a nucleosome. UBF1 was found to be enriched in pull down assays using nucleosomes containing specific histone H3 modifications (Bartke et al., 2010).

The pseudo-NORs have again provided a useful source for addressing if UBF binds to a nucleosomal template. Pseudo-NOR formation is dependent on extensive UBF binding to ectopic XEn DNA. As best we can tell the array is uniformly bound by UBF. Micrococcal nuclease digestion of nuclei from the pseudo-NOR cell line reveals that the XEn DNA is packaged as nucleosomes, concluding that *in vivo* UBF is capable of binding to nucleosomes (Wright et al., 2006).

We hypothesise that UBF has a chromatin interaction motif that is responsible for driving the specificity of UBF binding. In the previous chapter I demonstrated that UBF is evolutionarily conserved across the animal phylum, even in the most primitive metazoan, and that *Ciona* UBF can specifically recognise and bind to human NORs. This suggests that if a chromatin interaction motif is present in human UBF there is a strong chance that it is evolutionarily conserved. Therefore to identify the presence of a chromatin interaction motif within UBF I performed careful sequence analysis comparing the UBFs from the different species. To analyse UBF binding to rDNA *in vivo* I needed to develop specific tools. I generated a fluorescently tagged human UBF construct will enable us to study UBFs associated with rDNA throughout the cell cycle.

6.2 Results

6.2.1 Identification of an evolutionary conserved novel SANT domain within the N-terminus of UBF

We hypothesise that UBF's specificity for binding to rDNA is driven by its ability to recognise rDNA chromatin, and this is fuelled largely by the fact that rDNA sequences are rapidly evolving yet UBF retains its ability to target exclusively the rDNA. I have demonstrated that UBF is present across the animal phylum and the specificity for UBF binding to rDNA is conserved in *Ciona* UBF. This suggests that the mechanism driving UBF's binding specificity is evolutionarily conserved. I exported each protein sequence as a FASTA file and generated alignments using ClustalW2 (EMBL-EBI). The alignments enabled us to identify an evolutionarily conserved region within the N-terminal dimerisation domain of UBF, located from the 21st to 78th amino acid residue in human UBF. Interestingly this conserved region was even present in *Trichoplax* UBF (Figure 6.1). The fact that *Trichoplax* UBF was found to possess this conserved N-terminal region provides more convincing evidence that the orf we identified in *Trichoplax* is UBF, despite lacking the C-terminal tail. The evolutionary conservation of a domain suggests that the domain is performing an important function. Furthermore, this conserved domain in UBF is a single exon present in all the UBF orfs that we have identified. This suggests that exon shuffling is involved in the conservation of this conserved UBF domain throughout evolution, as hypothesised by Walter Gilbert (Gilbert, 1987).

The sequence of this N-terminal conserved region is identical between human, mouse, opossum and lizard UBF, and highly homologous in *Xenopus* UBF. However the most striking feature of this conserved region was the evolutionary spatial conservation of three tryptophan residues, which are considered rare amino acids (indicated by black boxes, Figure 6.1). Also evident from the alignment was the evolutionary conservation of a proline between the first and second

tryptophan and a cysteine between the second and third tryptophan (indicated by blue boxes, Figure 6.1).

Figure 6.1 ClustalW2 alignments reveal the presence of an evolutionarily conserved domain in the N-terminal dimerisation domain of UBF
UBF orfs from vertebrate species and the new non-vertebrate species identified in chapter 5 were converted to protein sequences. The protein sequences were subsequently imported into ClustalW2 (EMBL-EBI) as FASTA files. ClustalW2 generates an alignment of the UBF protein sequences from species across the animal phylum. A schematic of UBF1 and the position of the conserved region is indicated above the alignment. The black boxes highlight the evolutionarily conserved tryptophan residues and the blue boxes highlight the evolutionarily conserved proline and cysteine. '*' denotes fully conserved residues, ':' denotes strongly conserved residues and '.' denotes weakly conserved residues.

The SANT domain (switching-defective protein 3 (Swi3), adaptor 2 (Ada2), nuclear receptor co-repressor (N-CoR), transcription factor (TF)IIIB) is a motif found in a number of chromatin remodelling enzymes. The SANT domain was initially identified based on its homology with the DNA-binding domain (DBD) of c-Myb (Aasland, 1996). Both the Myb-DBD and the SANT domain are structurally similar, both comprising three α-helices, each of which contains a bulky aromatic residue, which together form a hydrophobic core that is critical to the overall structural fold (Figure 6.2 (A)) (Ogata et al., 1994, Tahirov et al., 2001, Aasland, 1996). The Myb DBD structure indicates that the third 'recognition' α-helix makes sequence specific contact with DNA, with several subsequent basic residues positioned with the potential to make contact with the phosphate group of DNA (Ogata et al., 1994). In most instances, SANT domains do not have basic residues at the C-terminus of the third α-helix. Furthermore the key residues in the third α-helix of the Myb DBD that make contact with DNA are not conserved in the SANT domain. In fact the SANT domains contains hydrophobic residues in the 'recognition' α-helix that are expected to inhibit DNA binding (Boyer et al., 2004). Despite the sequence and structural similarities, the SANT domain appears to have functionally evolved from the Myb DNA binding domain. SANT domains themselves appear to lack any enzymatic activity but are

functionally involved in histone acetylation and deacetylation, as well as ATP-dependent chromatin remodelling (Boyer et al., 2002, Sterner et al., 2002). A SANT domain present in c-Myb has been demonstrated to interact with the N-terminal tail of histone H3 and facilitates chromatin remodelling by making it accessible to histone acetyltansferases (HATs) (Mo et al., 2005).

The SANT domain is characterised by the presence of three spatially conserved tryptophan residues, extremely similar to that observed within the novel conserved domain in the N-terminal region of UBF (indicated by black boxes, Figure 6.2 (B)). In addition to the similar spatial conservation of the tryptophan residues the cysteine residue that is positioned between the second and third tryptophan in the novel conserved UBF domain is also evident in the SANT domain (indicated by blue box, Figure 6.2 (B)). An alignment of this novel SANT-like domain in UBF with the second SANT domain in Myb is shown to emphasize the sequence similarity (Figure 6.2 (C)). Identification of this evolutionarily conserved novel SANT-like domain in the dimerisation domain of UBF, supports our hypothesis that the specificity of UBF binding is driven by a chromatin interaction motif. In the latter part of this chapter I begin to investigate the role that this novel SANT-like domain plays in UBFs ability to recognise and target rDNA chromatin. However in order to conduct such investigations I needed to generate appropriate experimental tools that would enable me to analyse UBFs association with rDNA *in vivo*.

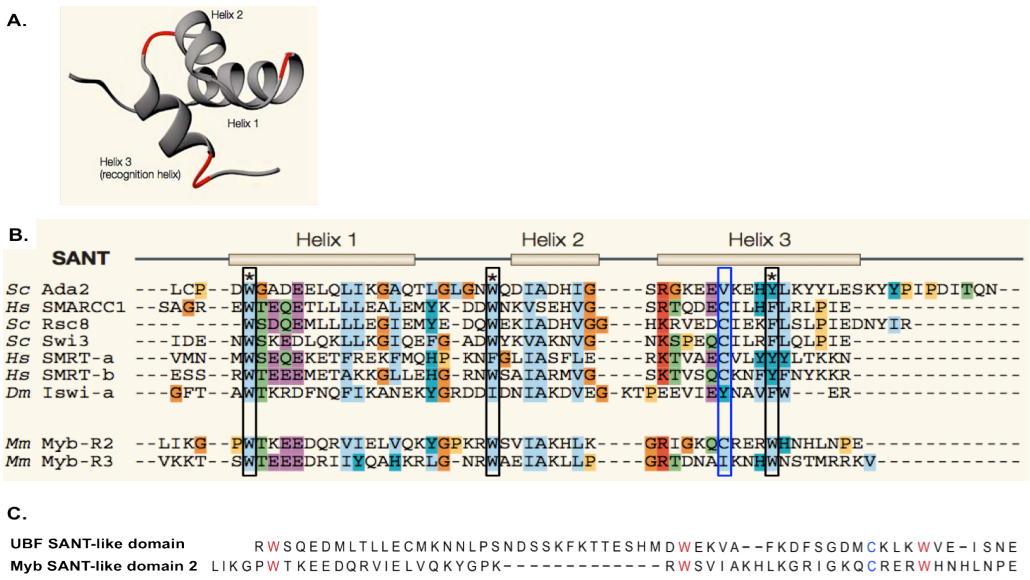

Figure 6.2 The SANT domain is a highly conserved motif
(A) Ribbon diagram of Myb DNA-binding domain, based on the solution structure of Myb R2 (Tahirov et al., 2001), is composed of three α-helices that have similar topography to the SANT domain. The third 'recognition' helix makes sequence specific contacts with DNA, however this function does not appear to be conserved in the SANT domain. (B) Alignment of SANT domain sequences and Myb sequences. Asterisks and black boxes indicate the conserved bulky hydrophobic residues. The blue box highlights a highly conserved cysteine residue. On the extreme left is the first two letters of the species name (*Dm, Drosophila melanogaster; Hs, Homo sapiens; Mm, Mus musculus; Sc, Saccharomyces cerevisiae*). Figure adapted from (Boyer et al., 2004). (C) Alignment of novel SANT-like domain in UBF with the second SANT domain in Myb. The conserved tryptophan residues are highlighted in red and cysteine in (blue).

6.2.2 Generation of a fluorescently tagged human UBF construct that mimics endogenous UBF

In the literature UBF is only tagged on the N-terminus, however there is no evidence of N-terminal tagged UBF targeting mitotic NORs, which is a defining characteristic of endogenous UBF. Furthermore, the punctate staining characteristic of endogenous UBF in the nucleolus is non-existent when UBF is tagged at the N-terminus (Figure 6.3) (Chen and Huang, 2001). From our collaborative work with Olivier Gadal we know that N-terminally tagged UBF1 is incapable of rescuing the lethality in a *hmo1*Δ iΔ yeast strain, whereas untagged UBF1 can restore growth. Additionally the newly identified evolutionarily conserved SANT-like domain is situated within the N-terminal region of UBF. Evolutionary conservation of a domain is a good indicator that it is performing an essential role. Therefore we reasoned that tagging UBF at the N-terminus, which is in close proximity to the conserved SANT-like domain, could be interfering with UBFs ability to perform its essential functions. Taking this into account I generated a fluorescent C-terminal tagged version of UBF1 and analysed if this construct can function similar to endogenous UBF and target NORs throughout the cell cycle.

The human UBF1 orf, lacking a stop codon, had previously been cloned in the McStay lab into the Gateway™ pENTR™/D-TOPO®, hence by employing Gateway™ technology we can clone the UBF orf into any destination vector. In the lab a lot of time has been invested into generating a catalogue of Gateway™ destination vectors that enables us to fuse an N- or C-terminal tag to a protein of interest. I will briefly describe how we constructed the Gateway™ destination vector for C-terminal tagging, as this is the construct I utilised for tagging human UBF1.

The pcDNA™-DEST40 Gateway™ destination vector, which is used for C-terminal fusion of V5-6xHIS tag (Figure 6.4 (A)), was manipulated to replace the V5-6xHIS tag for a fluorescent tag such as GFP (Green Fluorescent Protein). I made use of unique ApaI and PmeI restriction sites to extract the V5-6xHis tag from the pcDNA™-DEST40 vector. The GFP orf was amplified using *Pfu* with an ApaI containing forward primer and a PmeI containing reverse primer. The PCR product was digested with ApaI and PmeI and cloned into the pcDNA™-DEST40 vector to replace the V5-6xHis tag. The resulting modified destination vector was termed DEST-GFP-Cterm(neo), the neo signifies that the construct contains a neomycin resistance orf for mammalian selection (Figure 6.4 (B)).

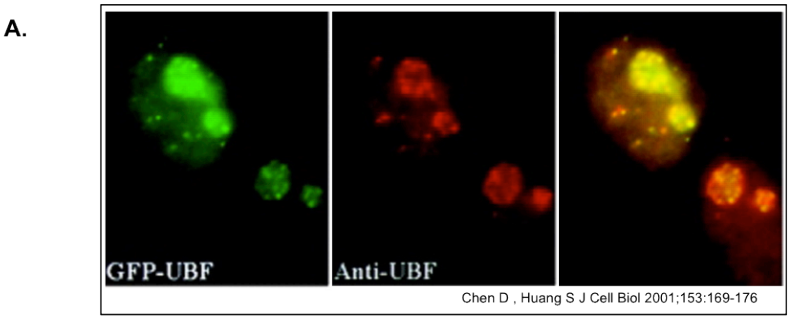

Figure 6.3 N-terminal GFP tagged UBF
The localization of N-terminal tagged UBF and the endogenous UBF in HeLa cells. Figure from (Chen and Huang, 2001).

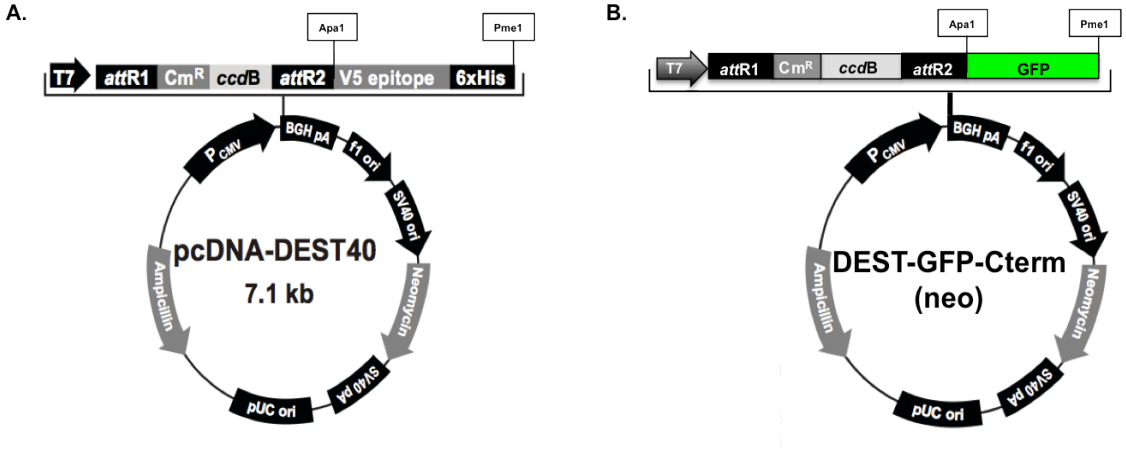

Figure 6.4 Generation of the gateway GFP construct for C-terminal tagging
(A) Schematic of pcDNA-DEST40 Gateway® destination vector. The unique ApaI and PmeI restriction sites either side of the C-terminal V5/6xHis tag are indicated. Figure adapted from the Invitrogen™ website www.invitrogen.com
(B) Schematic of the modified pcDNA-DEST40 Gateway® destination vector to contain a C-terminal GFP tag in place of the V5/6xHis tag. The ApaI and PmeI restriction sites were utilized to generate the DEST-GFP-Cterm(neo) construct.

To verify that the GFP orf was being expressed from the DEST-GFP-Cterm(neo) construct I cloned the orf of RPA190, the largest RNA Pol I subunit, into DEST-GFP-Cterm(neo), using the Gateway™ technology. The resulting construct DEST-RPA190-GFP-Cterm was transfected into the HT1080 human cell line. RPA190 was observed to target nucleoli demonstrating that the construct can fuse GFP to the inserted orf and reveal its localisation by fluorescence. For extra verification the DEST-GFP-Cterm(neo) construct was sequenced.

Having established that the DEST-GFP-Cterm(neo) is functioning correctly I decided to clone UBF1 orf from pENTR/D-TOPO_hUBF1Δstop into this GFP destination vector. Diagnostic restriction digests of the resulting DEST-hUBF1-GFP-Cterm(neo) construct implied that the construct was correct. However no expression of UBF1-GFP was observed in initial transfections performed in HT1080 human cells. We presumed that there was a mutation in the

UBF1 orf as I have already established that the DEST-GFP-Cterm(neo) is capable of expressing GFP. A DNA sample was sent for sequencing and the resulting sequence traces were visualised using 4peaks (mekentosj.com) and aligned with the UBF1 orf, using DNA Strider 1.4 or Serial Cloner 2.5 (serial-cloner.en.softonic.com). The location of the mutation was identified in the C-terminal acidic tail. As mentioned in section 2.1 virtually all UBF cloning proved problematic, with UBF picking up point mutations on a regular basis, particularly in the C-terminal region. Our reasoning for the frequency of these mutations is that UBF is being selected against in *E.coli*, due to a toxic effect caused by the C-terminal acidic tail. Because of these sporadic mutations, any manipulation to UBF DNA proved tedious and time consuming, with multiple rounds of cloning required for generating a UBF construct. Moreover DNA sequencing of the entire UBF orf had to be routinely performed each time UBF was manipulated and cultured in *E.coli*. The fact that we are tagging at the C-terminus of UBF means that we are routinely sequencing from the C-terminal end to ensure accurate fusion of the tag, and therefore able to identify any sporadic mutations that occur frequently at this region. When N-terminally tagging UBF, the sequencing may not have been performed from the C-terminus and therefore if mutations were present they would not have been detected.

After several rounds of cloning and using multiple different strategies, the DEST-hUBF1-GFP-Cterm(neo) construct was generated and verified by DNA sequencing. To establish if tagging UBF on the C-terminus interferes with its functioning *in vivo*, I transiently transfected DEST-hUBF1-GFP-Cterm(neo) into the HT1080 human cell using the standard calcium phosphate method. In parallel I co-transfected with the mCherry-Tubulin construct, which was kindly provided by Dr. Agnieszka Kaczmarczyk, which acts as a control by revealing cells that have been positively transfected. Cells were fixed 24hr after transfection with 4% PFA and mounted in DAPI. In positively transfected cells, mCherry-Tubulin reveals the cells microtubules and those cells that were expressing mCherry-Tubulin had also incorporated the DEST-hUBF1-GFP-Cterm(neo) construct. The staining pattern observed for cells expressing C-terminal tagged UBF was dramatically different from that observed in the literature for N-terminal tagged UBF (Figure 6.3)(Chen and Huang, 2001). C-terminally tagged UBF appears as punctate staining in the nucleolus, similar to that observed when immunostaining cells with α-hUBF antibodies. More importantly, in metaphase cells we observe that C-terminally tagged UBF targets mitotic NORs (Figure 6.5).

To further validate that the DEST-hUBF1-GFP-Cterm(neo) construct mimics endogenous UBF I transiently transfected the pseudo-NOR cell line with the construct. I demonstrate that similar to endogenous UBF the C-terminal tagged UBF can target pseudo-NORs at interphase and also during mitosis (pseudo-NORs are indicated by arrowheads, Figure 6.6). In metaphase cells the pseudo-NORs are easily distinguished due to their much larger size when compared to endogenous NORs.

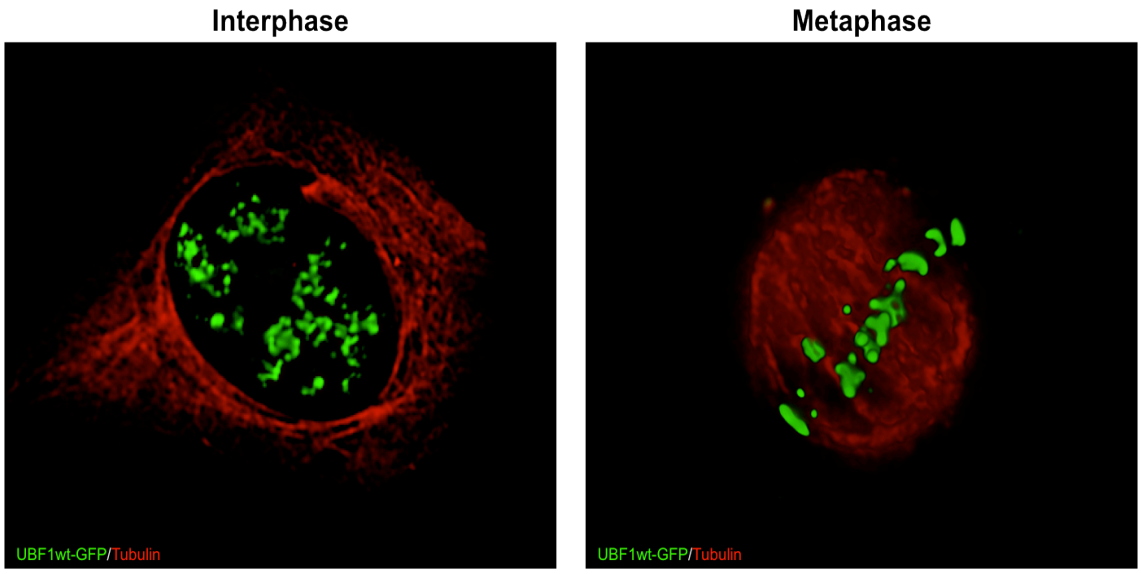

Figure 6.5 C-terminal tagged human UBF1 mimics endogenous UBF
HT1080 cells were co-transfected with DEST-hUBF1-GFP-Cterm and mCherry-Tubulin using the standard Calcium Phosphate method outlined in 2.3.7. Cells were fixed with 4% PFA before mounting in DAPI. C-terminal tagged human UBF1 targets nucleoli during interphase (left) as well as mitotic NORs (right).

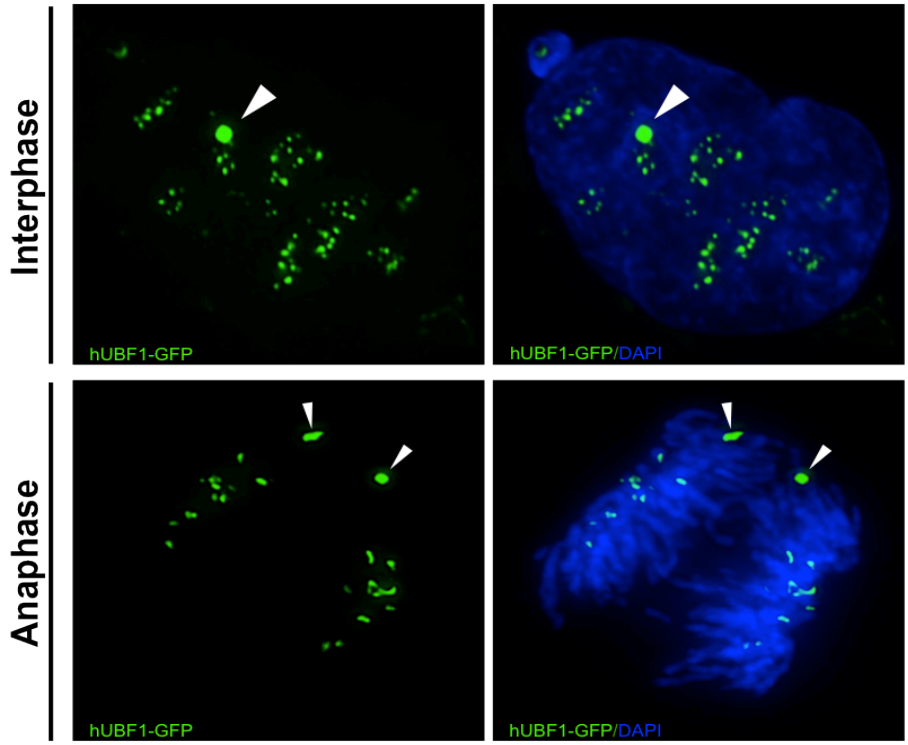

Figure 6.6 C-terminal tagged human UBF1 targets pseudo-NORs
The pseudo-NOR containing cell line was transiently transfected with DEST-hUBF1-GFP-Cterm using the standard Calcium Phosphate method outlined in 2.3.7. Cells were fixed with 4% PFA before mounting in DAPI. C-terminal tagged human UBF1 targets to nucleoli and the pseudo-NOR during interphase (top), as well as endogenous NORs and pseudo-NOR during mitosis (bottom). White arrowheads indicate pseudo-NOR.

Having demonstrated that the C-terminal tagged UBF mimics endogenous UBF, by targeting NORs throughout the cell cycle, I decided to use this construct to perform live cell imaging experiments. Live cell imaging with the DEST-hUBF1-GFP-Cterm construct will provide a powerful assay system for studying UBFs association with rDNA *in vivo* as well as UBFs mobility throughout the cell cycle. The DEST-hUBF1-GFP-Cterm(neo) was transfected into the pseudo-NOR cell line using the standard calcium phosphate protocol and I generated a stable clone constitutively expressing UBF1-GFP. The stable clone of cells was seeded in a glass-bottomed dish (MatTek) and HEPES (pH 7.2) was added to a final concentration of 20mmol/L immediately before cells were transferred to the heated stage on the DeltaVision Olympus microscope. Live cell movie was captured overnight and the resulting movie is presented on the CD included with my thesis. This short movie monitors UBFs localisation through an entire cell cycle. It begins with an interphase cell in which UBF is observed as punctate staining within the nucleolus and the pseudo-NOR is evident as a large distinctive nuclear body. As the cell approaches mitosis the rDNA becomes more condensed, eventually appearing as prominent foci. As the cell progresses through mitosis UBF remains associated with NORs. The NORs from sister chromatids are observed to move to opposite spindle poles around which nucleoli subsequently reform. The pseudo-NORs are again evident after cell division. This live cell movie validates that C-terminal tagged UBF1 remains bound to NORs throughout the cell cycle, hence mimicking endogenous UBF.

6.2.3 Functional analysis of the novel SANT domain identified with the N-terminal dimerisation domain of UBF

The novel SANT like domain that I have identified in the N-terminal region of UBF is highly conserved through evolution suggesting that it is involved in performing an important function associated with UBF. To determine if this novel domain is critical for UBF functioning I decided to perform mutational analyses. We hypothesise that if this novel SANT-like domain in UBF is a chromatin interaction motif, then performing mutational analyses within this domain will alter UBF's ability to target rDNA.

The obvious candidate residues for mutation were the tryptophan residues, as these residues are considered rare amino acids and more importantly are evolutionarily conserved in UBF among species across the animal phylum. Before performing the mutagenesis I first cloned the N-terminal half of UBF from the unique NotI and XhoI sites in pENTR/D-TOPO_hUBF1Δstop construct into pBluescript (SK-) (Stratagene). The reasoning for sub-cloning half the UBF orf is due the difficulty we have in manipulating UBF. We rationalised that using only half the UBF orf might limit the frequency of sporadic mutations.

Primers were designed to convert the codon for each of the conserved tryptophan residues to a codon for an alanine residue. Mutagenesis reactions were performed using the primers in table 2.2 and QuikChange® Lightning kit (Stratagene), outlined in section 2.1.15. The pBluescript(SK-)UBF1(NotI/XhoI) construct was used as the DNA template for the initial mutation of the tryptophan residues individually. Each mutation was verified by DNA sequencing. I then performed mutagenesis using pBluescript(SK-) UBF1_*W1A* construct as the template DNA to generate UBF1_*W1AW2A* and UBF1_*W1AW3A* double mutants. Similarly DNA from these double mutants was verified by sequencing with UBF1_*W1AW2A* subsequently used as the DNA template in the final mutagenesis reaction to generate the pBluescript(SK-)UBF1_*W1AW2AW3A* construct. The constructs generated include those shown in table 6.1.

Construct	Description
pBluescript (SK-) UBF1(NotIXhoI) *W1A*	First tryptophan mutated to Alanine
pBluescript (SK-) UBF1(NotIXhoI) *W2A*	Second tryptophan mutated to Alanine
pBluescript (SK-) UBF1(NotIXhoI) *W3A*	Third tryptophan mutated to Alanine
pBluescript (SK-) UBF1(NotIXhoI) *W1AW2A*	First and second tryptophan mutated to Alanine
pBluescript (SK-) UBF1(NotIXhoI) *W1AW3A*	First and third tryptophan mutated to Alanine
pBluescript (SK-) UBF1(NotIXhoI) *W1AW2AW3A*	First, second and third tryptophan mutated to Alanine

Table 6.1 Constructs containing mutated tryptophan residues within the SANT-like domain of UBF

To analyse if mutating these tryptophan residues impacts on the ability of UBF to target rDNA chromatin I made use of the DEST-hUBF1-GFP-Cterm construct. This construct has unique NotI and XhoI restriction sites facilitating replacement of the wild type SANT-like domain in the dimerisation domain of UBF with each of the mutants. One would expect that this cloning strategy would be straightforward, however generation of these UBF1 mutant-GFP constructs also proved problematic with random mutations occurring again in the C-terminal region of UBF. Consequently, only half of the desired constructs were successfully generated and confirmed by DNA sequencing. The UBF1 mutant-GFP constructs generated are displayed in (Figure 6.7).

These constructs were transfected into human cells to establish if the conserved tryptophan residues play a key role in UBFs ability to recognise rDNA chromatin *in vivo*. I co-transfected each of the UBF1 mutant constructs with the mCherry-Tubulin construct, which acts as a control for determining which cells have been positively transfected and also monitoring the overall efficiency of the transfection. In parallel to these transfections I also co-transfected wild type UBF1-GFP with the mCherry-Tubulin construct to directly compare the localisation of wild type UBF to the UBF mutants. All transient transfections were performed at the same time using the standard Calcium Phosphate method. Cells were fixed with 4% PFA 36 hours after transfection and mounted in DAPI.

Figure 6.7 Schematic of point mutations of the evolutionary conserved tryptophan residues
A cartoon of C-terminal GFP tagged human UBF1 is displayed and the position of the conserved domain within the dimerisation domain is highlighted by red lines. The wild type UBF protein sequence of the conserved region is shown on top and the three mutants shown below. Asterisks indicate the conserved tryptophan residues. A large blue 'A' denotes the mutation of tryptophan to alanine.

In control cells wild-type UBF1-GFP specifically targets the nucleolus, appearing as punctate staining characteristic of that observed for endogenous UBF (top row, Figure 6.8). Analysing cells transfected with the DEST-hUBF1-*W1A2AW3A*-GFP-Cterm construct we observed a dramatic change in the pattern of staining for UBF when compared to wild type UBF. Mutating the three conserved tryptophan residues results in the redistribution of UBF from the nucleolus with UBF now dispersed throughout the nucleus (second row, Figure 6.8). The dramatic change in UBF's localisation reveals that these three conserved tryptophan residues are fundamental in UBF's ability to target rDNA. To establish if the mutation of all three tryptophan residues is necessary to cause the redistribution of UBF1 I analysed the effect on UBF's localisation when solely the first or the third tryptophan residue is mutated. Interestingly I observed the same redistribution of UBF1 from the nucleolus for these single tryptophan residue mutations (third and bottom row, Figure 6.8). These *in vivo* studies reveal the critical nature of the conserved tryptophan residues in specifying UBF's ability to recognise rDNA chromatin. The fact that I observe the same redistribution of UBF, whether a single tryptophan residue or all three tryptophan residues are mutated, reveals that each tryptophan residue in this novel SANT-like domain is critical for directing UBF localisation.

A defining characteristic of UBF is its ability to remain bound to mitotic NORs. I therefore analysed the effect that mutating the tryptophan residues has on UBF's ability to bind mitotic NORs. Wild-type UBF1-GFP targets mitotic NORs, with the mCherry-Tubulin indicating that the cell is in metaphase (top row, Figure 6.9). As a consequence of mutating the three conserved tryptophan residues UBF loses its ability to target mitotic NORs and instead surrounds the metaphase chromosomes (second row, Figure 6.9). This inability to target mitotic NORs is also observed when either the first or the third conserved tryptophan residue is mutated (third and bottom row, Figure 6.9). These mutational studies reveal that the evolutionary conserved tryptophan residues of the novel SANT-like domain in the N-terminal region of UBF are critical to UBF's ability to bind to rDNA chromatin.

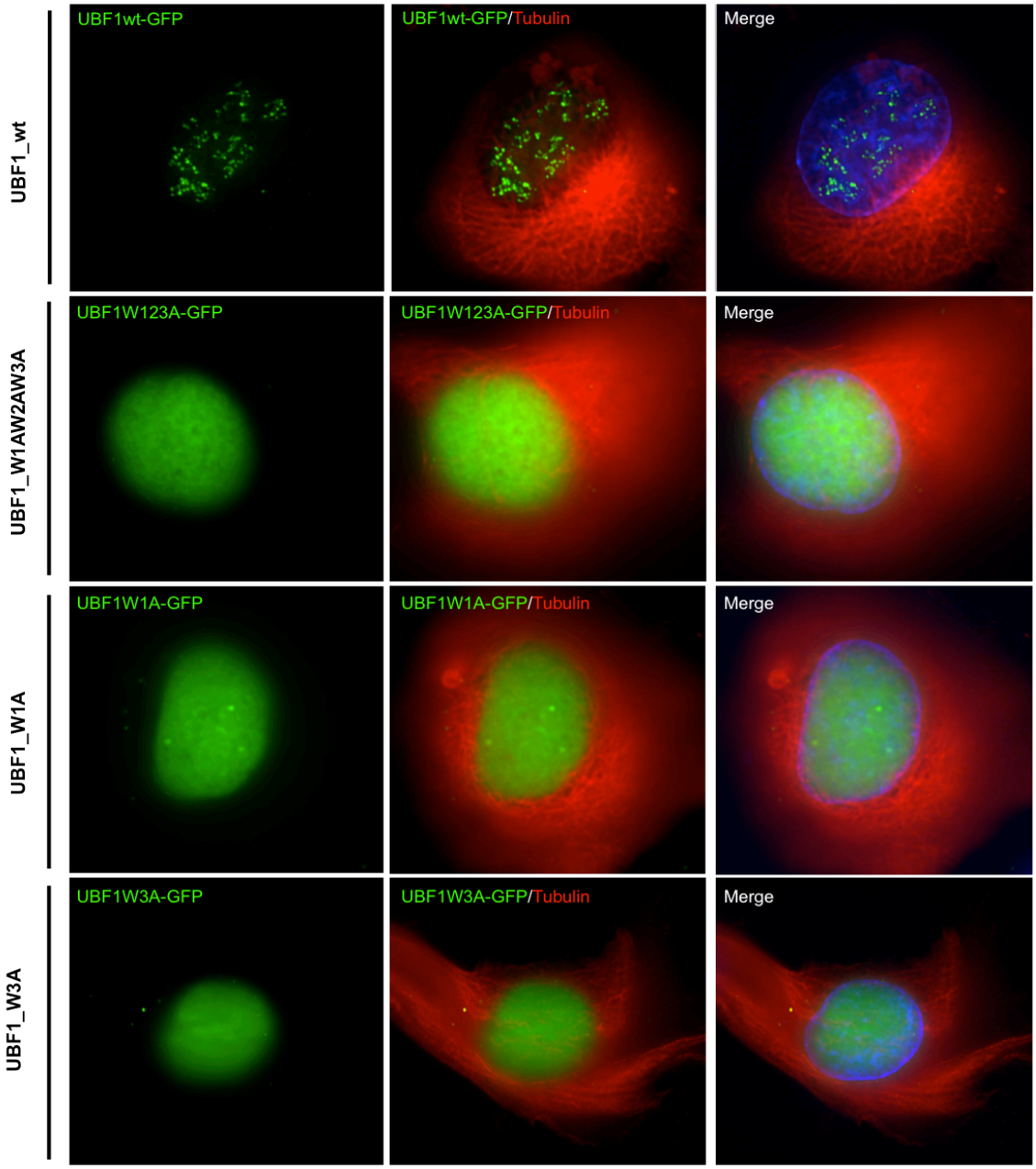

Figure 6.8 Mutating the conserved tryptophan residues results in the redistribution of UBF from the nucleolus

HT1080 cells were co-transfected with mCherry-Tubulin and DEST-hUBF1-GFP-Cterm or one of the UBF mutants using the standard Calcium Phosphate method outlined in 2.3.7. Cells were fixed with 4% PFA before mounting in DAPI. The localization of wild type UBF and UBF mutants in interphase cells was analysed. A merge of wild type UBF or UBF mutants with tubulin is displayed in the second panel in each row. The last panel displays a merge of wild type or mutant UBF, tubulin and DAPI.

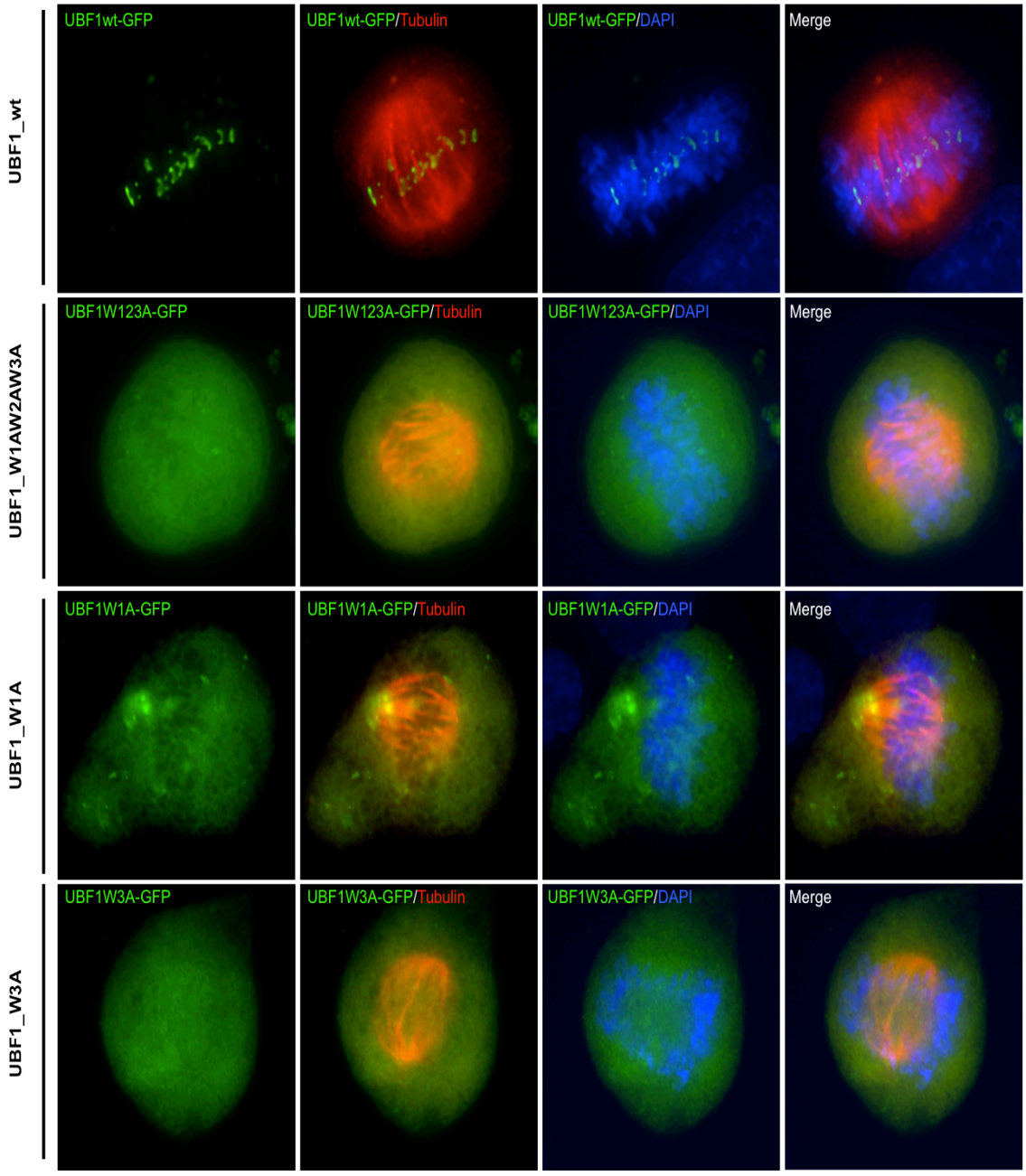

Figure 6.9 Mutating the conserved tryptophan residues results in UBFs inability to target mitotic NORs

HT1080 cells were co-transfected with mCherry-Tubulin and DEST-hUBF1-GFP-Cterm or one of the UBF mutants using the standard Calcium Phosphate method outlined in 2.3.7. Cells were fixed with 4% PFA before mounting in DAPI. The localization of wild type UBF and UBF mutants in metaphase cells was analysed. A merge of wild type or mutant UBF with tubulin or DAPI is displayed in the second and third panel, respectively, in each row. The last panel displays a merge of all three signals.

6.3 Discussion

In this chapter I have begun to address how UBF, a protein that lacks any sequence specificity for DNA binding, targets rDNA specifically *in vivo*. We hypothesise that UBF's ability to recognise rDNA is not solely reliant on the underlying sequence and that in actual fact UBF recognises the rDNA chromatin. If this is true UBF must contain a chromatin interaction motif. Performing multiple sequence alignments, we identified an evolutionarily conserved domain located in the N-terminal region of UBF, between amino acid residues 21 and 78. This novel domain is even present in *Trichoplax* UBF, revealing just how conserved this domain is and suggesting that it must be performing an important function.

By conducting further sequence analysis we reveal that the novel domain within the dimerisation domain of UBF contains three spatially conserved tryptophan residues. This spatial arrangement of three tryptophan residues is a signature of the SANT domain, a novel motif found in a number of chromatin remodelling factors (Boyer et al., 2004). For instance a SANT domain present in c-Myb functions as a histone interaction motif by binding to the N-terminal tail of histone H3 and positioning it for acetylation (Mo et al., 2005).

In order to perform functional analysis on this SANT-like domain in UBF I needed to establish a method for assaying UBF binding to rDNA *in vivo*. I generated a C-terminal GFP tagged human UBF1 construct and demonstrated that this fusion protein mimics endogenous UBF by targeting NORs throughout the cell cycle. In the literature UBF tagged at the N-terminus does not appear as punctate staining within the nucleolus and there is no evidence of it binding to mitotic NORs (Chen and Huang, 2001). By tagging at the N-terminus we believe that this is interfering with the correct functioning of the SANT-like domain within the N-terminal dimerisation domain of UBF. Interfering with the function of the SANT-like domain would thereby inhibit UBF's ability to recognise the rDNA chromatin and this would explain why N-terminal tagged UBF is incapable of targeting mitotic NORs.

By performing mutational analysis I sought to determine if the conserved novel SANT-like domain is required for specifying UBF binding to rDNA chromatin. Mutating the evolutionarily conserved tryptophan residues in the SANT-like domain of UBF reveals the critical nature of these residues for targeting UBF to rDNA. These mutational studies, combined with the similar spatial conservation of the tryptophan residues in this novel UBF domain and the SANT domain, provides evidence in support of our hypothesis that UBF recognises the rDNA chromatin rather than the underlying DNA sequence. Future analyses are required to prove that this novel SANT-like domain in the N-terminal region of UBF is in actual fact a chromatin interaction motif. I will discuss in the following chapter future studies that could be conducted to further characterise this SANT-like domain in UBF and establish if it is interacting with chromatin.

7 Conclusions and Future Directions

7.1 Conclusions

UBF binds across the entire rDNA repeats of active NORs (O'Sullivan et al., 2002) and remains bound to active NORs throughout the entire cell cycle (Roussel et al., 1993). A defining characteristic of active NORs is their appearance as secondary constrictions on metaphase chromosomes due to the decondensed state of the rDNA chromatin. We hypothesised that UBF binding to active rDNA repeats is responsible for establishing the open chromatin state associated with active NORs. In this thesis I have analysed the effect of reducing UBF levels on the chromatin state of active NORs. Making use of an inducible human UBFshRNA cell line, UBFKD cell line, I established that chronic depletion of UBF using 1μg/ml doxycycline correlates with a severe growth arrest with evidence suggestive of cell death by apoptosis. This finding along with our knowledge that UBF knockout mouse is embryonic lethal (personal communication with Tom Moss) reveals the essential nature of UBF.

Interestingly, using a significantly lower concentration of doxycycline, 2ng/ml, I was able to establish conditions in the UBFKD cell line in which I could reduce endogenous UBF levels by 4.5-fold without inducing a growth defect. 3D-immunoFISH revealed that this 4.5-fold reduction in UBF levels correlates with rDNA chromatin condensation and an increase in the proportion of silent NORs dissociated from nucleoli when compared directly to parental HT1080 cell line. To further reinforce our finding that UBF depletion correlates with rDNA chromatin condensation and an increase in the proportion of silent NORs, I employed the karyotypically normal human cell line, hTERT RPE-1. RNAi-mediated depletion of UBF resulted in rDNA chromatin condensation when compared to cells treated with control siRNA. Making use of the distal junction DNA probe, which hybridises to each human acrocentric chromosome, I was able to count the proportion of NORs that become silenced and dissociated from nucleoli as a consequence of UBF depletion. As a consequence of a 5.3-fold reduction in UBF levels the average number of silent NORs shifts from zero to three in RPE-1 cells.

In order to analyse the consequence of UBF depletion on the chromatin state of secondary constrictions I utilised the *Potorous tridactylus* (PtK) marsupial cell line. The rDNA repeats in these cells are located on the X-chromosome, therefore female cells have two NORs and male cells have a single NOR (Scheer and Rose, 1984, Robert-Fortel et al., 1993). Preparation of PtK metaphase spreads from RNAi-mediated UBF depleted cells revealed the loss of the secondary constriction. Additionally, RNAi-mediated depletion of UBF in the pseudo-NOR cell line results in the loss of the novel secondary constriction (unpublished work from the McStay group), which is present on a non-acrocentric chromosome as a consequence of extensive UBF binding to ectopic arrays. By combining the 3D-immunoFISH and chromosome analyses I have demonstrated that UBF is an essential player in maintaining the open decondensed chromatin state associated with active NORs.

Interestingly secondary constrictions are a characteristic of most if not all eukaryotes, however UBF was thought to be restricted to vertebrate. This notion was largely driven by the lack of a UBF-like protein in model organisms such as *Drosophila, C.elegans,* yeast and *Arabidopsis.* By performing tblastn searches I have demonstrated that UBF is not restricted to vertebrates but is present across the animal phyla, even in the most primitive metazoan *Trichoplax adhaerans*. To confirm that the newly identified UBF's from the tblastn searches were functioning like human UBF, I demonstrated that *Ciona intestinalis* UBF binds to human rDNA repeats throughout the entire cell cycle. I conclude that the ability of UBF to specifically recognise NORs has been conserved through evolution.

Plants appear to lack UBF, despite the fact that secondary constrictions were initially identified in plants (Heitz, 1931, McClintock, 1934). In *S. cerevisiae* a nucleolar HMG box protein, Hmo1, has been suggested to perform similar functions to UBF in yeast. Hmo1 is required for efficient rDNA transcription (Gadal et al., 2002), binds across the entire *S. cerevisiae* rDNA repeat *in vivo* (Hall et al., 2006) and Hmo1 binds to actively transcribed *S. cerevisiae* rRNA genes that are largely devoid of histone molecules (Merz et al., 2008). In collaboration with Olivier Gadal (Toulouse, France) we have addressed the question as to whether or not UBF and Hmo1 are functional counterparts. In the Gadal lab they have demonstrated that N-terminal tagged human UBF1 and UBF2 can target yeast nucleoli. Deletion of Hmo1 results in a growth defect that cannot be rescued by overexpressing human UBF1. However untagged human UBF1 can rescue the lethality observed in the *hmo1*Δ*rpa49*Δ yeast strain. This reveals that human UBF1 cannot fully substitute for Hmo1 but can perform some of Hmo1 functions in yeast. I performed the reciprocal experiments and demonstrated that Hmo1 can target human rDNA repeats throughout the cell cycle, as well as target pseudo-NORs, when expressed in human cells. Making use of the inducible human UBFshRNA cell line, UBFKD, I generated a stable pool of cells in which I could simultaneously deplete endogenous human UBF and induce expression of Hmo1. Growth curves reveal that Hmo1 expression cannot rescue the growth defect associated with UBF depletion. I conclude from these experiments that the requirement for a nucleolar specific HMG box protein to organise rDNA chromatin has been conserved through evolution. I predict that at some point in the future a nucleolar HMG box protein will be shown to be essential for the formation of NORs in plants where they were first described.

UBF binds specifically to rDNA repeats throughout the cell cycle, however this is at odds with UBFs lack of sequence specificity for DNA binding (Copenhaver et al., 1994). In the final part of my thesis I have begun to investigate how UBF specifically targets rDNA. We hypothesised that UBF might contain a chromatin interaction motif that enables UBF to bind to rDNA chromatin rather than the underlying rDNA sequence. A major feature driving our hypothesis is that rDNA is rapidly evolving yet UBFs ability to target rDNA is evolutionarily conserved, evident by *Ciona* UBFs ability to target human rDNA. I performed sequence analysis and

identified an evolutionarily conserved domain within the N-terminal dimerisation domain of UBF. This domain was present in all the newly identified UBFs in species across the animal phyla, including *Trichoplax* UBF. A striking feature of this conserved domain was the conserved spatial arrangement of three tryptophan residues, which are considered rare amino acids. This spatial arrangement of three tryptophan residues is a signature of the SANT domain, a novel motif found in a number of chromatin remodelling factors (Boyer et al., 2004). Mutational analysis of these tryptophan residues, within the SANT-like domain (SLD) in UBF, reveals the critical nature of these residues for UBFs ability to target rDNA. The similar spatial arrangement of the tryptophan residues in the SANT domain and the UBF SLD, combined with the mutational studies, provide evidence in support of our hypothesis that UBF recognises rDNA chromatin rather than the underlying DNA sequence.

7.2 Future Directions

I have established that UBF maintains the open chromatin state associated with active NORs and I have demonstrated that the proportion of silent NORs increases as a consequence of UBF depletion. One future experiment would be to determine if there is a hierarchy among the acrocentric chromosomes for the silencing of an NOR or is it completely random. To address this question one would have to obtain DNA probes that are specific to the short arms of each individual acrocentric chromosome and perform FISH using these probes.

In solution, UBF forms dimers through its N-terminal dimerisation domain (McStay et al., 1991). In the literature there is no evidence that SANT domains dimerise, however due to the location of the SANT-like domain (SLD) within the dimerisation domain it is possible that it may be facilitating the dimerisation of UBF. In the lab we have the GFP-trap® (Chromotek) system, which can be utilised in combination with the wild type human UBF1-GFP construct and mutant human UBF SANT domain-GFP constructs. Performing pilot experiments using the GFP-trap® system and the wild type UBF1-GFP construct I have detected by western blotting that the UBF1-GFP construct can pull-down both splice variants of UBF. Hence using this system will enable one to determine if the SLD is involved in UBF dimerisation. Interestingly, mutation of the first tryptophan residue of the SLD in *Xenopus* UBF has already been shown not to effect dimerisation (McStay et al., 1991).

My thesis work has shown that C-terminal tagging of UBF does not affect its ability to localise to NORs, but can this form of UBF substitute for endogenous UBF? In order to test this one could construct an shRNA resistant version of UBF-GFP and introduce it into the UBFKD cells under a Tet inducible promoter. Addition of doxycycline should in principle result in replacement of endogenous UBF with the UBF-GFP fusion protein, allowing its functionality to

be assessed. Assuming that UBF-GFP is fully functional this would provide an ideal platform for further studing the SLD my thesis work has identified.

Initially I would like to confirm that the SLD is conserved not only in sequence but also in function. I propose to replace the domain in human UBF with that from the primitive metazoan *Trichoplax*. I will assess both localisation and function. As the transcription machinery and the rDNA regulatory sequences diverge rapidly through evolution, conservation of function would imply that the SLD is recognising some conserved feature associated with rDNA, the obvious candidate being a specific chromatin/histone signature.

I envisage complementary approaches to identify the nature of such a signature. *In vitro* binding assays with individual histones or nucleosomes will confirm the ability of the SLD to recognise chromatin. Combining α-UBF ChIP and western blotting may reveal the particular histone signature that is read by the SLD *in vivo*. A number of studies suggest that *in vitro* approaches are appropriate. UBF has been demonstrated to displace linker histone H1 *in vitro* (Kermekchiev et al., 1997). Additionally it has been observed that UBF selectively binds to reconstituted and immobilised nucleosomes bearing either H3K4me3 or H3K9me3 modifications (Bartke et al., 2010). The Myb domain that most closely resembles UBF's SLD binds to the N-terminal tail of histone H3 in vitro (Mo et al., 2005).

UBF is a key regulator in ribosome biogenesis. UBF propagates the activity status of NORs through cell division, allowing the rapid onset of rDNA transcription and nucleolar reformation. I anticipate that future work on the SLD in UBF will solve the mystery surrounding UBF's ability to specifically recognise and organise rDNA chromatin, thereby facilitating our understanding as to how UBF performs its essential functions.

The work described in this thesis establishes UBF as a master regulator of ribosome biogenesis and suggests future experiments aimed at understanding how it performs this complex but essential role.

References

AAGAARD, L. & ROSSI, J. J. 2007. RNAi therapeutics: principles, prospects and challenges. *Advanced drug delivery reviews,* 59**,** 75-86.

AASLAND, R. 1996. The SANT domein: a putative DNA-binding domain in the SWI-SNF and ADA complexes, the transcriptional co-repressor N-CoR and TFIIIB. *Trens. Biochem. Sci.,* 21**,** 87-88.

AHMAD, Y., BOISVERT, F.-M., GREGOR, P., COBLEY, A. & LAMOND, A. I. 2009. NOPdb: Nucleolar Proteome Database—2008 update. *Nucleic acids research,* 37**,** D181-D184.

ALZUHERRI, H. M. & WHITE, R. J. 1999. Regulation of RNA polymerase I transcription in response to F9 embryonal carcinoma stem cell differentiation. *Journal of Biological Chemistry,* 274**,** 4328-4334.

ANDERSEN, J. S., LAM, Y. W., LEUNG, A. K. L., ONG, S.-E., LYON, C. E., LAMOND, A. I. & MANN, M. 2005. Nucleolar proteome dynamics. *Nature,* 433**,** 77-83.

ANDERSEN, J. S., LYON, C. E., FOX, A. H., LEUNG, A. K. L., LAM, Y. W., STEEN, H., MANN, M. & LAMOND, A. I. 2002. Directed proteomic analysis of the human nucleolus. *Current Biology,* 12**,** 1-11.

APRIKIAN, P., MOOREFIELD, B. & REEDER, R. H. 2001. New Model for the Yeast RNA Polymerase I Transcription Cycle. *Molecular and cellular biology,* 21**,** 4847-4855.

ARABI, A., WU, S., RIDDERSTRALE, K., BIERHOFF, H., SHIUE, C., FATYOL, K., FAHLEN, S., HYDBRING, P., SODERBERG, O., GRUMMT, I., LARSSON, L.-G. & WRIGHT, A. P. H. 2005. c-Myc associates with ribosomal DNA and activates RNA polymerase I transcription. *Nat Cell Biol,* 7**,** 303-310.

ARIS, J. P. & BLOBEL, G. 1991. cDNA cloning and sequencing of human fibrillarin, a conserved nucleolar protein recognized by autoimmune antisera. *Proceedings of the National Academy of Sciences,* 88**,** 931.

ARMACHE, K. J., MITTERWEGER, S., MEINHART, A. & CRAMER, P. 2005. Structures of complete RNA polymerase II and its subcomplex, Rpb4/7. *Journal of Biological Chemistry,* 280**,** 7131-7134.

ASSFALG, R., LEBEDEV, A., GONZALEZ, O. G., SCHELLING, A., KOCH, S. & IBEN, S. 2012. TFIIH is an elongation factor of RNA polymerase I. *Nucleic acids research,* 40**,** 650-659.

AZUM-GELADE, M. C., NOAILLAC-DEPEYRE, J., CAIZERGUES-FERRER, M. & GAS, N. 1994. Cell cycle redistribution of U3 snRNA and fibrillarin. Presence in the cytoplasmic nucleolus remnant and in the prenucleolar bodies at telophase. *Journal of Cell Science,* 107**,** 463-475.

BAER, M., NILSEN, T. W., COSTIGAN, C. & ALTMAN, S. 1990. Structure and transcription of a human gene for H1 RNA, the RNA component of human RNase P. *Nucleic acids research,* 18**,** 97-103.

BARTKE, T., VERMEULEN, M., XHEMALCE, B., ROBSON, S. C., MANN, M. & KOUZARIDES, T. 2010. Nucleosome-Interacting Proteins Regulated by DNA and Histone Methylation. *Cell,* 143**,** 470-484.

BARTSCH, I., SCHONEBERG, C. & GRUMMT, I. 1988. Purification and characterization of TTFI, a factor that mediates termination of mouse ribosomal DNA transcription. *Molecular and cellular biology,* 8**,** 3891-3897.

BAUERLE, K. T., KAMAU, E. & GROVE, A. 2006. Interactions between N-and C-terminal domains of the Saccharomyces cerevisiae high-mobility group protein HMO1 are required for DNA bending. *Biochemistry,* 45**,** 3635-3645.

BAZETT-JONES, D., LEBLANC, B., HERFORT, M. & MOSS, T. 1994. Short-range DNA looping by the Xenopus HMG-box transcription factor, xUBF. *Science,* 264**,** 1134-1137.

BECKMANN, H., CHEN, J. L., O'BRIEN, T. & TJIAN, R. 1995. Coactivator and promoter-selective properties of RNA polymerase I TAFs. *Science,* 270**,** 1506-1509.

BELL, S. P., PIKAARD, C. S., REEDER, R. H. & TJIAN, R. 1989. Molecular mechanisms governing species-specific transcription of ribosomal RNA. *Cell,* 59**,** 489.

BENAVENTE, R., ROSE, K. M., REIMER, G., HÜGLE-DÖRR, B. & SCHEER, U. 1987. Inhibition of nucleolar reformation after microinjection of antibodies to RNA polymerase I into mitotic cells. *The Journal of cell biology,* 105**,** 1483-1491.

BERGER, A. B., DECOURTY, L., BADIS, G., NEHRBASS, U., JACQUIER, A. & GADAL, O. 2007. Hmo1 is required for TOR-dependent regulation of ribosomal protein gene transcription. *Molecular and cellular biology,* 27**,** 8015.

BERMEJO, R., CAPRA, T., GONZALEZ-HUICI, V., FACHINETTI, D., COCITO, A., NATOLI, G., KATOU, Y., MORI, H., KUROKAWA, K., SHIRAHIGE, K. & FOIANI, M. 2009. Genome-Organizing Factors

Top2 and Hmo1 Prevent Chromosome Fragility at Sites of S phase Transcription. *Cell,* 138**,** 870-884.

BERNS, M. W., FLOYD, A. D., ADKISSON, K., CHENG, W. K., MOORE, L., HOOVER, G., USTICK, K., BURGOTT, S. & OSIAL, T. 1972. Laser microirradiation of the nucleolar organizer in cells of the rat kangaroo (Potorous tridactylis)* 1:: Reduction of nucleolar number and production of micronucleoli. *Experimental Cell Research,* 75**,** 424-432.

BIRD, A. P., TAGGART, M. H. & GEHRING, C. A. 1981. Methylated and unmethylated ribosomal RNA genes in the mouse. *Journal of molecular biology,* 152**,** 1-17.

BIRNSTIEL, M. L., WALLACE, H., SIRLIN, J. & FISCHBERG, M. 1966. Localization of the ribosomal DNA complements in the nucleolar organizer region of Xenopus laevis. *National Cancer Institute Monograph,* 23**,** 431.

BLEICHERT, F. & BASERGA, S. 2011. Small Ribonucleoproteins in Ribosome Biogenesis. *The Nucleolus***,** 135-156.

BLOOM, S. & GOODPASTURE, C. 1976. An improved technique for selective silver staining of nucleolar organizer regions in human chromosomes. *Human genetics,* 34**,** 199-206.

BOHNSACK, M. T., KOS, M. & TOLLERVEY, D. 2008. Quantitative analysis of snoRNA association with pre-ribosomes and release of snR30 by Rok1 helicase. *EMBO reports,* 9**,** 1230-1236.

BOISVERT, F.-M., LAM, Y. W., LAMONT, D. & LAMOND, A. I. 2010. A Quantitative Proteomics Analysis of Subcellular Proteome Localization and Changes Induced by DNA Damage. *Molecular & Cellular Proteomics,* 9**,** 457-470.

BOISVERT, F. M., VAN KONINGSBRUGGEN, S., NAVASCUÉS, J. & LAMOND, A. I. 2007. The multifunctional nucleolus. *Nature Reviews Molecular Cell Biology,* 8**,** 574-585.

BOULON, S., WESTMAN, B. J., HUTTEN, S., BOISVERT, F.-M. & LAMOND, A. I. 2010. The Nucleolus under Stress. *Molecular cell,* 40**,** 216-227.

BOYER, L. A., LANGER, M. R., CROWLEY, K. A., TAN, S., DENU, J. M. & PETERSON, C. L. 2002. Essential Role for the SANT Domain in the Functioning of Multiple Chromatin Remodeling Enzymes. *Molecular cell,* 10**,** 935-942.

BOYER, L. A., LATEK, R. R. & PETERSON, C. L. 2004. The SANT domain: a unique histone-tail-binding module? *Nature Reviews Molecular Cell Biology,* 5**,** 158-163.

BRADSHER, J., AURIOL, J., DE SANTIS, L. P., IBEN, S., VONESCH, J.-L., GRUMMT, I. & EGLY, J.-M. 2002. CSB Is a Component of RNA Pol I Transcription. *Molecular cell,* 10**,** 819-829.

BRANDENBURGER, Y., ARTHUR, J. F., WOODCOCK, E. A., DU, X. J., GAO, X., AUTELITANO, D. J., ROTHBLUM, L. I. & HANNAN, R. D. 2003. Cardiac hypertrophy in vivo is associated with increased expression of the ribosomal gene transcription factor UBF. *FEBS letters,* 548**,** 79-84.

BROWN, D. D. & GURDON, J. 1964. Absence of ribosomal RNA synthesis in the anucleolate mutant of Xenopus laevis. *Proceedings of the National Academy of Sciences of the United States of America,* 51**,** 139.

BROWN, S. E. & SZYF, M. 2007. Epigenetic programming of the rRNA promoter by MBD3. *Molecular and cellular biology,* 27**,** 4938-4952.

BRUMMELKAMP, T. R., BERNARDS, R. & AGAMI, R. 2002. A system for stable expression of short interfering RNAs in mammalian cells. *Science's STKE,* 296**,** 550.

CABURET, S., CONTI, C., SCHURRA, C., LEBOFSKY, R., EDELSTEIN, S. J. & BENSIMON, A. 2005. Human ribosomal RNA gene arrays display a broad range of palindromic structures. *Genome research,* 15**,** 1079-1085.

CAPERTA, A. D., NEVES, N., MORAIS-CECÍLIO, L., MALHÓ, R. & VIEGAS, W. 2002. Genome restructuring in rye affects the expression, organization and disposition of homologous rDNA loci. *Journal of Cell Science,* 115**,** 2839-2846.

CARMO-FONSECA, M., MENDES-SOARES, L. & CAMPOS, I. 2000. To be or not to be in the nucleolus. *Nat Cell Biol,* 2**,** E107-E112.

CASAFONT, I., NAVASCUÉS, J., PENA, E., LAFARGA, M. & BERCIANO, M. T. 2006. Nuclear organization and dynamics of transcription sites in rat sensory ganglia neurons detected by incorporation of 5′ -fluorouridine into nascent RNA. *Neuroscience,* 140**,** 453-462.

CAVANAUGH, A. H., HEMPEL, W. M., TAYLOR, L. J., ROGALSKY, V., TODOROV, G. & ROTHBLUM, L. I. 1995. Activity of RNA polymerase I transcription factor UBF blocked by Rb gene product. *Nature,* 374**,** 177-180.

CAVANAUGH, A. H., HIRSCHLER-LASZKIEWICZ, I., HU, Q., DUNDR, M., SMINK, T., MISTELI, T. & ROTHBLUM, L. I. 2002. Rrn3 Phosphorylation Is a Regulatory Checkpoint for Ribosome Biogenesis. *Journal of Biological Chemistry,* 277**,** 27423-27432.

CHAMBON, P. 1975. Eukaryotic nuclear RNA polymerases. *Annual review of biochemistry,* 44**,** 613-638.

CHEN, D. & HUANG, S. 2001. Nucleolar Components Involved in Ribosome Biogenesis Cycle between the Nucleolus and Nucleoplasm in Interphase Cells. *The Journal of cell biology,* 153**,** 169-176.

CHEN, H.-K., PAI, C.-Y., HUANG, J.-Y. & YEH, N.-H. 1999. Human Nopp140, Which Interacts with RNA Polymerase I: Implications for rRNA Gene Transcription and Nucleolar Structural Organization. *Molecular and cellular biology,* 19**,** 8536-8546.

CHOO, K., EARLE, E. & MCQUILLAN, C. 1990. A homologous subfamily of satellite III DNA on human chromosomes 14 and 22. *Nucleic acids research,* 18**,** 5641-5648.

CLEMENTE-BLANCO, A., MAYAN-SANTOS, M., SCHNEIDER, D. A., MACHIN, F., JARMUZ, A., TSCHOCHNER, H. & ARAGON, L. 2009. Cdc14 inhibits transcription by RNA polymerase I during anaphase. *Nature,* 458**,** 219-222.

CLOS, J., BUTTGEREIT, D. & GRUMMT, I. 1986. A purified transcription factor (TIF-IB) binds to essential sequences of the mouse rDNA promoter. *Proceedings of the National Academy of Sciences,* 83**,** 604.

COMAI, L., TANESE, N. & TJIAN, R. 1992. The TATA-binding protein and associated factors are integral components of the RNA polymerase I transcription factor, SL1. *Cell,* 68**,** 965-976.

CONCONI, A., WIDMER, R. M., KOLLER, T. & SOGO, J. M. 1989. Two different chromatin structures coexist in ribosomal RNA genes throughout the cell cycle. *Cell,* 57**,** 753-761.

COPENHAVER, G. P. & PIKAARD, C. S. 1996. Two‐dimensional RFLP analyses reveal megabase‐sized clusters of rRNA gene variants in Arabidopsis thaliana, suggesting local spreading of variants as the mode for gene homogenization during concerted evolution. *The Plant Journal,* 9**,** 273-282.

COPENHAVER, G. P., PUTNAM, C. D., DENTON, M. L. & PIKAARD, C. S. 1994. The RNA polymerase I transcription factor UBF is a sequence-tolerant HMG-box protein that can recognize structured nucleic acids. *Nucleic acids research,* 22**,** 2651-2657.

CRAMER, P., ARMACHE, K. J., BAUMLI, S., BENKERT, S., BRUECKNER, F., BUCHEN, C., DAMSMA, G., DENGL, S., GEIGER, S. & JASIAK, A. 2008. Structure of eukaryotic RNA polymerases. *Annu. Rev. Biophys.,* 37**,** 337-352.

DAMMANN, R., LUCCHINI, R., KOLLER, T. & SOGO, J. M. 1993. Chromatin structures and transcription of rDNA in yeast Saccharomyces cerevisiae. *Nucleic acids research,* 21**,** 2331-2338.

DAMMANN, R., LUCCHINI, R., KOLLER, T. & SOGO, J. M. 1995. Transcription in the yeast rRNA gene locus: distribution of the active gene copies and chromatin structure of their flanking regulatory sequences. *Molecular and cellular biology,* 15**,** 5294-5303.

DATTA, P. K., BUDHIRAJA, S., REICHEL, R. R. & JACOB, S. T. 1997. Regulation of Ribosomal RNA Gene Transcription during Retinoic Acid-Induced Differentiation of Mouse Teratocarcinoma Cells. *Experimental Cell Research,* 231**,** 198-205.

DENISSOV, S., VAN DRIEL, M., VOIT, R., HEKKELMAN, M., HULSEN, T., HERNANDEZ, N., GRUMMT, I., WEHRENS, R. & STUNNENBERG, H. 2007. Identification of novel functional TBP-binding sites and general factor repertoires. *The EMBO journal,* 26**,** 944-954.

DEV, V., TANTRAVAHI, R., MILLER, D. & MILLER, O. 1977. Nucleolus organizers in Mus musculus subspecies and in the RAG mouse cell line. *Genetics,* 86**,** 389-398.

DHALIWAL, M., PATHAK, S., SHIRLEY, L. & FLANAGAN, J. 1988. Ag-NOR staining in the Bennett wallaby, Macropus rufogriseus: evidence for dosage compensation. *Cytobios,* 56**,** 29.

DRAGON, F., GALLAGHER, J. E. G., COMPAGNONE-POST, P. A., MITCHELL, B. M., PORWANCHER, K. A., WEHNER, K. A., WORMSLEY, S., SETTLAGE, R. E., SHABANOWITZ, J., OSHEIM, Y., BEYER, A. L., HUNT, D. F. & BASERGA, S. J. 2002. A large nucleolar U3 ribonucleoprotein required for 18S ribosomal RNA biogenesis. *Nature,* 417**,** 967-970.

DRAKAS, R., TU, X. & BASERGA, R. 2004. Control of cell size through phosphorylation of upstream binding factor 1 by nuclear phosphatidylinositol 3-kinase. *PNAS,* 101**,** 9272-9276.

DRYGIN, D., RICE, W. G. & GRUMMT, I. 2010. The RNA polymerase I transcription machinery: an emerging target for the treatment of cancer. *Annual review of pharmacology and toxicology,* 50**,** 131-156.

DUNDR, M., HOFFMANN-ROHRER, U., HU, Q., GRUMMT, I., ROTHBLUM, L. I., PHAIR, R. D. & MISTELI, T. 2002. A kinetic framework for a mammalian RNA polymerase in vivo. *Science,* 298**,** 1623-1626.

DUNDR, M., MISTELI, T. & OLSON, M. O. J. 2000. The dynamics of postmitotic reassembly of the nucleolus. *The Journal of cell biology,* 150**,** 433-446.

EARLEY, K., LAWRENCE, R. J., PONTES, O., REUTHER, R., ENCISO, A. J., SILVA, M., NEVES, N., GROSS, M., VIEGAS, W. & PIKAARD, C. S. 2006. Erasure of histone acetylation by Arabidopsis HDA6 mediates large-scale gene silencing in nucleolar dominance. *Genes & development,* 20**,** 1283-1293.

FREED, E. F., PRIETO, J. L., MCCANN, K. L., MCSTAY, B. & BASERGA, S. J. 2012. NOL11, Implicated in the Pathogenesis of North American Indian Childhood Cirrhosis, Is Required for Pre-rRNA Transcription and Processing. *PLoS Genetics,* 8**,** e1002892.

FRENCH, S. L., OSHEIM, Y. N., CIOCI, F., NOMURA, M. & BEYER, A. L. 2003. In exponentially growing Saccharomyces cerevisiae cells, rRNA synthesis is determined by the summed RNA polymerase I loading rate rather than by the number of active genes. *Molecular and cellular biology,* 23**,** 1558-1568.

GADAL, O., LABARRE, S., BOSCHIERO, C. & THURIAUX, P. 2002. Hmo1, an HMG-box protein, belongs to the yeast ribosomal DNA transcription system. *EMBO J,* 21**,** 5498-5507.

GALLAGHER, J. E. G., DUNBAR, D. A., GRANNEMAN, S., MITCHELL, B. M., OSHEIM, Y., BEYER, A. L. & BASERGA, S. J. 2004. RNA polymerase I transcription and pre-rRNA processing are linked by specific SSU processome components. *Genes & development,* 18**,** 2506-2517.

GANLEY, A. R. D. & KOBAYASHI, T. 2007. Highly efficient concerted evolution in the ribosomal DNA repeats: Total rDNA repeat variation revealed by whole-genome shotgun sequence data. *Genome research,* 17**,** 184-191.

GANOT, P. & BORTOLIN, M. L. 1997. Site-specific pseudouridine formation in preribosomal RNA is guided by small nucleolar RNAs. *Cell,* 89**,** 799-810.

GAUTIER, T., ROBERT-NICOUD, M., GUILLY, M. & HERNANDEZ-VERDUN, D. 1992. Relocation of nucleolar proteins around chromosomes at mitosis. A study by confocal laser scanning microscopy. *Journal of Cell Science,* 102**,** 729-737.

GHOSHAL, K., MAJUMDER, S., DATTA, J., MOTIWALA, T., BAI, S., SHARMA, S. M., FRANKEL, W. & JACOB, S. T. 2004. Role of human ribosomal RNA (rRNA) promoter methylation and of methyl-CpG-binding protein MBD2 in the suppression of rRNA gene expression. *Journal of Biological Chemistry,* 279**,** 6783-6793.

GILBERT, W. The exon theory of genes. 1987. Cold Spring Harbor Laboratory Press, 901-905.

GOESSENS, G. 1984. Nucleolar structure. *Int. Rev. Cytol,* 87**,** 107-158.

GONZALEZ, I. L. & SYLVESTER, J. E. 1995. Complete sequence of the 43-kb human ribosomal DNA repeat: analysis of the intergenic spacer. *Genomics,* 27**,** 320-328.

GORSKI, J. J., PATHAK, S., PANOV, K., KASCIUKOVIC, T., PANOVA, T., RUSSELL, J. & ZOMERDIJK, J. C. B. M. 2007. A novel TBP-associated factor of SL1 functions in RNA polymerase I transcription. *The EMBO journal,* 26**,** 1560-1568.

GRANDI, P., RYBIN, V., BASSLE, J., PETFALSKI, E., STRAUS, D., MARZIOCH, M., SCHÄFER, T., KUSTER, B., TSCHOCHNER, H. & TOLLERVEY, D. 2002. 90S pre-ribosomes include the 35S pre-rRNA, the U3 snoRNP, and 40S subunit processing factors but predominantly lack 60S synthesis factors. *Molecular cell,* 10**,** 105.

GRANDORI, C., GOMEZ-ROMAN, N., FELTON-EDKINS, Z. A., NGOUENET, C., GALLOWAY, D. A., EISENMAN, R. N. & WHITE, R. J. 2005. c-Myc binds to human ribosomal DNA and stimulates transcription of rRNA genes by RNA polymerase I. *Nat Cell Biol,* 7**,** 311-318.

GROB, A., COLLERAN, C. & MCSTAY, B. 2011. UBF an Essential Player in Maintenance of Active NORs and Nucleolar Formation. *The Nucleolus***,** 83-103.

GROZDANOV, P., GEORGIEV, O. & KARAGYOZOV, L. 2003. Complete sequence of the 45-kb mouse ribosomal DNA repeat: analysis of the intergenic spacer. *Genomics,* 82**,** 637-643.

GRUENEBERG, D. A., PABLO, L., HU, K.-Q., AUGUST, P., WENG, Z. & PAPKOFF, J. 2003. A Functional Screen in Human Cells Identifies UBF2 as an RNA Polymerase II Transcription Factor That Enhances the β-Catenin Signaling Pathway. *Molecular and cellular biology,* 23**,** 3936-3950.

GRUMMT, I. 2003. Life on a planet of its own: regulation of RNA polymerase I transcription in the nucleolus. *Genes & development,* 17**,** 1691.

GRUMMT, I., KUHN, A., BARTSCH, I. & ROSENBAUER, H. 1986. A transcription terminator located upstream of the mouse rDNA initiation site affects rRNA synthesis. *Cell,* 47**,** 901-911.

GRUMMT, I., MAIER, U., OHRLEIN, A., HASSOUNA, N. & BACHELLERIE, J. P. 1985. Transcription of mouse rDNA terminates downstream of the 3'end of 28S RNA and involves interaction of factors with repeated sequences in the 3'spacer. *Cell,* 43**,** 801.

GRUMMT, I. & PIKAARD, C. S. 2003. Epigenetic silencing of RNA polymerase I transcription. *Nat Rev Mol Cell Biol,* 4**,** 641-649.

GRUMMT, I., ROTH, E. & PAULE, M. R. 1982. Ribosomal RNA transcription in vitro is species specific.

HALL, D. B., WADE, J. T. & STRUHL, K. 2006. An HMG protein, Hmo1, associates with promoters of many ribosomal protein genes and throughout the rRNA gene locus in Saccharomyces cerevisiae. *Molecular and cellular biology,* 26**,** 3672.

HALTINER, M. M., SMALE, S. T. & TJIAN, R. 1986. Two distinct promoter elements in the human rRNA gene identified by linker scanning mutagenesis. *Molecular and cellular biology,* 6**,** 227-235.

HAMERTON, J., CANNING, N., RAY, M. & SMITH, S. 1975. A cytogenetic survey of 14,069 newborn infants. *Clinical genetics,* 8**,** 223-243.

HANADA, K. I., SONG, C., YAMAMOTO, K., YANO, K., MAEDA, Y., YAMAGUCHI, K. & MURAMATSU, M. 1996. RNA polymerase I associated factor 53 binds to the nucleolar transcription factor UBF and functions in specific rDNA transcription. *The EMBO journal,* 15**,** 2217.

HANNAN, K., HANNAN, R., SMITH, S., JEFFERSON, L., LUN, M. & ROTHBLUM, L. 2000a. Rb and p130 regulate RNA polymerase I transcription: Rb disrupts the interaction between UBF and SL-1. *Oncogene,* 19**,** 4988.

HANNAN, K. M., BRANDENBURGER, Y., JENKINS, A., SHARKEY, K., CAVANAUGH, A., ROTHBLUM, L., MOSS, T., POORTINGA, G., MCARTHUR, G. A. & PEARSON, R. B. 2003a. mTOR-Dependent Regulation of Ribosomal Gene Transcription Requires S6K1 and Is Mediated by Phosphorylation of the Carboxy-Terminal Activation Domain of the Nucleolar Transcription Factor UBF†. *Molecular and cellular biology,* 23**,** 8862-8877.

HANNAN, K. M., BRANDENBURGER, Y., JENKINS, A., SHARKEY, K., CAVANAUGH, A., ROTHBLUM, L., MOSS, T., POORTINGA, G., MCARTHUR, G. A., PEARSON, R. B. & HANNAN, R. D. 2003b. mTOR-Dependent Regulation of Ribosomal Gene Transcription Requires S6K1 and Is Mediated by Phosphorylation of the Carboxy-Terminal Activation Domain of the Nucleolar Transcription Factor UBF†. *Molecular and cellular biology,* 23**,** 8862-8877.

HANNAN, K. M., KENNEDY, B. K., CAVANAUGH, A. H., HANNAN, R. D., HIRSCHLER-LASZKIEWICZ, I., JEFFERSON, L. S. & ROTHBLUM, L. I. 2000b. RNA polymerase I transcription in confluent cells: Rb downregulates rDNA transcription during confluence-induced cell cycle arrest. *Oncogene,* 19**,** 3487.

HANNAN, R. D., STEFANOVSKY, V., TAYLOR, L., MOSS, T. & ROTHBLUM, L. I. 1996. Overexpression of the transcription factor UBF1 is sufficient to increase ribosomal DNA transcription in neonatal cardiomyocytes: implications for cardiac hypertrophy. *Proceedings of the National Academy of Sciences,* 93**,** 8750.

HAYANO, T., YANAGIDA, M., YAMAUCHI, Y., SHINKAWA, T., ISOBE, T. & TAKAHASHI, N. 2003. Proteomic analysis of human Nop56p-associated pre-ribosomal ribonucleoprotein complexes. *Journal of Biological Chemistry,* 278**,** 34309-34319.

HEITZ, E. 1931. Die ursache der gesetzmässigen zahl, lage, form und grösse pflanzlicher nukleolen. *Planta,* 12**,** 775-844.

HEIX, J. & GRUMMT, I. 1995. Species specificity of transcription by RNA polymerase I. *Current opinion in genetics & development,* 5**,** 652-656.

HEIX, J., VENTE, A., VOIT, R., BUDDE, A., MICHAELIDIS, T. M. & GRUMMT, I. 1998. Mitotic silencing of human rRNA synthesis: inactivation of the promoter selectivity factor SL1 by cdc2/cyclin B-mediated phosphorylation. *The EMBO journal,* 17**,** 7373-7381.

HEIX, J., ZOMERDIJK, J. C. B. M., RAVANPAY, A., TJIAN, R. & GRUMMT, I. 1997. Cloning of murine RNA polymerase I-specific TAF factors: Conserved interactions between the subunits of the species-specific transcription initiation factor TIF-IB/SL1. *Proceedings of the National Academy of Sciences,* 94**,** 1733-1738.

HELIOT, L., KAPLAN, H., LUCAS, L., KLEIN, C., BEORCHIA, A., DOCO-FENZY, M., MENAGER, M., THIRY, M., O'DONOHUE, M. F. & PLOTON, D. 1997. Electron tomography of metaphase nucleolar organizer regions: evidence for a twisted-loop organization. *Molecular biology of the cell,* 8**,** 2199-2216.

HELIOT, L., MONGELARD, F., KLEIN, C., O'DONOHUE, M. F., CHASSERY, J. M., ROBERT-NICOUD, M. & USSON, Y. 2000. Nonrandom distribution of metaphase AgNOR staining patterns on human acrocentric chromosomes. *The journal of histochemistry and cytochemistry: official journal of the Histochemistry Society,* 48**,** 13.

HENDERSON, A., WARBURTON, D. & ATWOOD, K. 1972. Location of ribosomal DNA in the human chromosome complement. *Proceedings of the National Academy of Sciences,* 69**,** 3394.

HENDERSON, S. & SOLLNER-WEBB, B. 1986. A transcriptional terminator is a novel element of the promoter of the mouse ribosomal RNA gene. *Cell,* 47**,** 891-900.

HENNING, D., SO, R. B., JIN, R., LAU, L. F. & VALDEZ, B. C. 2003. Silencing of RNA Helicase II/Guα Inhibits Mammalian Ribosomal RNA Production. *Journal of Biological Chemistry,* 278**,** 52307-52314.

HENRIQUEZ, R., BLOBEL, G. & ARIS, J. 1990. Isolation and sequencing of NOP1. A yeast gene encoding a nucleolar protein homologous to a human autoimmune antigen. *Journal of Biological Chemistry,* 265**,** 2209-2215.

HERNANDEZ-VERDUN, D., ROUSSEL, P. & GÉBRANE-YOUNÈS, J. 2002. Emerging concepts of nucleolar assembly. *Journal of Cell Science,* 115**,** 2265-2270.

HERNANDEZ-VERDUN, D., ROUSSEL, P., THIRY, M., SIRRI, V. & LAFONTAINE, D. L. J. 2010. The nucleolus: structure/function relationship in RNA metabolism. *Wiley Interdisciplinary Reviews: RNA,* 1**,** 415-431.

HISCOX, J. A. 2007. RNA viruses: hijacking the dynamic nucleolus. *Nat Rev Micro,* 5**,** 119-127.

JANSA, P., MASON, S. W., HOFFMANN-ROHRER, U. & GRUMMT, I. 1998. Cloning and functional characterization of PTRF, a novel protein which induces dissociation of paused ternary transcription complexes. *The EMBO journal,* 17**,** 2855-2864.

JANTZEN, H., CHOW, A., KING, D. & TJIAN, R. 1992. Multiple domains of the RNA polymerase I activator hUBF interact with the TATA-binding protein complex hSL1 to mediate transcription. *Genes & development,* 6**,** 1950-1963.

JANTZEN, H.-M., ADMON, A., BELL, S. P. & TJIAN, R. 1990. Nucleolar transcription factor hUBF contains a DNA-binding motif with homology to HMG proteins. *Nature,* 344**,** 830-836.

JASIAK, A. J., ARMACHE, K. J., MARTENS, B., JANSEN, R. P. & CRAMER, P. 2006. Structural biology of RNA polymerase III: subcomplex C17/25 X-ray structure and 11 subunit enzyme model. *Molecular cell,* 23**,** 71-81.

JEFFERIES, H. B. J., FUMAGALLI, S., DENNIS, P. B., REINHARD, C., PEARSON, R. B. & THOMAS, G. 1997. Rapamycin suppresses 5[prime]TOP mRNA translation through inhibition of p70s6k. *EMBO J,* 16**,** 3693-3704.

JIMENEZ-GARCIA, L., SEGURA-VALDEZ, M. L., OCHS, R., ROTHBLUM, L., HANNAN, R. & SPECTOR, D. 1994. Nucleologenesis: U3 snRNA-containing prenucleolar bodies move to sites of active pre-rRNA transcription after mitosis. *Molecular biology of the cell,* 5**,** 955.

JONES, M. H., LEARNED, R. M. & TJIAN, R. 1988. Analysis of clustered point mutations in the human ribosomal RNA gene promoter by transient expression in vivo. *Proceedings of the National Academy of Sciences,* 85**,** 669-673.

JORDAN, E. G. 1991. Interpreting nucleolar structure: where are the transcribing genes? *Journal of Cell Science,* 98**,** 437-442.

JORDAN, P., MANNERVIK, M., TORA, L. & CARMO-FONSECA, M. 1996. In vivo evidence that TATA-binding protein/SL1 colocalizes with UBF and RNA polymerase I when rRNA synthesis is either active or inactive. *The Journal of cell biology,* 133**,** 225-234.

KAMAU, E., BAUERLE, K. T. & GROVE, A. 2004. The Saccharomyces cerevisiae High Mobility Group Box Protein HMO1 Contains Two Functional DNA Binding Domains. *Journal of Biological Chemistry,* 279**,** 55234-55240.

KASAHARA, K., KI, S., AOYAMA, K., TAKAHASHI, H. & KOKUBO, T. 2008. Saccharomyces cerevisiae HMO1 interacts with TFIID and participates in start site selection by RNA polymerase II. *Nucleic acids research,* 36**,** 1343-1357.

KASAHARA, K., OHTSUKI, K., KI, S., AOYAMA, K., TAKAHASHI, H., KOBAYASHI, T., SHIRAHIGE, K. & KOKUBO, T. 2007. Assembly of regulatory factors on rRNA and ribosomal protein genes in Saccharomyces cerevisiae. *Molecular and cellular biology,* 27**,** 6686-6705.

KASS, S., CRAIG, N. & SOLLNER-WEBB, B. 1987. Primary processing of mammalian rRNA involves two adjacent cleavages and is not species specific. *Molecular and cellular biology,* 7**,** 2891-2898.

KASS, S., TYC, K., STEITZ, J. A. & SOLLNER-WEBB, B. 1990. The U3 small nucleolar ribonucleoprotein functions in the first step of preribosomal RNA processing. *Cell,* 60**,** 897.

KEENER, J., DODD, J. A., LALO, D. & NOMURA, M. 1997. Histones H3 and H4 are components of upstream activation factor required for the high-level transcription of yeast rDNA by RNA polymerase I. *Proceedings of the National Academy of Sciences,* 94**,** 13458.

KERMEKCHIEV, M., WORKMAN, J. L. & PIKAARD, C. S. 1997. Nucleosome binding by the polymerase I transactivator upstream binding factor displaces linker histone H1. *Molecular and cellular biology,* 17**,** 5833-5842.

KEYS, D. A., LEE, B. S., DODD, J. A., NGUYEN, T. T., VU, L., FANTINO, E., BURSON, L. M., NOGI, Y. & NOMURA, M. 1996. Multiprotein transcription factor UAF interacts with the upstream element of the yeast RNA polymerase I promoter and forms a stable preinitiation complex. *Genes & development,* 10**,** 887-903.

KEYS, D. A., VU, L., STEFFAN, J. S., DODD, J. A., YAMAMOTO, R. T., NOGI, Y. & NOMURA, M. 1994. RRN6 and RRN7 encode subunits of a multiprotein complex essential for the initiation of rDNA transcription by RNA polymerase I in Saccharomyces cerevisiae. *Genes & development,* 8**,** 2349-2362.

KISS-LÁSZLÓ, Z., HENRY, Y., BACHELLERIE, J. P., CAIZERGUES-FERRER, M. & KISS, T. 1996. Site-specific ribose methylation of preribosomal RNA: a novel function for small nucleolar RNAs. *Cell,* 85**,** 1077.

KLEIN, J. & GRUMMT, I. 1999. Cell cycle-dependent regulation of RNA polymerase I transcription: the nucleolar transcription factor UBF is inactive in mitosis and early G1. *Proceedings of the National Academy of Sciences,* 96**,** 6096.

KOBAYASHI, T., HECK, D. J., NOMURA, M. & HORIUCHI, T. 1998. Expansion and contraction of ribosomal DNA repeats in Saccharomyces cerevisiae: requirement of replication fork blocking (Fob1) protein and the role of RNA polymerase I. *Genes & development,* 12**,** 3821-3830.

KOBERNA, K., MALÍNSKÝ, J., PLISS, A., MAŠATA, M., VEČEŘOVÁ, J., FIALOVÁ, M., BEDNÁR, J. & RAŠKA, I. 2002. Ribosomal genes in focus. *The Journal of cell biology,* 157**,** 743-748.

KORTSCHAK, R. D., SAMUEL, G., SAINT, R. & MILLER, D. J. 2003. EST Analysis of the Cnidarian< i> Acropora millepora</i> Reveals Extensive Gene Loss and Rapid Sequence Divergence in the Model Invertebrates. *Current Biology,* 13**,** 2190-2195.

KROGAN, N. J., PENG, W.-T., CAGNEY, G., ROBINSON, M. D., HAW, R., ZHONG, G., GUO, X., ZHANG, X., CANADIEN, V., RICHARDS, D. P., BEATTIE, B. K., LALEV, A., ZHANG, W., DAVIERWALA, A. P., MNAIMNEH, S., STAROSTINE, A., TIKUISIS, A. P., GRIGULL, J., DATTA, N., BRAY, J. E., HUGHES, T. R., EMILI, A. & GREENBLATT, J. F. 2004. High-Definition Macromolecular Composition of Yeast RNA-Processing Complexes. *Molecular cell,* 13**,** 225-239.

KRYSTOSEK, A. 1998. Repositioning of Human Interphase Chromosomes by Nucleolar Dynamics in the Reverse Transformation of HT1080 Fibrosarcoma Cells. *Experimental Cell Research,* 241**,** 202-209.

KUHN, A. & GRUMMT, I. 1987. A novel promoter in the mouse rDNA spacer is active in vivo and in vitro. *The EMBO journal,* 6**,** 3487.

KUHN, A., VENTE, A., DORÉE, M. & GRUMMT, I. 1998. Mitotic phosphorylation of the TBP-containing factor SL1 represses ribosomal gene transcription1. *Journal of molecular biology,* 284**,** 1-5.

KUHN, A., VOIT, R., STEFANOVSKY, V., EVERS, R., BIANCHI, M. & GRUMMT, I. 1994. Functional differences between the two splice variants of the nucleolar transcription factor UBF: the second HMG box determines specificity of DNA binding and transcriptional activity. *The EMBO journal,* 13**,** 416.

KUHN, C.-D., GEIGER, S. R., BAUMLI, S., GARTMANN, M., GERBER, J., JENNEBACH, S., MIELKE, T., TSCHOCHNER, H., BECKMANN, R. & CRAMER, P. 2007. Functional Architecture of RNA Polymerase I. *Cell,* 131**,** 1260-1272.

KWON, H. & GREEN, M. R. 1994. The RNA polymerase I transcription factor, upstream binding factor, interacts directly with the TATA box-binding protein. *Journal of Biological Chemistry,* 269**,** 30140-30146.

LABHART, P. & REEDER, R. H. 1984. Enhancer-like properties of the 60/81 bp elements in the ribosomal gene spacer of Xenopus laevis. *Cell,* 37**,** 285.

LALO, D., STEFFAN, J. S., DODD, J. A. & NOMURA, M. 1996. RRN11 encodes the third subunit of the complex containing Rrn6p and Rrn7p that is essential for the initiation of rDNA transcription by yeast RNA polymerase I. *Journal of Biological Chemistry,* 271**,** 21062.

LAM, Y. W., EVANS, V. C., HEESOM, K. J., LAMOND, A. I. & MATTHEWS, D. A. 2010. Proteomics analysis of the nucleolus in adenovirus-infected cells. *Molecular & Cellular Proteomics,* 9**,** 117-130.

LANG, W. H. & REEDER, R. H. 1995. Transcription termination of RNA polymerase I due to a T-rich element interacting with Reb1p. *Proceedings of the National Academy of Sciences,* 92**,** 9781-9785.

LANGST, G., BLANK, T. A., BECKER, P. B. & GRUMMT, I. 1997. RNA polymerase I transcription on nucleosomal templates: the transcription termination factor TTF-I induces chromatin remodeling and relieves transcriptional repression. *EMBO J,* 16**,** 760-768.

LARSON, D. E., XIE, W. Q., GLIBETIC, M., O'MAHONY, D., SELLS, B. H. & ROTHBLUM, L. I. 1993. Coordinated decreases in rRNA gene transcription factors and rRNA synthesis during muscle cell differentiation. *Proceedings of the National Academy of Sciences,* 90**,** 7933.

LAWRENCE, R. J., EARLEY, K., PONTES, O., SILVA, M., CHEN, Z. J., NEVES, N., VIEGAS, W. & PIKAARD, C. S. 2004. A Concerted DNA Methylation/Histone Methylation Switch Regulates rRNA Gene Dosage Control and Nucleolar Dominance. *Molecular cell,* 13**,** 599-609.

LEARNED, R. M., CORDES, S. & TJIAN, R. 1985. Purification and characterization of a transcription factor that confers promoter specificity to human RNA polymerase I. *Molecular and cellular biology,* 5**,** 1358-1369.

LEUNG, A. K. L., GERLICH, D., MILLER, G., LYON, C., LAM, Y. W., LLERES, D., DAIGLE, N., ZOMERDIJK, J., ELLENBERG, J. & LAMOND, A. I. 2004. Quantitative kinetic analysis of nucleolar breakdown and reassembly during mitosis in live human cells. *The Journal of cell biology,* 166**,** 787-800.

LEVAN, G. 1970. Contributions to the chromosomal characterization of the PTK 1 rat‐kangaroo cell line. *Hereditas,* 64**,** 85-96.

LI, J., LANGST, G. & GRUMMT, I. 2006a. NoRC-dependent nucleosome positioning silences rRNA genes. *EMBO J,* 25**,** 5735-5741.

LI, J., LÄNGST, G. & GRUMMT, I. 2006b. NoRC-dependent nucleosome positioning silences rRNA genes. *The EMBO journal,* 25**,** 5735-5741.

LIANG, X. & FOURNIER, M. J. 2006. The helicase Has1p is required for snoRNA release from pre-rRNA. *Molecular and cellular biology,* 26**,** 7437-7450.

LIAU, M. C. & PERRY, R. P. 1969. Ribosome precursor particles in nucleoli. *The Journal of cell biology,* 42**,** 272-283.

LIU, M., TU, X., FERRARI‐AMOROTTI, G., CALABRETTA, B. & BASERGA, R. 2007. Downregulation of the upstream binding factor1 by glycogen synthase kinase3β in myeloid cells induced to differentiate. *Journal of cellular biochemistry,* 100**,** 1154-1169.

LLANOS, S., CLARK, P. A., ROWE, J. & PETERS, G. 2001. Stabilization of p53 by p14ARF without relocation of MDM2 to the nucleolus. *Nature cell biology,* 3**,** 445-452.

LU, J., KOBAYASHI, R. & BRILL, S. J. 1996. Characterization of a high mobility group 1/2 homolog in yeast. *Journal of Biological Chemistry,* 271**,** 33678-33685.

LUCCHINI, R. & SOGO, J. M. 1995. Replication of transcriptionally active chromatin. *Nature,* 374**,** 276-280.

LUCCHINI, R., WELLINGER, R. E. & SOGO, J. M. 2001. Nucleosome positioning at the replication fork. *The EMBO journal,* 20**,** 7294-7302.

LUGER, K., DECHASSA, M. L. & TREMETHICK, D. J. 2012. New insights into nucleosome and chromatin structure: an ordered state or a disordered affair? *Nat Rev Mol Cell Biol,* 13**,** 436-447.

LUGER, K., MADER, A. W., RICHMOND, R. K., SARGENT, D. F. & RICHMOND, T. J. 1997. Crystal structure of the nucleosome core particle at 2.8 A resolution. *Nature,* 389**,** 251-260.

MAIS, C., WRIGHT, J. E., PRIETO, J. L., RAGGETT, S. L. & MCSTAY, B. 2005. UBF-binding site arrays form pseudo-NORs and sequester the RNA polymerase I transcription machinery. *Genes & development,* 19**,** 50-64.

MAJUMDER, S., GHOSHAL, K., DATTA, J., SMITH, D. S., BAI, S. & JACOB, S. T. 2006. Role of DNA methyltransferases in regulation of human ribosomal RNA gene transcription. *Journal of Biological Chemistry,* 281**,** 22062-22072.

MASON, S. W., SANDER, E. E. & GRUMMT, I. 1997. Identification of a transcript release activity acting on ternary transcription complexes containing murine RNA polymerase I. *The EMBO journal,* 16**,** 163-172.

MAYER, C., BIERHOFF, H. & GRUMMT, I. 2005. The nucleolus as a stress sensor: JNK2 inactivates the transcription factor TIF-IA and down-regulates rRNA synthesis. *Genes & development,* 19**,** 933.

MAYER, C., ZHAO, J., YUAN, X. & GRUMMT, I. 2004. mTOR-dependent activation of the transcription factor TIF-IA links rRNA synthesis to nutrient availability. *Genes & development,* 18**,** 423-434.

MCCLINTOCK, B. 1934. The relation of a particular chromosomal element to the development of the nucleoli in Zea mays. *Cell and Tissue Research,* 21**,** 294-326.

MCGOWAN, P. O., SASAKI, A., HUANG, T. C. T., UNTERBERGER, A., SUDERMAN, M., ERNST, C., MEANEY, M. J., TURECKI, G. & SZYF, M. 2008. Promoter-wide hypermethylation of the ribosomal RNA gene promoter in the suicide brain. *PloS one,* 3**,** e2085.

MCSTAY, B., FRAZIER, M. W. & REEDER, R. H. 1991. xUBF contains a novel dimerization domain essential for RNA polymerase I transcription. *Genes & development,* 5**,** 1957.

MCSTAY, B. & GRUMMT, I. 2008. The epigenetics of rRNA genes: from molecular to chromosome biology. *Annual review of cell and developmental biology,* 24**,** 131-157.

MCSTAY, B. & REEDER, R. H. 1986. A termination site for Xenopus RNA polymerase I also acts as an element of an adjacent promoter. *Cell,* 47**,** 913-920.

MCSTAY, B., SULLIVAN, G. J. & CAIRNS, C. 1997. The Xenopus RNA polymerase I transcription factor, UBF, has a role in transcriptional enhancement distinct from that at the promoter. *The EMBO journal,* 16**,** 396-405.

MEIER, U. T. 2005. The many facets of H/ACA ribonucleoproteins. *Chromosoma,* 114**,** 1-14.

MEIER, U. T. & BLOBEL, G. 1994. NAP57, a mammalian nucleolar protein with a putative homolog in yeast and bacteria. *The Journal of cell biology,* 127**,** 1505-1514.

MERANER, J., LECHNER, M., LOIDL, A., GORALIK-SCHRAMEL, M., VOIT, R., GRUMMT, I. & LOIDL, P. 2006. Acetylation of UBF changes during the cell cycle and regulates the interaction of UBF with RNA polymerase I. *Nucleic acids research,* 34**,** 1798-1806.

MERRY, D., PATHAK, S. & VANDEBERG, J. 1983. Differential NOR activities in somatic and germ cells of< i> Monodelphis domestica</i>(Marsupialia, Mammalia). *Cytogenetic and Genome Research,* 35**,** 244-251.

MERZ, K., HONDELE, M., GOETZE, H., GMELCH, K., STOECKL, U. & GRIESENBECK, J. 2008. Actively transcribed rRNA genes in S. cerevisiae are organized in a specialized chromatin associated with the high-mobility group protein Hmo1 and are largely devoid of histone molecules. *Genes & development,* 22**,** 1190-1204.

MIESFELD, R. & ARNHEIM, N. 1984. Species-specific rDNA transcription is due to promoter-specific binding factors. *Molecular and cellular biology,* 4**,** 221-227.

MILLER, G., PANOV, K. I., FRIEDRICH, J. K., TRINKLE-MULCAHY, L., LAMOND, A. I. & ZOMERDIJK, J. C. B. M. 2001. hRRN3 is essential in the SL1-mediated recruitment of RNA polymerase I to rRNA gene promoters. *The EMBO journal,* 20**,** 1373-1382.

MILLER JR, O. & BAKKEN, A. H. 1972. Morphological studies of transcription. *Acta Endocrinologica,* 71**,** S155-S177.

MILLER, O. L. & BEATTY, B. R. 1969. Visualization of Nucleolar Genes. *Science,* 164**,** 955-957.

MISHIMA, Y., FINANCSEK, I., KOMINAMI, R. & MURAMATSU, M. 1982. Fractiontion and reconstitution of factors required for accurate transcription of mammalian ribosomal RNA genes: identification of a species-depandent initiation factor. *Nucleic acids research,* 10**,** 6659-6670.

MO, X., KOWENZ-LEUTZ, E., LAUMONNIER, Y., XU, H. & LEUTZ, A. 2005. Histone H3 tail positioning and acetylation by the c-Myb but not the v-Myb DNA-binding SANT domain. *Genes & development,* 19**,** 2447-2457.

MONTGOMERY JR, T. S. H. 1898. Comparative cytological studies, with especial regard to the morphology of the nucleolus. *Journal of Morphology,* 15**,** 265-582.

MOSS, T. 1982. Transcription of cloned Xenopus laevis ribosomal DNA microinjected into Xenopus oocytes, and the identification of an RNA polymerase I promoter. *Cell,* 30**,** 835-842.

MOSS, T. & BIRNSTIEL, M. L. 1979. The putative promoter of a Xenopus laevis ribosomal gene is reduplicated. *Nucleic acids research,* 6**,** 3733-3744.

MOUGEY, E., O'REILLY, M., OSHEIM, Y., MILLER, O., BEYER, A. & SOLLNER-WEBB, B. 1993. The terminal balls characteristic of eukaryotic rRNA transcription units in chromatin spreads are rRNA processing complexes. *Genes & development,* 7**,** 1609.

NÉMETH, A., GUIBERT, S., TIWARI, V. K., OHLSSON, R. & LÄNGST, G. 2008. Epigenetic regulation of TTF-I-mediated promoter–terminator interactions of rRNA genes. *The EMBO journal,* 27**,** 1255-1265.

NI, J., TIEN, A. L. & FOURNIER, M. J. 1997. Small Nucleolar RNAs Direct Site-Specific Synthesis of Pseudouridine in Ribosomal RNA. *Cell,* 89**,** 565-573.

NIEWMIERZYCKA, A. & CLARKE, S. 1999. S-Adenosylmethionine-dependent Methylation in Saccharomyces cerevisiae IDENTIFICATION OF A NOVEL PROTEIN ARGININE METHYLTRANSFERASE. *Journal of Biological Chemistry,* 274**,** 814-824.

NOGI, Y., YANO, R. & NOMURA, M. 1991. Synthesis of large rRNAs by RNA polymerase II in mutants of Saccharomyces cerevisiae defective in RNA polymerase I. *Proceedings of the National Academy of Sciences,* 88**,** 3962.

NOMURA, M., NOGI, Y. & OAKES, M. 2004. Transcription of rDNA in the yeast Saccharomyces cerevisiae. *The Nucleolus***,** 128-53.

O'MAHONY, D. J. & ROTHBLUM, L. I. 1991. Identification of two forms of the RNA polymerase I transcription factor UBF. *Proceedings of the National Academy of Sciences,* 88**,** 3180.

O'SULLIVAN, A. C., SULLIVAN, G. J. & MCSTAY, B. 2002. UBF binding in vivo is not restricted to regulatory sequences within the vertebrate ribosomal DNA repeat. *Molecular and cellular biology,* 22**,** 657.

OAKES, C. C., SMIRAGLIA, D. J., PLASS, C., TRASLER, J. M. & ROBAIRE, B. 2003. Aging results in hypermethylation of ribosomal DNA in sperm and liver of male rats. *Proceedings of the National Academy of Sciences,* 100**,** 1775.

OCHS, R. L., LISCHWE, M. A., SHEN, E., CARROLL, R. E. & BUSCH, H. 1985. Nucleologenesis: composition and fate of prenucleolar bodies. *Chromosoma,* 92**,** 330-336.

OGATA, K., MORIKAWA, S., NAKAMURA, H., SEKIKAWA, A., INOUE, T., KANAI, H., SARAI, A., ISHII, S. & NISHIMURA, Y. 1994. Solution structure of a specific DNA complex of the Myb DNA-binding domain with cooperative recognition helices. *Cell,* 79**,** 639-648.

ORRICK, L. R., OLSON, M. O. J. & BUSCH, H. 1973. Comparison of nucleolar proteins of normal rat liver and Novikoff hepatoma ascites cells by two-dimensional polyacrylamide gel electrophoresis. *Proceedings of the National Academy of Sciences,* 70**,** 1316.

PADDISON, P. J., CAUDY, A. A., BERNSTEIN, E., HANNON, G. J. & CONKLIN, D. S. 2002. Short hairpin RNAs (shRNAs) induce sequence-specific silencing in mammalian cells. *Genes & development,* 16**,** 948-958.

PANOV, K. I., FRIEDRICH, J. K., RUSSELL, J. & ZOMERDIJK, J. C. B. M. 2006a. UBF activates RNA polymerase I transcription by stimulating promoter escape. *EMBO J,* 25**,** 3310-3322.

PANOV, K. I., PANOVA, T. B., GADAL, O., NISHIYAMA, K., SAITO, T., RUSSELL, J. & ZOMERDIJK, J. C. B. M. 2006b. RNA polymerase I-specific subunit CAST/hPAF49 has a role in the activation of transcription by upstream binding factor. *Molecular and cellular biology,* 26**,** 5436-5448.

PECULIS, B. A. & STEITZ, J. A. 1993. Disruption of U8 nucleolar snRNA inhibits 5.8S and 28S rRNA processing in the Xenopus oocyte. *Cell,* 73**,** 1233-1245.

PEYROCHE, G., LEVILLAIN, E., SIAUT, M., CALLEBAUT, I., SCHULTZ, P., SENTENAC, A., RIVA, M. & CARLES, C. 2002. The A14–A43 heterodimer subunit in yeast RNA pol I and their relationship to Rpb4–Rpb7 pol II subunits. *Proceedings of the National Academy of Sciences,* 99**,** 14670.

PIKAARD, C. S. & LAWRENCE, R. J. 2002. Uniting the paths to gene silencing. *Nature genetics,* 32**,** 340-341.

PIKAARD, C. S., MCSTAY, B., SCHULTZ, M. C., BELL, S. P. & REEDER, R. H. 1989. The Xenopus ribosomal gene enhancers bind an essential polymerase I transcription factor, xUBF. *Genes & development,* 3**,** 1779.

PIKAARD, C. S., PAPE, L., HENDERSON, S., RYAN, K., PAALMAN, M., LOPATA, M., REEDER, R. & SOLLNER-WEBB, B. 1990. Enhancers for RNA polymerase I in mouse ribosomal DNA. *Molecular and cellular biology,* 10**,** 4816-4825.

POORTINGA, G., HANNAN, K. M., SNELLING, H., WALKLEY, C. R., JENKINS, A., SHARKEY, K., WALL, M., BRANDENBURGER, Y., PALATSIDES, M. & PEARSON, R. B. 2004. MAD1 and c-MYC regulate UBF and rDNA transcription during granulocyte differentiation. *The EMBO journal,* 23**,** 3325-3335.

POORTINGA, G., WALL, M., SANIJ, E., SIWICKI, K., ELLUL, J., BROWN, D., HOLLOWAY, T. P., HANNAN, R. D. & MCARTHUR, G. A. 2011. c-MYC coordinately regulates ribosomal gene chromatin remodeling and Pol I availability during granulocyte differentiation. *Nucleic acids research,* 39**,** 3267-3281.

PRIETO, J.-L. & MCSTAY, B. 2008. Pseudo-NORs: A novel model for studying nucleoli. *Biochimica et Biophysica Acta (BBA) - Molecular Cell Research,* 1783**,** 2116-2123.

PRIETO, J. L. & MCSTAY, B. 2007. Recruitment of factors linking transcription and processing of pre-rRNA to NOR chromatin is UBF-dependent and occurs independent of transcription in human cells. *Genes & development,* 21**,** 2041.

PUTNAM, C. D., COPENHAVER, G. P., DENTON, M. L. & PIKAARD, C. S. 1994. The RNA polymerase I transactivator upstream binding factor requires its dimerization domain and high-mobility-group (HMG) box 1 to bend, wrap, and positively supercoil enhancer DNA. *Molecular and cellular biology,* 14**,** 6476-6488.

PUVION-DUTILLEUL, F. 1983. Morphology of transcription at cellular and molecular levels. *Int. Rev. Cytol,* 84**,** 57-101.

PUVION-DUTILLEUL, F., PUVION, E. & BACHELLERIE, J. P. 1997. Early stages of pre-rRNA formation within the nucleolar ultrastructure of mouse cells studied by in situ hybridization with a 5′ ETS leader probe. *Chromosoma,* 105**,** 496-505.

RAO, D. D., VORHIES, J. S., SENZER, N. & NEMUNAITIS, J. 2009. siRNA vs. shRNA: similarities and differences. *Advanced drug delivery reviews,* 61**,** 746-759.

RAŠKA, I. 2003. Oldies but goldies: searching for Christmas trees within the nucleolar architecture. *Trends in Cell Biology,* 13**,** 517-525.

RAŠKA, I., DUNDR, M., KOBERNA, K., MELČÁK, I., RISUEÑO, M.-C. & TÖRÖK, I. 1995. Does the Synthesis of Ribosomal RNA Take Place within Nucleolar Fibrillar Centers or Dense Fibrillar Components? A Critical Appraisal. *Journal of Structural Biology,* 114**,** 1-22.

REITER, A., HAMPERL, S., SEITZ, H., MERKL, P., PEREZ-FERNANDEZ, J., WILLIAMS, L., GERBER, J., NÉMETH, A., LÉGER, I. & GADAL, O. 2012. The Reb1-homologue Ydr026c/Nsi1 is required for efficient RNA polymerase I termination in yeast. *The EMBO journal*.

RITOSSA, F. & SPIEGELMAN, S. 1965. Localization of DNA complementary to ribosomal RNA in the nucleolus organizer region of Drosophila melanogaster. *Proceedings of the National Academy of Sciences of the United States of America,* 53**,** 737.

ROBERT-FORTEL, I., JUNERA, H., GÉRAUD, G. & HERNADEZ-VERDUN, D. 1993. Three-dimensional organization of the ribosomal genes and Ag-NOR proteins during interphase and mitosis in PtK 1 cells studied by confocal microscopy. *Chromosoma,* 102**,** 146-157.

ROBINS, A., HAYMAN, D. & WELLS, J. 1984. Ribosomal gene reiteration in a marsupial species with an X-linked nucleolar organizer. *Australian journal of biological sciences,* 37**,** 211-216.

RODRIGO, R. M., RENDON, M. C., TORREBLANCA, J., GARCIA-HERDUGO, G. & MORENO, F. J. 1992. Characterization and immunolocalization of RNA polymerase I transcription factor UBF with anti-NOR serum in protozoa, higher plant and vertebrate cells. *Journal of Cell Science,* 103**,** 1053-1063.

ROEDER, R. G. & RUTTER, W. J. 1969. Multiple Forms of DNA-dependent RNA Polymerase in Eukaryotic Organisms. *Nature,* 224**,** 234-237.

ROUSSEL, P., ANDRÉ, C., COMAI, L. & HERNANDEZ-VERDUN, D. E. 1996. The rDNA transcription machinery is assembled during mitosis in active NORs and absent in inactive NORs. *The Journal of cell biology,* 133**,** 235-246.

ROUSSEL, P., ANDRÉ, C., MASSON, C., GÉRAUD, G. & HERNANDEZ-VERDUN, D. 1993. Localization of the RNA polymerase I transcription factor hUBF during the cell cycle. *Journal of Cell Science,* 104**,** 327-337.

RUGGERO, D. & PANDOLFI, P. P. 2003. Does the ribosome translate cancer? *Nature Reviews Cancer,* 3**,** 179-192.

RUSSELL, J. & ZOMERDIJK, J. C. B. M. 2005. RNA-polymerase-I-directed rDNA transcription, life and works. *Trends in biochemical sciences,* 30**,** 87-96.

SAITOH, Y. & LAEMMLI, U. K. 1994. Metaphase chromosome structure: Bands arise from a differential folding path of the highly AT-rich scaffold. *Cell,* 76**,** 609-622.

SAKAI, K., OHTA, T., MINOSHIMA, S., KUDOH, J., WANG, Y., DE JONG, P. J. & SHIMIZU, N. 1995. Human ribosomal RNA gene cluster: identification of the proximal end containing a novel tandem repeat sequence. *Genomics,* 26**,** 521-526.

SANIJ, E., POORTINGA, G., SHARKEY, K., HUNG, S., HOLLOWAY, T. P., QUIN, J., ROBB, E., WONG, L. H., THOMAS, W. G. & STEFANOVSKY, V. 2008. UBF levels determine the number of active ribosomal RNA genes in mammals. *The Journal of cell biology,* 183**,** 1259-1274.

SANTORO, R. & GRUMMT, I. 2001. Molecular Mechanisms Mediating Methylation-Dependent Silencing of Ribosomal Gene Transcription. *Molecular cell,* 8**,** 719-725.

SANTORO, R. & GRUMMT, I. 2005. Epigenetic Mechanism of rRNA Gene Silencing: Temporal Order of NoRC-Mediated Histone Modification, Chromatin Remodeling, and DNA Methylation. *Molecular and cellular biology,* 25**,** 2539-2546.

SANTORO, R., LI, J. & GRUMMT, I. 2002. The nucleolar remodeling complex NoRC mediates heterochromatin formation and silencing of ribosomal gene transcription. *Nat Genet,* 32**,** 393-396.

SAVINO, T. M., BASTOS, R., JANSEN, E. & HERNANDEZ-VERDUN, D. 1999. The nucleolar antigen Nop52, the human homologue of the yeast ribosomal RNA processing RRP1, is recruited at late stages of nucleologenesis. *Journal of Cell Science,* 112**,** 1889-1900.

SAVINO, T. M., GÉBRANE-YOUNÈS, J., DE MEY, J., SIBARITA, J. B. & HERNANDEZ-VERDUN, D. 2001. Nucleolar assembly of the rRNA processing machinery in living cells. *The Journal of cell biology,* 153**,** 1097-1110.

SCHEER, U. & ROSE, K. M. 1984. Localization of RNA polymerase I in interphase cells and mitotic chromosomes by light and electron microscopic immunocytochemistry. *Proceedings of the National Academy of Sciences,* 81**,** 1431.

SCHERL, A., COUTÉ, Y., DÉON, C., CALLÉ, A., KINDBEITER, K., SANCHEZ, J. C., GRECO, A., HOCHSTRASSER, D. & DIAZ, J. J. 2002. Functional proteomic analysis of human nucleolus. *Molecular biology of the cell,* 13**,** 4100-4109.

SCHERRER, K., LATHAM, H. & DARNELL, J. E. 1963. Demonstration of an unstable RNA and of a precursor to ribosomal RNA in HeLa cells. *Proceedings of the National Academy of Sciences of the United States of America,* 49**,** 240.

SCHMICKEL, R. D. 1973. Quantitation of human ribosomal DNA: hybridization of human DNA with ribosomal RNA for quantitation and fractionation. *Pediatric research,* 7**,** 5-12.

SHAV-TAL, Y., BLECHMAN, J., DARZACQ, X., MONTAGNA, C., DYE, B. T., PATTON, J. G., SINGER, R. H. & ZIPORI, D. 2005. Dynamic sorting of nuclear components into distinct nucleolar caps during transcriptional inhibition. *Molecular biology of the cell,* 16**,** 2395-2413.

SHIELS, C., COUTELLE, C. & HUXLEY, C. 1997. Contiguous Arrays of Satellites 1, 3, and [beta] Form a 1.5-Mb Domain on Chromosome 22p. *Genomics,* 44**,** 35-44.

SINCLAIR, A. H., BERTA, P., PALMER, M. S., HAWKINS, J. R., GRIFFITHS, B. L., SMITH, M. J., FOSTER, J. W., FRISCHAUF, A. M., LOVELL-BADGE, R. & GOODFELLOW, P. N. 1990. A gene from the human sex-determining region encodes a protein with homology to a conserved DNA-binding motif. *Nature,* 346**,** 240-244.

SINKKONEN, L., HUGENSCHMIDT, T., FILIPOWICZ, W. & SVOBODA, P. 2010. Dicer is associated with ribosomal DNA chromatin in mammalian cells. *PloS one,* 5**,** e12175.

SIRRI, V., URCUQUI-INCHIMA, S., ROUSSEL, P. & HERNANDEZ-VERDUN, D. 2008. Nucleolus: the fascinating nuclear body. *Histochemistry and cell biology,* 129**,** 13-31.

SOLDANI, C., BOTTONE, M. G., PELLICCIARI, C. & SCOVASSI, A. I. 2009. Nucleolus disassembly in mitosis and apoptosis: dynamic redistribution of phosphorylated-c-Myc, fibrillarin and Ki-67. *European Journal of Histochemistry,* 50**,** 273-280.

SOLLNER-WEBB, B., WILKINSON, J., ROAN, J. & REEDER, R. H. 1983. Nested control regions promote Xenopus ribosomal RNA synthesis by RNA polymerase I. *Cell,* 35**,** 199.

SRIVASTAVA, L., LAPIK, Y. R., WANG, M. & PESTOV, D. G. 2010. Mammalian DEAD Box Protein Ddx51 Acts in 3′ End Maturation of 28S rRNA by Promoting the Release of U8 snoRNA. *Molecular and cellular biology,* 30**,** 2947-2956.

SRIVASTAVA, M., BEGOVIC, E., CHAPMAN, J., PUTNAM, N. H., HELLSTEN, U., KAWASHIMA, T., KUO, A., MITROS, T., SALAMOV, A., CARPENTER, M. L., SIGNOROVITCH, A. Y., MORENO, M. A., KAMM, K., GRIMWOOD, J., SCHMUTZ, J., SHAPIRO, H., GRIGORIEV, I. V., BUSS, L. W., SCHIERWATER, B., DELLAPORTA, S. L. & ROKHSAR, D. S. 2008. The Trichoplax genome and the nature of placozoans. *Nature,* 454**,** 955-960.

STEFANOVSKY, V., LANGLOIS, F., GAGNON-KUGLER, T., ROTHBLUM, L. I. & MOSS, T. 2006a. Growth factor signaling regulates elongation of RNA polymerase I transcription in mammals via UBF phosphorylation and r-chromatin remodeling. *Molecular cell,* 21**,** 629-639.

STEFANOVSKY, V. Y., LANGLOIS, F., BAZETT-JONES, D., PELLETIER, G. & MOSS, T. 2006b. ERK modulates DNA bending and enhancesome structure by phosphorylating HMG1-boxes 1 and 2 of the RNA polymerase I transcription factor UBF. *Biochemistry,* 45**,** 3626-3634.

STEFANOVSKY, V. Y., PELLETIER, G., BAZETT-JONES, D. P., CRANE-ROBINSON, C. & MOSS, T. 2001a. DNA looping in the RNA polymerase I enhancesome is the result of non-cooperative in-phase bending by two UBF molecules. *Nucleic acids research,* 29**,** 3241-3247.

STEFANOVSKY, V. Y., PELLETIER, G., HANNAN, R., GAGNON-KUGLER, T., ROTHBLUM, L. I. & MOSS, T. 2001b. An Immediate Response of Ribosomal Transcription to Growth Factor Stimulation in Mammals Is Mediated by ERK Phosphorylation of UBF. *Molecular cell,* 8**,** 1063-1073.

STERNER, D. E., WANG, X., BLOOM, M. H., SIMON, G. M. & BERGER, S. L. 2002. The SANT domain of Ada2 is required for normal acetylation of histones by the yeast SAGA complex. *Journal of Biological Chemistry,* 277**,** 8178-8186.

STROHNER, R., NEMETH, A., JANSA, P., HOFMANN-ROHRER, U., SANTORO, R., LÄNGST, G. & GRUMMT, I. 2001. NoRC—a novel member of mammalian ISWI-containing chromatin remodeling machines. *The EMBO journal,* 20**,** 4892-4900.

STULTS, D. M., KILLEN, M. W., PIERCE, H. H. & PIERCE, A. J. 2008. Genomic architecture and inheritance of human ribosomal RNA gene clusters. *Genome research,* 18**,** 13-18.

SULLIVAN, G. J., BRIDGER, J. M., CUTHBERT, A. P., NEWBOLD, R. F., BICKMORE, W. A. & MCSTAY, B. 2001. Human acrocentric chromosomes with transcriptionally silent nucleolar organizer regions associate with nucleoli. *The EMBO journal,* 20**,** 2867-2877.

SYLVESTER, J. E., GONZALEZ, I. L. & MOUGEY, E. B. 2004. Structure and organization of vertebrate ribosomal DNA. *The Nucleolus***,** 58-72.

TAGARRO, I., WIEGANT, J., RAAP, A. K., GONZÁLEZ-AGUILERA, J. J. & FERNÁNDEZ-PERALTA, A. M. 1994. Assignment of human satellite 1 DNA as revealed by fluorescent in situ hybridization with oligonucleotides. *Human genetics,* 93**,** 125-128.

TAHIROV, T. H., SASAKI, M., INOUE-BUNGO, T., FUJIKAWA, A., SATO, K., KUMASAKA, T., YAMAMOTO, M. & OGATA, K. 2001. Crystals of ternary protein-DNA complexes composed of DNA-binding domains of c-Myb or v-Myb, C/EBP or C/EBP and tom-1A promoter fragment. *Acta Crystallographica Section D: Biological Crystallography,* 57**,** 1655-1658.

THERMAN, E., SUSMAN, B. & DENNISTON, C. 1989. The nonrandom participation of human acrocentric chromosomes in Robertsonian translocations. *Annals of human genetics,* 53**,** 49-65.

THURIAUX, P., MARIOTTE, S., BUHLER, J.-M., SENTENAC, A., VU, L., LEE, B.-S. & NOMURA, M. 1995. Gene RPA43 in Saccharomyces cerevisiae Encodes an Essential Subunit of RNA Polymerase I. *Journal of Biological Chemistry,* 270**,** 24252-24257.

TIAN, Q., KOPF, G. S., BROWN, R. S. & TSENG, H. 2001. Function of basonuclin in increasing transcription of the ribosomal RNA genes during mouse oogenesis. *Development,* 128**,** 407-416.

TOLLERVEY, D., LEHTONEN, H., JANSEN, R., KERN, H. & HURT, E. C. 1993. Temperature-sensitive mutations demonstrate roles for yeast fibrillarin in pre-rRNA processing, pre-rRNA methylation, and ribosome assembly. *Cell,* 72**,** 443.

TRAVERS, A. A. 2003. Priming the nucleosome: a role for HMGB proteins? *EMBO reports,* 4**,** 131-136.

TSAI, R. Y. L. & MCKAY, R. D. G. 2002. A nucleolar mechanism controlling cell proliferation in stem cells and cancer cells. *Genes & Dev.,* 16**,** 2991-3003.

TSENG, H., BIEGEL, J. A. & BROWN, R. S. 1999. Basonuclin is associated with the ribosomal RNA genes on human keratinocyte mitotic chromosomes. *Journal of Cell Science,* 112**,** 3039-3047.

TUAN, J. C., ZHAI, W. & COMAI, L. 1999. Recruitment of TATA-Binding Protein–TAFI Complex SL1 to the Human Ribosomal DNA Promoter Is Mediated by the Carboxy-Terminal Activation Domain of Upstream Binding Factor (UBF) and Is Regulated by UBF Phosphorylation. *Molecular and cellular biology,* 19**,** 2872-2879.

TYCOWSKI, K. T., SHU, M. D. & STEITZ, J. A. 1994. Requirement for intron-encoded U22 small nucleolar RNA in 18S ribosomal RNA maturation. *Science,* 266**,** 1558-1561.

TYCOWSKI, K. T., SMITH, C. M., SHU, M.-D. & STEITZ, J. A. 1996. A small nucleolar RNA requirement for site-specific ribose methylation of rRNA in Xenopus. *Proceedings of the National Academy of Sciences,* 93**,** 14480-14485.

VALDEZ, B. C., HENNING, D., SO, R. B., DIXON, J. & DIXON, M. J. 2004. The Treacher Collins syndrome (TCOF1) gene product is involved in ribosomal DNA gene transcription by interacting with upstream binding factor. *Proceedings of the National Academy of Sciences of the United States of America,* 101**,** 10709.

VAN DE WETERING, M., OOSTERWEGEL, M., DOOIJES, D. & CLEVERS, H. 1991. Identification and cloning of TCF-1, a T lymphocyte-specific transcription factor containing a sequence-specific HMG box. *The EMBO journal,* 10**,** 123.

VAN DE WETERING, M., OVING, I., MUNCAN, V., FONG, M. T. P., BRANTJES, H., VAN LEENEN, D., HOLSTEGE, F. C. P., BRUMMELKAMP, T. R., AGAMI, R. & CLEVERS, H. 2003. Specific inhibition of gene expression using a stably integrated, inducible small-interfering-RNA vector. *EMBO reports,* 4**,** 609-615.

VOIT, R. & GRUMMT, I. 2001. Phosphorylation of UBF at serine 388 is required for interaction with RNA polymerase I and activation of rDNA transcription. *Proceedings of the National Academy of Sciences,* 98**,** 13631.

VOIT, R., HOFFMANN, M. & GRUMMT, I. 1999. Phosphorylation by G1-specific cdk–cyclin complexes activates the nucleolar transcription factor UBF. *The EMBO journal,* 18**,** 1891-1899.

VOIT, R., SCHÄFER, K. & GRUMMT, I. 1997. Mechanism of repression of RNA polymerase I transcription by the retinoblastoma protein. *Molecular and cellular biology,* 17**,** 4230-4237.

VOIT, R., SCHNAPP, A., KUHN, A., ROSENBAUER, H., HIRSCHMANN, P., STUNNENBERG, H. & GRUMMT, I. 1992. The nucleolar transcription factor mUBF is phosphorylated by casein kinase II in the C-terminal hyperacidic tail which is essential for transactivation. *The EMBO journal,* 11**,** 2211.

WANG, L., GOUT, I. & PROUD, C. G. 2001. Cross-talk between the ERK and p70 S6 Kinase (S6K) Signaling Pathways. *Journal of Biological Chemistry,* 276**,** 32670-32677.

WARNER, J. R. 1999. The economics of ribosome biosynthesis in yeast. *Trends in biochemical sciences,* 24**,** 437-440.

WATKINS, N. J., SÉGAULT, V., CHARPENTIER, B., NOTTROTT, S., FABRIZIO, P., BACHI, A., WILM, M., ROSBASH, M., BRANLANT, C. & LÜHRMANN, R. 2000. A Common Core RNP Structure Shared between the Small Nucleoar Box C/D RNPs and the Spliceosomal U4 snRNP. *Cell,* 103**,** 457-466.

WEBER, J. D., TAYLOR, L. J., ROUSSEL, M. F., SHERR, C. J. & BAR-SAGI, D. 1999. Nucleolar Arf sequesters Mdm2 and activates p53. *Nat Cell Biol,* 1**,** 20-26.

WINDLE, J. J. & SOLLNER-WEBB, B. 1986. Two distant and precisely positioned domains promote transcription of Xenopus laevis rRNA genes: analysis with linker-scanning mutants. *Molecular and cellular biology,* 6**,** 4585-4593.

WITTNER, M., HAMPERL, S., STÖCKL, U., SEUFERT, W., TSCHOCHNER, H., MILKEREIT, P. & GRIESENBECK, J. 2011. Establishment and Maintenance of Alternative Chromatin States at a Multicopy Gene Locus. *Cell,* 145**,** 543-554.

WORTON, R., SUTHERLAND, J., SYLVESTER, J., WILLARD, H., BODRUG, S., DUBE, I., DUFF, C., KEAN, V., RAY, P. & SCHMICKEL, R. 1988. Human ribosomal RNA genes: orientation of the tandem array and conservation of the 5' end. *Science,* 239**,** 64-68.

WRIGHT, J., MAIS, C., PRIETO, J. & MCSTAY, B. A role for upstream binding factor in organizing ribosomal gene chromatin. 2006. 77-84.

XIAO, L., KAMAU, E., DONZE, D. & GROVE, A. 2011. Expression of yeast high mobility group protein HMO1 is regulated by TOR signaling. *Gene,* 489**,** 55-62.

XU, Y., YANG, W., WU, J. & SHI, Y. 2002. Solution structure of the first HMG box domain in human upstream binding factor. *Biochemistry,* 41**,** 5415-5420.

YAMAMOTO, K., YAMAMOTO, M., HANADA, K., NOGI, Y., MATSUYAMA, T. & MURAMATSU, M. 2004. Multiple protein-protein interactions by RNA polymerase I-associated factor PAF49 and role of PAF49 in rRNA transcription. *Molecular and cellular biology,* 24**,** 6338-6349.

YAO, F., SVENSJÖ, T., WINKLER, T., LU, M., ERIKSSON, C. & ERIKSSON, E. 1998. Tetracycline repressor, tetR, rather than the tetR-mammalian cell transcription factor fusion derivatives, regulates inducible gene expression in mammalian cells. *Human gene therapy,* 9**,** 1939-1950.

YOUNG, D. W., HASSAN, M. Q., PRATAP, J., GALINDO, M., ZAIDI, S. K., LEE, S.-H., YANG, X., XIE, R., JAVED, A., UNDERWOOD, J. M., FURCINITTI, P., IMBALZANO, A. N., PENMAN, S., NICKERSON, J. A., MONTECINO, M. A., LIAN, J. B., STEIN, J. L., VAN WIJNEN, A. J. & STEIN, G. S. 2007. Mitotic occupancy and lineage-specific transcriptional control of rRNA genes by Runx2. *Nature,* 445**,** 442-446.

YUAN, X., ZHAO, J., ZENTGRAF, H., HOFFMANN-ROHRER, U. & GRUMMT, I. 2002. Multiple interactions between RNA polymerase I, TIF-IA and TAFI subunits regulate preinitiation complex assembly at the ribosomal gene promoter. *EMBO reports,* 3**,** 1082-1087.

ZHAI, W. & COMAI, L. 2000. Repression of RNA Polymerase I Transcription by the Tumor Suppressor p53. *Molecular and cellular biology,* 20**,** 5930-5938.

ZHANG, S., WANG, J. & TSENG, H. 2007. Basonuclin regulates a subset of ribosomal RNA genes in HaCaT cells. *PloS one,* 2**,** e902.

ZHANG, Y. & LU, H. 2009. Signaling to p53: Ribosomal Proteins Find Their Way. *Cancer Cell,* 16**,** 369-377.

ZHAO, J., YUAN, X., FRÖDIN, M. & GRUMMT, I. 2003. ERK-Dependent Phosphorylation of the Transcription Initiation Factor TIF-IA Is Required for RNA Polymerase I Transcription and Cell Growth. *Molecular cell,* 11**,** 405-413.

ZHOU, Y., SANTORO, R. & GRUMMT, I. 2002. The chromatin remodeling complex NoRC targets HDAC1 to the ribosomal gene promoter and represses RNA polymerase I transcription. *EMBO J,* 21**,** 4632-4640.

ZOMERDIJK, J., BECKMANN, H., COMAI, L. & TJIAN, R. 1994. Assembly of transcriptionally active RNA polymerase I initiation factor SL1 from recombinant subunits. *Science,* 266**,** 2015-2018.

Appendix: Scientific Communications

Oral Presentation

Selected for oral presentation in Sub-Nuclear Structures and Diseases conference 2012, The Møller Centre, Cambridge, UK, 28th-30th June 2012, *"UBF, a master regulator of ribosome biogenesis"*.

Poster Presentations

Sub-Nuclear Structures and Diseases Conference, Wellcome Trust Genome Campus, Hinxton, Cambridge, UK, 27th-30th July 2010.
Christine Colleran, José-Luis Prieto, Brian McStay. *"UBF, a master regulator of ribosome biogenesis"*.

College of Science Research Day, NUI Galway, Ireland, 12th April 2010.
Christine Colleran, José-Luis Prieto, Brian McStay. *"UBF, a master regulator of ribosome biogenesis"*.

Scientific Communication

Grob, A., **C. Colleran**, and B. McStay. 2011. *UBF an Essential Player in Maintenance of Active NORs and Nucleolar Formation.* Book chapter in *The Nucleolus*, Mark O.J. Olson (Editor): pg83-103